Neural circuit perturbations during attention switching

Myers-Joseph, Dylan

Awarding institution:
King's College London

Neural circuit perturbations during attention switching

Dylan Myers-Joseph

Thesis submitted for the degree of Doctor of Philosophy

December 2022

Centre for Developmental Neurobiology

Institute of Psychiatry, Psychology and Neuroscience

King's College London

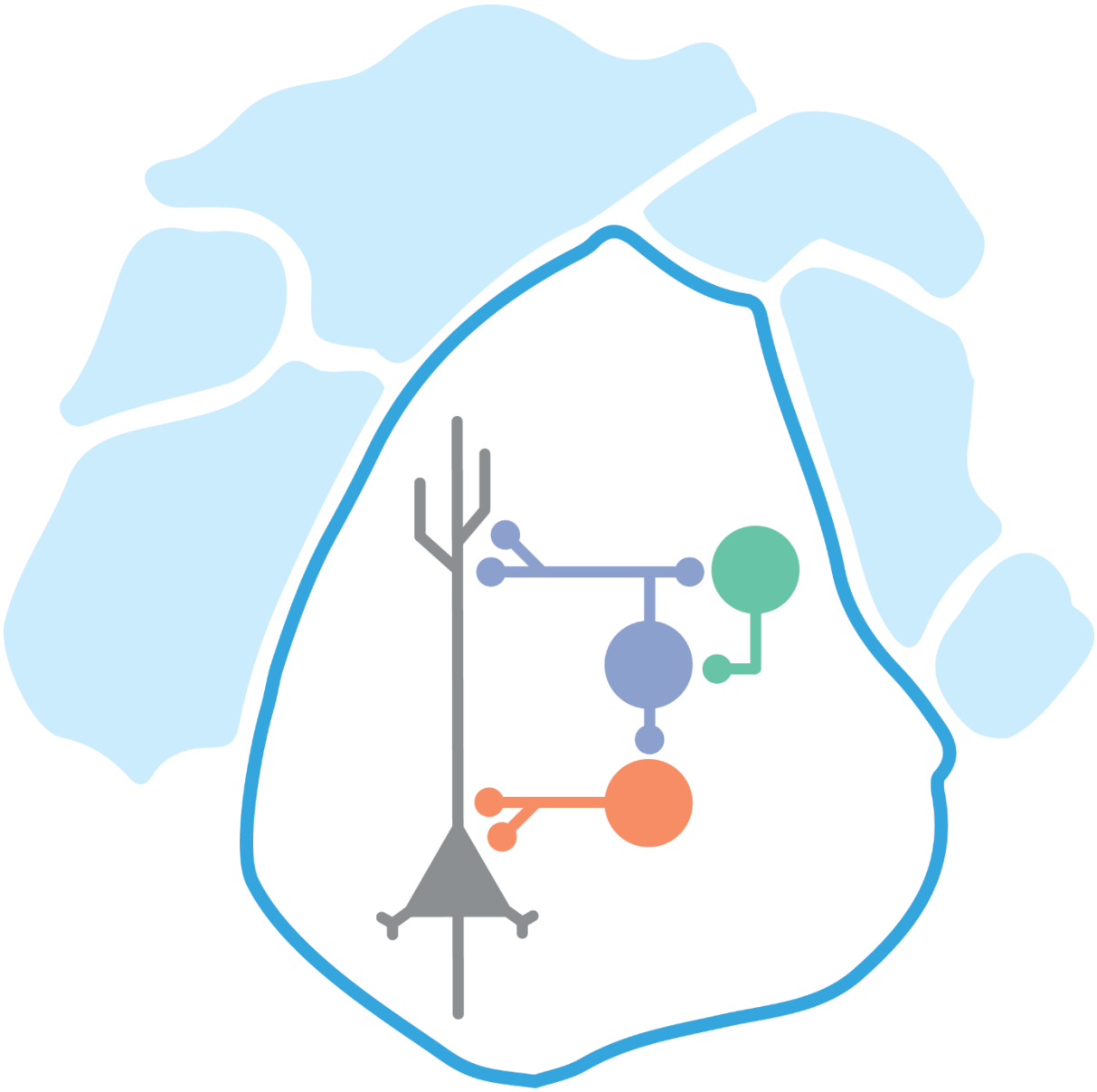

Abstract

The modulation of sensory processing by attention is a key feature of cognition. Much of the previous work on attention has been carried out in non-human primates. The primate visual system is hierarchically organised, and the intensity of attentional modulation has been found to be greater higher up in the hierarchy. The mapping of attention effects across mouse higher visual areas is unknown. Here I have recorded from 7 visual cortical areas whilst mice performed a cross-modal attention switching task. I found that primary visual cortex (V1) was the area most strongly modulated by attention, an inversion of the pattern expected from analogy to primate data. Although there has been a great deal of excellent work into attention, its neural circuit basis is poorly understood. I used all-optical methods to investigate whether two molecularly defined interneuron types are involved in the attentional modulation of visual stimulus selectivity in mouse V1 - vasoactive intestinal peptide expressing (VIP) and parvalbumin expressing (PV) interneurons.

First, VIP interneurons exert disinhibitory control over pyramidal neurons through inhibition of somatostatin expressing (SOM) interneurons. This disinhibitory motif is a candidate mechanism for the changes in neural activity with attention. I bi-directionally manipulated the activity of VIP interneurons as mice performed an attention switching task. I recorded the activity of VIP, SOM, PV interneurons and pyramidal neurons identified in the same tissue and found that while both attention and VIP manipulation affected the activity in all 4 cell classes, their effects on the stimulus selectivity of the neural population were orthogonal. In support of their independence, attention and VIP-SOM disinhibition produced distinct patterns of changes in activity and different changes in the noise correlations between and within the 4 recorded cell classes. Collectively, these experiments provide evidence against a role for VIP interneurons in the neural correlates of cross-modal attention and highlight the ability of cortical circuits to simultaneously contain multiple strong non-interacting modulations in the same neural population.

Second, PV interneurons are strongly modulated by attention and exert a powerful influence on the activity of cortical circuits. I optogenetically excited PV interneurons whilst recording activity in V1 of mice performing the same cross-modal attention switching task. The effects of PV activation had opposite effects on the network depending on the cognitive state of the

animal. Strengths of PV activation which inhibited non-PV visually evoked activity during calibration sessions elicited no-change or an increase in non-PV activity when the mouse viewed the same visual stimuli during the attention switching task. Additionally, activation of PV interneurons modified stimulus selectivity in an attention dependent manner. However, interpretation of these results is made difficult because monotonic changes in stimulus selectivity depend on non-monotonic and paradoxical changes in the activity of non-PV cells with increasing PV photoactivation. Further work is required to identify the causes and implications of these unexpected effects, but they suggest caution when interpreting the effects of perturbing interneuron activity.

Acknowledgements

I hope everybody I should thank here already knows how much I appreciate them, ideally because I've already told them in person, but it can't hurt to make some thanks explicit. It takes a village to raise a child, and I certainly feel I've grown and changed since I started the PhD, it would not have been the same without the lovely environment of the CDN.

First, enormous thanks to my supervisor Adil Khan, without his tutelage, support and enthusiasm this would not have been possible. I'd also like to thank my supervisor Juan Burrone and my thesis committee members Matthew Grubb and Samuel Cooke, for their insight and guidance at many key moments.

I'd like to thank all the lab past and present for being wonderful colleagues and friends. Nick Cole, we've been in this together since day one and I wouldn't have had it any other way. Matt Harvey, your company is enough to make me miss training mice in a dark room. Filipe Ferreira, the bravest little neuron that I've met. Francesca Ruggeri, thanks for putting up with me trying to teach you how to use MATLAB. Marian Fernandez-Otero, thanks for your positive presence and for being so willing to test my unfinished code.

Finally, thank you to my family, specifically to my parents, without whom I most certainly wouldn't be who or where I am today. And to my wife Lies, thank you so much for your love and support, although perhaps I should be thanking my time spent studying for us ending up together.

Declaration of contributions

The work presented in this thesis is my own and I have endeavoured to make it clear in the text where the work was done by other people. However, in case anything was missed.

Matthew Harvey performed the widefield imaging and wrote the analysis code to map the locations of higher visual areas (Figure 2.5).

Marian Fernandez-Otero performed all immunohistochemical labelling and confocal imaging of stained slices - used for the identification of SOM, PV and VIP interneurons in chapter 3. She also performed the manual steps of registering the *in vivo* and immunolabelled images and identified stained cells.

Francesca Ruggeri carried out the experiments presented in figure 3.17 during her masters project. She was trained and supervised by me and Nicholas Cole.

Table of Contents

Table of figures

Table of Tables

Abbreviations

A	Anterior visual area (Rodent)
ACC	Anterior cingulate cortex
AL	Anterolateral visual area (Rodent)
AM	Anteromedial visual area (Rodent)
Cg1	Primary cingulate areas (Rodent)
Cg2	Secondary cingulate areas (Rodent)

HVA	Higher visual areas
IT	Inferior Temporal gyrus (primate)
V1	Primary visual cortex
V2	Secondary visual cortex (primate)
V3	Visual area three (primate)
V4	Visual area four (primate)
VIP	Vasoactive Intestinal Peptide
LI	Laterointermediate visual area (Rodent)
LM	Lateromedial visual area (Rodent)
LP	Lateral Posterior nucleus of the thalamus (Rodent)
M	Medial visual area (Rodent)
MST	Medial Superior Temporal area (primate)
MT	Middle temporal visual area (primate)
RL	Rostrolateral visual area (Rodent)
P	Posterior visual area (Rodent)
PFC	Prefrontal cortex
PL	Prelimbic cortex
PM	Posteromedial visual area (Rodent)
POR	Postrhinal visual area (Rodent)
PV	Parvalbumin
PYR	Pyramidal neurons
ROI	Region of interest
SC	Superior colliculus
SOM	Somatostatin
5HT3aR	Serotonin receptor 5HT3a

Chapter 1 – Introduction

We are all intimately familiar with attention; it would be hard to read these words without it. The brain receives a deluge of sensory information at any one moment, attention is the process through which this flood of information is parsed to amplify the subset of information necessary to guide current behaviour. The overall aim of this thesis is to investigate the neural circuit basis of attentional modulation in visual cortex.

Most of the research on attention has been focused on visual attention, in part because more of the primate brain is devoted to vision than other sensory modalities (Felleman and Van Essen, 1991). Non-invasive neural recording techniques such as electroencephalography (EEG), electrocorticography (EcoG), magnetoencephalography (MEG), and functional magnetic resonance imaging (fMRI) have made it possible to study the neural correlates of attention in humans (Kastner and Ungerleider, 2000; Posner and Rothbart, 2007; Carrasco, 2011). Historically, it has only rarely been possible to record the activity of individual neurons in humans (Kastner and Ungerleider, 2000; Posner and Rothbart, 2007; Carrasco, 2011). Although the recent development of the neuropixel probes has made it possible to record from dozens of neurons simultaneously in human subjects (Paulk et al., 2022; Chung et al., 2022) opening significant opportunities for human experiments into cognitive phenomena, such experiments are rare.

Non-human experiments have therefore allowed more precision and experimental control. Historically, macaques have been the primary subjects of attention research, because of the similarity of our brains to theirs and their ability to learn the complex behavioural tasks involved in attention experiments. However, neural correlates of attention have been found across the animal kingdom, even appearing in invertebrates such as the dragonfly (Wiederman and O'Carroll, 2013).

There is increasing interest in the mouse as a model organism for attention research (Speed and Haider, 2021). A wealth of experimental tools is now available allowing investigation of neural circuit mechanisms in a way not available in primates. Genetically encoded calcium indicators allow the simultaneous recording of enormous numbers of neurons (Stringer et al., 2021), while advances in electrophysiological probes allow temporally precise measurements

from multiple areas across the mouse brain simultaneously (Steinmetz et al., 2018). Transgenic mouse driver lines make genetically identified cell-classes accessible for experimentation. For example, PV-cre mouse lines allow expression of excitatory opsins in parvalbumin expressing interneurons allowing interneuron mediated inhibition of cortical activity (Li et al., 2019). Cell-type targeted delivery of opsins allows for the interrogation of the mouse brain using light alone, to rapidly probe the activity of multiple brain regions (Guo et al., 2014; Voitov and Mrsic-Flogel, 2022), or when combined with holographic light delivery - to manipulate single cells or test the effect of complex patterns of activity (Packer et al., 2015; Marshel et al., 2019).

1.1 - Different forms of attention

Attention is the prioritised representation of certain stimuli at the expense of the unattended ones. To understand the neural circuit basis of attention, it is important to recognise the similarities and distinctions between different forms of attention. One broad dichotomy is between bottom-up (exogeneous) attention, where the spotlight of attention is captured by a stimulus of sufficient salience, and top-down (endogenous) attention which is directed according to an internal rule or strategy. Here I will focus on endogenous attention, which can be divided into sub-types according to which sensory information is being highlighted: spatial attention, feature-based attention, and cross-modal attention. Research into these different forms of attention has yielded slightly different effects on neural circuits and necessitated the use of distinct behavioural tasks. It is an open question as to whether these forms of attention manifest through the same basic mechanisms (Reynolds and Heeger, 2009; Moore and Zirnsak, 2017).

1.1.1 – Spatial Attention

Spatial attention is perhaps the most well studied, it involves the direction of attention towards locations in the visual field. Macaques have proved effective for these investigations because they can be instructed to fixate on locations in visual space. However, recent experiments in mice have shown them capable of spatial attention, and different behavioural paradigms have been used increasing their potential as a model organism for investigating

this cognitive phenomenon (Wang and Krauzlis, 2018; McBride et al., 2019; Speed et al., 2020; Wang and Krauzlis, 2020; You and Mysore, 2020; Hu and Dan, 2022; Kanamori and Mrsic-Flogel, 2022). In one such task, at the start of each trial an auditory cue on the left or right of the mouse signalled the hemifield of visual space that should be attended to. Mice were then required to perform a go/no-go task using the visual stimuli presented on the cued side, whilst ignoring the conflicting visual stimuli on the opposite side (Hu and Dan, 2022). An alternative visual spatial attention task required the mice to attend to one of two locations on a screen for blocks of trials at a time, rather than the location to be attended being cued on a per trial basis. Mice performed a go/no-go task with the visual gratings presented in the attended location, whilst a neutral visual grating (which was never rewarded) was presented in the unattended location (Kanamori and Mrsic-Flogel, 2022).

Moreover, many of the behavioural and neural correlates of spatial attention are similar in primates and mice (Covered well in (Speed and Haider, 2021)). Behavioural performance increases with attention, with an improved hit rate for attended stimuli and improved perceptual sensitivity (d') (Reynolds et al., 2000; Cohen and Maunsell, 2009; Mitchell et al., 2009; Wang and Krauzlis, 2018; Luo and Maunsell, 2019; McBride et al., 2019; Ruff and Cohen, 2019; Speed et al., 2020; Wang and Krauzlis, 2020; You and Mysore, 2020). Subjects also detected stimuli more quickly with attention (Posner et al., 1980; Wang and Krauzlis, 2018; Speed et al., 2020), and were better at discriminating between different orientations (Cohen and Maunsell, 2009; Mitchell et al., 2009; Wang and Krauzlis, 2018, 2020; You and Mysore, 2020).

For both mice and primates, there is increased neural activity in response to the attended stimuli (Moran and Desimone, 1985; McAdams and Maunsell, 1999; Reynolds et al., 1999; Cohen and Maunsell, 2009; Sundberg et al., 2009; Ruff et al., 2020; Speed et al., 2020), noise correlations are decreased which increases the amount of information that can be encoded by the population (Cohen and Maunsell, 2009; Mitchell et al., 2009; Ruff and Cohen, 2019; Speed et al., 2020), and there is a subtractive shift in contrast response curves such that the responses to low-contrast stimuli are enhanced more by attention than for high contrast stimuli (Reynolds et al., 2000, 2000; Sundberg et al., 2009; Speed et al., 2020), among other similar neural changes.

1.1.2 – Feature-based attention

Attention can also be directed towards visual features, without regard for their spatial location. Tasks investigating this form of attention might require the subject to search for a target with a particular feature, such as shape or colour, whilst ignoring the other features.

Neural correlates of feature-based attention have been found in various areas of the monkey visual system (Chelazzi et al., 1993; Bichot and Schall, 1999; Sheinberg and Logothetis, 2001; Bichot et al., 2005, 2015). As an example, in middle temporal visual area (MT) where neurons are tuned for visual motion, focusing attention on a direction of movement enhanced the responses of neurons that were tuned for the same direction and suppressed neurons with opposed tuning. This effect occurs even though the stimuli being enhanced are far apart from one another in the visual field (Treue and Martínez-Trujillo, 1999). Likewise, human psychophysical experiments find that feature-based attention enhances behavioural performance throughout the visual field (Rossi and Paradiso, 1995; Sàenz et al., 2003) (Although other explanations have been put forward, see (Theeuwes, 2013)).

Many of the changes in neural activity with feature-based attention have been found to be similar to spatial attention; potentially because they act through the same mechanisms, with spatial location being one feature that can be selected for (Treue and Martínez-Trujillo, 1999; Maunsell and Treue, 2006; Cohen and Maunsell, 2011). It is also possible that although the mechanisms or effects of different types of attention might be similar, the neurons that implement the attentional modulations could be different.

1.1.3 - Cross-modal attention

Attention can also be transferred between sensory modalities, rather than between stimulus features or locations, this is cross-modal attention. As might be expected given that we have multiple senses, there are several distinct behavioural paradigms used to investigate this form of attention. One such task used in monkeys and humans involves participants being presented with rapid interleaved streams of visual and auditory stimuli (Hackley et al., 1990; Alho et al., 1992; Woods et al., 1992; Mehta et al., 2000a). Based on a cue at the start of a trial the subject is required to alternate between attending to either the visual or auditory

stimuli. For each modality the stream of stimuli forms an “oddball” target detection task, with one high-probability stimulus and a second low-probability “oddball” stimulus. The subject must selectively respond to only the infrequently presented “oddball” stimulus in the attended modality.

Cross-modal attention switching tasks have also been developed for mice, one of which is the task I will be using in this thesis and which I will discuss in detail in chapter 2 (Poort et al., 2015, 2022). A different example of a mouse cross modality switching task is employed by the Halassa lab (Wimmer et al., 2015; Schmitt et al., 2017; Rikhye et al., 2018). In that task, freely moving mice choose to respond with a left or right nose-poke based on simultaneously presented visual and auditory stimuli. The direction indicated by the visual and auditory stimuli may be in conflict, and the mice are informed about which modality should be attended to based on an auditory cue provided upon initiating a trial.

Some of the changes in neural activity associated with transferring attention across sensory modalities are similar to the pattern for the other forms of attention I just described (Mehta et al., 2000a; Maunsell, 2015; Poort et al., 2022). The mechanisms that mediate the modulations of visual attention could be the same for other modalities. Indeed, visual attention could be part of a mechanism that operates across all of cortex, an area such as the PFC may hold information about the current context and bias activity in sensory regions to coordinate attention across modalities (Miller and Cohen, 2001).

1.2 - How might attention differ between the primate and the mouse?

There are broad similarities between the primate and rodent brains (Ventura-Antunes et al., 2013; Beauchamp et al., 2022), and although similarities have been found between mouse and primate neural and behavioural correlates of attention, there are some differences in the neural substrate of the two groups that may alter the mechanisms employed or potentially limit comparisons (Speed and Haider, 2021).

One important difference is that primates make saccadic eye movements, sampling the world by bringing it in to focus on the fovea, whilst mice lack a fovea. However, recent work has found that there is a region of mouse visual cortex which has heightened spatial resolution, the “focea” (van Beest et al., 2021). This region is not aligned with the direction of gaze like

the primate fovea, but instead corresponds to a region of space in front of, and slightly above, the mouse. In freely moving mice, compensatory head movements maintain the location of the focea within the visual field, potentially because during forward motion it points toward the "focus of expansion" the point at which optic flow is absent and where the optic flow seems to emanate from.

If mice manipulate this region of increased spatial resolution for visual tasks other than locomotion, it does not appear to be through eye movements. Saccade like eye movements have been observed in head-fixed mice, but head and eye tracking reveals that mouse eye movements are associated with vestibular mechanisms that stabilise the visual field during head movements (Meyer et al., 2020). Additionally, a study which tracked the eye movements of mice as they hunted crickets found that visual tracking of their prey was achieved through head movements rather than independent targeted eye movements (Michaiel et al., 2020). Whether the direction of the focea towards points of interest with head-movement is analogous to overt attention in primates, or whether visual attention in mice is more agnostic to orienting movements and more like covert attention in primates remains to be seen.

In mice, the lack of a detailed central visual point and the use of head and body movements to sample the environment may cause substantial differences in the mechanisms used to modify visual information. For example, it is possible that this explains why locomotion modulates visual activity in head-fixed mice (Niell and Stryker, 2010; Polack et al., 2013; Fu et al., 2014; Pakan et al., 2016), while eye-movements do the same for primates (Morris and Krekelberg, 2019; Speed and Haider, 2021).

A second difference is the organisation within and between brain regions. Rodents lack the orientation columns found in primate V1, mouse V1 may display more sensorimotor integration than in the primate (Froudarakis et al., 2019), and mouse V1 recieves more cross modal input from other primary sensory cortices than in the primate (Clavagnier et al., 2004; Charbonneau et al., 2012). This is potentially indicative of the evolutionary parcellation of the primate brain into more distinct areas with specialised functionality. These differences may change the way that top-down attentionally modulation targets these areas.

Thirdly, the size of primate and mouse brains also imposes differences simply because of the time required to communicate between areas. Top-down projections in the mouse modulate

sensory signals at very early time-points, while modulations in monkeys can take hundreds of milliseconds to develop (Gregoriou et al., 2014; Liu et al., 2021).

Finally, the difference in cognitive ability of monkeys allows task designs to control for behavioural effects that may not be possible in mice. The disambiguation of the results from mouse behavioural tasks can therefore be less clear (Speed and Haider, 2021).

1.3 - Attentional modulations and higher visual areas

To understand the neural circuits underlying attentional modulation, it is important to first identify the regions in the mouse visual cortex which demonstrate substantial attentional modulation. Although the organisation of visual processing and attentional modulation across cortical regions is well characterised in primates, it is less understood in the rodent visual cortex.

1.3.1 – Primate visual cortex is organised into hierarchical parallel processing streams

Visual information flows from the retina to the lateral geniculate nucleus of the thalamus to primary visual cortex and into higher visual cortical areas, the primate visual system has a hierarchical organisation (Felleman and Van Essen, 1991). Areas higher up in the chain represent progressively more complex combinations of features, becoming invariant to properties such as spatial location or size.

Broadly, primate extrastriate visual cortex has been divided into two anatomically and functionally separate pathways (Mishkin et al., 1983). The dorsal stream involved in visually guided action and spatial perception (Kravitz et al., 2011), and the ventral stream involved in object recognition (Mishkin et al., 1983). However, not all areas within a stream are necessarily involved at all times and the processing of different functional properties can involve the activity of the same areas, meaning that the specific functional network active within a stream may vary from moment to moment according to context (Galletti and Fattori, 2018).

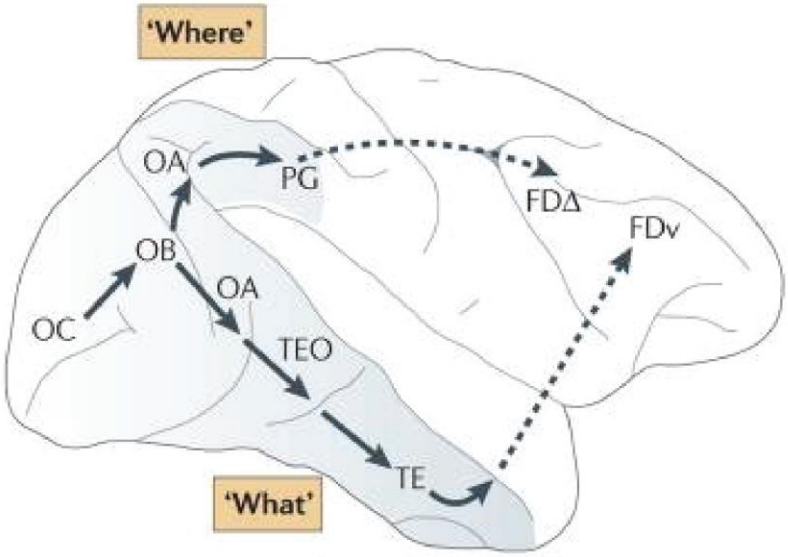

Figure 1.1: Dorsal and ventral streams of macaque visual processing.

The first version (Mishkin et al., 1983) of the dorsal and ventral streams of visual processing in the macaque. The ventral stream stretches from the primary visual cortex (area OC) to area TE in the inferior temporal cortex, with another projection from area TE to ventral prefrontal region FDv. The dorsal stream also starts in the primary visual cortex and extends to area PG in the inferior parietal lobule, with another projection from area PG to dorsolateral prefrontal region FDΔ. Through lesion studies in monkeys the ventral stream was determined to mediate object recognition ("What") and the dorsal stream was found to mediate spatial vision ("Where"). However, now the dorsal stream may be more accurately described as supporting visually guided actions, a "How" pathway. Reproduced from (Kravitz et al., 2011) PMC author manuscript.

1.3.2 - Mouse visual cortex is also organised into hierarchical parallel processing streams

Mouse cortex also contains a network of higher visual areas (HVA), capable of supporting complex visual behaviours (Glickfeld and Olsen, 2017), although primate cortex is parcellated into more distinct modular areas than mouse cortex (Laramée and Boire, 2015). Successively more detailed maps of mouse visual cortex have been made using a range of techniques (Glickfeld and Olsen, 2017): cytoarchitecture (Caviness, 1975), electrophysiology (Wagor et al., 1980), anterograde tracing (Olavarria and Montero, 1989; Wang and Burkhalter, 2007), and intrinsic imaging (Garrett et al., 2014).

Most recently mesoscale calcium imaging was used to make a retinotopic map of mouse visual cortex (Zhuang et al., 2017). Imaging experiments have the advantage of identifying all visually responsive areas, in this case defining the boundaries between regions as the points when the sign of the retinotopic field flips (For the specific method (Garrett et al., 2014; Zhuang et

al., 2017)). However, the areas identified may be dependent on the visual stimuli presented, and the HVAs mapped by different techniques do not always align. For the purposes of this thesis, I am using the list of areas proposed as a consensus by Glickfield and Olsen (2017): lateromedial (LM), anterolateral (AL), rostrolateral (RL), anterior (A), anteromedial (AM), posteromedial (PM), lateraintermediate (LI), posterior (P), and postrhinal (POR). I have additionally included the medial (M) area which has not been well defined in the mouse, but was found through intrinsic and calcium imaging, as well as in the rat (Olavarria and Montero, 1984).

Mouse visual cortex is also hierarchically organised, at least for V1 and 5 of the higher visual areas mentioned above (Siegle et al., 2021). However, as is expected given that mice rely less on vision, have poorer visual acuity and fewer visual cortical areas than primates, there are fewer levels to the hierarchy (Coogan and Burkhalter, 1993; D'Souza et al., 2020).

Based on their functional properties and connectivity (Andermann et al., 2011; Marshel et al., 2011; Roth et al., 2012), mouse higher visual areas have been split into parallel processing streams. Areas AM, PM, M, and AL form the dorsal stream and areas LM, LI, P, and POR form the ventral stream (Wang et al., 2011, 2012; Wang and Burkhalter, 2013; Smith et al., 2017), although there is evidence a more nuanced arrangement might be more accurate (Han et al., 2022).

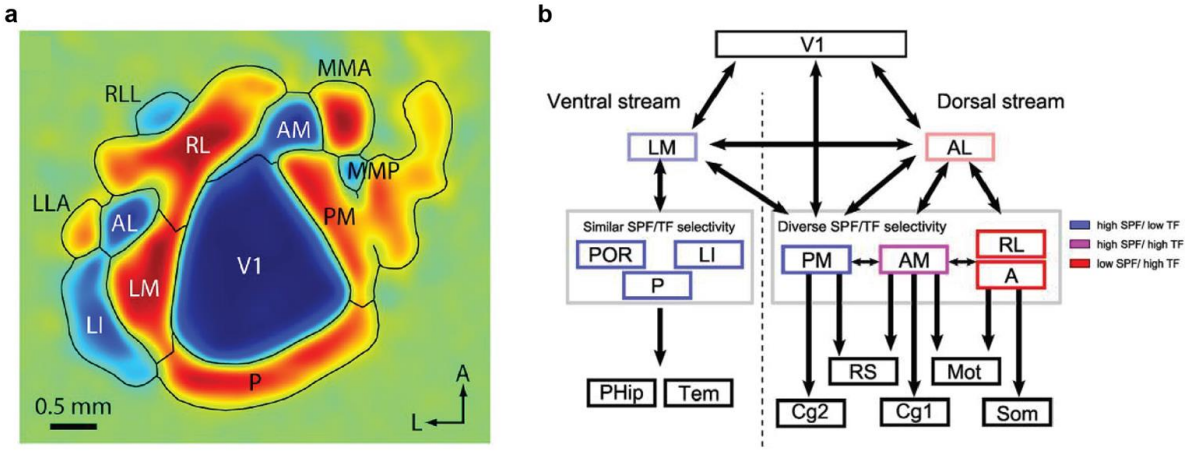

Figure 1.2: Mice have hierarchically organised visual areas arranged into dorsal and ventral streams.

a) The average of field sign maps taken from retinotopic mapping in Emx1-Ai96 and Emx1-Ai93 mice, with area labels and borders. Reproduced from (Zhuang et al., 2017). **b)** Diagram constructed from the anatomical and function data on mouse higher visual areas (HVA). The arrangement of the visual streams is based on (Wang et

al., 2012). The putative ventral stream contains four lateral HVAs (LM, LI, POR, and P) (Wang et al., 2012) that share similar spatiotemporal selectivity. Area LM has been proposed as a gateway to the ventral stream (Wang et al., 2011). Areas LI, P, and POR project to parahippocampal (PHip) and temporal cortices (Tem) (Wang et al., 2012). The putative dorsal stream contains five anterior/medial HVAs (AL, PM, AM, RL, and A) (Wang et al., 2012). Like area LM for the ventral stream, area AL has been proposed as a gateway to the dorsal stream (Wang et al., 2011). The anatomical targets (Wang et al., 2012) and spatiotemporal selectivity of the four HVAs downstream of AL is not uniform and Murakami et al divided them into three groups. Reproduced from (Murakami et al., 2017).

1.3.3 - Attentional modulations are stronger higher up the primate visual hierarchy

In primates top-down attention modulates visual responses as early as the dorsal lateral geniculate nucleus (dLGN) with the intensity of the attentional modulation increasing up the visual hierarchy (Mehta et al., 2000a, 2000b; Cook and Maunsell, 2002; O'Connor et al., 2002; Maunsell and Treue, 2006; Montijn et al., 2012; Klein et al., 2014; Martin et al., 2019). These results appear to hold true for spatial, feature-based and cross-modal attention. Based on the latency of the modulation, attention may start in higher areas and backpropagate down the visual hierarchy (Buffalo et al., 2010). The stimuli used to measure attention may affect the intensity of modulation and the earliest detectable area, for this reason some of the studies investigating this have used simple diffuse light (Mehta et al., 2000a). As far as I am aware no studies have mapped the pattern of attentional modulations across the mouse visual hierarchy. Here, I recorded from 7 visual cortical areas (including V1) whilst mice performed an attention switching task. Of the recorded areas I found that only V1, AM and PM were significantly attentionally modulated, and that V1 was the most strongly affected. This is an inversion of the pattern that would be expected from primate results.

1.4 - Where is the source of the top-down signal?

Miller and Cohen (2001) proposed a model which addresses where the top-down signals that induce attentional modulations might be generated and how attentional modulations play a part in the end goal of altering behaviour. The activity of frontal areas like the prefrontal cortex (PFC) has been found to reflect different behavioural task rules through distinct patterns of network activity, in both primates and rodents (Rich and Shapiro, 2009; Durstewitz et al., 2010; Karlsson et al., 2012). The PFC could then project onto sensory cortex, supplying a

contextual signal that biases perception. The motor areas that receive information from sensory cortex may then produce a different behaviour from that which would have been elicited had the top-down contextual signal been absent (Miller and Cohen, 2001).

In support of this model, the frontal eye field is an oculomotor area within primate prefrontal cortex. In spatial attention tasks, direct stimulation of the frontal eye field elicits attention-like effects in visual cortical areas (Moore and Fallah, 2001; Moore and Armstrong, 2003). Furthermore, there are reciprocal connections between anterior cingulate cortex (ACC) and V1 in mice (Zhang et al., 2016; Leinweber et al., 2017), and optogenetic studies have given evidence for a causal role of long-range projections from the PFC in controlling various behaviours (Warden et al., 2012; Challis et al., 2014; Lee et al., 2014a; Otis et al., 2017), including visual discrimination (Zhang et al., 2014). Countering the importance of the PFC in attention, unihemispheric removal of the entire lateral PFC (including the FEF) reduced attentional modulation in V4, but did not abolish it (Gregoriou et al., 2014), suggesting that while PFC is involved it does not do the job alone.

Activity in sensory cortex can drive behaviour. Whilst rats performed a frequency discrimination task, optogenetic manipulation of neurons projecting from auditory cortex to striatum predictably biased the rat's decisions (Znamenskiy and Zador, 2013). When the strength of corticostriatal synapses was tracked over the course of learning it matched the association between rewarded direction and tone (Xiong et al., 2015). Also, in mice, V1 neurons directly innervate a section of dorsomedial striatum (Khibnik et al., 2014). These results might outline a general mechanism through which sensory representations can influence motor actions.

Attentional modulations in primary visual cortex might also come from another region, even if PFC is the original source of the signal. As discussed earlier, in primates attention effects are stronger higher up in the hierarchy. The top-down input could be generated or applied first there and then be passed down to V1 through feedback connections (Buffalo et al., 2010). These higher visual areas may not necessarily be cortical, in mice the lateral posterior nucleus (LP) is a higher thalamic nucleus, sits further up the visual hierarchy than V1 (Siegle et al., 2021), and can enhance stimulus selectivity in V1 (Fang et al., 2020). LP is a homolog of the visual pulvinar in primates, the silencing of which attenuates attentional effects in area V4

(Zhou et al., 2016). Another possibility is that the attentional modulation in V1 could be sourced from the midbrain, in a mouse visual spatial attention task the motor layers of superior colliculus were found to be attentionally modulated earlier than V1 (Hu and Dan, 2022).

Alternatively, the attentional modulation in visual cortex might instead be inherited, with the top-down signal arriving first in the lateral geniculate nucleus (LGN) - allowing it to act as more than a relay for retinal information (Casagrande et al., 2005). In further support for the thalamus as key site of attentional modulation, in mice the PFC biases activity in the visual thalamic reticular nucleus in a cross-modality attention switching task (Wimmer et al., 2015). The reticular nucleus does not project to cortex and instead regulates thalamic activity.

The exact combination of areas involved may depend upon the stimuli attention is amplifying. For example, if attention is focused on the colour of an object, it may be directed towards a cortical visual area that better represents that feature. In favour of this, some of the effects observed with spatial attention depend on the size of the neurons receptive field, which increases up the visual hierarchy (Moran and Desimone, 1985). Changes in the strength of attentional modulation may therefore follow the receptive field size of the modulated area.

1.5 - The heterogeneity of cortical inhibition

Inhibition exerts a powerful influence over the way that cortical activity evolves. Although they represent a minority of neurons in cortex, the connections of inhibitory interneurons spread wide and can sculpt the activity of the entire neuronal population (Kepecs and Fishell, 2014; Cardin, 2018). Control of inhibitory interneuron activity could be a key mechanism through which top-down attention signals modulate stimulus evoked activity.

The cortex contains a rich zoo of different types and subtypes of GABAergic inhibitory interneurons with differences in morphology, connectivity, molecular expression and intrinsic firing properties (Rudy et al., 2011; Kepecs and Fishell, 2014; Harris et al., 2018). However, broadly three molecularly defined interneuron subtypes make up almost all neocortical GABAergic interneurons, separated by whether they express the Ca2+-binding protein parvalbumin (PV), the neuropeptide somatostatin (SOM), or the ionotropic serotonin receptor 5HT3a (5HT3aR) (Rudy et al., 2011).

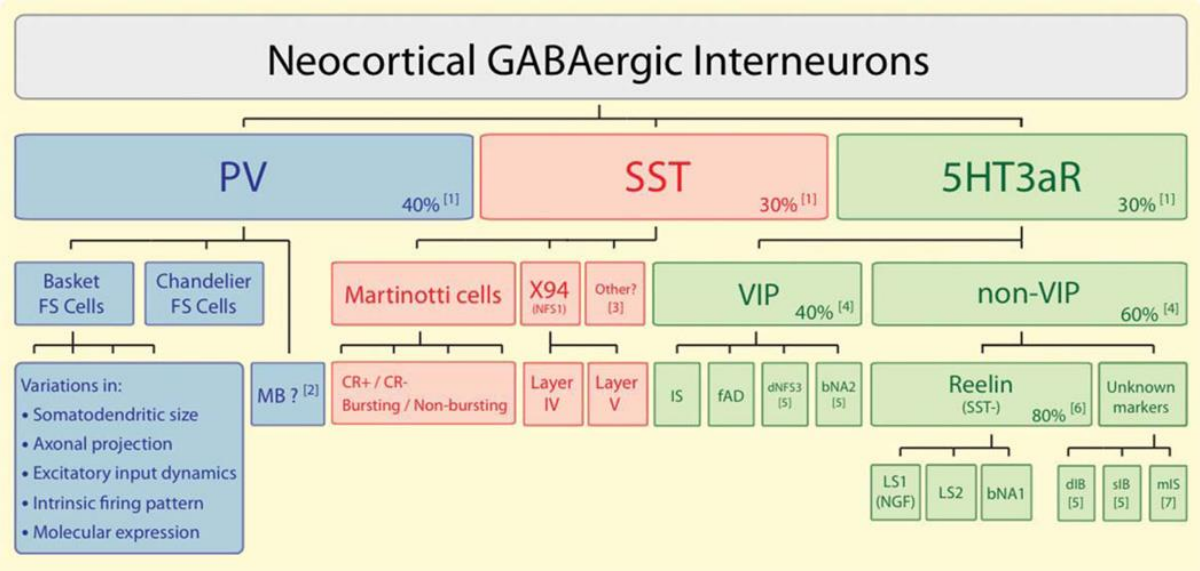

Figure 1.3: Classes of neocortical inhibitory interneurons.

Almost all neocortical GABAergic neurons can be grouped according to their expression of either parvalbumin (PV), somatostatin (SST here, SOM in the rest of the text), or the ionotropic serotonin receptor 5HT3a (5HT3aR). Each group is made up of several subgroups, and each subgroup can be divided into several functionally distinct classes of interneurons. Many PV interneurons display a fast-spiking (FS) firing pattern. Two anatomically separable subgroups of FS neurons exist, basket cells, and chandelier cells. Variation in the properties of basket cells has been observed. A third potential subgroup of non-FS, PV-expressing neurons are MB (multipolar bursting) neurons. Among SST interneurons, Martinotti cells are the majority and the most well characterised. Subdivisions within this group exist, see (Rudy et al., 2011) for details. The other major subgroup of SST are neurons identified in the X94 mouse line, which have abundant axonal projections to layer IV. The X94 subgroup is present in both layer IV and V. A smaller proportion of SST interneurons have been identified that don't belong to either subgroup - "other" (McGarry et al., 2010). The subgroups of 5HT3aR-expressing interneurons are less clear but can be broadly separated according to whether or not they express the neuropeptide VIP. The distinct interneuron classes in each of these subgroups have been incompletely described. However, some classes have been frequently observed. For VIP interneurons these are: bipolar or bitufted neurons with a "fast adapting" (fAD) or an irregular spiking (IS) firing pattern. For non-VIP interneurons these are: neurogliaform (NGF) cells with a late spiking firing pattern (LS1), and multipolar neurons with an LS2 firing pattern. See (Rudy et al., 2011) for the numbered notes in the figure. Reproduced from (Rudy et al., 2011) PMC author manuscript.

1.5.1 - Parvalbumin expressing interneurons

PV expressing interneurons constitute approximately 40% of neocortical interneurons and have been historically identifiable in electrophysiological recordings thanks to their distinctive

fast and narrow spiking (Kawaguchi et al., 1987; Ascoli et al., 2008). Two major subclasses of PV interneurons have been documented. Basket cells, which are multipolar and synapse at the soma and the proximal dendrite of their target cells, and chandelier cells which target the axon initial segment and are less well understood (Kawaguchi and Kubota, 1997; Ascoli et al., 2008). There are likely subtypes within these groups particularly among basket cells (Rudy et al., 2011). PV interneurons span layers II to VI of neocortex but are most predominantly found in layer IV (Rudy et al., 2011). Basket cells perform potent, fast and temporally precise inhibition of their target cells, and are probably crucial components in maintaining cortical excitation/inhibition balance (Hasenstaub et al., 2005; Haider and McCormick, 2009).

1.5.2 - Somatostatin expressing interneurons

Approximately 30% of GABAergic neocortical interneurons express SOM. Expression of SOM has often been associated with Martinotti cells (McGarry et al., 2010; Rudy et al., 2011). Martinotti cells are present throughout layers II-VI, but are most numerous in layer V. They inhibit the apical and basal dendrites of pyramidal neurons with ascending axons that arborize and spread out horizontally in layer I, allowing them to exert inhibitory control over the apical tufts of pyramidal neurons (Kawaguchi and Kubota, 1997; Wang et al., 2004). Excitatory inputs onto Martinotti cells are often strongly facilitating, unlike PV interneurons, meaning Martinotti cells may be preferentially active when the network activity is high and repetitive activity in a single pyramidal neuron may drive them to fire (Kapfer et al., 2007; Silberberg and Markram, 2007). Other subtypes of SOM interneurons have also been observed, which vary in the overlap of their properties with Martinotti cells (Ma et al., 2006; McGarry et al., 2010).

1.5.3 - 5HT3aR expressing interneurons

Finally, the remaining approximately 30% of interneurons express 5HT3aR, this group is particularly heterogeneous (Rudy et al., 2011) and includes within it all of the neurons that express vasoactive intestinal peptide (VIP) - which in primary somatosensory cortex was estimated to be approximately 40% of 5HT3aR interneurons (Lee et al., 2010). VIP expression has been shown to be non-overlapping with PV and SOM expression (Kawaguchi and Kubota, 1997; Xu et al., 2010).

VIP expressing interneurons display a heterogeneity of transcriptomic, physiological and morphological features; including neurons with bipolar, bitufted and multipolar structures (Harris et al., 2018; Hodge et al., 2019; Prönneke et al., 2020). In visual cortex, the somata of VIP interneurons are primarily in layer II/III, their axons are distributed across layers I/II, IV and VI, and their dendrites are spread across layers I and II (Hajós et al., 1988; Zilles et al., 1991; Ji et al., 2016). Modulation of this (5HT3aR/VIP) group of neurons by serotonin and acetylcholine suggests they may be involved in changing brain activity during certain states and behavioural contexts (Lee et al., 2010; Fu et al., 2014).

1.5.4 - Connectivity of molecularly identified interneurons

The development of interneuron-specific transgenic mouse lines has opened up significant opportunities for interrogating the cortical circuit. The molecularly defined groups of GABAergic interneurons just discussed inhibit more than excitatory pyramidal neurons, making specific connections with one another to form an inhibitory network (Pfeffer et al., 2013; Campagnola et al., 2022). Pfeffer et al., used transgenic mouse lines to express Cre in molecularly defined interneurons, and in combination with optogenetic stimulation, electrophysiological recordings and single-cell molecular profiling they were able to identify the pattern of connections between PV, SOM and VIP expressing interneurons. They expressed ChR2 in either PV, SOM or VIP interneurons in mouse visual cortex and by comparing the effects of photostimulation on neighbouring pyramidal neurons and GABAergic interneurons, they investigated the postsynaptic preferences of interneuron types. In cortical layers II/III and V they found that PV interneurons primarily inhibit one another, avoiding other interneurons. In contrast, SOM interneurons avoid inhibiting each other (but see (Campagnola et al., 2022)), but contact all other interneurons. Finally, VIP interneurons preferentially inhibit SOM interneurons, avoiding pyramidal cells, allowing them to exert disinhibitory control over pyramidal neurons through the inhibition of SOM (Pi et al., 2013).

In support of this, VIP and SOM interneurons are contacted by distinct populations of pyramidal neurons, and an increase in activity of a small number of VIP or SOM interneurons can recruit other members of the same type (Karnani et al., 2016b). Additionally, VIP interneurons in V1 have been found to display highly synchronised behaviour, similar to PV

interneurons (Knoblich et al., 2019). This specialisation of interneurons allows individual cells to fulfil distinct roles in cortical processing (Kepecs and Fishell, 2014).

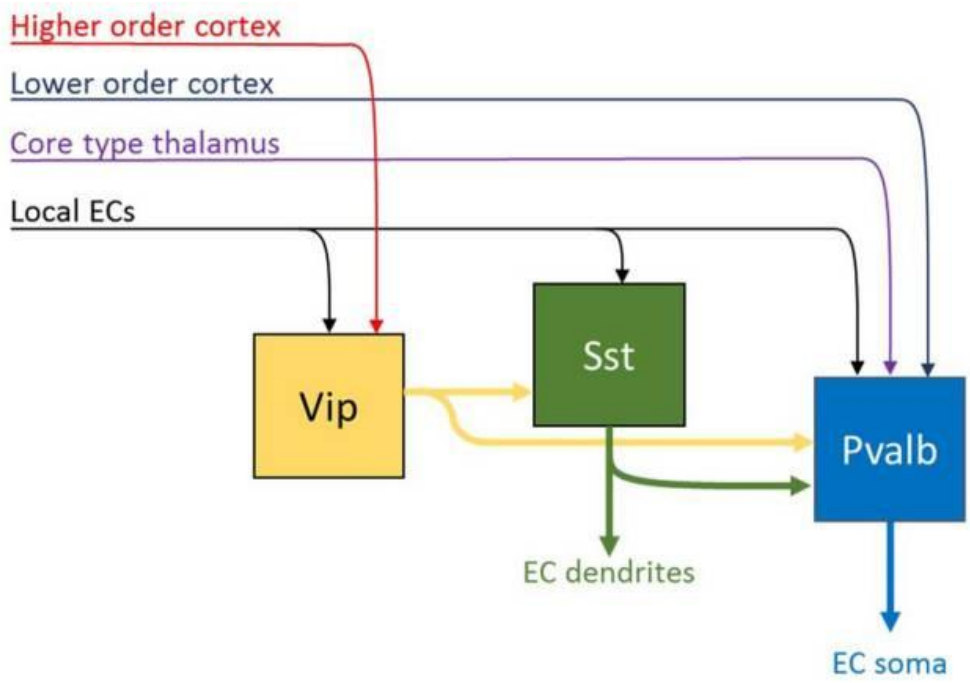

Figure 1.4: Connections between and inputs to the three main inhibitory neuron classes.

VIP interneurons inhibit mainly other interneurons and receive input from higher cortical areas. SOM interneurons (here SST) inhibit PV (here Pvalb) interneurons and the dendrites of excitatory cells (EC). PV interneurons strongly inhibit excitatory neurons at the soma and receive feedforward input from lower cortical areas and the thalamus. All interneurons receive input from local excitatory cells. Reproduced from (Harris and Shepherd, 2015) PMC author manuscript.

1.5.5 – Differences in inhibition between mice and humans

How homologous is the inhibitory circuitry found in mice and humans? Loomba et al. (2022) used three-dimensional electron microscopy data to compare synaptic connectivity between mice, macaques and humans. In line with recent transcriptomic data (Bakken et al., 2021) they found an approximately 2.5-fold increase in the proportion of interneurons in human compared to mouse cortex. However, this expansion in the number of interneurons was not accompanied by a corresponding shift in the excitation-inhibition balance, but rather an increase in the complexity of the interneuron-to-interneuron network of connections.

A core set of neocortical interneuron types appears to be maintained across mice and primates. The expression of the same genes (SOM, PV, VIP and LAMP5) in non-overlapping

subsets of neocortical interneurons was found to account for almost all neocortical interneurons in these species (Kreinen et al., 2020). However, it remains to be seen whether this increase in interneuron network complexity from mouse to human is due to an amplification of existing interneuron subtypes or the presence of new subtypes, but in either situation it will likely limit direct translation of findings in mice to humans. More likely, understanding of neural computational principles and broader mechanisms will be transferable, and the comprehension of the behaviour of neural networks gained from studying mice will lead to more rapid progress in understanding the aspects of human networks which are dissimilar from the mouse.

1.6 - Division of cortical labour between interneuron subtypes

A range of types of inhibitory cortical interneurons means a greater number of tools available to the cortical circuit and therefore more computational power (Silver, 2010; Cardin, 2018). Significant among the computational functions of interneurons are the arithmetic operations they can perform on encoded signals and their effect on the timing of neural activity.

1.6.1 - Interneurons can perform distinct computations

Arithmetic operations allow neurons, and the environmental and behavioural states that affect them, to transform the way that information is processed. These elementary operations can be summarised in the way that they effect the input-output (I/O) relationship of the neuron (Silver, 2010; Ferguson and Cardin, 2020). Additive and subtractive effects maintain the shape of the neurons input-output relationship but shift the curve as a whole, such as a change in a neurons basal firing rate. Multiplicative or divisive effects alter the slope of a neurons input-output relationship, a change in neuronal gain (Salinas and Thier, 2000), altering the sensitivity of a neuron to its inputs without changing the selectivity of the neuron for those inputs (Salinas and Sejinowski, 2001).

Pyramidal neurons have complex dendritic arbors which form many interconnected electrical compartments. The arithmetic operation performed by shunting inhibition may depend on its location and intensity on the postsynaptic cell. If the inhibition is strong and close to the soma it may have a divisive effect, but if it is small and distributed across dendrites it may be

subtractive (Blomfield, 1974; Vu and Krasne, 1992; Holt and Koch, 1997; Silver, 2010). Given that molecularly defined interneuron subtypes systematically target distinct portions of pyramidal neurons they have been proposed to perform different arithmetic operations.

Based on their connections alone we would expect PV interneurons to have a divisive effect and SOM interneurons to have a subtractive one. Wilson et al. optogenetically activated PV or SOM interneurons while recording the orientation tuning of other neurons (Wilson et al., 2012). As expected, they found that PV interneurons divided responses, preserving stimulus selectivity, whereas SOM interneurons had a subtractive effect that sharpened selectivity. Similarly, Attalah et al. optogenetically excited or inhibited the activity of PV interneurons and recorded a primarily divisive effect on the activity of pyramidal neurons (Atallah et al., 2012). However, Lee et al. found the opposite, with activation of PV interneurons having a subtractive effect, sharpening stimulus selectivity of V1 neurons and improving perceptual discrimination. Whereas the same manipulations on SOM interneurons were primarily divisive (Lee et al., 2012).

This contradiction may be resolved when considering the strength of the activation of PV interneurons, with more potent PV activation sharpening the tuning of pyramidal neurons. Tuning becomes sharper as more of the inhibited neurons responses are forced to its minimum activity - an ‘iceberg’ effect (Atallah et al., 2014; El-Boustani et al., 2014; Lee et al., 2014b). The differing effects of SOM excitation are harder to reconcile, with the effect appearing to rest on the duration of SOM photoactivation. Tuning curves were sharpened when photoactivation was applied for the first second of visual stimulus presentation, but not when applied for the full 4s of the visual stimulus (Lee et al., 2014b). El-Boustani et al. showed that this difference in arithmetic effects could be due to the relative timing of the activation of SOM interneurons and pyramidal neurons, with co-activation being divisive (El-Boustani and Sur, 2014; El-Boustani et al., 2014).

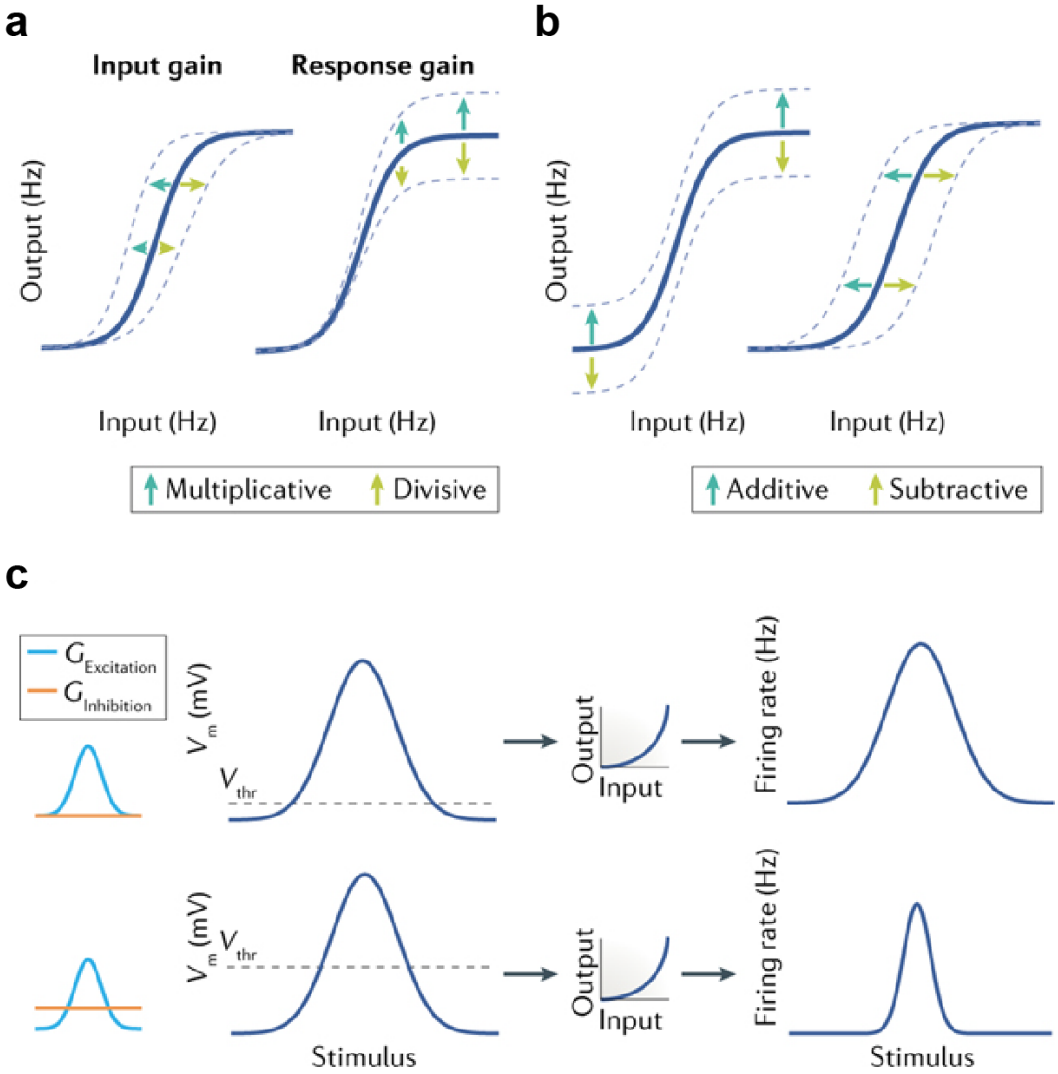

Figure 1.5:The effect of arithmetic operations on a neurons input-output relationship.

a) Multiplicative and divisive modulations change the slope of a neurons input-output (I/O) function without changing the minimum current needed to produce an action potential. This alters neural gain, changing the sensitivity of the neuron without changing selectivity. If the modulation increases gain it is multiplicative, if it decreases gain it is divisive. These modulations can apply to either the input or the output. **b)** Additive and subtractive modulations move the whole curve without changing its slope. These transformations retain the sensitivity of a neuron to its inputs but alter its selectivity by changing the input required for the neuron to reach its response threshold. Like the modulations in **a** additive and subtractive modulations can apply to the input or output of a neuron. **c)** Subtractive effects can be produced by divisive modulations. A change in spike threshold (V_{thr}) can sharpen a neurons tuning curve through an "iceberg" effect, by changing the relationship between a neurons firing-rate responses and its underlying subthreshold membrane potential (V_m). These effects can be produced by inhibitory synaptic input. Inhibitory and excitatory synaptic input conductance are $G_{inhibition}$ and $G_{excitation}$ respectively. Reproduced from (Ferguson and Cardin, 2020) PMC author manuscript.

1.6.2 - Interneuron subtypes may not be paired directly with one arithmetic operation

Manipulation of these cell types doesn't happen in isolation; inhibitory interneurons are embedded in a recurrently connected network. SOM interneurons inhibit PV interneurons, meaning that in addition to inhibiting the apical dendrites of pyramidal neurons, SOM activation can reduce inhibition at the soma (Cottam et al., 2013; Pfeffer et al., 2013). Optogenetic activation experiments are therefore difficult to interpret. The optogenetic activation of either SOM or PV interneurons can produce a combination of subtractive and divisive effects. These results can be explained by a network model which can turn subtractive inhibition of neurons into divisive inhibition of the network and vice versa, depending on the strength of suppression and the spiking threshold of the modelled neuron (Seybold et al., 2015). Additionally, results from Philips and Hasentaub demonstrated that bidirectional optogenetic manipulations can have conflicting effects. Their inhibition of SOM interneurons produced primarily multiplicative changes and inhibition of PV produced primarily additive ones on the tone-evoked responses of auditory cortical neurons. Meanwhile, activation of SOM and PV had similar effects on frequency tuning curves, with both producing matched combinations of subtraction and division. They created a model of a densely connected network, which took into account not just the effects of direct inhibition, but also the effect of the network wide alteration of a neuron's inputs. Within this model, even relatively small changes in spontaneous activity alters whether the effects of tonic activation or inactivation of interneuron populations are consistent or asymmetric (Phillips and Hasenstaub, 2016).

1.6.3 - Arithmetic operations in attention

Documented changes in neural responses with attention have aligned with different arithmetic operations. In some cases, attention increases neural gain multiplicatively, scaling neural activity (McAdams and Maunsell, 1999; Treue and Martínez-Trujillo, 1999). In others there was a sharpening of tuning with attention, either of individual neurons (Spitzer et al., 1988) or at the level of the population as a whole (Martinez-Trujillo and Treue, 2004), more consistent with subtractive changes.

Various models have been used to try to explain the changes to a neurons tuning curve with attention. Among them, the normalisation model neatly captures both the multiplicative

scaling and sharpening of neurons tuning curves across different attention paradigms (Reynolds and Heeger, 2009). Normalisation involves neurons responses being divided by a common factor usually including the summed activity of a population of neurons. Crucially, these models do not identify what the circuits or neural mechanisms might be that produce these changes. There are multiple methods through which normalisation could be implemented, and the actions of the inhibitory interneurons described above are among them (Carandini and Heeger, 2012).

Mechanistic models have also been described, which define ways that phenomenological models such as the normalisation model could be implemented in the circuit. A model which used a recurrently connected excitatory-inhibitory network managed to capture both the decrease in noise correlations and increase in firing rate seen with attention. Additionally, this model predicted that attentional modulation would favour inhibitory interneurons and was consistent with top-down cholinergic recruitment of VIP interneurons playing a central role in attention (Kanashiro et al., 2017). These results further emphasise interneurons as candidate mediators of attentional modulations. Experiments investigating the activity and roles of different interneuron subtypes during attention tasks will help to constrain and refine future mechanistic models.

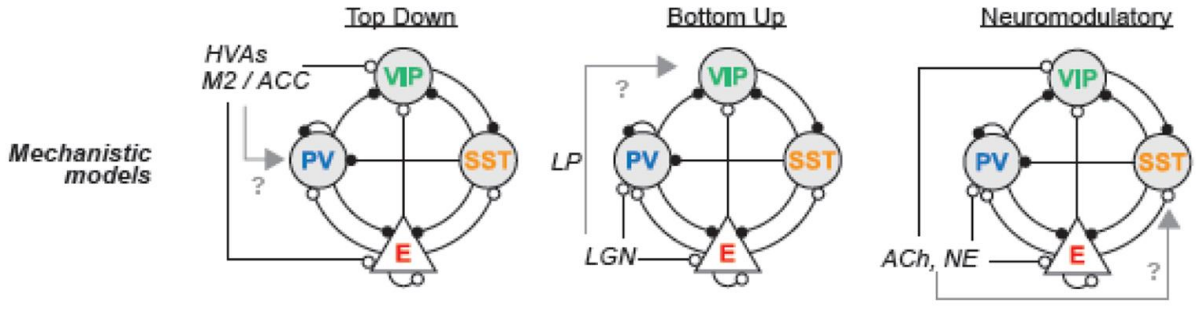

Figure 1.6: Mechanistic models for visual attention.

Mechanistic models try to provide a plausible biophysical implementation of attentional modulation. These models can better describe the effects on the local circuit and the sources of attentional modulation, if the roles of excitatory (E) and major subtypes of inhibitory neurons (PV, parvalbumin; VIP, vasoactive intestinal peptide; SST, somatostatin) in the cortex are better defined. As described in section 1.4, in the mouse, potential sources of attentional signals include: top-down inputs from higher visual areas (HVAs) or secondary motor/anterior cingulate cortex (M2/ACC) (Zhang et al., 2014; Leinweber et al., 2017), and bottom-up inputs from lateral geniculate nucleus (LGN) or lateral posterior nucleus (LP) (Roth et al., 2016; Speed et al., 2020). Not discussed in

1.6 but mentioned in 1.8 are neuromodulatory inputs including acetylcholine (ACh) and noradrenaline (NE). Open circles are excitatory; closed circles are inhibitory. Reproduced from (Speed and Haider, 2021) PMC author manuscript.

1.6.4 - Interneurons can regulate the timing of activity in the neural network

The properties of inhibitory interneurons influence their effect on temporal patterns of cortical activity, meaning different populations of interneurons may promote different rhythms of activity in the cortex (Cardin, 2018). In neocortex, feedforward inputs first recruit excitation followed by inhibition which constructs a narrow temporal window restricting sensory evoked spiking (Higley and Contreras, 2006). The properties of this window could shape tuning for sensory inputs (Wehr and Zador, 2003; Zhou et al., 2012). For example, when investigating direction selectivity of whisker deflection in barrel cortex, excitation proceeded inhibition when the direction was preferred but the difference in timing decreased at non-preferred orientations (Wilent and Contreras, 2005).

PV interneurons are rapidly activated by afferent inputs (Pouille and Scanziani, 2001; Beierlein et al., 2003; Cruikshank et al., 2007) and as mentioned earlier provide strong shunting inhibition onto pyramidal neurons. PV inputs may only be effective for a brief time, Inhibitory postsynaptic potentials (IPSPs) at PV synapses depress quickly when activity is high. Using this short effective window, PV interneurons may increase the temporal precision of the informative first spike in cortical neurons responding to sensory input (Panzeri et al., 2001; Pouille and Scanziani, 2001; Cardin et al., 2010; Resulaj et al., 2018).

Later in the response to sensory stimuli, the inputs of SOM (Li et al., 2014) and VIP interneurons may be more important (Mesik et al., 2015). Unlike PV, SOM interneurons are activated by repeated, facilitating inputs (Kapfer et al., 2007; Silberberg and Markram, 2007). The profile of short-term plasticity at SOM synapses also differs from PV interneurons. SOM IPSPs only depress slightly with repeated activation and so can provide a more sustained inhibitory presence on the inputs to pyramidal dendrites than PV interneurons provide at the soma (Murayama et al., 2009; Lovett-Barron et al., 2012). The synapses of VIP interneurons also show distinct dynamics, with VIP to SOM synapses displaying frequency dependent facilitation (Walker et al., 2016).

Due to these distinct properties, PV and SOM interneurons likely play different roles in the

rhythms of cortical activity, evoking gamma and beta frequency oscillations respectively. Optogenetic excitation of PV interneurons in barrel cortex suppresses the responses of local neurons to sensory stimuli, and rhythmic activation of PV interneurons at 40Hz produced an amplification in the LFP at that frequency (Cardin et al., 2009). Similarly, activation of PV cells in infralimbic and prelimbic cortex promoted gamma frequency oscillations, while optogenetic inhibition of PV cells suppressed gamma oscillations (Sohal et al., 2009). Whereas SOM interneurons preferentially promoted slower cortical oscillations in range of 5-30Hz, with the inhibition of SOM interneurons selectively suppressing visually evoked beta oscillations, and PV and SOM interactions producing intermediate frequencies (20-30Hz) (Chen et al., 2017; Veit et al., 2017). The behavioural state of the animal can also modify the rhythms of cortical activity. Attention can increase the gamma frequency (20-80 Hz) synchronisation of neurons (Fries et al., 2001; Börgers et al., 2005). Local increases in synchronisation may allow downstream neurons to better integrate synchronised inputs, effectively amplifying the signals modulated by attention.

Recurrent inhibition that precisely tracks excitation can generate asynchrony in neural networks, reducing the correlations between neurons, even in cases where neurons receive identical inputs (Renart et al., 2010; Tetzlaff et al., 2012; Graupner and Reyes, 2013; Helias et al., 2014). Indeed, pharmacological reductions of inhibitory activity increased noise correlations (Sippy and Yuste, 2013). A reduction in noise correlations leads to an improvement in population coding (Ly et al., 2012; Middleton et al., 2012; Franke et al., 2017). This is of particular interest here as attention has also been found to decorrelate cortical activity (Cohen and Maunsell, 2009; Ruff and Cohen, 2019; Speed et al., 2020).

1.7 - Behaviour modifies the activity of VIP, SOM and PV interneurons

Interneurons are recruited by behaviour, and different groups of interneurons may be more involved in certain brain states and behavioural contexts. Some early evidence for this, recorded in mouse barrel cortex, shows that fast-spiking interneurons were more active during quiet wakefulness, but non-fast-spiking interneurons were more depolarised and increased their firing rates during an alert state - whisking (These were most likely 5HT3aR neurons due to the superficial recording location and the abundance of those neurons there)

(Gentet et al., 2010).

Inhibitory neurons likely modulate circuit activity over different timescales (Kuchibhotla et al., 2017). Over longer durations, interneurons are involved in the plasticity of cortical circuits with learning: SOM interneurons exhibited a decrease in axonal boutons with motor skill training, disruption of SOM interneurons impaired learning (Chen et al., 2015), and inhibition is involved in critical period plasticity in visual cortex (Fagiolini and Hensch, 2000; van Versendaal et al., 2012; Kuhlman et al., 2013), among other examples (Froemke et al., 2007; Chen et al., 2011; Donato et al., 2013).

Interneurons are also important for acute changes in cortical network activity, with multiple interneuron cell types often being involved simultaneously. One example for this is data from Kuchibhotla et al. Mice switched between two contexts involving auditory stimuli, discrimination of pure tones and passive listening to the same stimuli. The signal for the change in context was removal or addition of the reward tube that the mice licked to respond in the task. Two-photon imaging of auditory cortex revealed context dependent modulation of sensory information, with the discrimination task leading to selective activation of some neurons and general suppression of others. PV, SOM and VIP interneurons all increased their baseline activity with task engagement, but while PV and SOM were responsive to stimuli during the task, VIP interneurons were suppressed. Optogenetic suppression of the 3 groups had opposing effects, implicating SOM and PV in suppression of pyramidal neuron activity and VIP in disinhibition. They found that inhibition of any of the interneuron cell types impaired task performance and therefore a combination is key for gating contextual information (Kuchibhotla et al., 2017). The changes in interneuron activity with behavioural context may be due to neuromodulators. Pharmacological block of muscarinic ACh receptors had a biased effect on interneuron activity, and reduced task performance and contextual changes in excitatory neurons (Kuchibhotla et al., 2017).

There is also good evidence for different interneuron cell-types being involved in distinct aspects of behaviours. Pinto and Dan (2015) performed calcium imaging of the prefrontal cortex (PFC) whilst mice performed an auditory go/no-go task. Using transgenic mouse lines for cell-type specific expression of Cre they were able to investigate the activity of VIP, SOM and PV interneurons during this behaviour. Interneurons of the same sub-type were found to

have similar functional properties, each encoding different task related signals. PV interneurons responded to all task events: sensory, motor and outcome. SOM displayed motor related activity (primarily responding to licking) but did not respond for the sensory stimuli or the outcome of a trial. VIP had strongly outcome related activity, with greater VIP activity in response to the preparatory cue at the start of a trial when the proceeding trial was incorrect (punished) compared to when it was rewarded (Pinto and Dan, 2015). This suggests that VIP interneurons could be involved here in adjusting behaviour based on action outcomes, a vital aspect of cognitive control that the frontal cortex is known to be required for (Schall et al., 2002; Ridderinkhof et al., 2004; Narayanan et al., 2013). VIP interneurons also respond to reinforcement signals in auditory cortex (Pi et al., 2013). Additionally, the activity of SOM interneurons suppresses input to pyramidal neurons over a large region by inhibiting dendrites, contributing to surround suppression and potentially gating information - for example from motor activity - from entering the cortical area (Silberberg and Markram, 2007; Adesnik et al., 2012; Zhang et al., 2014). In line with this, VIP-SOM disinhibition allows processes such as associative learning about unexpected events (Letzkus et al., 2011; Krabbe et al., 2019), by gating the plasticity of inputs onto pyramidal neurons (Williams and Holtmaat, 2019). However, the specific preferences and roles of interneurons may vary from region to region.

Behaviour may affect the activity of multiple interneuron cell-types, sometimes simultaneously, but brain state and neuromodulatory inputs affect different cell-types differently (Gentet et al., 2012; Alitto and Dan, 2013; Lee et al., 2013; Pi et al., 2013; Fu et al., 2014; Zhang et al., 2014). Furthermore, during sensation and behaviour interneuron sub-types have been proposed to act as functionally homogeneous units (Kvitsiani et al., 2013; Pi et al., 2013; Hangya et al., 2014; Kato et al., 2015; Pinto and Dan, 2015; Karnani et al., 2016b), which increases the possibility that manipulation of molecularly defined cell-types might produce useful information about the function of those cell-types in cortical circuitry processing active behaviour.

1.8 - The role of VIP interneurons in attention

VIP interneurons are of particular interest because they are positioned at the top of a

hierarchical disinhibitory microcircuit (Hangya et al., 2014; Kepecs and Fishell, 2014; Harris and Shepherd, 2015), increasing the activity of pyramidal neurons by inhibiting SOM interneurons (Lee et al., 2013; Pfeffer et al., 2013; Pi et al., 2013). Disinhibition opens interesting computational options to the network (Letzkus et al., 2015), such as the gating of signals by releasing them from a normally present layer of inhibition in the cortex (Vogels and Abbott, 2009).

VIP interneurons have been found to enhance the firing of pyramidal neurons in various cortical regions, including: visual (Fu et al., 2014; Ayzenshtat et al., 2016; Jackson et al., 2016; Karnani et al., 2016a; Shapiro et al., 2022b), somatosensory (Lee et al., 2013), auditory (Pi et al., 2013; Karnani et al., 2016a), and frontal areas (Garcia-Junco-Clemente et al., 2017; Kamigaki and Dan, 2017; Lee et al., 2019). Although, the signals which VIP interneurons are amplifying likely change from region to region. In barrel cortex, VIP interneuron activity increased with whisking due to projections from motor cortex (Lee et al., 2013), and VIP interneuron activity in visual cortex has been associated with locomotion (Fu et al., 2014). However, although VIP interneurons increased the activity of excitatory neurons in auditory cortex, movement reduced stimulus related spike rates (Bigelow et al., 2019).

Critically, VIP interneuron mediated disinhibition has been proposed as a key mechanism underlying attentional modulation (Sridharan and Knudsen, 2015; Batista-Brito et al., 2018). Potentially because VIP interneurons can create holes in the 'blanket of inhibition' that cortex is normally covered by, allowing selective amplification of the attended stimulus (Karnani et al., 2016a). Activation of cingulate cortex has even been found to increase V1 activity and behavioural performance on a visual discrimination task, likely through VIP mediated disinhibition (Zhang et al., 2014).

1.8.1 - VIP interneurons receive cholinergic input

Neuromodulators can dramatically change the dynamics of neural circuits, and are important for brain states like sleep, arousal and mood (Bargmann and Marder, 2013). There is substantial evidence for a central role for acetylcholine in attention (Everitt and Robbins, 1997; Sarter et al., 2005, 2009). Acetylcholine signalling is heightened during tasks requiring attention (Parikh et al., 2007; Sarter et al., 2009) and its phasic release may be involved in the

rapid allocation of attention (Disney et al., 2007; Herrero et al., 2008). Also, performance on attention tasks (such as the five-choice serial reaction time task (5CSRTT) in rats) is impaired by lesions and pharmacological interventions targeting cholinergic signalling (Muir et al., 1992; McGaughy et al., 2000). In macaque V1, acetylcholine can enhance the gain of visual stimulus responses, and nicotinic acetylcholine receptors (nAChRs) were found to be expressed by inhibitory interneurons and feedforward thalamic synapses (Disney et al., 2007). Additionally, the prefrontal cortex can perform top-down regulation of other areas by controlling acetylcholine release in them (Nelson et al., 2005).

GABAergic interneuron subtypes respond differently to neuromodulators (Gao et al., 2003; Bacci et al., 2005; Kruglikov and Rudy, 2008). For example, serotoninergic afferents synapse onto SOM but not VIP interneurons (Paspalas and Papadopoulos, 2001). Meanwhile, cholinergic agonists affect the activity SOM and VIP, but not PV interneurons (Kawaguchi, 1997). The basal forebrain is the primary source of cholinergic input to cortex. In mice, optogenetic manipulation of cholinergic axon terminals in V1 was also capable of improving behavioural performance on a visual discrimination task at the scale of trials, rapidly enhancing and desynchronising cortical activity (Pinto et al., 2013). VIP interneurons are specifically activated by basal forebrain input through nicotinic acetylcholine receptors (nAChRs), allowing phasic acetylcholine release to disinhibit pyramidal neurons (Porter et al., 1999; Alitto and Dan, 2013). (Poorthuis et al., 2014; Gasselin et al., 2021).

1.8.2 - Modulation of VIP interneurons by locomotion may parallel changes with attention

The circuit changes associated with locomotion and attention in mice are qualitatively very similar, locomotion: enhances neural activity whilst preserving orientation selectivity (Niell and Stryker, 2010; Keller et al., 2012), improves spatial selectivity (Mineault et al., 2016) and interacts with spatial integration (Ayaz et al., 2013), improves stimulus discriminability by decorrelating neural activity (Erisken et al., 2014; Dadarlat and Stryker, 2017), and even increases gamma frequency oscillations (Niell and Stryker, 2010; Saleem et al., 2017). Locomotion is also associated with neuromodulator signalling, including acetylcholine (Polack et al., 2013; Reimer et al., 2016). Importantly, cholinergic input from the basal forebrain activates VIP interneurons during locomotion, potentially increasing visual responses in V1

(Fu et al., 2014). It seems possible that locomotion and attention could operate using the same circuit mechanisms (Speed and Haider, 2021).

1.8.3 - Do the modulations from VIP interneurons and attention interact?

If, as hypothesised, attention is mediated by VIP-SOM disinhibition then there are two major predictions. First, attention and VIP modulations should have similar effects on pyramidal neurons, and the magnitude of attentional modulations observed in the task should depend on the activity of VIP interneurons. Second, the activity of different cell-classes and the interactions between those classes should be influenced in a similar way by attention and VIP manipulation. I tested these hypotheses through the optogenetic manipulation of VIP interneurons whilst simultaneously imaging activity in V1 of pyramidal, SOM, PV, and VIP interneurons, in mice performing a cross-modality attention-switching task.

I observed an enhancement of stimulus selectivity in V1 with attention, an increase in activity with VIP photoactivation, and a decrease in activity with VIP photoinhibition. Modulations from attention and VIP manipulation induced distinct changes in the network. VIP photoactivation increased pyramidal, VIP and PV activity and mostly suppressed SOM activity, whilst attention induced heterogeneous changes with a clear reduction present in the evoked activity of all four cell-types measured here. When combined, attention and VIP manipulation do not interact and appear orthogonal at the level of the neural population. These results indicate that attentional modulation of stimulus selectivity in mouse V1 is not mediated by VIP-SOM disinhibition. Additionally, they highlight the computational power of the cortical circuit and its previously reported capacity to overlay multiple non-interacting signals in the same neural populations (Mante et al., 2013; Rigotti et al., 2013; Stringer et al., 2019).

1.9 - PV interneurons may be involved in mediating attention

As discussed earlier, PV interneurons provide strong shunting inhibition at the pyramidal cell soma and are involved in regulating the temporal patterns of the circuit. They have therefore often been positioned as providing a broad inhibition, maintaining excitatory-inhibitory balance to keep their local network in check (Scholl et al., 2015; Kaplan et al., 2016). They've even been used as a proxy for direct inhibition of excitatory neurons (Lien and Scanziani, 2018;

Li et al., 2019). Although, their actual role in the network is likely more nuanced (Cardin, 2018). PV interneurons may also be involved in attention. In macaque area V4 narrow-spiking neurons (putative PV-expressing interneurons) were modulated by attention and were actually more strongly modulated than their broad-spiking neighbours (Mitchell et al., 2007). PV interneurons are also attentionally modulated during a cross-modality attention switching task in mice which I am using in this thesis (Poort et al., 2022).

1.9.1 - Optogenetic manipulation of PV interneurons can produce unexpected effects

The brain is a complex interconnected system and transient manipulations should generally be interpreted carefully, deficits observed could be due to diaschisis - disruption of connected regions - rather than because a network component is essential (Otchy et al., 2015; Hong et al., 2018). Likewise, the cortex contains networks of recurrently connected interneurons, and investigations which manipulate their activity can produce unexpected, conflicting or paradoxical results. Ideally manipulations of circuits should mimic physiological changes to increase interpretability (Phillips and Hasenstaub, 2016; Wolff and Ölveczky, 2018; Li et al., 2019).

An increase in input to inhibitory cells can cause a seemingly paradoxical decrease in their steady state activity (Tsodyks et al., 1997). Models like inhibitory stabilised networks and supralinear stabilised networks can account for this unexpected effect of manipulating interneuron activity (Ozeki et al., 2009; Rubin et al., 2015; Litwin-Kumar et al., 2016; Kato et al., 2017; Sanzeni et al., 2020) and modelling of neural networks in general can help to resolve the effects of network manipulations.

I aimed to investigate the role of PV interneurons in the attentional modulation of V1 using a cross-modal attention switching task in mice. I found that both PV and non-PV cells changed their stimulus selectivity with attention. The optogenetic excitation of PV interneurons that I applied did affect the attentional modulation of V1, but it also produced unexpected and paradoxical effects on the activity of non-PV cells in a manner dependent on the behavioural task the mice were involved in. Further work will be required to fully resolve these results.

1.10 - Thesis aims

There are similarities in the neural correlates of attention in mice and primates. While mouse V1 has been shown to be attentionally modulated, the relationship of mouse higher visual areas and attention is unexplored. Additionally, the neural circuit mechanisms that underlie attentional modulation are relatively poorly understood. Many interneuron subtypes have been identified and their properties and activity during active behaviour described, chief among which are PV, SOM and VIP interneurons. PV interneurons are strongly modulated by attention and VIP interneurons have been proposed to mediate attentional modulation through a disinhibitory motif. However, the role of these interneurons in attention has not been directly tested. In this thesis I pursued three main aims:

1. To map the attentional modulations of mouse higher visual cortical areas (Chapter 2).
2. To investigate whether VIP interneurons mediate the attentional modulation of mouse V1 through disinhibition (Chapter 3).
3. To investigate whether PV interneurons mediate the attentional modulation of mouse V1 (Chapter 4).

Chapter 2 – Attentional modulation of mouse cortical visual areas

2.1 - Introduction

A blackbird searching for the ripe blackberries on the vine, the man reading in a cafe shifting to eavesdropping on an interesting conversation nearby - the need to triage the flood of information available to the senses is ubiquitous. Attention enhances the processing of selected stimuli at the expense of others, specialising to the task at hand. The top-down modulation of visual cortical circuits by attention is one of the most intensely studied neural correlates of cognition (Maunsell, 2015; Moore and Zirnsak, 2017; Speed and Haider, 2021). The stimulus selectivity of neurons in visual cortex generally increases with attention, an alteration that is believed to underlie the improvements in behavioural discriminability of attended stimuli (Reynolds and Chelazzi, 2004; Kanamori and Mrsic-Flogel, 2022; Poort et al., 2022). To increase stimulus selectivity and produce more distinct cortical representations of the stimuli, the stimulus-evoked firing rates of neurons change; these changes may be either increases (McAdams and Maunsell, 1999; Speed et al., 2020; Kanamori and Mrsic-Flogel, 2022), decreases (Moran and Desimone, 1985; Luck et al., 1997), or a combination of the two (Mitchell et al., 2007; Poort et al., 2022). Other changes in neural activity may also help improve the ability of downstream circuits to separate the attended stimuli, such as reductions in noise correlations (Cohen and Maunsell, 2009; Mitchell et al., 2009). However, surprisingly little is known about the circuit mechanisms that produce attentional modulation in visual cortex.

The neural basis of attention has been mainly studied in non-human primates. Although primate visual acuity is much greater and experiments with primates allow the use of particularly complex behavioural paradigms, there are many similarities in the primate and mouse visual systems and the powerful experimental tools available in mice allow more detailed investigation of the circuit mechanisms of attention (Huberman and Niell, 2011). We know from previous work that mouse primary visual cortex is also attentionally modulated (Poort et al., 2015, 2022; Khan et al., 2018; Wang and Krauzlis, 2018; Speed et al., 2020; Hu and Dan, 2022; Kanamori and Mrsic-Flogel, 2022).

Although mice rely less on vision than primates, they nevertheless have a series of hierarchically organised cortical areas dedicated to vision (Wang and Burkhalter, 2007; Garrett et al., 2014; Glickfeld and Olsen, 2017; Zhuang et al., 2017; Siegle et al., 2021). The primate visual system is arranged into distinct processing streams (Maunsell, 1992; Ungerleider and Mishkin, 1982). Based on their differing functional properties (Andermann et al., 2011; Marshel et al., 2011; Roth et al., 2012) extrastriate mouse visual cortex has been divided in the literature into dorsal and ventral visual streams like those seen in primates (Wang et al., 2011, 2012; Wang and Burkhalter, 2013; Smith et al., 2017). However, a more nuanced arrangement has also been suggested where the dorsal stream separates into multiple sub-groups (Han et al., 2022) (Murakami et al., 2017); an alternative framework that has also been put forward for primate visual processing (Kravitz et al., 2011). Both human and non-human primate studies have found that the magnitude of attentional modulation is not the same at all stages of visual processing, increasing from LGN to V1 and up the hierarchy of cortical visual areas (Mehta et al., 2000a, 2000b; Cook and Maunsell, 2002; O'Connor et al., 2002; Montijn et al., 2012; Klein et al., 2014; Martin et al., 2019). Additionally, the latency to modulation is shorter in higher visual areas, suggesting that top-down attentional modulations backpropagate down the visual stream (Buffalo et al., 2010). To the best of my knowledge no previous work has examined differences in attentional modulation across mouse visual cortical areas, which is the aim of this chapter.

Here I have recorded neural activity from 7 cortical visual areas (including V1) in mice performing a cross-modality attention-switching task using two-photon calcium imaging. I found that primary visual cortex (V1), posteromedial area (PM) and anteromedial area (AM) of mouse visual cortex were significantly modulated by attention. The major finding from these results is that both in terms of the magnitude of change in stimulus selectivity with attention and in terms of the proportion of recorded neurons that were attentionally modulated, activity in V1 is more strongly affected by attention than any of the higher visual areas that I recorded here. This result is an inversion of the pattern of modulations which could be expected based on the primate visual cortical hierarchy. Secondly, my data together with the published connectivity of between PM and AM and analogy between findings in mouse and primate data shows that PM and AM may form an attentionally modulated sub-

stream for visual processing. To make this claim stronger the precise set of stimuli and circumstances under which this stream is active should be added, which is left for further study.

2.2 – Results

2.2.1 – A cross-modal attention switching task

To investigate the neural circuit mechanisms of attentional modulation, I trained mice to perform a cross modality attention switching task (Fig. 2.1a, b). Head-fixed mice were trained to alternate between blocks of visual discrimination trials and blocks of olfactory discrimination trials; effectively switching between performing a go/no-go task in two different modalities.

In both block types, mice initiated a trial by maintaining running speed above threshold (>5cm/s) for 2.8s plus a random jitter (mean 0.4s). In a visual block, mice could trigger a reward (a drop of soya milk) by licking the reward delivery spout in response to the presentation of one of two visual grating stimuli (Fig. 2.2b). If the mouse licked in response to the other (non-rewarded) grating no reward was delivered and the mouse was punished with a timeout (4s), during which the non-rewarded visual stimulus remained on screen (Fig. 2.2c). If the mouse continued to lick during the timeout the punish time was reset, further delaying the next trial and the next possible reward.

Similarly, in an odour block the mice could trigger a drop of reward by licking the delivery spout in response to one of two odours delivered through a tube placed above the mouse's nose (Fig. 2.2d). A lick in response to the non-rewarded odour triggered the same timeout as the non-rewarded visual stimulus (Fig. 2.2e). Aside from the modality of the stimuli being differentiated, odour and visual block trials differed in that the same visual grating stimuli that were relevant to the task and attended to during the visual block were presented on 70% of olfactory block trials (Fig. 2.1b). However, during the olfactory block the gratings were irrelevant to the task and licking in response to them had no effect. The irrelevant visual stimuli were presented before the odour for 1.8 seconds regardless of the animal's response, and 1.8s (+0.2s (mean)) after their offset one of the two odours was presented. This ensured that the visual stimuli in the two blocks were identical and matched for running behaviour

during the time-period analysed.

During the visual block, mice accurately discriminated between the two visual gratings. Whereas during the odour block they ignored the same visual gratings while accurately discriminating between the two odour stimuli (Fig. 2.1c, behavioural d' attend visual 3.47 ± 0.77 median ± IQR, ignore visual 0.55 ± 0.87, sign-rank test p = 7.56×10^{-10}, d' discriminating olfactory stimuli 3.90 ± 0.67, n=50 sessions, 15 mice).

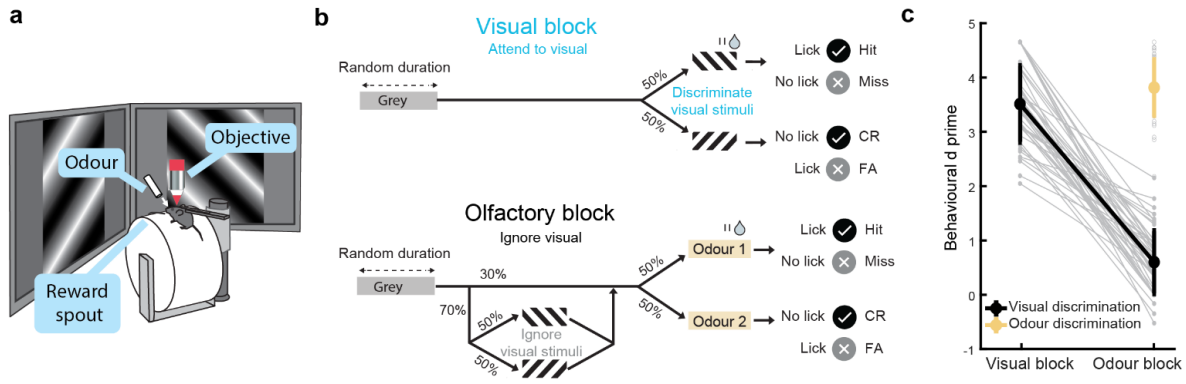

Figure 2.1: Mice perform a cross-modality attention switching task.

a) Schematic of the experimental apparatus. **b)** Schematic of the behavioural task. Top, visual block: mice were rewarded for licking the reward spout when gratings of a specific orientation were presented (+15 degrees from vertical, rewarded grating) and not when gratings of a second orientation were presented (-15 degrees from vertical, unrewarded grating). Olfactory block: mice were rewarded for licking when odour 1 was presented and not when odour 2 or either of the visual gratings were presented. CR indicates correct rejection. FA indicates false alarm. **c)** Behavioural discrimination performance (behavioural d') across attention. Connected points indicate visual discrimination, individual points in the odour block represent olfactory discrimination. Grey lines and points are individual sessions (n = 50 sessions, 15 mice), coloured lines show the average of all sessions.

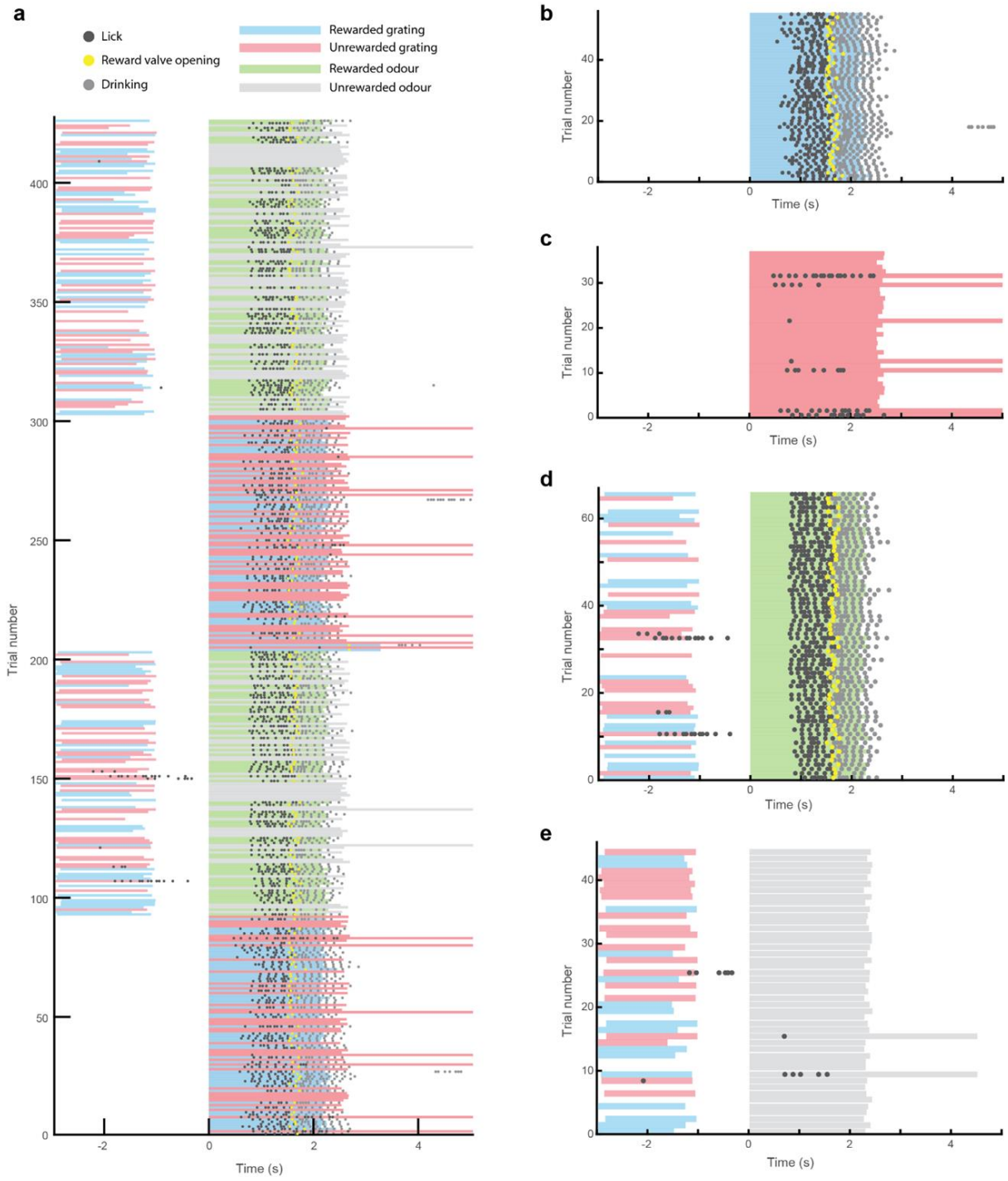

Figure 2.2: Mice accurately discriminate between stimuli in the attention switching task.

a) Raster plots of a whole example session aligned to the onset of the task relevant stimuli on each trial (Odour in the odour block, visual in the visual block). Coloured bars indicate the time the stimuli were presented. Dots indicate licking times. **b)** Raster plots of licking during rewarded visual trials from the first visual block in the example session in **a.** Trials are arranged chronologically and aligned to stimulus onset. **c)** Same as **b** but for unrewarded visual trials from the first visual block. **d)** Raster plots of licking during rewarded odour trials for the

first odour block in the example session in **a.** Trials are arranged chronologically and aligned to odour onset. Irrelevant visual stimuli are marked using the same colours as in the visual block. **e)** Same as in **d**, but for unrewarded odours from the first odour block.

2.2.2 – Attentional modulation of stimulus selectivity

Before mapping the effects of the attention switching task in mouse higher visual areas (HVA), I recorded the neural activity in primary visual cortex (V1) as it is the largest and most well studied mouse visual area and previous research has found neural correlates of attention in V1 (Wang and Krauzlis, 2018; Speed et al., 2020; Kanamori and Mrsic-Flogel, 2022; Poort et al., 2022). To observe neural activity, I expressed the calcium indicator GCaMP7f in V1 neurons non-specifically using a viral vector in VIP-cre mice (Further experiments involving these mice will be presented in chapter 3), and through two-photon calcium imaging I recorded the responses of neurons in layer 2/3. Coarse retinotopic mapping was performed before each recording session to ensure the stimuli presented on the screen were located correctly for the currently recorded patch of V1.

Many neurons displayed a clear preference for one of the two visual stimuli over the other, quantified as a selectivity index - the difference in responses to the rewarded and unrewarded grating stimuli, normalised by the pooled standard deviation (Fig 2.3a). This means that cells that had a stronger preference for the rewarded and non-rewarded stimuli had more extreme positive and negative selectivity values respectively, and therefore higher absolute selectivity values. Many neurons also modified the magnitude of their responses when the mouse was attending vs ignoring the same visual stimuli, in such a way that their selectivity also changed with attention. The majority of changes in selectivity with attention produced more extreme values (Fig. 2.3b,c), 29% of all recorded neurons increased their absolute selectivity when the mice were attending to the visual stimuli compared to when the same visual stimuli were ignored.

In line with previous work (Poort et al., 2015) (Khan et al., 2018; Poort et al., 2022), this attentional modulation can be seen as a broadening of the distribution of selectivity values with attention when viewing the population as a whole (Fig. 2.3d) and is quantified by a significant increase of the absolute stimulus selectivity of the whole neural population (Fig. 2.3e, (average absolute selectivity ignore, 0.35 ± 0.10 median ± IQR, attend 0.61 ± 0.28, sign-rank test, $P = 7.56 \times 10^{-10}$, N = 50 sessions). When restricting the analysis only to neurons that significantly enhanced their selectivity with attention, I found that the increase in average absolute selectivity is produced through a combination of increased responses to the preferred stimulus and decreased responses to the non-preferred stimulus.

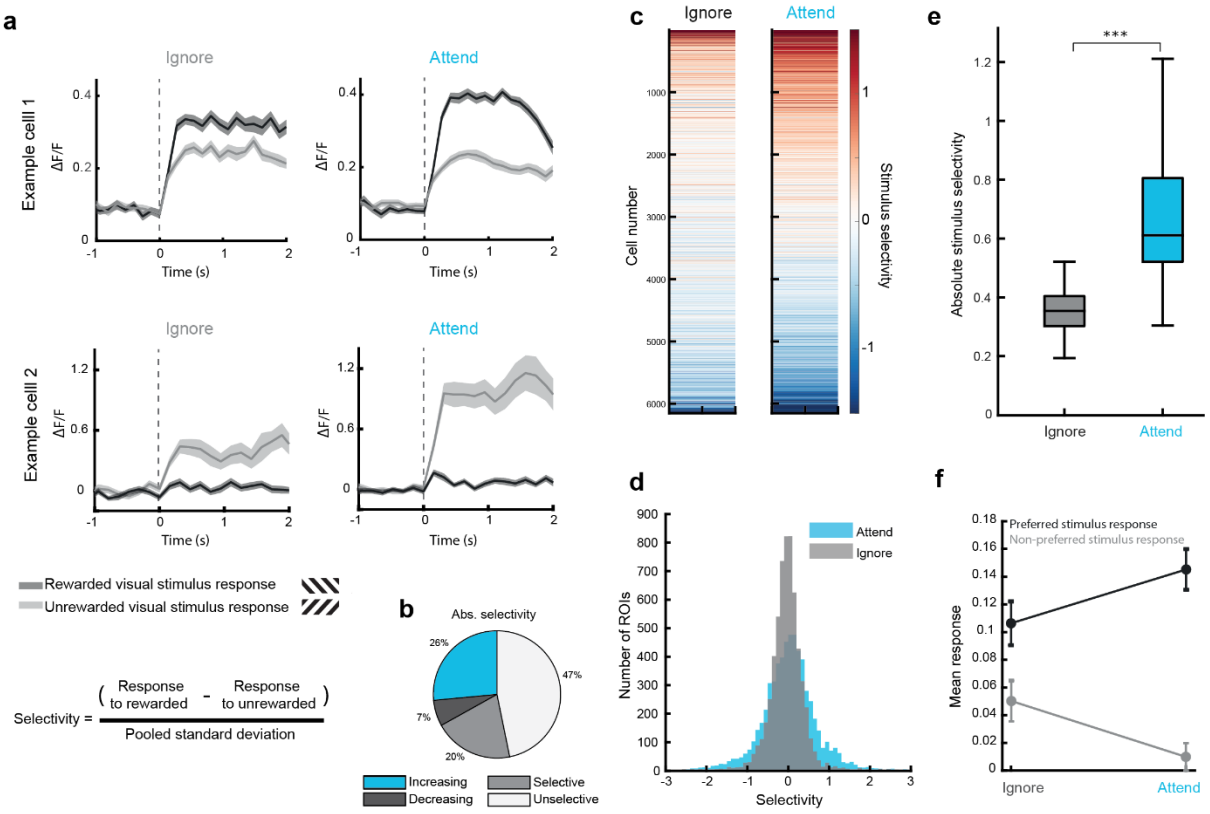

Figure 2.3: Top-down modulation of V1 neurons during the attention-switching task.

a) Average responses from 2 example cells to the rewarded and unrewarded visual gratings in the odour and visual blocks, showing an increase in selectivity in the attend condition. Top, a cell with a preference for the rewarded grating stimulus (positive selectivity). Bottom, a cell with a preference for the unrewarded grating stimulus (negative selectivity). **b)** Proportions of all cells (n = 6153 neurons, 15 mice) according to how they responded to the two visual gratings and how their responses changed with attention. Increasing - cells that significantly increase their absolute selectivity with attention. Decreasing - cells that significantly decrease their absolute selectivity with attention. Selective - cells that were significantly selective for one of the two visual stimuli, but which did not change significantly with attention. Unselective - cells that were not significantly

selective either when attending to or ignoring the stimuli. Details of the statistical tests used to assess whether cells were significantly selective and for significant changes in selectivity can be found in section 5.10. These results were corrected using the Benjamini-Hochberg procedure with a false discovery rate of 0.05. **c)** Stimulus selectivity of the same cells in the attend and ignore conditions (columns). Cells were ordered by their mean selectivity across both contexts (n = 6153 neurons, 15 mice). **d)** Histograms of stimulus selectivity when ignoring and attending the visual stimuli (n = 6153 neurons, 15 mice). **e)** Box plots of absolute stimulus selectivity during the ignore and attend conditions (n = 50 sessions, 15 mice, $p = 7.56\times10^{-10}$, Wilcoxon signed-rank test). **f)** Average baseline subtracted responses to the preferred and non-preferred visual stimuli in the ignore and attend conditions for cells that significantly increased their stimulus selectivity with attention (n = 50 sessions, 15 mice, error bars indicate SEM).

2.2.3 – Changes in selectivity with attention are not explained by changes in behaviour

Alongside the change in task relevance for the visual gratings there are associated overt behavioural changes between block types in the mouse's response to the visual stimuli. For the rewarded visual grating, the mouse transitions from not responding to the visual stimuli in the odour block to slowing down and licking in response to the same visual grating in the visual block (Fig 2.4a). Mouse visual cortex has been shown to encode behavioural information (Niell and Stryker, 2010; Fu et al., 2014; Stringer et al., 2019). It is therefore imperative to eliminate the possibility that changes in behaviour are the source of the observed attentional modulations. This has been assessed before for the previous version of this task (Poort et al., 2015) and I have performed similar analyses here.

<u>Decoding block type using running or neural data</u>

I trained a linear decoder to predict whether the visual stimuli were presented during an odour or visual block using either the population activity of V1 neurons or the running speed of the mouse. Both decoders can identify block type with 70-90% accuracy 1 second after stimulus presentation (Fig. 2.4b). However, individual behavioural sessions systematically vary in terms of the difference in running speed between the attended and ignored visual stimulus trials after visual stimulus onset (Fig 2.4a).

When binning the behavioural sessions according to the time-point of divergence in running speed with block type, the decoder using running speed from sessions in the slowest bin identifies trial type latest and with the least accuracy (Fig 2.4b). The decoder using sessions

with the fastest divergence in running speed with block type had performance higher than chance in the first time-bin after visual stimulus onset (50ms, Wilcoxon signed rank test, p = 0.019, n = 17 sessions). Whereas the decoder using sessions with the slowest divergence only had performance higher than chance at 250ms after visual stimulus onset (Wilcoxon signed rank test, p = 0.005, n = 16 sessions).

If the attentional modulation of neural activity were due to changes in running speed, we might expect the performance of the decoder using neural data to show a similar effect to the decoder using running speed, this is not what I observe. Instead, for the decoder trained on neural information, the different bins of time of divergence in running speed produced overlapping decoder performance curves (Fig 2.4b). The decoders trained on the neural data from the slowest and fastest diverging sessions both performed significantly higher than chance in the first time-bin after visual stimulus onset (158ms, Wilcoxon signed rank test, fast - $p = 2.93x10^{-4}$, slow - $p = 7.76x10^{-4}$). Meaning that for sessions with the slowest divergence in running speed when attending vs ignoring the visual stimuli, the decoder trained on neural data performed better than chance ~100ms before the decoder based on running speed, despite better temporal resolution for the running speed data. This suggests there is information in the V1 neural population indicating whether the stimulus is attended or ignored before and beyond the mouse's choice of motor action.

Correlation of attentional modulation and variance in neural activity explained by locomotor or licking behaviour

There are other behavioural changes aside from running that could account for changes in neural activity, most significant among which may be licking, which the mouse does to respond to stimuli in the task. For this reason, most of my analyses on neural activity in this thesis look at the first second after visual stimulus onset, to limit the impact of licking behaviour. If changes in neural activity are due to changes in behaviour, we might expect those changes in behaviour to be useful in predicting neural activity. I fit a cross validated ridge regression model on each individual neurons activity and tested their performance on held out data. I trained a full model using both the following task parameters - visual stimulus, odour stimulus, block type, interaction between visual stimuli and block type - and the

behavioural parameters, licking activity and running activity. I also trained a second model identical to the full model except for the omission of the behavioural parameters. As a measure of the influence of behaviour on each neurons activity I found the difference in R^2 between the full model and the no-behaviour model by dividing the no-behaviour R^2 by the full model R^2 to estimate the proportion of explained variance accounted for by behaviour; I then subtracted this value from 1 to get the proportion of the full model R^2 reduced by removing behaviour. The change in R^2 provides a measure of the influence of overt behaviour on each cell, and this can then be compared to the change in selectivity with attention. For all non-VIP cells, a larger change in R^2 did not correlate with a larger change in selectivity. In fact there is a significant negative correlation (larger changes in R^2 correlated with smaller changes in selectivity with attention, ($r(6151) = -0.170$, $p = 5.51 \times 10^{-41}$) (Fig1.5c). This same significant negative correlation is present when taking only significantly selective cells ($r(2763) = -0.138$, $p = 3.69 \times 10^{-13}$), only unselective cells ($r(3386) = -0.173$, $p = 2.77 \times 10^{-24}$) or only significantly attentionally modulated cells ($r(2419) = -0.145$, $p = 7.96 \times 10^{-13}$), demonstrating that it is not simply a large number of unresponsive neurons dominating the pattern. In addition, VIP interneurons display a strong positive correlation between their change in model predictions with behaviour and their change in selectivity ($r(350) = 0.332$, $p = 1.76 \times 10^{-10}$), in line with previous reports that they are minimally responsive to visual stimuli and modulated by locomotion (Fu et al., 2014). Experiments involving VIP interneurons will be revisited in chapter 4.

Finally, I filtered the neural population taking all non-VIP cells with a change in R^2 less than the median of the population - those least effected by behaviour. The change in absolute selectivity with attention for this population remains significant (Wilcoxon sign rank test, $p = \sim 0$, $n = 3086$, Fig 1.5d). Taken together the increase in selectivity seen with attention is not readily accounted for by any changes in the behaviour parameters measured here.

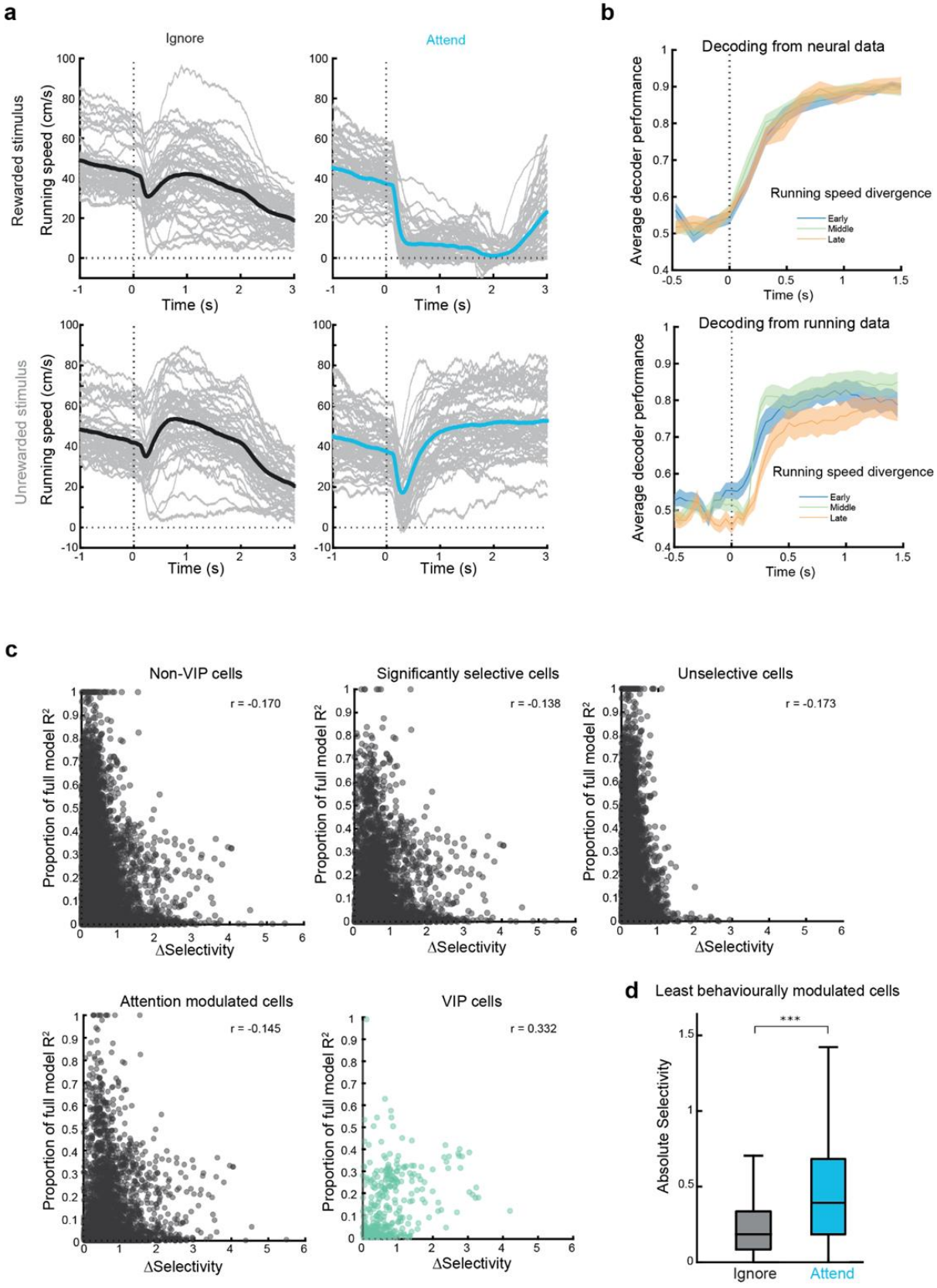

Figure 2.4: Changes in running and licking cannot account for the increase in stimulus selectivity with attention.

a) Running speed aligned to rewarded and unrewarded visual stimulus onset (dashed line) - top and bottom respectively. Left - trials from the odour block, right - trials from the visual block. Grey traces are the individual session averages, coloured lines are the overall average. **b)** Top - performance of a decoder when decoding block type from neural activity in 158ms bins aligned to the visual stimulus onset. The data was divided into three groups of sessions by the time of divergence of running speed between attend and ignore conditions. Early, middle and late represent 0-33rd, 34th-66th and 67th-100th percentiles. Bottom, same as top, but for a decoder using running speed instead of neural activity. While the decoder using running data clearly follows the sequence of running divergence, the decoder using neural data does equally well in all three running conditions, demonstrating that the running divergence does not contribute to the distinct activity levels in the attend and ignore conditions. **c)** Cells with stronger influence of running and licking do not account for attentional modulation. Absolute change in selectivity for the visual stimuli with attention (Delta selectivity) plotted against the reduction in R2 when removing running and licking behaviour information from a ridge regression model predicting the activity of each neuron: 1 - (no-behaviour model R2)/(full model R2). Larger values indicate a greater influence of running and licking. From top left to bottom right: All non-VIP cells, all significantly selective non-VIP cells, all non-VIP cells that were not significantly selective, all non-VIP cells that significantly increased their selectivity with attention, all VIP interneurons. **d)** Average absolute stimulus selectivity during the ignore and attend conditions (n = 3086 cells, 15 mice, non-VIP neurons, p = ~0) when taking only neurons whose activity is least influenced by running and licking behaviour (bottom 50% of the median change in model R^2.

2.2.4 – Functional retinotopic mapping of higher visual areas

In primates, attentional modulations increase intensity higher in the hierarchy of visual areas. I investigated the neural activity in mouse higher visual areas during our attention switching task as to the best of my knowledge the effects of attentional modulation in mouse HVAs have not previously been examined. Higher visual areas were found through functional retinotopic mapping in very similar fashion to previous work (Zhuang et al., 2017). Retinotopic mapping was performed with Matthew Harvey, who operated the widefield microscope and constructed the retinotopic maps from the resulting data.

I used a transgenic mouse line expressing GCaMP6s in excitatory neurons to ensure even indicator expression across areas. Within the 4-5mm craniotomy up to 7 HVAs were visible and accessible for two-photon imaging per mouse: primary visual cortex (V1), lateromedial area (LM), rostrolateral area (RL), anteromedial area (AM), posteromedial area (PM), medial area (M), and anterolateral area (AL) (Fig 2.5a).

Whilst mice performed the attention switching task, one visual area was recorded from per mouse per day in a pseudo random order. Recordings were taken from the centre of the

mapped retinotopic area. Coarse retinotopic mapping was performed before each recording session to position stimuli correctly. These sessions were not designed to function as an analysis of visual field coverage but within these coarse retinotopic mapping sessions many of the previously published visual field coverage preferences were replicated. LM and RL which have been shown to prefer nasal coordinates (Zhuang et al., 2017), responded to the nasal portion of the screen (Fig 2.5c). Likewise, PM and AM both of which prefer more temporal coordinates responded on average to more temporal parts of the screen than LM and RL (Zhuang et al., 2017).

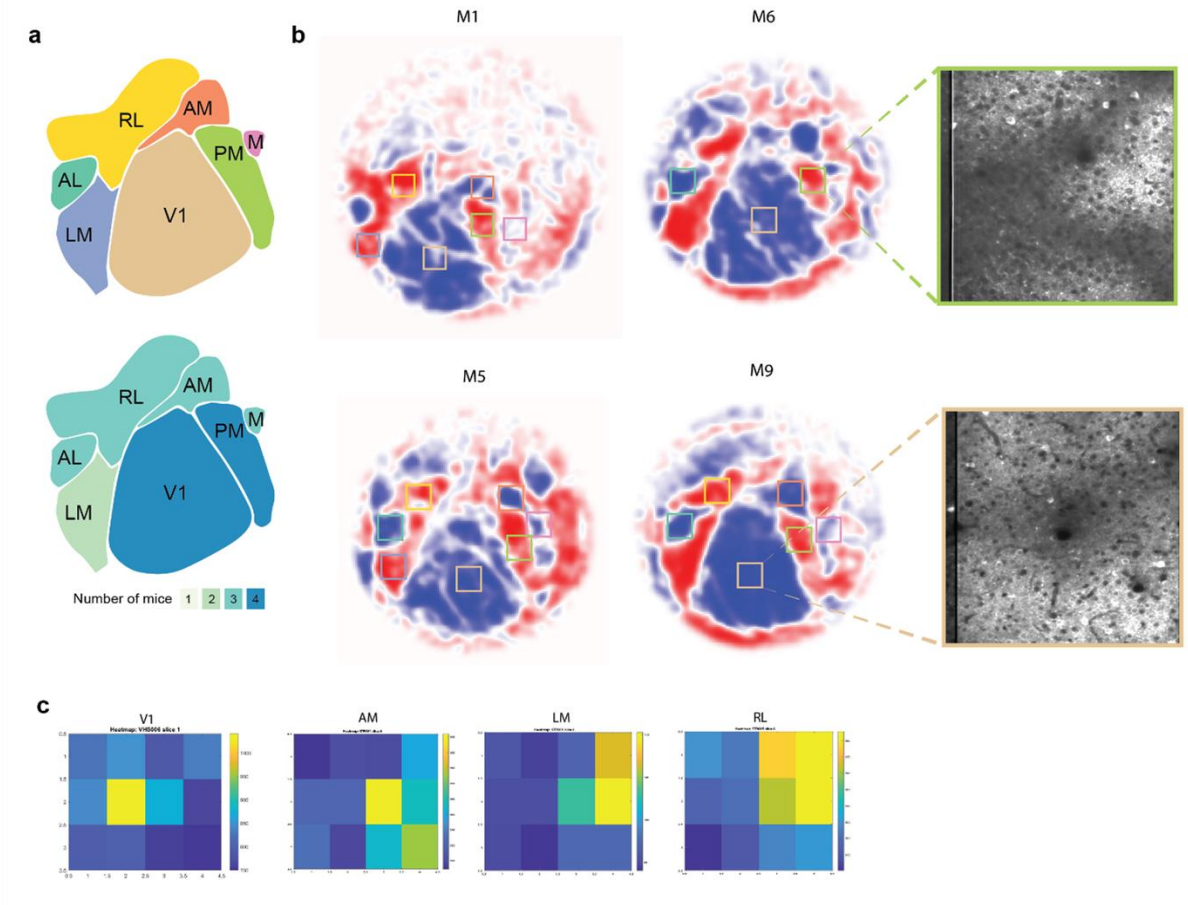

Figure 2.5: Functional retinotopic mapping reliably identifies higher visual areas.

a) Top - Schematic of average HVA locations. Bottom - same schematic colour coded according to the number of mice in which a recording of sufficient quality was taken from that higher visual area. Primary visual cortex (V1), lateromedial area (LM), rostrolateral area (RL), anteromedial area (AM), posteromedial area (PM), medial area (M), and anterolateral area (AL). **b)** Sign-maps of retinotopic areas constructed from widefield calcium imaging responses to spherically corrected vertically or horizontally drifting inverting checker-board bars presented to the mice. Maps from each of the 4 mice used in this chapter are presented. Coloured squares indicate the

approximate recording locations for colour coded HVA's in the schematic in a. Expanded view on right shows two example planes from 2 imaging sites. **c)** Results from the coarse retinotopic mapping used to identify the approximate retinotopic location of the two-photon imaging site at the start of each day. Each heatmap shows the average fluorescence of the entire imaging plane when a rapidly alternating black and white square was presented in that quadrant of the monitor screen in front of the mouse's contralateral eye. Each heatmap is an example map for different visual areas, left to right: V1, AM, LM, RL.

The stimuli used for retinotopic mapping do not extend over the entirety of the visual field and so may not reach the edge of the receptive fields of each visual area. This could lead to error in the identification of visual field edges, based on the reversal of visual field sign. What then is the precision of the higher visual area locations that we have found? Zhuang et al. compared the functional retinotopic map obtained through calcium imaging to the architechtonic borders between visual areas. The largest mismatch they found was at the V1 - LM/RL border with differences of 312 ± 88 µm across 4 mice. Given that they also found a misalignment between architectonic and projection-based retinotopic borders using the Allen Mouse Brain Connectivity Atlas, this could indicate that the architectonic border of V1 is related to a function other than the reversal of the retinotopic map, rather than a failure of spatial precision in functional mapping (Zhuang et al., 2017).

However, if the mismatch in the V1 border is due to a spatial inaccuracy of functional retinotopic mapping, the magnitude of the potential mismatch in comparison with an approximate width of between 500-650um for the HVAs recorded may pose a problem. The recordings of HVAs in this thesis were made using an ~450 x 450um 2-photon imaging field of view which was aligned to the middle of the retinotopically mapped regions – meaning that they would be vulnerable to contamination by cells from the borders of V1.

2.2.5 – Attentional modulation in mouse higher visual areas

When looking at the effect of attention switching on all neurons, V1, AM, and PM showed a significant increase in the absolute selectivity of the whole population of recorded neurons with attention after holm-bonferroni multiple comparisons correction (Fig. 2.6e). Of these three, V1 had the highest absolute population selectivity in the attend condition (Fig. 2.6c) and the largest changes in absolute selectivity with attention. As V1 is also the largest of the three areas significantly modulated by attention, experiments for subsequent chapters of this

thesis will focus on V1. AL, LM and RL showed no significant change in absolute selectivity with attention, while area M showed a significant decrease in selectivity with attention, however this result was not robust - subsequent analysis across multiple task difficulties (detailed later) did not find a significant main effect for attention. Results before multiple comparisons correction for Wilcoxon signed rank test of absolute selectivity when attending vs ignoring the visual stimuli: AL p=0.413 n=618 cells, AM $p=7.13x10^{-28}$ n=635 cells, LM p=0.032 n=511 cells, M $p=2.07x10^{-20}$ n=1539 cells, PM $p=6.32x10^{-08}$ n=1120 cells, RL p=0.608 n=772 cells, V1 p=~0 n=2260 cells.

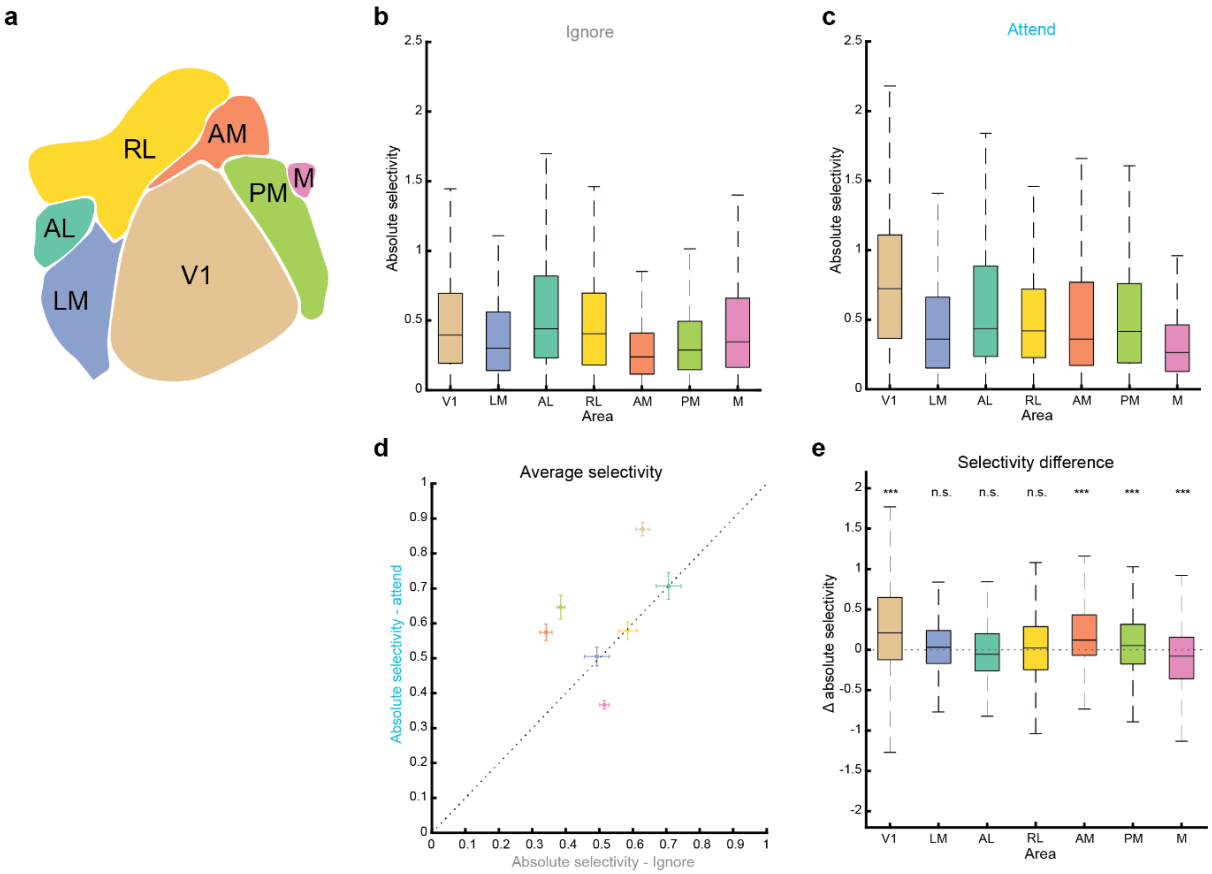

Figure 2.6: Absolute selectivity of the neural population with attention across higher visual areas.

a) Schematic indicating colour coding of all HVA's for the plots. **b)** Mean absolute selectivity for the visual stimuli in the ignore condition, for all cells from each visual area. Visual areas are arranged starting with V1 and rotating clockwise. **c)** Same as in b, but for selectivity in response to the visual stimuli in the attend condition. **d)** Scatter of the mean absolute selectivity of the whole population of recorded cells in each area in the attend condition against the same in the ignore condition. Error bars indicate s.e.m. **e)** Selectivity difference with attention for

each recorded cell in all areas. Effectively the selectivity of each cell in **b** subtracted from the selectivity of that cell in **c**. ***= p<0.001. V1 n=2260 cells, 4 mice; LM n=511 cells 2 mice; AL n=618 cells, 3 mice; RL n=772 cells, 3 mice; AM n=635 cells, 3 mice; PM n=1120 cells, 4 mice; M n=1539 cells, 3 mice.

2.2.6 – Proportions of significantly modulated neurons and their responses

I have presented data about attentional modulations in V1 from two sets of mice so far, the VIP-cre mice in figure 2.3 and 2.4, and the transgenic GCaMP6s mice in the rest of this chapter. The pattern in both these sets of recordings is that most of the neurons are significantly selective for one of the two stimuli, and a majority of significantly selective neurons increase their selectivity with attention (Fig. 2.3d, Fig. 2.7a). It is likely that a larger proportion of recorded neurons are not selective for either visual stimulus in the figure 2.3 dataset as those mice expressed GCaMP7f in all neurons rather than only excitatory cells and so some interneurons are included. The significantly selective neurons of areas PM and AM display a similar pattern to V1, congruent with the increase in the area's absolute population selectivity (Fig. 2.7a), although both have an absolute minority of significantly selective cells.

Despite not showing significant increases in absolute population selectivity, areas RL, LM and AL all have large proportions of significantly selective cells indicating that they are strongly responding to the visual stimuli in the task. In addition, RL and LM have a substantial number of cells that increase their selectivity with attention, but the proportion of these cells is decreased relative to V1.

The changes with attention for significantly modulated neurons in V1 are characterised by a decrease in the average response to the unpreferred grating and an increase in the response to the preferred grating (Fig. 2.3f, Poort et al., 2022). For all cells in each HVA that significantly enhanced their absolute selectivity with attention, I plotted the mean response to visual stimuli with and without attention (Fig. 2.7b). Broadly these cells appear to follow the same pattern as V1.

I tested the effects of visual stimulus type and attention on mean responses using a two-way ANOVA (See table below for the results). All areas apart from RL had a significant main effect for the visual stimulus, indicating that the mean response was significantly different between the preferred and non-preferred stimuli, as expected. No HVAs had a significant main effect for attention indicating that attention did not simply shift mean responses up or down for

both visual stimuli. Only V1 and PM had a significant interaction effect between visual stimulus and attention, such that attention modulated mean responses and did so differently for the preferred and non-preferred visual stimuli.

To summarise, of the higher visual areas recorded, PM and AM significantly increase their selectivity for the visual stimuli with attention, potentially constituting a functional visual processing stream. Importantly, in terms of the proportion of recorded neurons modulated and absolute selectivity of the population when attending to the visual stimuli V1 shows the largest modulation by attention, an inversion of what might be expected given the primate data.

Table 2.1: Two-way ANOVA for the effects of visual stimulus type and attention on mean responses of cells that significantly enhance their selectivity with attention, for each HVA.

Area	Visual stimulus	Attention	Interaction
V1 (n = 869 cells)	3.43×10^{-13}	0.122	F(1,3472) = 6.128, p = 0.013
LM (n = 62 cells)	0.002	0.714	F(1,244) = 2.412, p = 0.122
AL (n = 24 cells)	0.016	0.245	F(1,92) = 3.093, p = 0.082
RL (n = 109 cells)	0.120	0.563	F(1,432) = 0.350, p = 0.555
AM (n = 132 cells)	4.20×10^{-5}	0.540	F(1,524) = 2.723, p = 0.100
PM (n = 207 cells)	4.01×10^{-4}	0.866	F(1,824) = 4.259, p = 0.039
M (n = 132 cells)	4.59×10^{-4}	0.658	F(1,524) = 1.303, p = 0.254

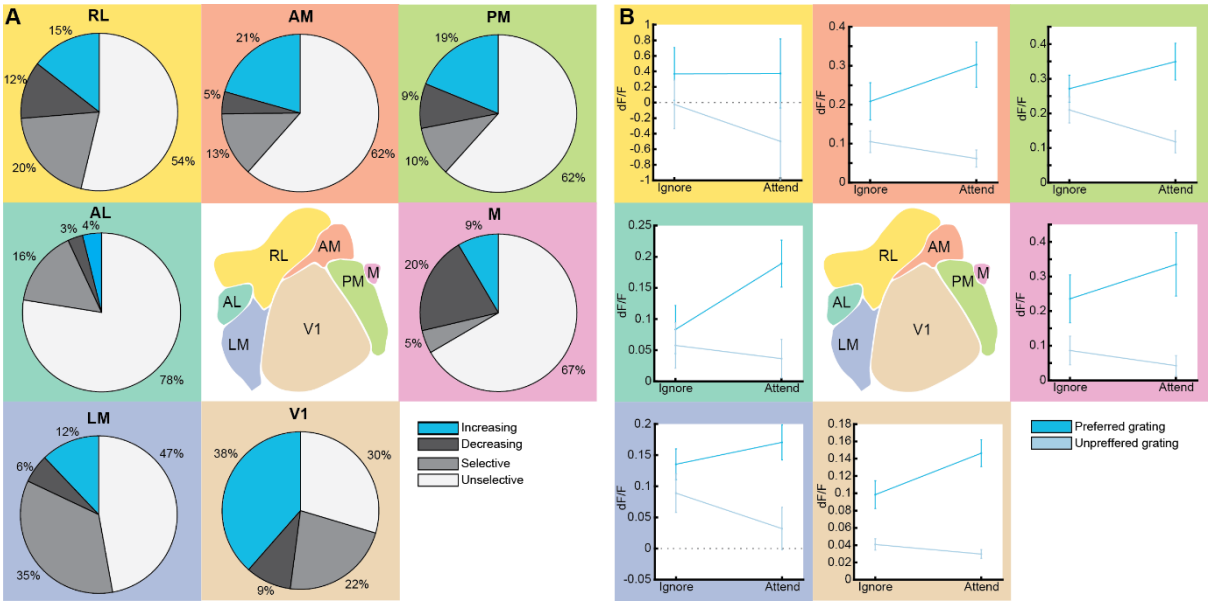

Figure 2.7: Proportions of cells significantly modulated by attention divided by higher visual area.

a) Proportions of neurons for all HVAs and from the same dataset as Figure 2.6, plots are arranged with reference to the central schematic. Increasing - cells that significantly increase their selectivity with attention. Decreasing - cells that significantly decrease their selectivity with attention. Selective - cells that were significantly selective for one of the two visual stimuli, but which did not change significantly with attention. Unselective - cells that were not significantly selective. V1 n=2260 cells, 4 mice; LM n=511 cells 2 mice; AL n=618 cells, 3 mice; RL n=772 cells, 3 mice; AM n=635 cells, 3 mice; PM n=1120 cells, 4 mice; M n=1539 cells, 3 mice. **b)** Saturated blue - mean visual stimulus evoked activity in response to each cells preferred stimulus (averaged 0-1s, baseline subtracted) of all cells that significantly increased their selectivity with attention (the cells making up the respective blue slices in **a**). Unsaturated blue - the same but for responses to the cells unpreferred visual stimulus. Plots are arranged with reference to the central schematic. V1 n=869 cells, 4 mice; LM n=62 cells 2 mice; AL n=24 cells, 3 mice; RL n=109 cells, 3 mice; AM n=132 cells, 3 mice; PM n=207 cells, 4 mice; M n=132 cells, 3 mice.

2.2.7 – Changes in selectivity with attention in higher visual areas are not accounted for by running and licking behaviour

The behavioural controls reported earlier in figure 2.4 were performed on the larger dataset of recording from V1 of VIP-cre mice. The results from that dataset cannot necessarily be assumed to be true in other visual areas. I performed some of the same controls on the three areas that were positively modulated by attention. AM and PM had no correlation between the change in selectivity and the proportion of explainable variance accounted for by recorded running and licking behaviour (Fig. 2.8c,e, PM $r(1118)=-.001$, $p=.981$; AM $r(632)=-.061$ $p=.122$). The neurons recorded in V1 of the HVA mice had a significant negative correlation between change in selectivity and proportion of model R^2 change with behaviour meaning neurons with larger attentional changes appear less accounted for by behaviour (Fig. 2.8a, V1 ($r(2258)=-.053$. $p=.012$). After filtering to retain the 50% of cells that were least effected by behaviour, all three areas still had significant increases in the absolute selectivity with attention (Fig. 2.8b,d,f).

I also performed the same analysis for area M to examine whether the unreliable result of decreased absolute selectivity with attention could be accounted for by behaviour. M also had no correlation between the effect of removing behaviour from the model and change in selectivity with attention (Fig. 2.8g, M $r(1537)=-.041$. $p=.105$)). Filtering for the least

behaviourally effected half of cells also retained a significant reduction in absolute selectivity with attention (Fig. 2.8h). From these results we can conclude that the changes in selectivity of HVAs when attending to visual stimuli in this task cannot be readily accounted for by behaviour.

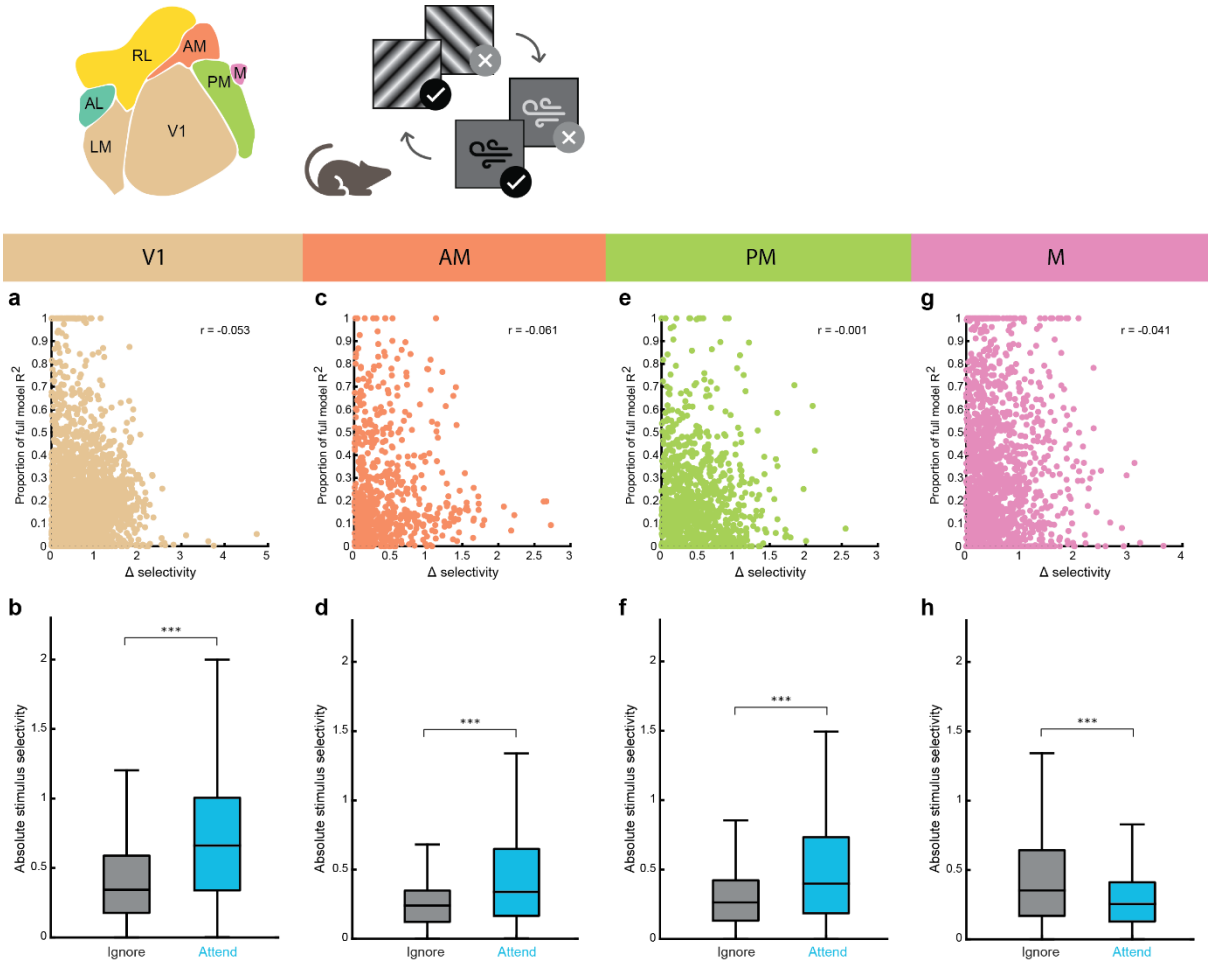

Figure 2.8: Attentional modulation in HVAs is also not explained by the mouse's running and licking.

a) For all cells recorded in V1, cells with stronger influence of running and licking do not account for attentional modulation. Absolute change in selectivity for the visual stimuli with attention (Delta selectivity) plotted against the reduction in R2 when removing running and licking behaviour information from a ridge regression model predicting the activity of each neuron: 1 - (no-behaviour model R2)/(full model R2). Larger values indicate a greater influence of running and licking. **b)** For cells recorded in V1 (4 mice). Average absolute stimulus selectivity during the ignore and attend conditions (n = 2260 cells) when taking only neurons whose activity is least influenced by running and licking behaviour (bottom 50% of the median change in model R^2, n = 1130 cells, p = ~0). **c-d)** Same as **a,b** but for data recorded from area AM (3 mice). **c**, n = 635 cells. **d** n = 317 cells, p = 2.75×10^{-15}. **e-f)** Same as **a,b** but for data recorded from area PM (4 mice). **e**, n = 1120 cells. **f** n = 560 cells, p = 1.02×10^{-10}. **g-h)** Same as **a,b** but for data recorded from area M (3 mice). **g**, n = 1539 cells. **h** n = 769 cells, p = 2.13×10^{-16}.

2.2.8 – Health of recording site across visual areas

A different number of active ROIs were identified in different visual areas despite the imaging field-of-view being the same size. One possibility is that the difference in the number of significantly attentionally modulated cells is due to the number of well recorded cells in each area. Recording sites were excluded from analysis based on blurry images or blebbing and other signs of poor health, but to assess whether differences in quality of recording site might account for the differences I have found here I attempted to quantify the health of the sites included in analysis.

The number of manually counted cells showing nuclear GCaMP6s fluorescence (a sign of cells being unhealthy) across the full volume (450 x 450 um FOV, 6 planes) – varied between 5 and 35 cells (Fig 2.9a). Although area M had the highest number of filled cells there was no clear pattern of significantly attentionally modulated regions having a lower number of filled cells. Therefore, using this marker, poor cell heath due to the calcium indicator does not seem to be varying systematically according to region. Cells could also show nuclear filling because of the elongated axial PSF and a lack of alignment between the centre of the cell and the imaging plane. There are more markers of cell health than nuclear filling and it would be valuable to develop a standardised scoring system to track and compare the health of recording cites.

The quality of imaged ROIs may be varying systematically even if obvious markers of health are not – to quantify this I tried to identify cells that had clear strong cytoplasmic fluorescence and no nuclear fluorescence – “good donuts”. For each ROI I calculated the Euclidean distance of each pixel from the centre of the ROI. I then calculated the mean fluorescence in the 20% of pixels that were furthest from the centre of the ROI and compared it to the mean fluorescence for the 20% of pixels that were closest to the centre (Fig 2.9b). ROIs were then classified as high quality if they had an outer fluorescence that was greater than the centre by one standard deviation. I found that V1 had the highest percentage of good donuts with all higher visual areas apart from AM and LM having significantly fewer good donut shaped cells than V1 (LM $X^2 = 4.49$, df = 1, p = .068; AL $X^2 = 41.03$, df = 1, $p = 5.99 \times 10^{-10}$; RL $X^2 = 76.27$, df = 1, $p < 1 \times 10^{-10}$; AM $X^2 = 2.50$, df = 1, p = .114; PM $X^2 = 13.72$, df = 1, $p = 6.37 \times 10^{-4}$; M $X^2 = 278.59$, df = 1, $p < 1 \times 10^{-10}$) (Fig 2.9c). Additionally, I found a substantial but not significant

positive correlation between the percentage of “good donut” cells in an area and the percentage of cells that significantly enhanced their selectivity with attention (Fig 2.9d, $r(5) = 0.661$, $p = .106$, $n = 7$ areas, 22 sessions 4 mice). To investigate whether the good donut cells are the source of the attentionally modulated neurons I plotted the overlap in the groups (Fig 2.9e). All recorded areas had substantially more good donuts than significantly attentionally modulated cells and for all areas a substantial portion of its significantly attentionally modulated cells were not classified as good donuts. Suggesting that the quality of the imaging site is unlikely to be the primary indicator of attentionally modulated neurons and/or that the “good donut” measure of site quality needs further refinement.

One potential source of the variation in the number of well recorded cells may be the use of a flat cranial window against a curved brain surface. Future investigations will be required to establish whether these differences can be mitigated by changes to surgical technique or whether there is an alternative source of variation such as preferential GCaMP expression in different brain regions for these transgenic mice. Repeats of these experiments which equalise quality across recording sites, for example by centring the window on lateral higher visual areas or using a curved window – assuming of course that this is the source of the variation, could establish whether the differences in attentional modulation found here can be in part attributed to variation in the number of high-quality ROIs recorded.

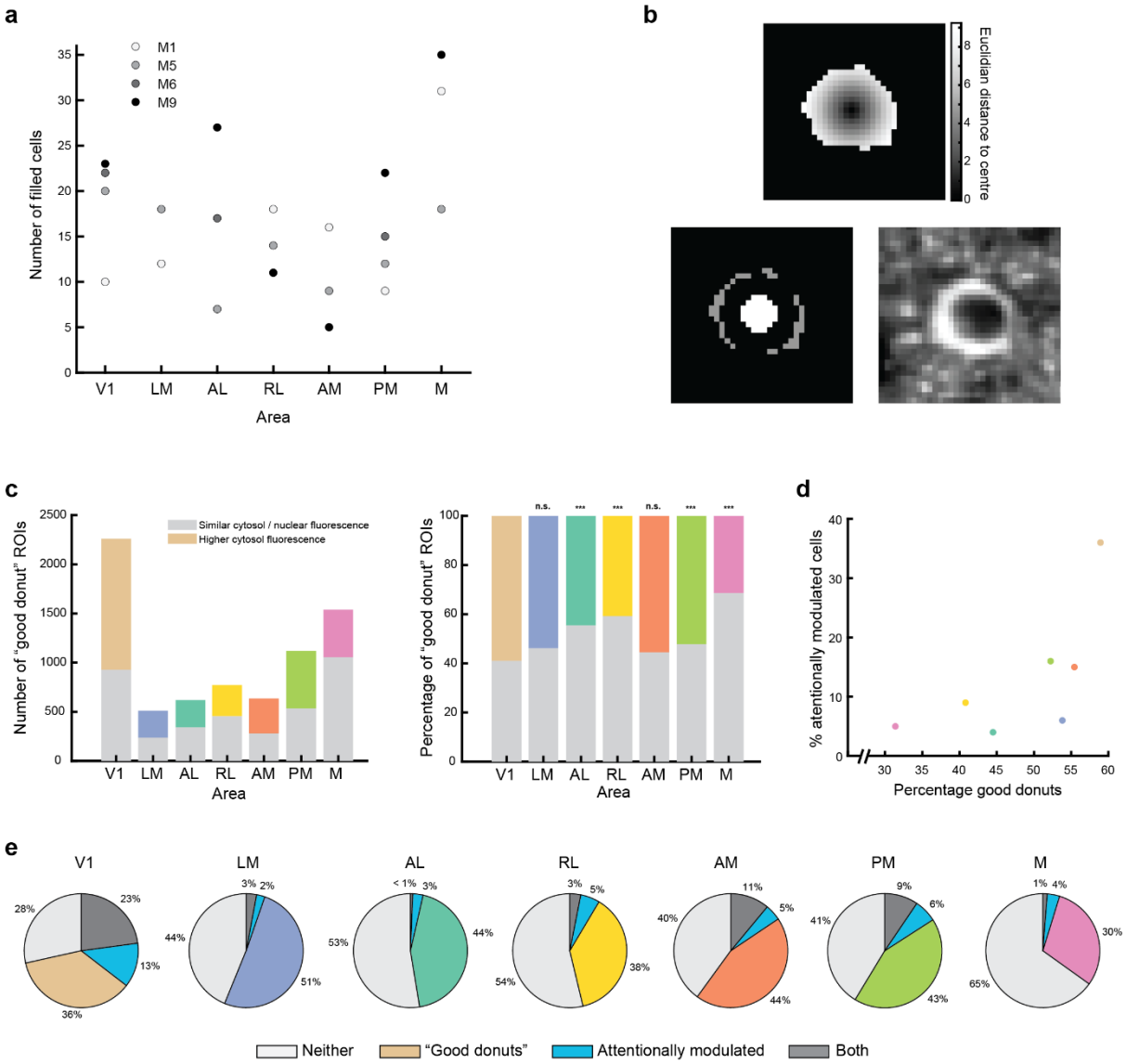

Figure 2.9: Differences in patterns of GCaMP6s expression across recorded higher visual areas

a) Numbers of manually counted cells with nuclear filled GcaMP6s across all 6 recording planes at each recording site and for each mouse. **B)** Top – Euclidean distance of each pixel within an example ROI from the centre of that ROI. Bottom left – The furthest 20% and closest 20% of pixels from the ROIs centre. Bottom right – The mean image of the fluorescence signal centred on the example ROI. **C)** Left – the proportion of cells which had a mean fluorescence for outer pixels greater than the mean fluorescence of the inner pixels by at least 1 standard deviation. Right – the same data as left but as percentages of the ROIs recorded for that visual area. *** = p<0.001, see text for details. **d)** Scatter of the percentage of cells that were good donuts within a visual area, compared to the percentage of cells that significantly enhanced their selectivity with attention (bootstrap test of significance change, p values corrected using the Benjamini-Hochberg procedure with FDR = 0.05). e) Pie charts of the percentage of cells within each visual area that were identified as good donuts, that significantly enhanced their selectivity (same statistical test as described in **d)** or that were both or neither of the above. (V1

n=2260 cells, 4 mice; LM n=511 cells 2 mice; AL n=618 cells, 3 mice; RL n=772 cells, 3 mice; AM n=635 cells, 3 mice; PM n=1120 cells, 4 mice; M n=1539 cells, 3 mice).

2.2.9 – Increases in selectivity with attention are reduced with rising perceptual difficulty

Increasing task demands have previously been shown to promote top-down modulation (Norman et al., 2022). I examined the effect of varying the difficulty in this task by changing the orientation difference between the pairs of discriminated visual stimuli. Mice were presented with interleaved trials of visual gratings coming from 3 different difficulties (30° - data in previous figures, 20° and 10° difference) (Fig 2.10a). V1 had a significant decrease in the selectivity change with attention at harder orientations, seemingly primarily driven by a lack of change in the attend condition. Two-way ANOVA results in the table below for the effect of difficulty (Orientation difference) and attention on stimulus selectivity.

PM and AM also had a significant effect of orientation on selectivity but had more similar selectivity differences across difficulties than V1, showing a dip primarily for 10°. Area M which had shown a significant reduction in selectivity with attention when looking solely at 30° (Fig. 2.6) does not have significant main effects for attention or difficulty when considering trials of all difficulties (Two-way ANOVA results below), bringing into question the robustness of the reduction in selectivity of this area. RL, LM and AL which did not have a significant change in selectivity with attention for 30° (Fig. 2.6) also did not have a significant effect on selectivity of attention or interaction of attention with difficulty. However, all three of these regions had a significant effect of the orientation differences alone on their selectivity.

One possible explanation is that the greater perceptual difficulty causes smaller changes in selectivity because the mice perform the task more poorly, and a larger number of incorrect trials included within the analysed pool is corrupting the results for the more difficult orientations. However, restricting the analysis to only correct trials did not alter the pattern of results, so this seems unlikely (Two-way ANOVA for results on selectivity in V1 using only correct trials: attention $p=6.24\times10^{-33,}$ orientation p=~0, interaction $F(1, 13554) = 25.481$, $p=9.00\times10^{-12}$).

Table 2.2: Two-way ANOVA results for the effect of visual stimulus orientation difference and attention on selectivity.

Area	Attention	Difficulty (orientation difference)	Interaction
V1	$p=1.79x10^{-22}$	p=~0	$F(1, 13554) = 35.090, p=6.31x10^{-16}$
LM	p=0.700	$1.31x10^{-05}$	F(1,3062)=0.325 p=0.569
AL	p=0.553	$p=3.64x10^{-04}$	F (1, 2213)=0.331 p=0.565
RL	p=0.126	$p=5.09x10^{-21}$	F (1, 4628)=0.677 p=0.411
AM	$p=7.32x10^{-7}$	p=0.017	F(1, 3806) = 1.012 p=0.314
PM	p=0.643	$p=1.98x10^{-11}$	$F(1, 6081) = 17.148, p=3.51x10^{-5}$
M	p=0.610	p=0.918	F(1, 8934) = 0.009, p=0.924

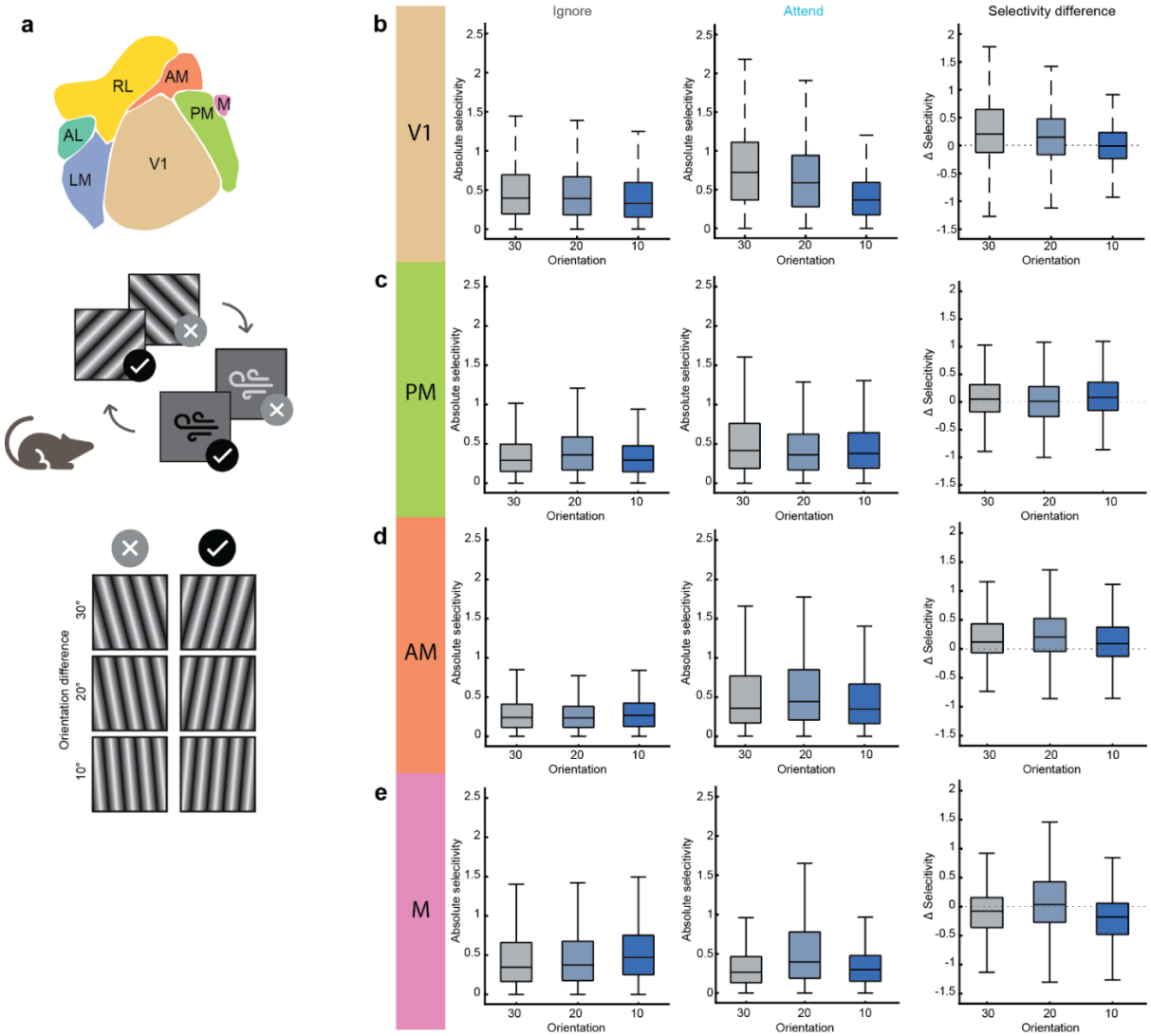

Figure 2.10: Selectivity as a function of orientation difference between the task visual stimuli.

a) Schematic of higher visual areas with colour code, and visual stimulus difficulties. **b)** Absolute population selectivity in V1 when ignoring visual stimuli of different orientation differences (left), absolute selectivity of the population when attending to visual stimuli of different orientation differences (middle), and the differences in selectivity with attention for the different orientation differences (attend - ignore) (right). n = 2260 cells, 4 mice. **c)** Same as in **b** but for data from area PM, n = 1120 cells, 4 mice. **d)** Same as in **b** but for data from area AM, n = 635 cells, 3 mice. **e)** Same as in **b** but for data from area M, n = 1539 cells, 3 mice.

It is possible that the change in selectivity of the population with attention might be diminished because fewer cells are selective for the harder difficulties, because of the increasing similarity of the rewarded and unrewarded stimuli. Unselective cells could therefore dampen the signal, even if a similar proportion of selective cells are attentionally modulated. This doesn't seem to be the case in V1, the proportion of unselective cells increases with difficulty, but there is also a decrease in the proportion of selective cells that increase their selectivity with attention (55.1% at 40°, 42.6% at 30°, 18.5% at 20°, Fig. 2.11a). Area PM (Fig. 2.11b) has a similar pattern to V1, while a simple trend for area AM is not clear (Fig. 2.11c).

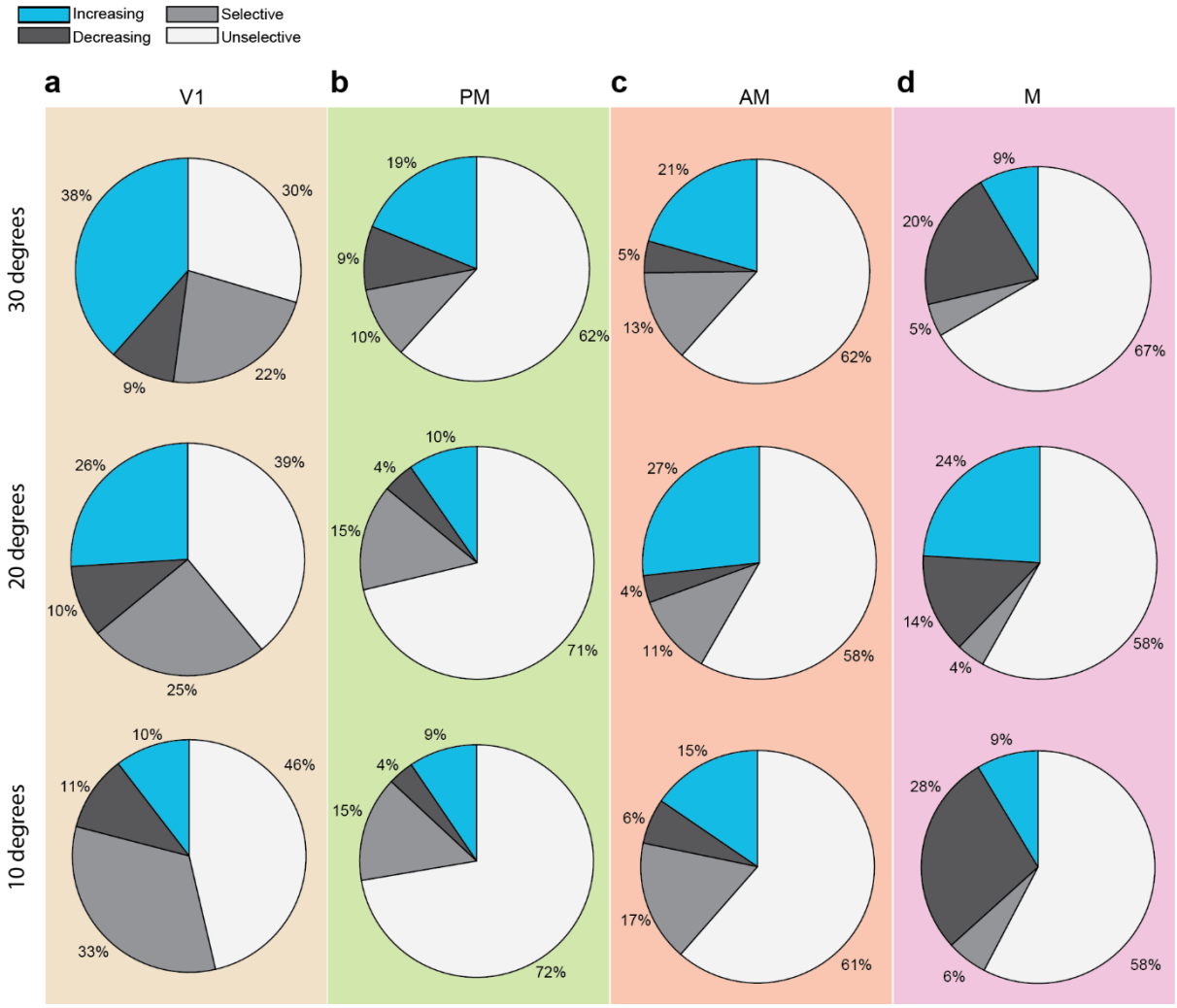

Figure 2.11: Proportions of cells significantly modulated by attention across different task difficulties.

a) Proportions of V1 neurons displaying significant selectivity or significant changes in selectivity with attention across different orientations with interleaved stimuli. Increasing - cells that significantly increase their selectivity with attention. Decreasing - cells that significantly decrease their selectivity with attention. Selective - cells that

were significantly selective for one of the two visual stimuli, but which did not change significantly with attention. Unselective - cells that were not significantly selective. n=2260 cells, 4 mice. **b)** Same as in **a** but for neurons in PM n=1120 cells, 4 mice. **c)** Same as in **a** but for neurons in AM n=635 cells, 3 mice. **d)** Same as in **a** but for neurons in M n=1539 cells, 3 mice.

An alternative explanation is that the interleaved trial structure imposes uncertainty about the perceptual decision being made (Kepecs et al., 2008; Zariwala et al., 2013) and the top-down signal enhancing selectivity is weaker or biased towards the most clearly separated gratings. Therefore, I recorded from V1 in mice performing the same attention switching task but discriminating between only one orientation pair in a single day. In these mice the change in absolute selectivity of the population was significant at all three orientations tested: 40° (Median ignore=0.312, Median attend=0.504, n = 1693 cells, $p = 9.19x10^{-10}$, Fig. 2.11a), 30° (Median ignore=0.292, median attend=0.328, n = 2090 cells, $p = 1.39x10^{-6}$, Fig. 2.11b) and 20° (Median ignore=0.188, median attend=0.385, n = 1629 cells, p = ~0, Fig. 2.11c), and the change in population selectivity was comparable at 40° and 20°. I was unable to record from 10° orientation difference in these mice as the task becomes too difficult and the mice demotivated. The attentional modulation does not decrease with difficulty when the same stimuli are presented for an entire session. Additionally, session-wise presentation of different orientations also showed a decrease in the total proportion of selective cells in V1. However, unlike the interleaved visual stimulus presentation, the proportion of selective cells that significantly enhance their selectivity with attention does not follow the same trend (47.5% at 40°, 32% at 30°, 54.8% at 20°, Figure 2.12d-f). Suggesting that the two different task structures and the predictability of visual stimuli are interacting differently with the attentional modulation of stimulus selectivity.

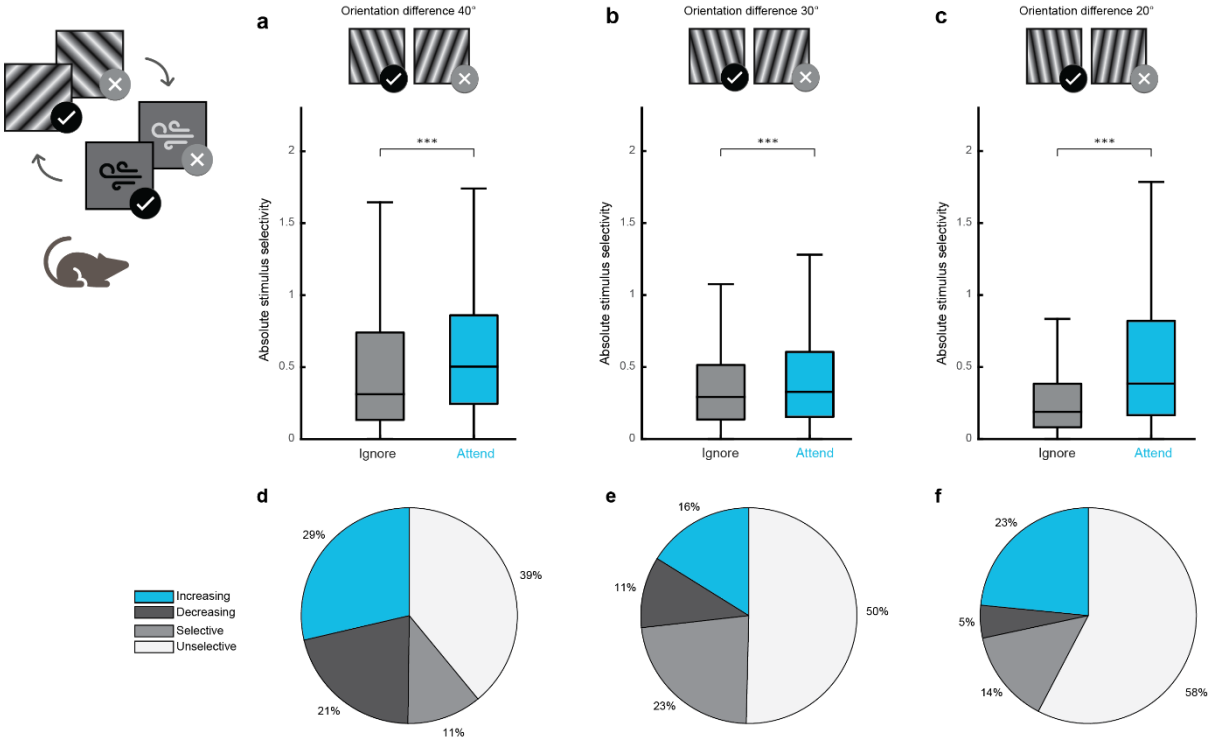

Figure 2.12: Stimulus selectivity does not decrease with difficulty when only one pair of orientations is presented per session.

a) Average absolute stimulus selectivity during the ignore and attend conditions at 40° orientation difference (n = 1693 cells, 4 mice, $p = 9.19 \times 10^{-10}$). **b)** Same as in **a** but for 30° orientation difference trials (n = 2090 cells, 4 mice, $p = 1.39 \times 10^{-6}$). **c)** Same as in **a** but for 20° orientation difference trials (n = 1629 cells, 4 mice, p = ~0). **d)** Proportions of V1 neurons displaying significant selectivity or significant changes in selectivity with attention for 40° orientation difference visual stimuli. Increasing - cells that significantly increase their selectivity with attention. Decreasing - cells that significantly decrease their selectivity with attention. Selective - cells that were significantly selective for one of the two visual stimuli, but which did not change significantly with attention. Unselective - cells that were not significantly selective. n = 1693 cells, 4 mice. **e)** Same as in **d**, but for 30° orientation difference visual stimuli, n = 2090 cells, 4 mice. **f)** Same as in **d**, but for 20° orientation difference visual stimuli, n = 1629 cells, 4 mice.

One might expect the differences in attentional modulation across the different stimulus pairs observed here to be accompanied by corresponding changes in behavioural performance. For interleaved trials there is a difference with difficulty, a two-way ANOVA of the effects of block type and visual stimulus difficulty on behavioural d', reveals a significant effect for both (block type $p = 6.00 \times 10^{-20}$, difficulty $p = 5.42 \times 10^{-07}$), but no interaction ($F(2,114) = 0.652$, $p = 0.322$) (Fig. 2.13a). However, multiple comparisons tests show that performance at 20° and 30° was similar, which suggests that differences in selectivity at these orientations are not due to

differences in behaviour. To further examine whether the differences in stimulus selectivity are associated with the changes in behaviour, I took the recordings from areas which were significantly modulated by attention (V1, PM and AM. n= 4 mice, 11 sessions total) and compared the behavioural d' in stable visual block trials to the average absolute selectivity of the neural population during those trials for 10° and 20° orientation differences individually. For neither 10° ($r(9) = -.282$, $p = .430$) nor 20° ($r(9) = -.596$, $p = .069$) was there a significant correlation between selectivity of the population and behavioural d', suggesting that changes in behaviour do not account for the differences in selectivity at different task difficulties.

For session-wise presentation of visual stimulus pairs, mice performed the task well at all 3 orientations with behavioural d' above 2 when the visual stimuli were relevant to the task. Statistical comparisons are not reported here as they are unreliable due to a small number of sessions (n=4), so further investigation would be required to properly quantify the differences between session-wise and interleaved behavioural performance.

The discrepancy between selectivity differences on interleaved and non-interleaved trials observed in this task might be similar to the effect observed by Zariwala et al., 2013. They found that when the odour stimuli on trials were predictable (came from a smaller possible set) there was an improvement in performance beyond that achievable by additional sampling time. Additionally, one can hypothesise that top-down modulations may be stronger when the stimuli they are enhancing are more predictable.

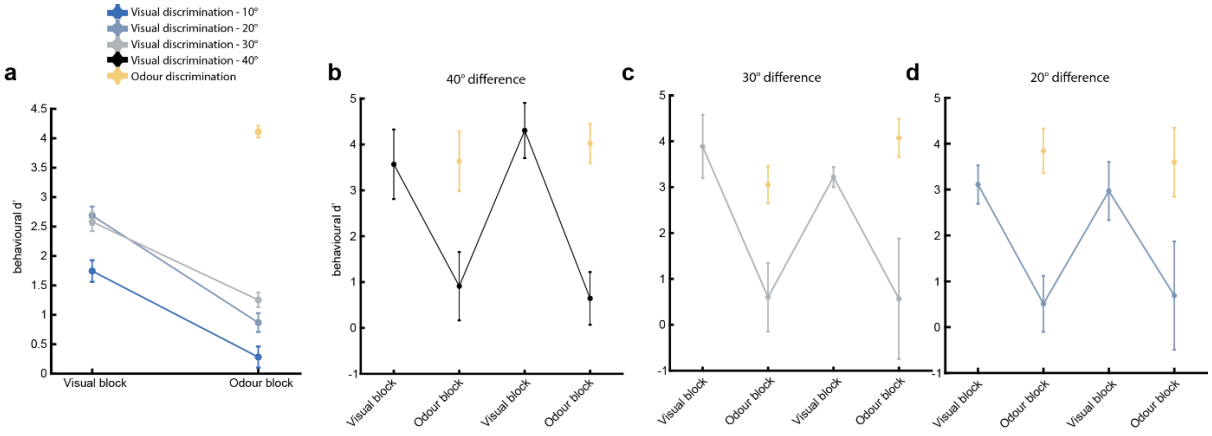

Figure 2.13: Behavioural discrimination for interleaved and session wise visual stimulus difficulties.

a) Behavioural discrimination performance (behavioural d') across attention (n = 22 sessions, 4 mice). Connected points indicate visual discrimination, individual points in the odour block represent olfactory discrimination. Different coloured lines show the average of all sessions at different visual discrimination difficulties. Error bars

indicate s.e.m. **b)** Same as in **a** but for sessions in which only 40° orientation difference visual stimuli were presented (n = 4 sessions, 4 mice). **c)** Same as in **a** but for sessions in which only 30° orientation difference visual stimuli were presented (n = 4 sessions, 4 mice). **d)** Same as in **a** but for sessions in which only 20° orientation difference visual stimuli were presented (n = 4 sessions, 4 mice).

2.3 - Discussion

The primate visual system has a hierarchical organisation (Felleman and Van Essen, 1991) as does that of the mouse (Siegle et al., 2021). Studies in humans and non-human primates show that attentional modulation increases as it ascends the cortical hierarchy, which we might expect to also see in mice (Mehta et al., 2000a; Buffalo et al., 2010; Martin et al., 2019). Using a cross-modality attention switching task and two-photon calcium imaging I have replicated the attentional modulation previously observed in mouse primary visual cortex (Poort et al., 2015, 2022; Khan et al., 2018) and found that of the 7 mouse visual cortical areas recorded, contrary to our prediction, V1 has the strongest modulation from attention. Along with V1, areas AM and PM had significant attentional modulations. AM and PM are part of the mouse dorsal visual stream and thus together potentially form an attentionally modulated sub-stream (Wang et al., 2011, 2012; Wang and Burkhalter, 2013; Smith et al., 2017).

2.3.1 – Differences in network organisation may explain differences in attentional modulation of V1 in mouse and primate.

The relative strength of attentional modulation in mouse V1 compared to primate V1 might be partially explained by fundamental differences in the organisation of their visual cortices. Perhaps unsurprisingly given primates increased reliance on vision over olfaction, rodents have fewer hierarchical levels in their visual system (Coogan and Burkhalter, 1993; D'Souza et al., 2020). The connections between points in the hierarchy are also distinct: while the only other visual areas macaque V1 projects to directly are V2, V3, V4 and middle temporal area MT (Felleman and Van Essen, 1991), mouse V1 projects to all visual areas (Wang et al., 2012; Gămănuţ et al., 2018).

Mouse V1 may also have a greater direct influence on non-visual brain areas than primate V1. Rodent V1 connects to a variety of cortical areas that are not directly connected to V1 in monkeys (Vogt and Miller, 1983; Miller and Vogt, 1984; Reep et al., 1994, 1996; Burwell and

Amaral, 1998). In addition, the mouse primary visual cortex receives more cross-modal projections from other primary cortices than in the primate (Clavagnier et al., 2004; Charbonneau et al., 2012). Mouse V1 may therefore be incorporating properties which are left to higher areas in the monkey visual stream, perhaps due to parcellation of primate cortex into a larger number of distinct functional areas (Laramée and Boire, 2015).

2.3.2 – Areas AM and PM may form part of an attentionally modulated visual sub-stream

It is interesting that of the higher visual areas only PM and AM were significantly modulated. Area PM receives strong inputs from V1, and PM and AM are strongly connected (Wang et al., 2012; Gămănuţ et al., 2018) making it plausible that the attentional modulation seen in AM and PM is inherited directly from V1.

Mouse visual processing appears to be organised into functional sub-modules. V1 neurons projecting to the same HVAs share the same spatial frequency, temporal frequency, orientation and direction tuning (Glickfeld et al., 2013; Matsui and Ohki, 2013). However, the network of areas is not completely segregated, individual L2/3 V1 neurons project out of V1 to multiple HVAs in non-random combinations suggesting that they simultaneously contribute to the processing of multiple pathways (Han et al., 2018). V1 neurons projecting to AL and PM rarely make local connections to one another in V1 (Kim et al., 2018), reinforcing the idea that visual cortical processing in the mouse is divided up into multiple parallel streams. In addition, layer 5 feedback projections from AL and PM to V1 have distinct tuning preferences and enhance the activity of different populations of V1 neurons (Huh et al., 2018). This restricted recurrent connectivity may allow top-down input to modulate the activity of these streams independently. The data presented here suggests that the V1, PM, AM may constitute an attentional parallel processing stream.

As a potential mechanism supporting this, subcortical modulation - including neuromodulators implicated in attention - can be regionally localised and could differently affect neighbouring parallel pathways. The nucleus basalis is a key source of cortical acetylcholine and enhances visual responses during locomotion and arousal (Hasselmo and Sarter, 2011; Carcea and Froemke, 2013). Pafundo et al., 2016 found that basal forebrain mediated increases in gain were confined to V1 and did not spread to LM.

That AM and PM might be part of a parallel processing stream for attention is supported by earlier reports. PM connects strongly to retrosplenial and secondary cingulate areas (Cg2) (Wang et al., 2012) while AM projects to primary cingulate areas (Cg1) (Wang et al., 2012). In rodents, stimulation of area Cg1 evokes eye movements (Brecht et al., 2004) and AM and parietal areas contribute to spatial memory tasks (Harvey et al., 2012). PM and AM may therefore be analogous to the proposed primate parieto-prefrontal dorsal sub-stream, important for spatial working memory and the initiation and control of eye movements, and which includes areas MT and MST (Kravitz et al., 2011). Attentional modulation has been reported along the primate dorsal visual pathway in areas MT and MST (Treue and Maunsell, 1996) and area MT has been found to display feature-based attentional modulations, with increased gain in direction selective neurons (Treue and Martínez-Trujillo, 1999). This pathway may be especially relevant to attention as it feeds into prefrontal cortex, necessary for the top-down executive control of visuospatial processing.

PM and AM are also indirectly linked to frontal areas, the lateral posterior thalamic nucleus (LP, mouse pulvinar) has 3 anatomically and functionally distinct sub-regions. One of these subregions, the medial LP, receives input near exclusively from anterior cingulate and orbital cortex and along with sending reciprocal feedback connections it projects onto dorsal stream visual areas including AM and PM (Bennett et al., 2019). In addition, activation of LP suppresses V1 neurons and increases feature selectivity (Fang et al., 2020), and silencing of the pulvinar has been found to reduce attentional effects in monkey V4 (Zhou et al., 2016).

2.3.3 – Areas without significant attentional modulation were still responsive to the stimuli

All 7 areas had a substantial number of recorded neurons that were selective for the visual stimuli. However, all recorded higher visual areas had a greater number of unselective cells than V1. This fits with data from De Vries et al., 2020 who surveyed the response properties of neurons in 6 HVAs across L2/3 to L6 and found that in HVAs a greater proportion of neurons do not respond reliably to any stimuli. Perhaps because a larger proportion of neurons in these HVAs are signalling more complex combinations of different sensory modalities, internal states and behaviours (Olcese et al., 2013). However, I observed that the proportion of neurons that increase their selectivity with attention in RL, LM, AL and M is still lower than in

PM, AM and V1 when looking at only significantly selective neurons. One possibility is that the selectivity of some higher visual areas does not significantly change because the signal is high dimensional and distributed across many neurons. To test this, I trained a decoder to distinguish the rewarded and unrewarded stimuli in the attend and ignore conditions based on the activity in V1, AL and M (logistic regression classifier, cross-validated and tested on out of sample data). The decoder performance was not significantly different in the attend and ignore contexts in any of the 3 areas. For V1 and AL this is because the decoder reaches a ceiling of already near perfect performance in the ignore condition. An alternative method will be required to answer this question.

If it is possible for a simple decoder to already reliably distinguish stimuli in the ignore condition, why would the attentional modulation of visual cortex be necessary? A recent study indicates that far greater sensory information is present in V1 than is demonstrated by a mouse's behavioural performance (Stringer et al., 2021). It may be that the attentional modulations are useful in altering the processing by downstream regions of the responses to attended stimuli.

Areas LM and AL are involved in perception of simple visual features such as orientation (Jin and Glickfeld, 2020) and previous measurements have found their average orientation selectivity to be similar to or greater than V1 in nearly all higher visual areas (Andermann et al., 2011; Marshel et al., 2011). Indeed, absolute selectivity in AL was only just significantly greater than the selectivity in V1 in the ignore condition (Wilcoxon rank sum test $p = 0.034$), but LM and AL were not attentionally modulated here.

Different higher visual areas have different stimulus preferences (de Vries et al., 2020). Am I seeing less attentional modulation in some HVAs because they are being presented with non-preferred stimuli? The stimuli used in this task are not tailored specifically to the preferences of any particular region. AL, AM and LM have been found to prefer higher temporal frequencies and lower spatial frequencies while PM prefers higher spatial frequencies and lower temporal frequencies (Andermann et al., 2011; Marshel et al., 2011; Roth et al., 2012). The spatial (0.1 cpd) and temporal frequencies (2Hz) used here are slightly higher than the average preferences found for cells in these areas by Marshel et al., 2011. However, Marshel et al., 2011 perform their mapping in anaesthetised animals, a manipulation which has been

found to reduce average spatial and temporal frequency preferences (Alitto et al., 2011). Andermann et al., 2011 performed a similar study without anaesthesia on only AL, PM and V1 and based on their data the stimuli used here might be expected to drive AL and PM similarly well.

2.3.4 – Attentional modulation decreases with increasing difficulty when difficulties are interleaved

In a different mouse visual attention task, top-down modulation was only found to be involved when task demand was high (Norman et al., 2022). To examine whether changes in difficulty altered the strength of attentional modulation in the attention switching task presented here, I increased the task difficulty by interleaving trials with a smaller angle between the rewarded and unrewarded visual stimuli (making them harder to distinguish from one another). The selectivity of the neural population in both V1 and PM significantly reduced with increasing visual discrimination difficulty and the changes interacted with the attentional modulation, reducing the change in selectivity for the harder stimulus pairs (Fig. 2.10).

I also observed a consistent decrease in selectivity with increasing task difficulty for higher visual areas that were not attentionally modulated. It is therefore possible that the changes in selectivity could simply be due to the properties of the stimulus pairs. Indeed, fewer cells were significantly selective in V1 for the more difficult visual stimulus pairs, but the proportions of significantly attentionally modulated selective cells also decreased (Figure 2.11a). However, recordings from a different group of mice in which different difficulty visual stimulus pairs were presented on a per-session basis rather than interleaved, showed no trend in the changes in absolute selectivity of the population with task difficulty. Although the number of significantly selective cells decreased with difficulty, the proportion of selective cells that were attentionally modulated did not trend downwards as for the interleaved stimulus presentations (Fig. 2.12d-f).

Changes in attentional modulation have been seen to accompany changes in behavioural performance, as in a recent spatial attention task in mice (Speed et al., 2020). My data shows that when visual stimulus trials of different difficulties were interleaved there was a decrease for the hardest pair, but no change for the two difficulties that overlapped with the session-

wise difficulty recordings (Fig. 2.13). It would be interesting to see the results of testing with more mice or across a wider range of difficulties. It would be especially interesting to see whether the results parallel differences that have been reported in the behavioural performance of rats discriminating between the same odour stimuli either in block-wise or interleaved trial designs. Decision accuracy increased when the predictability of stimuli increased, when the number of stimuli the rats potentially had to discriminate between was decreased from 8 to 2, despite no change in performance when varying the amount of time the animal was allowed to sample the stimuli for (Zariwala et al., 2013).

The variation of attentional modulation with perceptual difficulty may be due to the interleaved presentation of visual stimuli increasing the uncertainty about the boundary between rewarded and unrewarded stimuli (Grinband et al., 2006; Kepecs et al., 2008). As uncertainty about the decision boundary increases the specificity of the top-down attentional modulation applied to the circuit could decrease, accounting for the differences in attentional modulation between these two stimulus presentation strategies.

Alternatively, the internal rules the mice are using to perform the task may be different from those that I am anticipating, and an unexpected mechanism may be more parsimonious. Mice may sometimes sub-optimally integrate information for behavioural tasks. In a go/no-go orientation discrimination task the circuit did not discount the distractor stimulus, leaving the mice vulnerable to making systematic behavioural errors when stimuli with systematic differences in orientation are interleaved (Jin et al., 2019). Further experiments will be required to clarify the effects of manipulating task difficulty observed here.

2.3.5 – Caveats and future work

Studies have found larger attentional modulations in the ventral primate visual stream than the dorsal (Mehta et al., 2000a). It may be that the putative mouse ventral stream areas (laterointermediate (LI), posterior (P), or postrhinal (POR)) display attentional modulations, but I was unable to record from them in these mice. Further work could investigate the responses in these regions.

Given previous data showing streams of processing in mouse visual cortex it would be interesting to know whether there is a bias in connectivity to HVAs from V1 based on a neuron's modulation with attention. AL has been reported as a gateway to the visual stream,

but it is less modulated here than downstream areas (Wang et al., 2011; Fehérvári and Yagi, 2016). However, strong direct connections between V1 and the HVAs exist and may be favoured for this computation. Do attentionally modulated neurons in V1 preferentially project to PM and AM?

Primate areas MT and MST which I have discussed as being potentially analogous to mouse areas AM and PM, are involved in the encoding of the motion of objects (Galletti and Fattori, 2018). It may be that we see greater attentional modulation in these areas because of the properties of the stimulus the mouse is being asked to attend to. It would be interesting to see if the dominance of these areas persists when stimulus properties are varied (for example, using static stimuli) in an otherwise identical version of the task. Similarly, is the same pattern of HVAs activated when mice are engaged in a task designed for probing the effects of spatial attention? (Speed and Haider, 2021).

Lastly, changes such as stimulus selectivity have been found to be neural correlates of attention, but an examination of a single metric at the scale of individual neurons is likely insufficient to assess whether an area is involved in a complex behaviour. Like the parable of the blind men and the elephant we are likely receiving information (however accurate) about parts of the phenomenon. The changes in stimulus selectivity could be manifestations of changes happening at the neuronal population level and downstream regions may be reading out this population activity. For example, the same transformation may be applied to all cells in a stimulus specific manner making it visible at the population level but complex to examine at the level of individual cells because of the ways it changes individual tuning curves (Failor et al., 2022). An examination of population activity could provide powerful insights that would not have been possible by observing one neuron at a time, such as (Vyas et al., 2020; Chadwick et al., 2023).

Chapter 3 - Attentional modulation is orthogonal to disinhibition by VIP interneurons in primary visual cortex

3.1 - Introduction

As discussed in the previous chapter, attention enacts significant changes on the way sensory information is processed in cortical circuits. However, the circuit basis of attentional modulation in visual cortex is poorly understood. The cortex contains a diverse array of interconnected GABAergic inhibitory interneurons with a variety of morphological and functional properties; the presence of these cells makes complex dynamics possible within cortical circuits (Markram et al., 2004; Pfeffer et al., 2013; Kepecs and Fishell, 2014; Tremblay et al., 2016; Campagnola et al., 2022). VIP positive cells make up around 15% of all interneurons (Rudy et al., 2011), they are poised to modify cortical activity most saliently through their disinhibition of pyramidal cells by inhibiting SOM positive interneurons (Lee et al., 2013; Pfeffer et al., 2013; Pi et al., 2013). This disinhibitory motif has been found in a range of different brain regions including: sensory cortex (Lee et al., 2013; Pi et al., 2013; Fu et al., 2014; Ayzenshtat et al., 2016; Jackson et al., 2016; Karnani et al., 2016a; Bigelow et al., 2019; Shapiro et al., 2022b), motor cortex (Garcia-Junco-Clemente et al., 2017), prefrontal cortex (Kamigaki and Dan, 2017; Lee et al., 2019) and the amygdala (Krabbe et al., 2019). It opens up interesting computational possibilities (Vogels and Abbott, 2009; Letzkus et al., 2015), potentially performing different functions at different timescales, in the longer term gating the plasticity of inputs onto pyramidal neurons which allows for associative learning among other functions (Krabbe et al., 2019; Williams and Holtmaat, 2019). More relevant for this study, are the effects of VIP activity in the short term, with increased VIP firing positively modulating the gain of local pyramidal cell activity (Letzkus et al., 2015; Guet-McCreight et al., 2020).

The disinhibition of visual cortex through top-down inputs from frontal cortex onto VIP interneurons has been put forward as a core-mechanism of attentional modulation and found to enhance the activity of pyramidal neurons and improve visual discrimination (Zhang et al., 2014). Additionally, a theoretical model employing selective disinhibition has reproduced many of the effects of attention (Sridharan and Knudsen, 2015). This effect is similar to the

suggestion that the increase in gain of visual cortical responses with locomotion (Niell and Stryker, 2010) is mediated by VIP-SOM disinhibition (Fu et al., 2014). The modulatory effect of locomotion itself bears a resemblance to attentional modulation and has even been positioned as a potential surrogate to study the mechanisms of attention (Mineault et al., 2016; Speed and Haider, 2021). Additionally, cholinergic inputs to visual cortex appear important for attentional modulation in V1 (Disney et al., 2007; Herrero et al., 2008; Pinto et al., 2013). VIP interneurons are activated by acetylcholine (Alitto and Dan, 2013), making it possible that VIP interneurons mediate the increase in visual gain with cholinergic signalling during attention (Poorthuis et al., 2014; Gasselin et al., 2021).

V1 activity is clearly modulated by both VIP driven disinhibition and attention, there are two main scenarios for what may happen when both modulations co-exist in the same network. First, as described above they may be aligned, and similar to the effect of contrast and attention in monkey area MT (Martínez-Trujillo and Treue, 2002), attention and VIP activity could transform cortical activity along the same dimension. Alternatively, they may act independently in the network, operating in non-aligned or orthogonal ways on the activity of the same neuronal population. This would be similar to the way in which movement and the representation of visual stimuli have been found to be orthogonal in mouse V1, allowing the encoding of both sets of information without either signal degrading the other (Stringer et al., 2019). However, the relationship between VIP driven and attentional modulations has not been directly investigated.

To investigate these predictions, I applied an all-optical approach in V1, optogenetically manipulating the activity of VIP interneurons to mimic physiological activity levels while simultaneously imaging the activity of PYR, PV, SOM, and VIP cells, in mice performing an cross-modal attention (Disney et al., 2007; Herrero et al., 2008) task. As described in chapter 2, the alternation between attending and ignoring the same visual stimuli induced a robust modulation of V1 visual stimulus responses. The optogenetic activation of VIP interneurons produced a clear enhancement of activity in V1. Identification of SOM interneurons through post-hoc immunolabelling of recordings, revealed that this enhancement is disinhibitory due to a reduction in SOM activity. Conversely, photoinhibition of VIP cells reduced V1 activity. Critically, when VIP manipulations were interleaved with attentional changes the two

modulations did not interact, and even appear to be orthogonal at the level of population activity. In support of this, the two modulations also differed in their effect on the interactions between the recorded interneuron classes and in the direction in which they modulated firing rate. Therefore, the attentional modulation of stimulus selectivity in V1 is not mediated by VIP-SOM disinhibition. These results also add to a body of work proclaiming the versatility of the cortical circuit in its ability to overlay multiple non-interacting signals within the same neural population.

3.2 – VIP activation and attentional modulation do not interact

3.2.1 – VIP activation strongly modulates cortical activity

I tested the hypothesis that VIP interneuron mediated disinhibition is involved in the attentional modulation of V1 neurons discussed in the previous chapter. I expressed the red-shifted excitatory opsin Chrimson in VIP interneurons alongside GCaMP7f non-specifically. This allowed an all-optical approach, photostimulating VIP interneurons whilst recording the activity of VIP and non-VIP neurons in the same patch of cortex. The optogenetic laser light and the monitor displaying the visual stimuli were blanked during the linear phase of each line scan of the two-photon microscope providing near simultaneous optogenetic activation and calcium imaging. This also allowed me to observe the activity of neurons during periods of optogenetic stimulation without correcting for an optogenetic light induced imaging artefact. Additionally, the laser used for excitation of the GCaMP7f did not appear to stimulate Chrimson. To test this, I compared the mean VIP activity over the first second of imaging to the mean activity over the 10th second as that was the latest timepoint in which for all sessions the mouse had not yet initiated a trial. I found no significant difference in VIP activity between these two windows ($p = 0.278$ Wilcoxon signed rank test, $n = 17$ sessions, 7 mice. Median ± IQR, 1^{st} second 1.44 ± 0.87, 10^{th} second 1.18 ± 0.72).

VIP interneurons were first optogenetically excited with no visual stimuli (only grey screens). This served as both a baseline observation for the effect of the optogenetic manipulation and as a calibration session for the selection of the laser powers to be used with visual stimuli. For each recording site I selected a ‘low’ and ‘high’ light power based on the shape of the laser power-response curves generated from the optogenetic laser only session. I chose the highest

power that was below saturation of the average laser evoked VIP cell response and a second power which produced approximately half of the effect of the high power. These laser powers were typically 0.6 mW (low, range 0.5 to 0.6 mW) and 1.5 mW (high, range 1.5 to 2.25 mW). Optogenetic activation of VIP cells produced a robust excitation of both the VIP cell population and the non-VIP neuron population, consistent with VIP's known role as controlling a disinhibitory motif (fig 3.1d). To examine whether the photoactivation of VIP interneurons was within a physiological range I compared the amplitude of their activity during spontaneous locomotion with their activity during photoactivation. Mean VIP interneuron activity with low and high laser power was 1.32 ΔF/F and 1.77 ΔF/F respectively. The average 50th, 75th and 95th percentiles of activity during locomotion without laser for all VIP interneurons was 0.78 ΔF/F, 1.23 ΔF/F, and 2.06 ΔF/F respectively, which confirmed that both laser powers evoked activity in VIP interneurons within the range observed without optogenetic intervention during spontaneous locomotion.

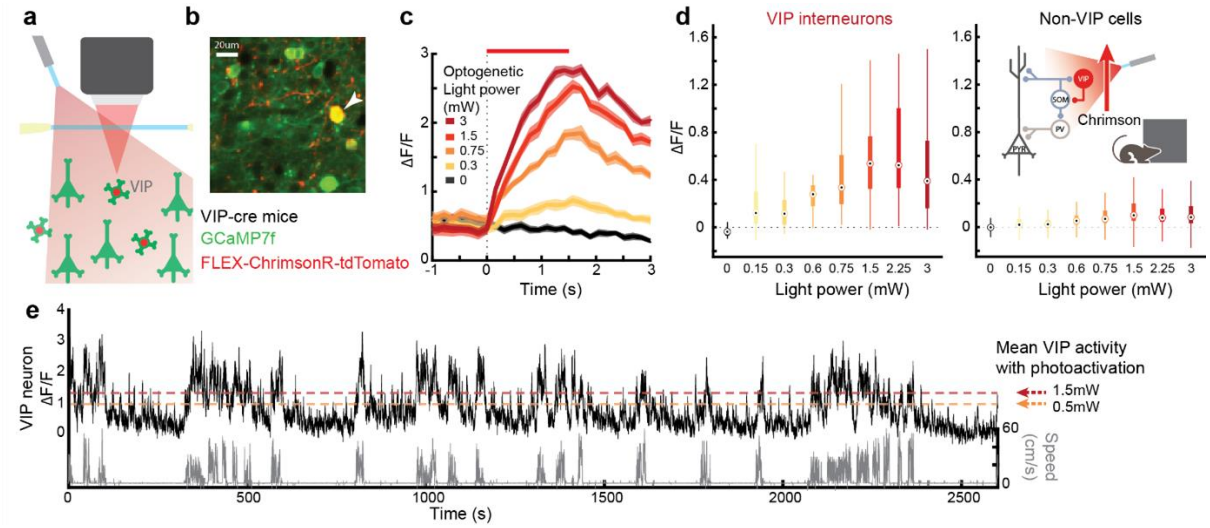

Figure 3.1: VIP activation promotes cortical activity.

a) Schematic of near-simultaneous imaging and optogenetic stimulation. **b)** Example region of an in vivo imaged plane showing all neurons expressing GCaMP7f and a VIP interneuron (arrowhead) additionally expressing Chrimson-tdTomato. **c)** Mean responses of an example VIP interneuron to different light powers. Responses are aligned to optogenetic light onset (dashed line). Red bar indicates optogenetic stimulation duration (1.5s), shading indicates SEM. **d)** Box plots of optogenetically evoked activity (mean 0-1s, baseline subtracted) across different light powers for VIP interneurons (left, n = 91 cells, 6 mice) and non-VIP cells (right, n = 2233 cells, 6 mice). Inset: schematic of the VIP-SOM disinhibitory circuit (studied further below) with VIP interneuron activation during passive grey screen viewing. **e)** Example activity trace showing running evoked activity of an

example VIP interneuron (black) and running speed (grey), dashed lines indicate mean optogenetically evoked activity in VIP interneurons (orange, low power, red, high power).

3.2.2 – VIP activation modulates responses to visual stimuli

After the optogenetic sessions with a grey screen, mice were presented with visual grating stimuli moving in 8 different directions at 45° increments, which they viewed passively. On interleaved trials VIP interneurons were photoactivated during the visual stimulus presentation epoch. I constructed tuning curves for all cells and aligned them according to the preferred direction of each neuron. As expected, VIP interneurons increased their activity at all directions with photoactivation (Fig 3.2a).

Many non-VIP cells showed clear tuning to the visual stimuli alone and their activity was strongly altered by the VIP activation, in most cases increasing their firing rates (Fig 3.2b). The disinhibition of non-VIP cells occurred at all orientations, and by comparing the average responses at each orientation I found that VIP activation caused a primarily multiplicative enhancement in orientation tuned non-VIP cells (Fig. 3.2b, laser response $\sim$ $\beta0+\beta1$(no laser response). Low power: $\beta1=1.568$, $\beta0=0.009$. High power: $\beta1=1.634$, $\beta0=0.032$. n=1044 cells, 8 mice). Control mice with the same laser stimulation but no opsin expression did not show any significant changes in VIP interneuron or non-VIP cell activity, ruling out laser-evoked artefacts at these laser powers (Fig 3.2c,d). Purely multiplicative increases are unlikely to change stimulus selectivity (McAdams and Maunsell, 1999). Therefore, these results suggest that VIP interneurons are not involved in the modulation of stimulus selectivity I observed with attention. However, testing this hypothesis directly necessitates the manipulation of VIP activity during the attention-switching task.

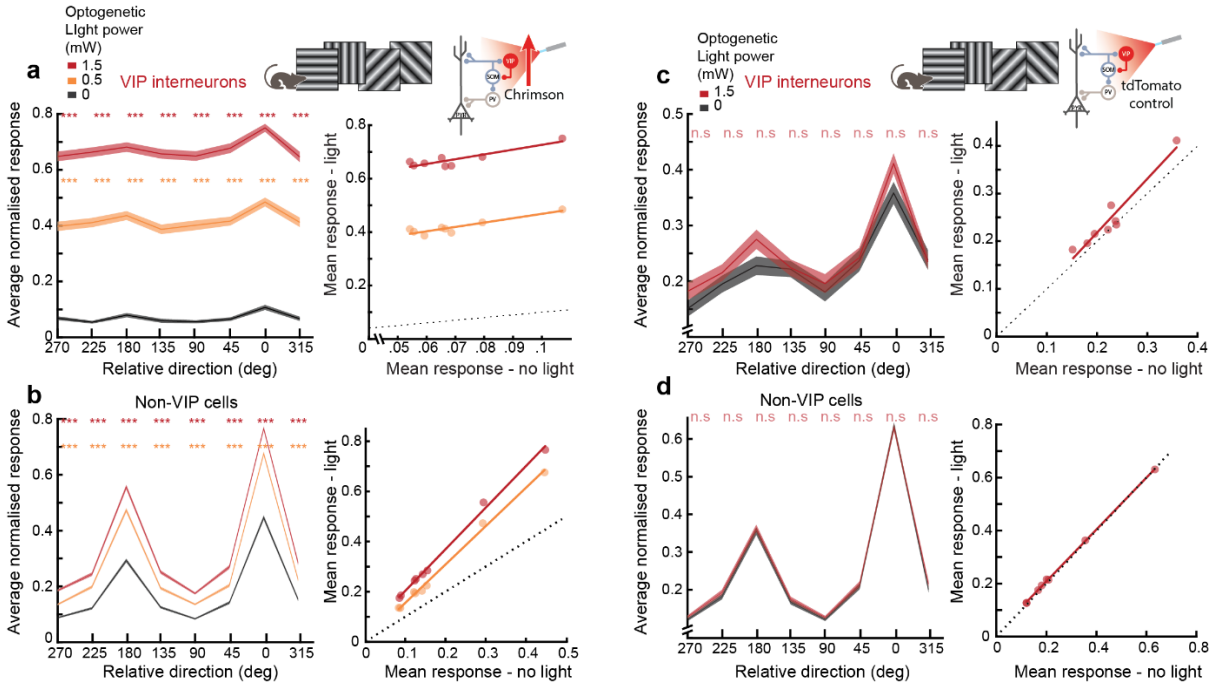

Figure 3.2: VIP activation multiplicatively increases non-VIP visually evoked responses.

a) Left, stimulus evoked normalised activity in response to different oriented drifting gratings, averaged across all VIP interneurons (n = 141 cells) aligned to their preferred direction. ***, p<0.001 Wilcoxon signed-rank test for photoactivation compared to non-photoactivation conditions at each direction, corrected for multiple comparisons. Right, the same data shown as average activity with and without optogenetic light. Linear regression, low power, slope = 1.823, intercept = 0.327. High power, slope = 2.081, intercept = 0.52, 8 mice. **b)** Same as f, for all orientation selective non-VIP neurons, n = 1044 cells. Low power, slope = 1.568, intercept = 0.009. High power, slope = 1.634, intercept = 0.032, 8 mice. **c, d)** Same as **a, b**, for control mice expressing only tdTomato and no opsin, n.s. indicates non-significant, n = 61 VIP interneurons, and 434 non-VIP cells, 3 mice.

3.2.3 – VIP interneuron activity may be more associated with behaviour than attention

I investigated whether VIP interneuron activity was modified by attention. When comparing average activity, I found significantly higher pre-stimulus activity in the attend condition than in the ignore condition (Fig. 3.3a). However, as VIP interneurons activity is correlated with locomotion it seems likely that this difference is due to changes in behaviour as the pre-stimulus average running speed also increases from the ignore to the attend condition (Fig. 3.3b). Indeed, I also found that changes in selectivity of VIP interneurons correlate with how much of their activity can be explained by behaviour (Fig. 2.4c). When correcting for pre-

stimulus differences, the average stimulus evoked VIP cell activity has no difference between the ignore and attend conditions or between visual stimuli within those conditions (Fig. 3.3c). Further indication that VIP interneurons are unlikely to be mediating the attentional modulation of V1.

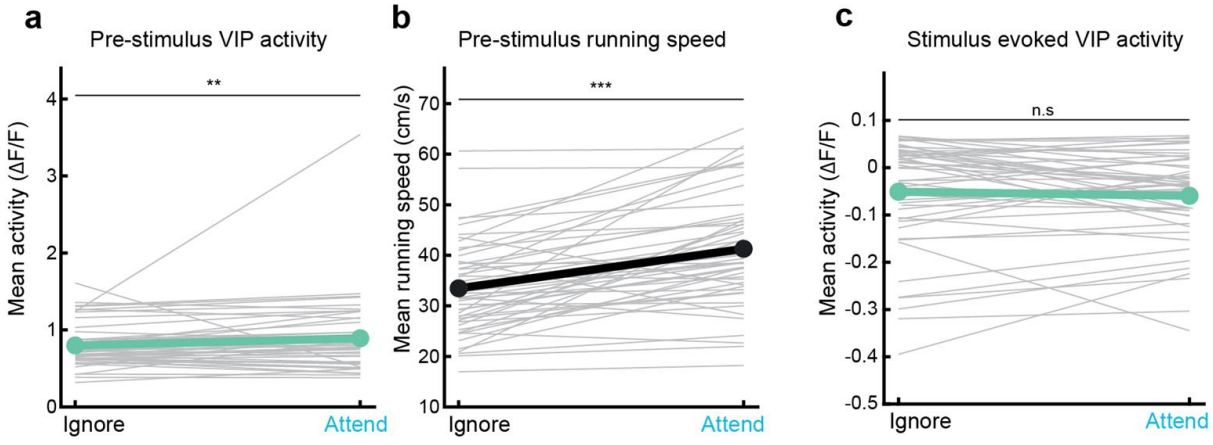

Figure 3.3: Changes in VIP interneuron activity with context accompany changes in behaviour.

a) Average pre-stimulus VIP interneuron activity -0.1 to -1s relative to visual stimulus onset in the ignore and attend conditions of the task. Grey lines are the individual session averages, coloured lines are the overall average (**, $p < 0.01$, n = 50 sessions, 15 mice). **b)** Average running speed -0.1 to -1s relative to visual stimulus onset in the ignore and attend conditions of the task. Grey lines are the individual session averages, coloured lines are the overall average (***, $p < 0.001$, n = 50 sessions, 15 mice). **c)** Average stimulus evoked VIP interneuron activity 0-1s after visual stimulus onset (baseline subtracted) in the ignore and attend conditions of the task. Grey lines are the individual session averages, coloured lines are the overall average (n = 50 sessions, 15 mice, n.s. indicates not significant).

3.2.4 – VIP activation during attention-switching

To examine whether VIP-driven modulation underlies the attentional modulation described in chapter 1, I photoactivated VIP interneurons in randomly interleaved trials while mice performed the attention-switching task (Fig. 2.1). The optogenetic laser was switched on 100ms before the visual stimulus onset and turned off 1.5s into the visual stimulus presentation. During the first 1.5s of visual stimulus presentation the mouse licking cannot elicit a reward. This time-period was therefore chosen for the optogenetic manipulation to avoid contaminating the effect of the optogenetic manipulation with behavioural effects of consuming the reward- there was no effect of photoactivation on the mouse's behaviour; this

was likely also because the optogenetic manipulation was uni-hemispheric and activity in the other hemisphere was unperturbed (Fig. 3.4). Unperturbed behaviour was important because any neural changes observed with optogenetic stimulation could not be due to gross changes in behaviour or performance accuracy. As in the passive viewing condition, the activity of VIP and non-VIP cells was increased with increasing light power both when the visual stimuli were attended and when they were ignored (Fig 3.5b).

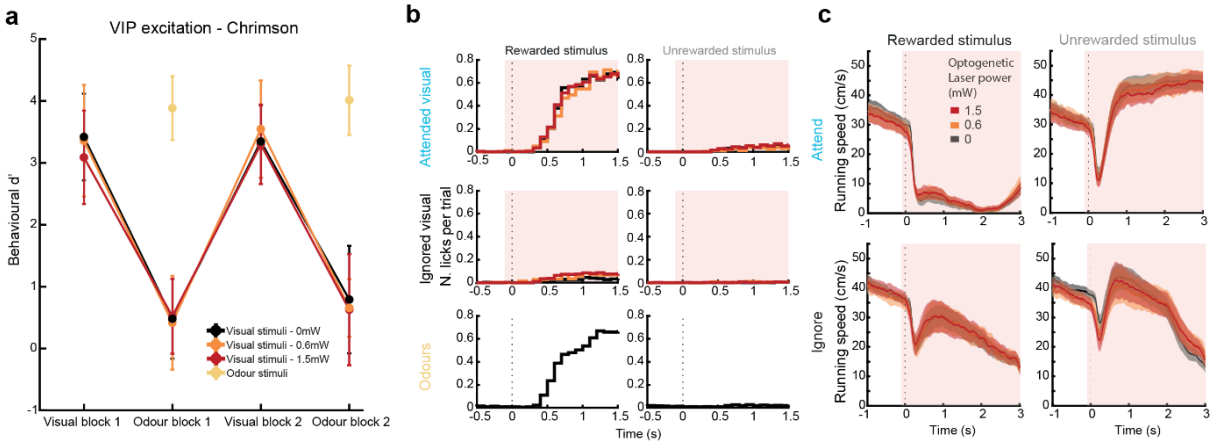

Figure 3.4: No change in behaviour with VIP photoactivation.

a) Behavioural d' for visual and odour stimuli across the first 4 blocks of attention switching, shown separately for different optogenetic light powers, for mice expressing the excitatory opsin Chrimson in VIP interneurons. No changes were observed in the discrimination accuracy of visual or odour stimuli with optogenetic light. Wilcoxon signed-rank tests comparing visual stimulus no light and light trials: low power, visual block p = 0.801, odour block p= 0.461; high power, visual block p = 0.167, odour block p = 0.958. Error bars indicate SEM. N = 17 sessions, 7 mice – same sessions for **a**, **b** and **c**. **b)** Average number of licks per trial aligned to stimulus onset for each of 6 trial types, with trials divided according to optogenetic light power (same colour legend as **a**). Licks shown in response to the visual stimuli in the visual block (top), visual stimuli in the odour block (middle), and odour stimuli (bottom), split into the stimulus rewarded in the relevant block (left) and unrewarded stimulus (right). Light red shading indicates light onset. **c)** Average running speed at different optogenetic laser powers aligned to visual stimulus onset (dashed line) in the visual block (top) and odour block (bottom). Split into rewarded stimulus (left) and unrewarded stimulus (right). Shaded areas indicate s.e.m. Light red shading indicates light onset.

To determine whether the optogenetic and attentional modulations were acting through the same mechanism, I selected neurons which showed a significant increase in stimulus selectivity with attention and plotted their response amplitudes to the two grating stimuli in

the ignore and attend conditions (Fig. 3.5c shows neurons with a preference for the unrewarded stimulus, similar results are seen for neurons which prefer the rewarded stimulus, data now shown). The responses of this group of neurons were affected by both attention and VIP activation. Increasing VIP photoactivation produced an even increase in the average activity (0 to 1s) of this population for both visual stimuli in both the attend and ignore conditions (Fig. 3.5d). A two-way ANOVA found significant main effects for both attention and laser on the responses for the rewarded stimulus, but no significant interaction effect between the two. Similarly, no interaction between VIP activation and attention was found for responses to the unrewarded stimulus or for cells that increased selectivity with attention, but which preferred the rewarded stimulus (See table below for all two-way ANOVA results). In control mice which expressed tdTomato but no opsin in VIP interneurons, there was no main effect from the optogenetic laser and no interaction between laser delivery and attention on the mean responses of cells that increased their selectivity with attention (Fig. 3.5e, see table below for results).

Although I found no interaction between attention and VIP activation on stimulus evoked responses, I next checked if VIP activation in the attend or ignore condition changed stimulus selectivity (Fig. 3.5f, see table below for statistics). Not only might we expect an increase in selectivity if VIP disinhibition was producing the attentional modulation, but we would likely also expect this effect to be attenuated in the attend condition for cells that increase their selectivity with attention, as they have already been enhanced. A two-way ANOVA on the data in Fig. 3.5f (all non-VIP cells which significantly increased their selectivity with attention) found a significant main effect on selectivity from attention ($p = 2.44\times10^{-11}$), but not from VIP activation ($p = 0.457$) and no interaction effect ($p = 0.153$). The same pattern of results is observed when widening the analysis from only non-VIP cells whose selectivity is enhanced by attention to either significantly selective cells or all non-VIP cells (summarised in tables below). Similarly, in the control mice expressing tdTomato but no opsin, there was only a significant effect of attention, but no significant effect of light or an interaction of the two (Fig. 3.5g, see table below for statistics) of neurons in control mice. Thus, attention and VIP driven disinhibition modify stimulus evoked activity in the same neurons, but the two effects do not interact.

Table 3.1: Two-way ANOVA results for the effect of attention and VIP activation on neurons mean responses.

Cell group	Visual stimulus	Attention effect	Laser effect	Interaction
Negatively selective	Preferred	p=0.133	p=0.011	F(2, 86) = 0.072, p=0.931
	Non-preferred	$p=1.31x10^{-5}$	$p=1.70x10^{-5}$	F(2, 86) = 0.376, p=0.688
Positively selective	Preferred	p=0.316	p= 0.005	F(2, 86) = 0.016, p=0.984
	Non-preferred	p=0.080	$p=4.65x10^{-4}$	F(2, 86) = 0.017, p=0.983

Table 3.2: Two-way ANOVA results for the effect of attention and optogenetic laser on neurons mean responses in mice expressing no opsin.

Cell group	Visual stimulus	Attention effect	Laser effect	Interaction
Negatively selective	Preferred	p=0.501	p=0.887	F(2, 96) = 0.365, p=0.695
	Non-preferred	$p=1.29x10^{-8}$	p=0.762	F(2, 96) = 0.022, p=0.979
Positively selective	Preferred	$p=1.84x10^{-8}$	p=0.833	F(2, 96) = 0.027, p=0.973
	Non-preferred	p=0.088	p=0.337	F(2, 96) = 0.538, p=0.586

Table 3.3: Two-way ANOVA results for the effects of attention and VIP activation on neurons stimulus selectivity.

Cell group	Attention effect	Laser effect	Interaction
All non-VIP	$P=4.50x10^{-4}$	p=0.060	F(1,64) = 0.955, p=0.332
Unselective	p=0.002	p=0.436	F(1,64) = 1.200, p=0.278
Significantly selective	P=0.012	p=0.050	F(1,64) = 0.512, p=0.477
Increasing with attention	$P=2.44x10^{-11}$	p=0.457	F(1,64) = 2.095, p=0.153
VIP	$p=5.84x10^{-4}$	p=0.070	F(1,60) = 1.351, p=0.250

Table 3.4: Two-way ANOVA results for the effects of attention and optogenetic laser on neurons stimulus selectivity, in mice expressing no opsin.

Cell group	Attention effect	Laser effect	Interaction
All non-VIP	$P=2.66x10^{-10}$	p=0.741	F(2,96) = 0.470, p=0.626
Unselective	$P=7.74x10^{-6}$	p=0.961	F(2,96) = 0.154, p=0.858
Significantly selective	$P=3.32x10^{-5}$	p=0.922	F(2,96) = 0.116, p=0.890
Increasing with attention	$P=2.69x10^{-17}$	p=0.364	F(2,96) = 0.734, p=0.483
VIP	$P=1.10x10^{-14}$	p=0.406	F(2,96) = 1.369, p=0.259

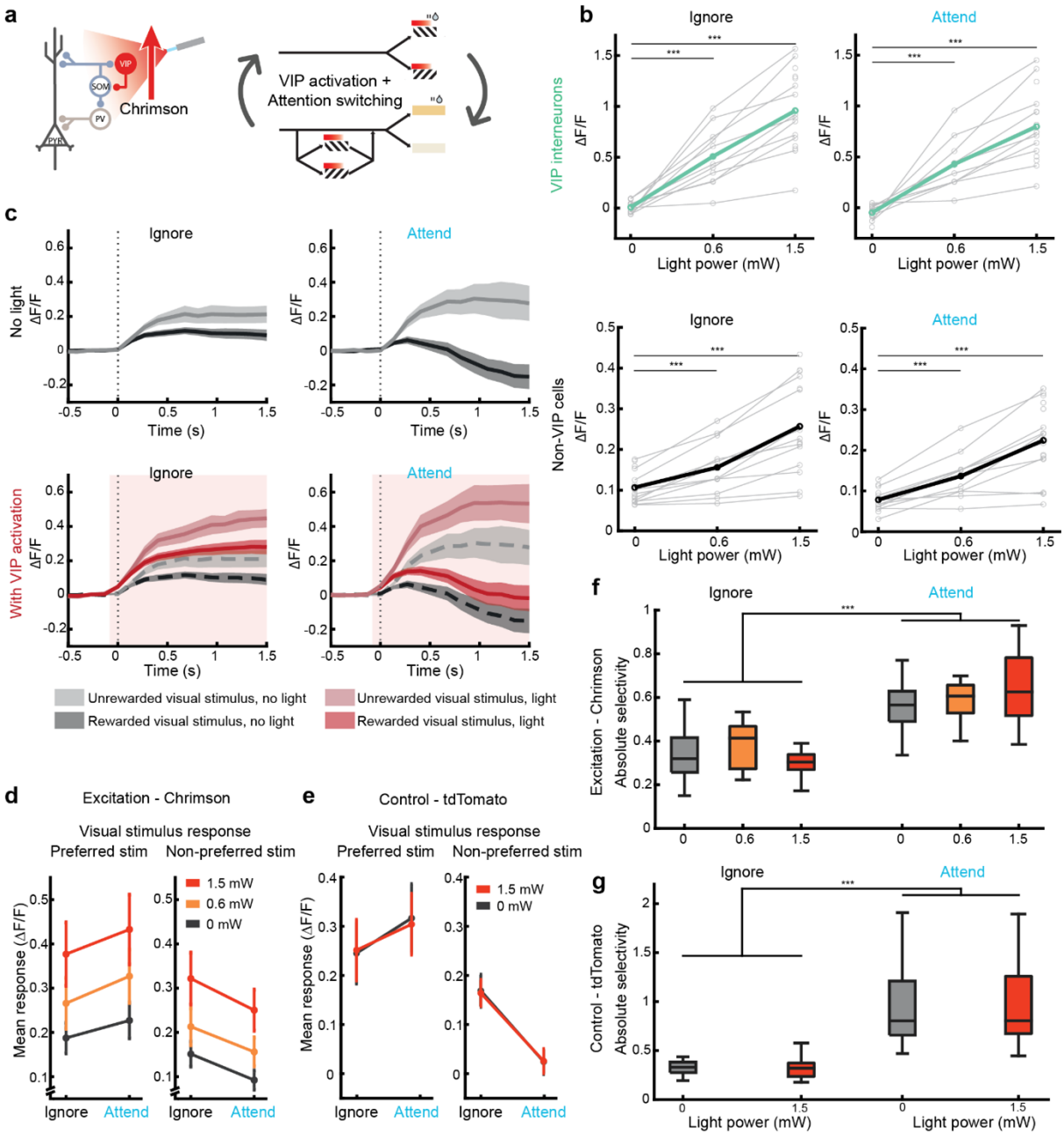

Figure 3.5: No-interaction between VIP activation and attentional modulation.

a) Schematic showing VIP photoactivation during the attention switching task. Light onset (red bars) was from -0.1s to 1.5s relative to visual stimulus onset. Light was ramped off over 0.2s. **b)** Mean visual stimulus evoked activity with increasing VIP photoactivation. Top, all VIP interneurons, bottom, all non-VIP cells. Left, responses when ignoring the visual stimuli, right, responses when attending the visual stimuli. Wilcoxon signed-rank test between photoactivation and non-photoactivation conditions, ***, $p < 0.001$, n = 17 sessions, 7 mice. Gray lines indicate individual session averages, coloured lines indicate overall average. **c)** Top, mean visual stimulus evoked activity for all non-VIP cells with preference for the unrewarded stimulus that significantly increased their selectivity with attention (mean of n=17 session averages, shading indicates SEM). Bottom, same

sessions, responses with additional VIP photoactivation (red). Responses from top are superimposed for comparison (grey dashed lines, light red shading indicates light onset). **d)** Black, mean visual stimulus evoked activity (averaged 0-1s) of all non-VIP cells with preference for the unrewarded stimulus that significantly increased their selectivity with attention, n = 17 sessions. Orange and red, same responses with additional VIP photoactivation. Error bars indicate SEM. **e)** Same as **d** for control mice expressing tdTomato, n = 17 sessions, 3 mice. **f)** Absolute stimulus selectivity with increasing VIP photoactivation for all non-VIP cells which significantly increased their selectivity with attention (n = 17 sessions). Stimulus selectivity measured when ignoring the visual stimuli (left) and attending the same stimuli (right). There was a significant effect of attention on selectivity, but not of VIP activation or an interaction between the two (2-way ANOVA, attention $p = 2.44\times10^{-11}$, other ps > 0.05). **g)** Same as **f** for control mice expressing tdTomato, n = 17 sessions, 3 mice.

3.3 – VIP inhibition does not attenuate attentional modulation

3.3.1 – Calibration of VIP inhibition.

VIP excitation did not interact with attentional modulation of stimulus selectivity. However, activation and inactivation of interneuron cell types can produce conflicting results (Phillips and Hasenstaub, 2016). To further investigate the role of VIP interneurons in shaping cortical stimulus evoked responses I also optogenetically inhibited VIP interneurons. The only methodological difference from the photoactivation experiments described in chapter 3.2 is that I expressed the inhibitory opsin ArchT in VIP interneurons rather than the excitatory opsin Chrimson.

I recorded a session in each mouse where the optogenetic laser was applied with only grey monitor screens. VIP cells were progressively inhibited at higher optogenetic laser powers in-vivo (Fig. 3.6c). V1 non-VIP cells did not display a reduction in activity with increasing photoinhibition of VIP interneurons (Fig. 3.6c), most likely because pyramidal neurons in V1 have low spontaneous activity (Niell and Stryker, 2010). Two laser powers were chosen for later passive visual stimulus presentation and full attention switching behaviour recordings. A high power which saturated the inhibition of spontaneous VIP interneuron activity and a second power which produced approximately half of the effect of the high power. Light powers were selected individually for each recording site and were typically 1.5mW for the low power (range 1.15 to 1.8mW) and 7.5mW for the high (range 5.7 to 9mW).

Due to optogenetic laser artefacts discussed later in this chapter, for the rest of this analysis

of VIP inhibition I will only be discussing the results of the lower laser power for the ArchT mice. The maximum power used to activate Chrimson was comparable to the low power for ArchT and so I was able to include both laser powers when analysing the Chrimson data set. Photoinhibition of VIP activity at the low laser power was highly effective, and comparable in magnitude to physiological changes. The average reduction in activity of VIP interneurons was 0.085 ΔF/F, and was comparable to the drop in stimulus evoked activity from locomoting (median = 0.504) to stationary (median = 0.392) of 0.11 ΔF/F.

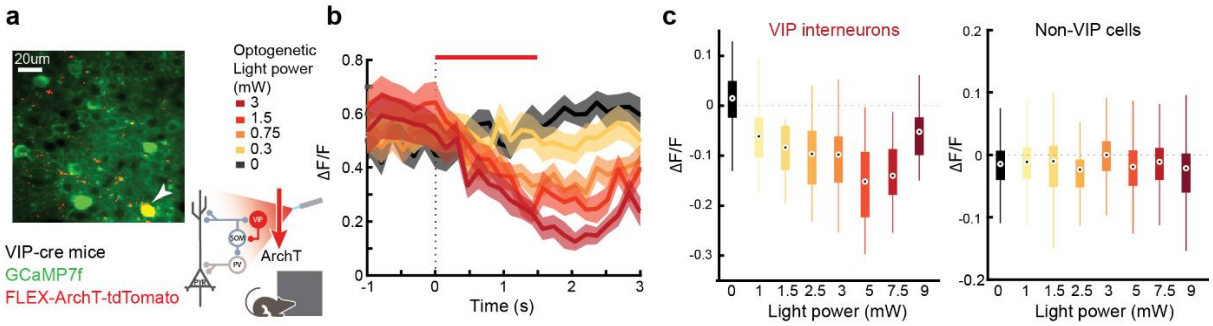

Figure 3.6: Optogenetic inhibition of VIP interneurons.

a) Example region of an in vivo imaged plane showing all neurons expressing GCaMP7f and a VIP interneuron (arrowhead) additionally expressing ArchT-tdTomato. **b)** Mean responses of an example VIP interneuron to different light powers. Responses are aligned to optogenetic light onset (dashed line). Red bar indicates optogenetic stimulation duration (1.5s), shading indicates SEM. **c)** Box plots of optogenetically inhibited activity (mean 0-1.5s, baseline subtracted) across different light powers for VIP interneurons (left, n = 92 cells, 5 mice) and non-VIP cells (right, n= 1648 cells, 5 mice).

3.3.2 – VIP inhibition modestly suppressed cortical responses during passive viewing

As in the photoexcitation experiments just described, passive mice were presented with visual grating stimuli moving in 8 different directions at 45° increments. On interleaved trials VIP interneurons were photoinhibited during the visual stimulus presentation epoch. The optogenetic laser produced the expected inhibition of VIP interneuron activity across orientations (Fig. 3.7a). Orientation tuned non-VIP cell activity was significantly reduced at each cells preferred orientation (Fig. 3.7b). It is likely that I do not see inhibition at orientations orthogonal to the preference for each cell because activity has reached a physiological floor. It is therefore difficult to establish whether VIP inhibition has a divisive or subtractive effect on non-VIP cell activity.

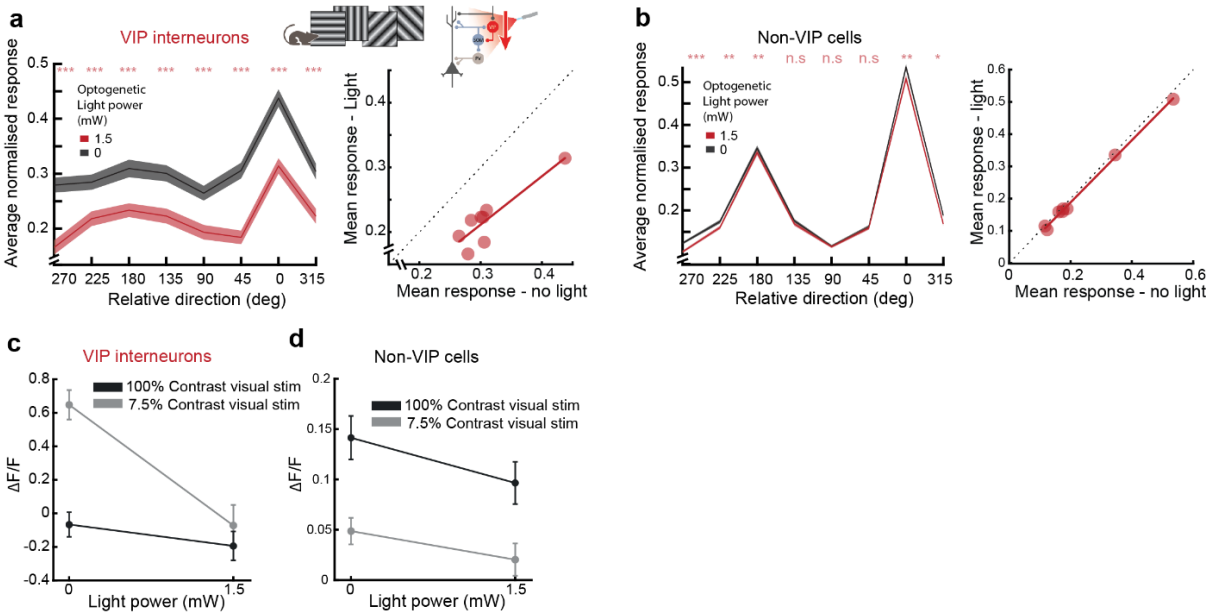

Figure 3.7: VIP inactivation modulates cortical responses to visual stimuli.

a) Left, stimulus evoked normalised activity in response to different oriented gratings, averaged across all VIP interneurons (n = 122 cells, 6 mice) aligned to their preferred direction. *, p<0.05, **, p<0.01, ***, p<0.001 Wilcoxon signed-rank test for photoinhibition compared to non-photoinhibition conditions at each direction, corrected for multiple comparisons. Right, the same data shown as average activity with and without optogenetic light. Linear regression, slope = 0.748, intercept = -0.012. **b)** Same as a, for all orientation selective non-VIP neurons, n = 953 cells, slope = 0.965, intercept = -0.005. High power, slope = 1.634, intercept = 0.032, 8 mice. **c)** Visual stimulus evoked VIP interneuron activity (mean 0-1.5s, baseline subtracted) in response to a drifting vertical grating at low and high contrast, with and without VIP photoinhibition, n = 37 cells, 5 mice. **d)** Same as c, for non-VIP cells, n = 528 cells, 5 mice.

To confirm the strength of my optogenetic inhibition, I tested another group of passively viewing mice which were presented with interleaved high and low contrast visual stimuli. Low contrast grating stimuli moving front to back have been reported to strongly activate VIP interneurons (Millman et al., 2020) (Although VIP interneurons have also been reported to be broadly or weakly tuned (Kerlin et al., 2010; Mesik et al., 2015; Szadai et al., 2022)). When restricting analysis to trials on which the mice were spontaneously running, photoinhibition reduced VIP cell activity to a similar level despite much higher initial activity due to the low contrast stimuli (Fig. 3.7c). A two-way ANOVA for the effect of contrast and optogenetic inhibition on VIP cell activity showed a significant main effect of contrast ($p = 3.65 \times 10^{-8}$) but not laser ($p = 0.08$) and a significant interaction between the two ($F(1, 144) = 5.043$, $p = 0.026$).

A two-way ANOVA of non-VIP cell activity for the same trials (Fig. 3.7d) showed a significant main effect for contrast ($p = 1.86x10^{-6}$) but no effect for optogenetic laser ($p = 0.096$) or interaction ($F(1,2108) = 0.760$, $p = 0.384$). The power of optogenetic laser I have selected was therefore capable of a potent reduction in VIP activity, although it only led to a modest reduction (if any) of the average non-VIP cell activity whilst passively viewing stimuli.

3.3.3 – VIP inactivation during attention-switching

To establish whether VIP activity was required for attentional modulation I optogenetically inhibited VIP interneurons on randomly interleaved trials while mice performed the attention-switching task. On optogenetic laser trials the light was active from 100ms before stimulus onset to the end of the visual stimulus. There was no significant effect on behaviour of the optogenetic laser power used in this analysis (Fig. 3.8). VIP interneurons showed a reduction in activity when inhibited during the behaviour, both in the attend and ignore conditions (Fig. 3.9b). However, no significant effect of VIP inhibition was seen on non-VIP activity (Fig. 3.9b).

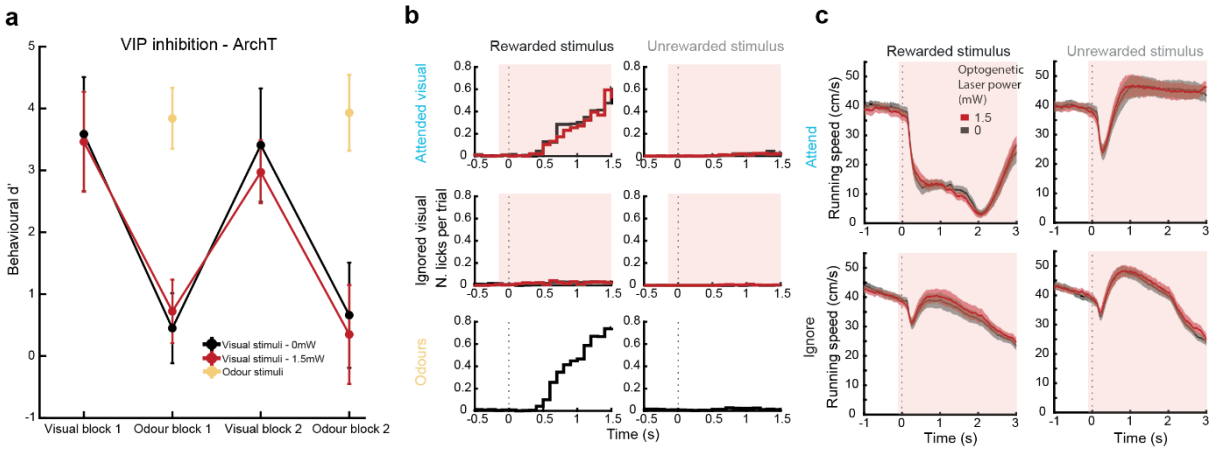

Figure 3.8: No change in behaviour with VIP photoinhibition.

a) Behavioural d' for visual and odour stimuli across the first 4 blocks of attention switching task trials, divided by optogenetic laser power. Wilcoxon signed rank tests comparing visual stimulus no laser and laser trials: visual block p = 0.831, odour block p = 0.644. Error bars indicate s.e.m. N = 16 sessions, 5 mice, same sessions for panels **a**, **b** and **c. b)** Average number of licks per trial aligned to stimulus onset (dashed line) for each of 6 main trial types, with trials divided according to optogenetic laser power. Visual stimuli in the visual block (top), in the odour block (middle), and odour stimuli (bottom). Split into rewarded stimulus (left) and unrewarded stimulus (right). Light red shading indicates light onset. **c)** Average running speed with and without optogenetic laser aligned to visual stimulus onset (dashed line) in the visual block (top) and odour block (bottom). Split into rewarded stimulus (left) and unrewarded stimulus (right). Shaded areas indicate s.e.m. Light red shading indicates light onset.

I selected the population of non-VIP cells that significantly increased their selectivity with attention and plotted their average activity in the first second after onset for the two visual stimuli with and without the optogenetic laser in the attend and ignore conditions.

VIP photoinhibition did not significantly affect the stimulus evoked responses of attentionally modulated neurons. Data for cells preferring the unrewarded stimulus can be seen in Fig. 3.9c and d, a two-way ANOVA of their response to the rewarded stimulus shows that there is a significant main effect for attention (p=0.001) but not for VIP inhibition (p=0.792), and no significant interaction effect (p=0.973). The results are similar for responses to the unrewarded stimulus and for positively selective cells (Fig 3.9e) - which prefer the rewarded grating - and show no-interaction between optogenetic inhibition and the attentional modulation (See table below for statistics). In accordance with these results there was no significant change in the absolute stimulus selectivity of the population with VIP inhibition

(Fig. 3.9f). A two-way ANOVA found a significant main effect on selectivity from attention (p=0.003), but not from VIP inactivation (p = 0.899) and no interaction between the two (p=0. 508). VIP interneurons do not appear to be involved in the increase in stimulus selectivity observed here with attention.

Table 3.5: Two-way ANOVA results for the effect of attention and VIP inhibition on neurons mean responses.

Cell group	Visual stimulus	Attention effect	Laser effect	Interaction
Negatively selective	Preferred	p=0.076	p=0.520	F(2, 88) = 0.141, p=0.868
	Non-preferred	p=0.001	p=0.792	F(2, 88) = 0.028, p=0.972
Positively selective	Preferred	$p=1.74x10^{-11}$	p=0.667	F(2, 88) = 0.017, p=0.983
	Non-preferred	p=0.033	p=0.846	F(2, 88) = 0.126, p=0.882

Table 3.6: Two-way ANOVA results for the effects of attention and VIP inhibition on neurons stimulus selectivity.

Cell group	Attention effect	Laser effect	Interaction
All non-VIP	$P=1.72x10^{-10}$	p=0.886	F(2,84) = 0.313, p=0.732
Unselective	$P=6.76x10^{-8}$	p=0.657	F(2,84) = 0.967, p=0.385
Significantly selective	$P=2.58x10^{-9}$	p=0.992	F(2,84) = 0.048, p=0.953
Increasing with attention	$P=1.13x10^{-16}$	p=0.878	F(2,84) = 0.465, p=0.630
VIP	$P=3.38x10^{-12}$	p=0.877	F(2,84) = 0.006, p=0.994

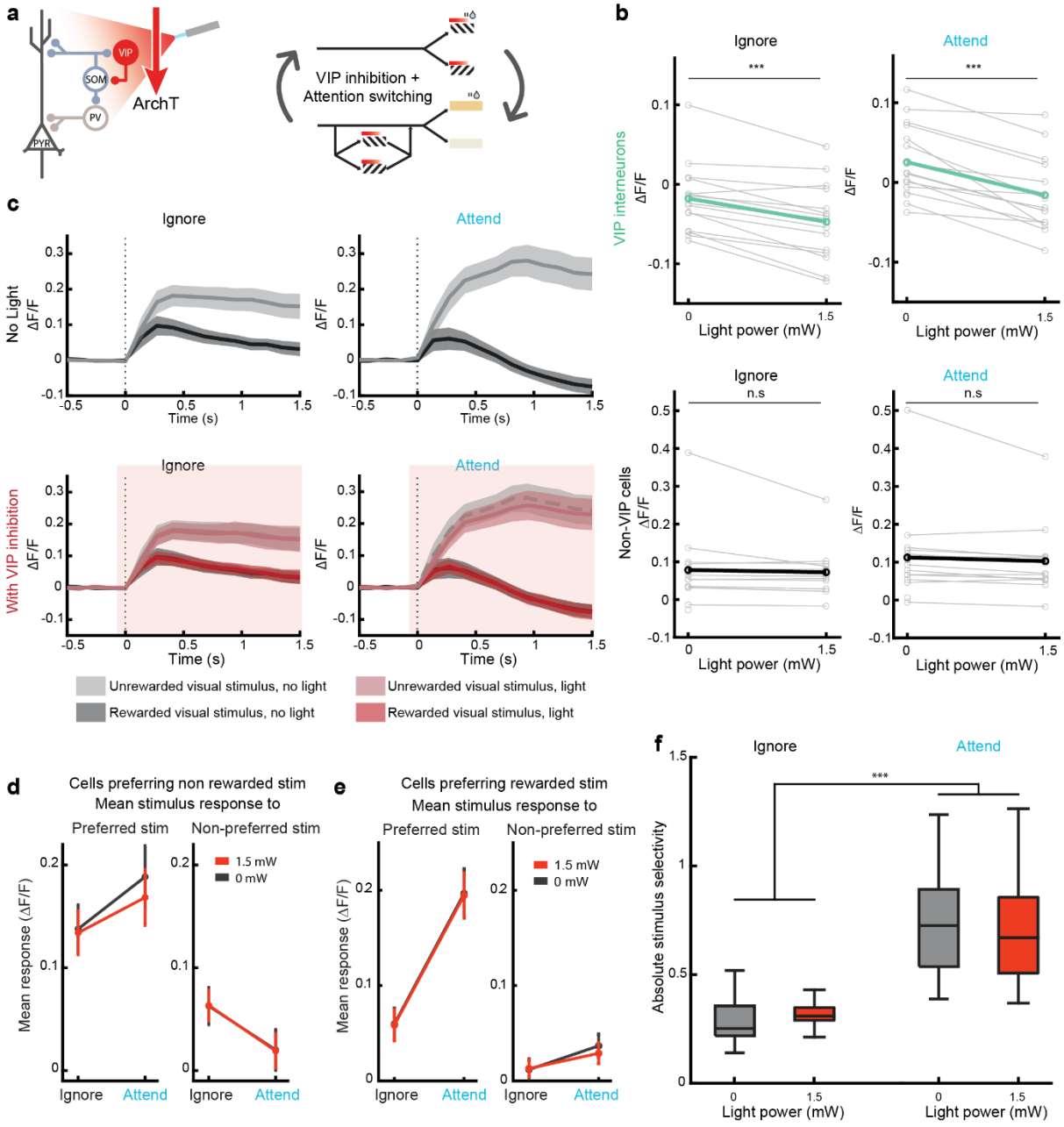

Figure 3.9: No effect of VIP inactivation on attentional modulation.

a) Schematic showing VIP photoinhibition during the attention switching task. Light onset (red bars) was from -0.1s to 1.5s relative to visual stimulus onset. Light was ramped off over 0.2s. **b)** Mean visual stimulus evoked activity (baseline subtracted) with increasing VIP photoinhibition. Top, all VIP interneurons, bottom, all non-VIP cells. Left, responses when ignoring the visual stimuli, right, responses when attending the visual stimuli. Wilcoxon signed-rank test between photoactivation and non-photoactivation conditions, ***, p< 0.001, n = 16 sessions, 5 mice. Grey lines indicate individual session averages, coloured lines indicate overall average. **c)** Top, mean visual stimulus evoked activity for all non-VIP cells with preference for the unrewarded stimulus that significantly increased their selectivity with attention (mean of n = 16 sessions, shading indicates SEM). Bottom, same sessions, responses with additional VIP photoinhibition (red). Responses from top are superimposed for

comparison (grey dashed lines, light red shading indicates light onset). **d)** Black, mean visual stimulus evoked activity (averaged 0-1s, baseline subtracted) of all non-VIP cells with preference for the unrewarded stimulus that significantly increased their selectivity with attention, n = 16 sessions. Red, same responses with additional VIP photoinhibition. Error bars indicate SEM. **e)** Same as **d** for cells with preference for the rewarded stimulus. **f)** Absolute stimulus selectivity without and with VIP photoinhibition for all non-VIP cells which significantly increased their selectivity with attention (n = 16 sessions). Stimulus selectivity measured when ignoring the visual stimuli (left) and attending the same stimuli (right). There was a significant effect of attention on selectivity, but not of VIP activation or an interaction between the two (2-way ANOVA, attention p = 1.13×10-16, other ps > 0.05).

3.3.4 – Higher optogenetic laser power produced artefacts

To determine if even further inhibition of VIP cells was possible, a second higher optogenetic laser power was used in mice expressing the inhibitory opsin ArchT, typically 7.5mW. The inhibitory effects plateaued at this higher power (fig 3.10a), with no significant difference between the low and high powers when attending (Paired t-test p= 0.886) or ignoring the visual stimuli (Paired t-test p= 0.823). Sustained activation of archaerhodopsin has been found to elicit paradoxically increased rates of spontaneous vesicle release (Mahn et al., 2016). Archaerhodopsin is a proton pump and this increase in spontaneous release appears to be due to pH-dependent calcium influx – it seems unlikely that I will be eliciting these sorts of changes as they were reported after minutes rather than seconds of activation. To control for any non-opsin effects of the laser light alone I conducted the same experiments as described above but for an opsin free control (first described in the VIP photoactivation experiments). The laser powers chosen for these mice were based on those used for the photoactivation and photoinhibition experiments, 1.5mW and 7.5mW. In no-opsin control mice the higher laser power produced an artefactual excitation of VIP and non-VIP cells, both in the attention switching task and when the mice were passively viewing visual stimuli (Fig. 3.10 b,c). Interestingly, in the same mice stimulated with only the optogenetic laser the artefactual light evoked activity was absent for VIP interneurons (Fig 3.10j). These results reinforce the importance of light only controls in animals performing the full behavioural task.

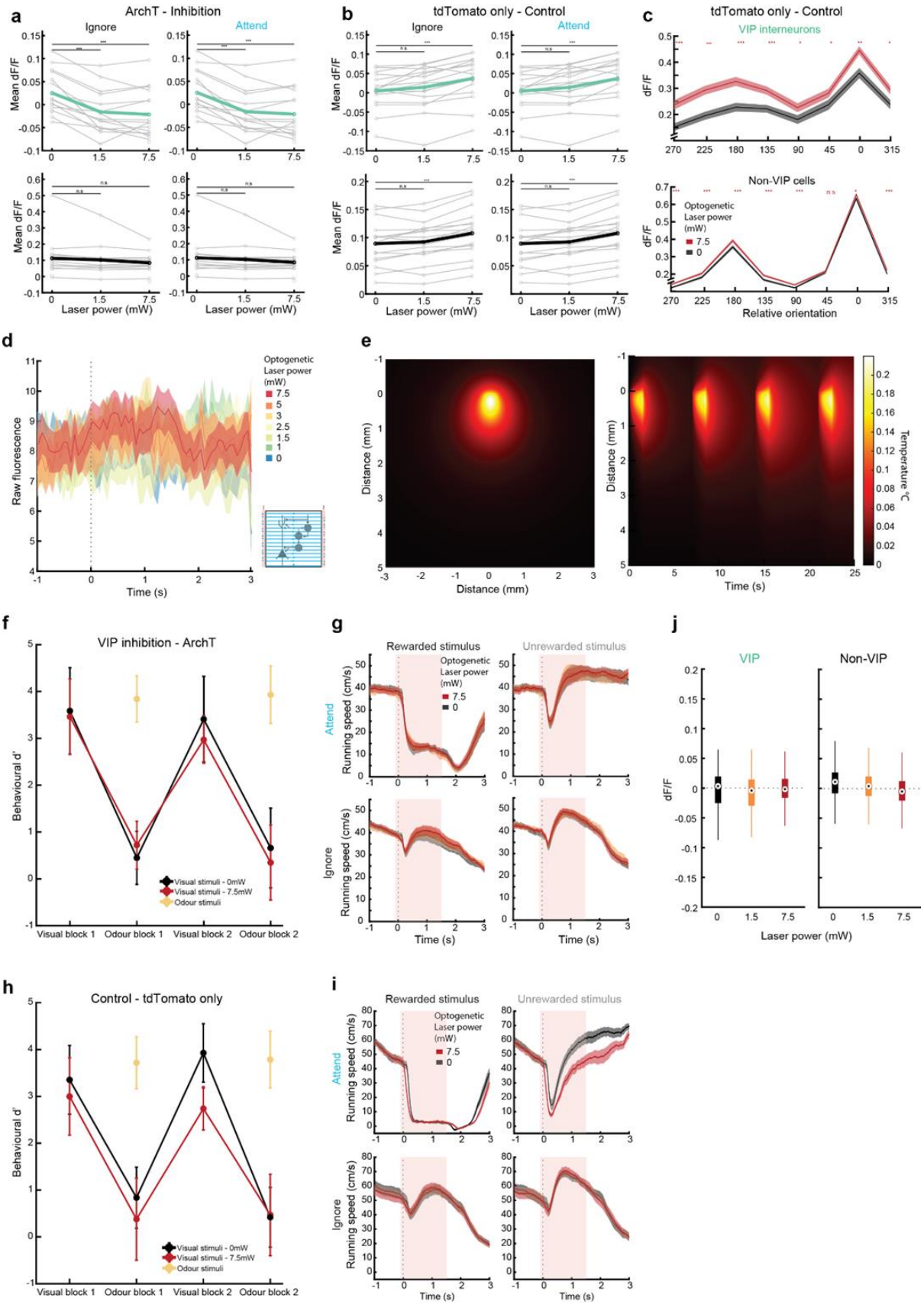
a
ArchT - Inhibition
Ignore
Attend
Mean dF/F
Laser power (mW)
b
tdTomato only - Control
Ignore
Attend
Mean dF/F
Laser power (mW)
c
tdTomato only - Control
VIP interneurons
dF/F
Non-VIP cells
Optogenetic Laser power (mW)
7.5
0
Relative orientation
d
Raw fluorescence
Optogenetic Laser power (mW)
7.5
5
3
2.5
1.5
1
0
Time (s)
e
Distance (mm)
Distance (mm)
Time (s)
Temperature °C
f
VIP inhibition - ArchT
Behavioural d'
Visual stimuli - 0mW
Visual stimuli - 7.5mW
Odour stimuli
Visual block 1
Odour block 1
Visual block 2
Odour block 2
g
Rewarded stimulus
Unrewarded stimulus
Attend
Ignore
Running speed (cm/s)
Optogenetic Laser power (mW)
7.5
0
Time (s)
j
VIP
Non-VIP
dF/F
Laser power (mW)
h
Control - tdTomato only
Behavioural d'
Visual stimuli - 0mW
Visual stimuli - 7.5mW
Odour stimuli
Visual block 1
Odour block 1
Visual block 2
Odour block 2
i
Rewarded stimulus
Unrewarded stimulus
Attend
Ignore
Running speed (cm/s)
Optogenetic Laser power (mW)
7.5
0
Time (s)

Figure 3.10: Increasing laser power saturates VIP inhibition and introduces an optogenetic artefact not seen at the same power without visual stimuli.

a) Average optogenetically evoked activity (baseline subtracted) with increasing light power for mice expressing ArchT in VIP interneurons. Top, all VIP interneurons, bottom, all non-VIP cells. Responses shown when ignoring the visual stimuli (left) or attending the visual stimuli (right). Wilcoxon signed-rank test between light activity and nonlight activity, ***, p< 0.001, n.s. indicates not significant, n = 16 sessions, 5 mice. Gray lines indicate individual session averages, coloured lines indicate overall average. **b)** Same as in a, for control mice expressing only tdTomato in VIP interneurons (n = 17 sessions, 3 mice). **c)** Passive visual stimulus presentation experiments with and without 7.5mW optogenetic laser. Normalised activity averaged across all VIP interneurons (top, n= 61 cells, 3 mice) and all orientation tuned non-VIP cells (bottom, n = 434, 3 mice) aligned to their preferred orientation. * = p<0.05, ** = p<0.01, *** = p<0.001 sign-rank test for optogenetic laser compared to non-laser at each orientation. **d)** Average raw fluorescence values aligned to optogenetic laser onset (dashed line) at 7 different powers when imaging a portion of a mouse's cranial window not expressing GCaMP7f. **e)** Modelled temperature change due to the optogenetic laser at 7.5mW. Modelling performed using code from Stujenske, et al., 2015. Left - maximum heat at each location centred on the optogenetic fibre in vertical and radial distance. Right - maximum heat over successive 7.5mW optogenetic laser activations at different depths centred on the optogenetic fibre. **f)** Behavioural d' for visual and odour stimuli across the first 4 blocks of attention switching, shown separately for different optogenetic light powers, for mice expressing ArchT in VIP interneurons. Wilcoxon signed-rank tests comparing visual stimulus no light and light trials: visual block p = 0.374, odour block p = 0.844 (n = 16 sessions, 5 mice). **g)** For mice expressing ArchT in VIP interneurons - Average running speed at different optogenetic laser powers aligned to visual stimulus onset (dashed line) in the visual block (top) and odour block (bottom). Split into rewarded stimulus (left) and unrewarded stimulus (right). Shaded areas indicate s.e.m. Light red shading indicates light onset (n = 16 sessions, 5 mice). **h)** Same as in **f**, but for mice expressing tdTomato but no opsin in VIP interneurons. Wilcoxon signed rank tests comparing visual stimulus no laser and laser trials: visual block p = 5.07×10^{-5}, odour block p = 0.132 (n = 17 sessions, 3 mice). **i)** Same as in **g**, but for mice expressing tdTomato but no opsin in VIP interneurons (n = 17 sessions, 3 mice). **j)** Average activity (baseline subtracted) for all VIP interneurons (left – n = 52 cells, 3 mice) and non-VIP cells (right – n = 644 cells, 3 mice) in response to the optogenetic laser alone for no-opsin control mice.

Light artefact is not due to heat or light leaking into PMTs

The artefact could be caused by optogenetic light leaking into the photomultiplier tubes (PMT) which collect the light from the fluorescent indicators. If this were the case, I would expect consistent results between the behavioural and optogenetic light only sessions. In addition, the visual stimulus monitors and the optogenetic laser are switched off during the turnaround times of the two-photon laser and the PMTs are blanked during this period. To confirm, I

recorded the effects of the optogenetic laser in both brain slices and non-fluorescent regions of the experimental mice. Very small fluctuations in the output of the PMT can be seen at the highest laser power, changes which are orders of magnitude smaller than the fluctuations in fluorescence when calcium imaging (Fig. 3.10d).

Changes in temperature are known to produce changes to the firing rates and physiological properties of neurons and alter behaviour (Long and Fee, 2008; Kim and Connors, 2012). I used the code available from Stujenske et al., 2015 to model the increase in temperature using the parameters of the optogenetic stimuli applied in no-opsin control mice and found that the maximum temperature increase at the fibre tip was only 0.22°C (Fig 3.10e). In addition, when modelling several high laser power trials in a row with the minimum inter-trial time seen in the task, heat dissipated between trials and did not accumulate past 0.22°C (Fig 3.10e). Stimulating in PFC Stujenske et al found that temperature changes of 0.22°C did not alter activity, and only saw changes at >1°C (Stujenske et al., 2015). It therefore seems unlikely that the artefactual effects are due to temperature changes. Indeed, the temperatures modelled here are likely to be an overestimate as in this setup the optogenetic fibre is in water above the window rather than embedded in tissue and so the locus of most intense heating is outside of the brain.

<u>The artefact is likely due to light reaching retina and overt behavioural changes</u>

In mice expressing ArchT there was no change in behavioural discrimination (d') of the visual stimuli at the high laser power (Wilcoxon sign-rank, attend p=0.375, ignore p=0.844) (Fig. 3.10f). However, for the no-opsin control mice there was a significant reduction in behavioural performance at the high laser power in the attend condition (Wilcoxon sign-rank, attend $p=5.07x10^{-5}$, ignore p=0.132) (Fig 3.10h). Also, while there is no clear change in the running activity of mice expressing ArchT with and without optogenetic laser (Fig. 3.10g), the no-opsin control mice slowed down earlier in visual blocks on optogenetic laser trials, likely because they were detecting the laser onset 100ms before the visual stimulus (Fig. 3.10i).

Although mice have been commonly assumed to be red-light blind, more recent work demonstrates that rodents can see red light (Niklaus et al., 2020). To attempt to prevent optogenetic light from reaching the mouse's eyes, opaque dental cement was used to attach the head-plates and a matte black metal cone was placed as a light guard around the

microscope objective during recordings. It seems most likely that the optogenetic artefact is due to light from the optogenetic laser reaching the mouse's retina by propagating through the brain and that the effects of its detection are compounded by behavioural changes the light provokes.

These results corroborate the findings of Danskin et al., 2015. They implanted an optogenetic cannula significantly further anterior than the illumination I have just described and showed that red light (640nm) but not blue (473nm) or yellow (589nm) produced retinal activation and behavioural artifacts at a power of 10mW (Danskin et al., 2015). The light source in my experiments is further from the eyes than in Danskin et al., 2015, and because of this there may be a weaker direct effect of the optogenetic laser on the retina, meaning that the artefact was difficult to detect or absent during the session with the optogenetic laser alone. The effect may have become more measurable because the same light power was delivered into the network in a different state, with changes in behaviour due to the light amplifying the direct feed-forward effects from the retina.

3.4 – Orthogonality of VIP and attentional modulations

3.4.1 – Attention and VIP modulations are orthogonal

Previous work has shown that by being represented orthogonally at the population level locomotor and visual activity can co-occur in the same network and not negatively influence each other's information coding (Stringer et al., 2019). I tested whether VIP and attentional modulations might also be orthogonal. I took two vectors separating the visual stimulus-evoked neural activity of non-VIP cells using dimensionality reduction through linear discriminant analysis (LDA). One vector distinguishing between attend and ignore conditions without optogenetic manipulation, and a second separating trials with and without optogenetic manipulation within the ignore condition (Fig. 3.11a). I calculated the cosine similarity of these two vectors as a measure of the alignment of VIP and attentional modulations.

To construct a null distribution, I took the cosine similarity for random axes extracted based on the covariance of the original data (10,000 samples, same method as (Elsayed et al., 2016). The cosine similarity of VIP and attentional modulation for each session was compared to its

own random mean. In the experiments with optogenetic excitation of VIP interneurons, attention and photostimulation had a significantly lower cosine similarity than the random vectors (Wilcoxon sign-rank test, p = 0.009, n=17 sessions) suggesting they are less aligned to one another than random axes from the same data. In the VIP inhibition or control experiments, the cosine similarity of VIP and attentional modulation was not significantly different from the cosine similarity for the random axes (Fig. 3.11b, Wilcoxon sign-rank test, p = 0.4, n=16 sessions, p = 0.7, n=17 sessions respectively), as expected given no significant difference in non-VIP cell activity with the optogenetic laser.

As a positive control I divided attended visual stimulus trials with no laser into two equal groups and extracted the axis separating rewarded from unrewarded stimuli for each and calculated the cosine similarity between the two halves of the data (50 repeats), these axes are expected to be aligned. In all three groups of mice these vectors had a higher cosine similarity than the random axes (Fig. 3.11b, sign-rank test Chrimson $p=2.93x10^{-04}$, ArchT $p=6.43x10^{-04}$, tdTomato p=0.002. n=16 n=17, and n=17 sessions respectively). These results indicate that, more than simply not interacting, the modulation of cortical activity through VIP interneurons and the modulation through attention are orthogonal to one another.

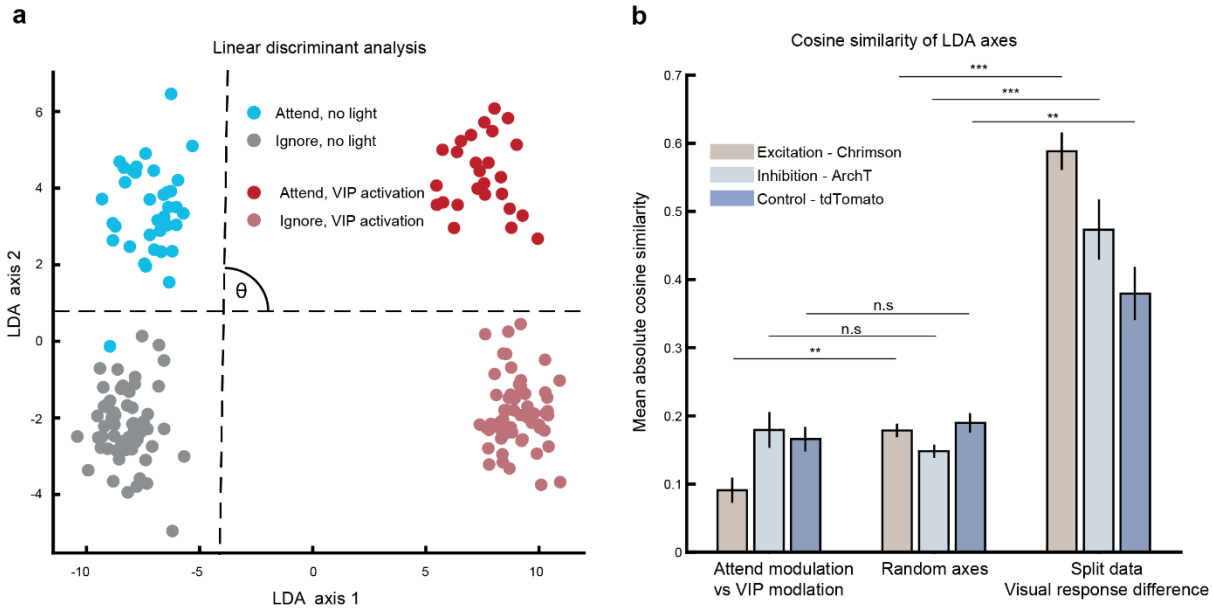

Figure 3.11: VIP and Attentional modulations are orthogonal.

a) Mean stimulus evoked activity from individual trials projected onto the first two axes obtained from

dimensionality reduction using linear discriminant analysis (LDA). Example session from a mouse expressing Chrimson. Dashed lines are indicative of the directions along which attention and VIP photoactivation most strongly modulated activity. **B)** Mean cosine similarity for pairs of axes in neural activity space (Chrimson n = 17 sessions, 7 mice, ArchT n = 16 sessions, 5 mice, tdTomato control n = 17 sessions, 3 mice). From left to right, absolute cosine similarity for: LDA axis separating VIP photoactivation vs no photoactivation trials and LDA axis separating attend vs ignore trials; pairs of random axes extracted based on the covariance of the original neural data (10,000 samples); two axes separating the rewarded vs unrewarded visual stimuli where each axis was found using half of the data (mean of 50 shuffled repeats). Significance tests were against the corresponding random axes median, ** $p<0.01$, *** $p<0.001$. From left to right p values for all tests: 0.009, 0.379, 0.653, 6.43×10^{-4}, 2.93×10^{-4}, 0.002.

3.4.2 – Attention orthogonalizes the population response to the task visual stimuli without changing population sparseness

Visuomotor associations can orthogonalize the population representation of different stimuli (Failor et al., 2023). Failor et al. found that this orthogonalization was underpinned by a sparsening of the population response. Is an orthogonalization of stimulus responses also observed with attention and if so, is it associated with sparsening? Addressing this question will also shed light on the issue of whether the brain orthogonalises representations primarily through sparsening, or by other mechanisms.

In the same fashion as Failor et al., I examined the orthogonality of the population responses to the two stimuli in this task – with and without attention. Orthogonality was quantified as the cosine similarity of the mean response vectors to the two stimuli. The trials were split into odd and even halves before computing the response vectors which ensured that the diagonal was not 1 by definition. I then compared the cosine similarity for the rewarded and unrewarded visual stimuli in the odour block, to the same in the visual block. For both mice expressing Chrimson (Fig. 3.12a) and for no-opsin control mice (Fig. 3.12c) there was a significant reduction in the cosine similarity of the population code for the two stimuli with attention – the visual stimulus responses orthogonalized with attention – reflecting the increase in selectivity we observe here with attentional modulation.

To quantify the population sparseness during different task conditions, I used the Treves-Rolls measure, where higher values mean more sparse representations (Treves and Rolls, 1991; Willmore and Tolhurst, 2001). For mice expressing the excitatory opsin Chrimson, both VIP

photoactivation and attention decreased the population sparseness (Fig. 3.12b). However, for the no-opsin control mice neither attention nor the application of the laser light produced a significant change in population sparseness (Fig. 3.12d). Changes in population sparseness for the Chrimson mice may be indicative of a change in the network other than attention due to VIP activation, as despite the conflicting changes in sparseness, both Chrimson expressing (Fig. 3.12b) and no-opsin control (Fig. 3.12d) mice displayed an orthogonalization of their responses to the task's visual stimuli with attention.

Thus, here a sparsening of population responses is not required for an orthogonalization of responses to visual stimuli. The sparsening of visual stimulus responses presented by Failor et al. occurs following multi-day task training, and so it may be that orthogonalization that occurs on shorter timescales (such as through application of attention) is produced by changes to the network other than sparseness.

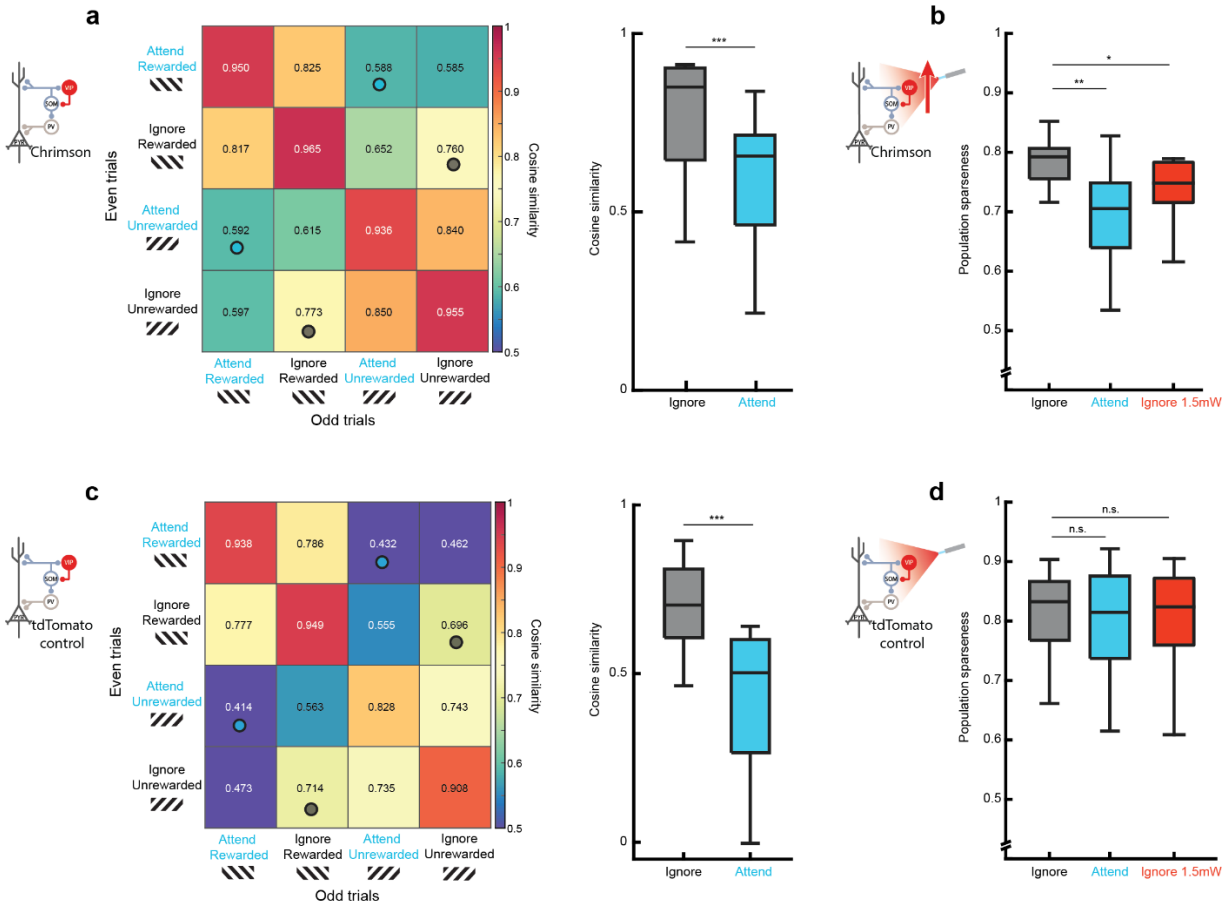

Figure 3.12: Attention orthogonalizes visual stimulus responses with and without changes in population

sparseness

a) Population sparseness in responses to rewarded visual stimulus in the no laser condition when ignored and attended to, and when ignored with VIP photoactivation – for mice expressing Chrimson (Wilcoxon signed rank tests, ignore vs attend p = 0.004, ignore no laser vs VIP photoactivation p = 0.050, n = 17 sessions, 7 mice). **b)** Left - mean cosine similarity between the mean population response for pairs of visual stimulus trials, split into even and odd trials and into ignore and attend conditions. Grey circles indicate the cosine similarities averaged for the ignore condition of the right-hand boxplot. Blue circles indicate the conditions averaged for the attend condition. Right – boxplot of the average cosine similarity for rewarded vs unrewarded mean population response when ignoring or attending to the stimuli (Wilcoxon signed rank tests, $p = 3.52x10^{-4}$, n = 17 sessions, 7 mice). **c)** Same as in **a** but for control mice expressing no opsin. (Wilcoxon signed rank tests, ignore vs attend p = 0.906, ignore no laser vs laser p = 0.554, n = 17 sessions, 3 mice). **d)** Same as in **b** but for control mice expressing no opsin. (Wilcoxon signed rank tests, $p = 3.52x10^{-4}$, n = 17 sessions, 3 mice).

3.4.3 – VIP-SOM mediated disinhibition produces multiplicative gain in pyramidal cells

After finding that modulations from VIP interneurons and attention did not interact and were orthogonal at the population level, I wanted to better understand whether the circuit mechanisms underlying these modulations were distinct from one another. Cortical VIP interneurons are known to disinhibit pyramidal neurons through their inhibition of SOM interneurons. However, this motif is embedded in a highly recurrently connected network (Pfeffer et al., 2013) and the effect that manipulation of one cell class will have on the rest of the network is not always clear (Seybold et al., 2015; Pakan et al., 2016; Garcia Del Molino et al., 2017). Indeed, the effect of VIP activation leading to SOM inhibition and thus PYR disinhibition has never been demonstrated in simultaneously measured VIP, SOM and PYR cells *in vivo.*

To examine the effects of VIP interneuron photoexcitation, brain sections from 4 out of 8 of the same mice were immunohistochemically stained and registered to *in vivo* images to identify the molecular identity of recorded neurons (Fig. 3.13a). PV, SOM and VIP positive interneurons (fig 2.1 k) were detected, and the remaining cells were labelled as putative pyramidal (PYR) neurons. Optogenetic excitation of VIP interneurons during passive presentation of oriented drifting grating stimuli modulated the stimulus responses of all 4 classes, increasing the average activity of VIP, PYR and PV cells and decreasing the activity of SOM interneurons on average (Fig. 3.13b,c,d).

Also observable after immunolabelling was a small number of putative pyramidal neurons

that are inhibited by VIP activation (Fig. 3.13b). It seems likely that this was due to the activation of CCK+ VIP interneurons that directly inhibit pyramidals.

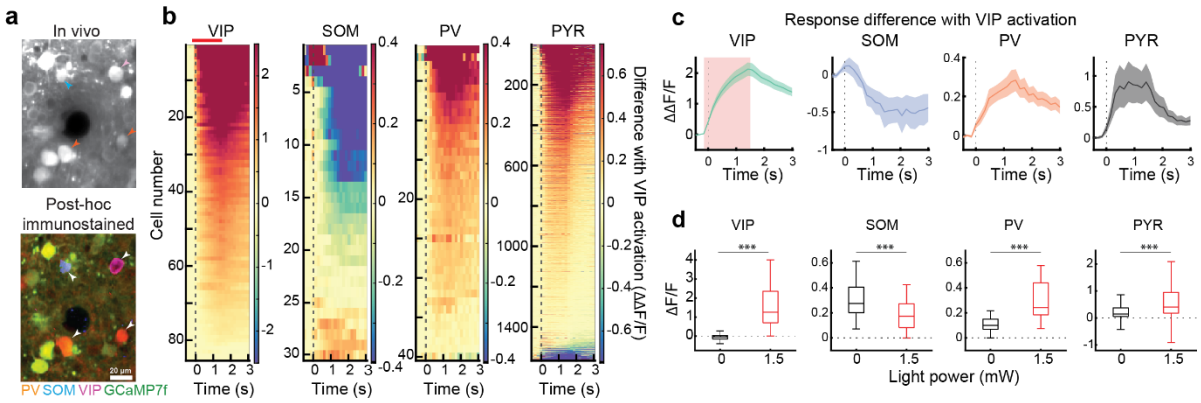

Figure 3.13: Non-VIP activation during VIP photostimulation is consistent with VIP-SOM disinhibitory motif.
a) Example region of an in vivo image plane with GCaMP7f-expressing neurons (top) and the same region after post-hoc immunostaining for PV, SOM, and VIP (orange, blue, and magenta, respectively) following image registration (bottom). Identified interneurons are indicated by arrowheads. **b)** Difference (VIP photoactivation condition minus no photoactivation condition) of average visual stimulus-evoked response for each cell in all 4 cell classes (average of all orientations of visual stimuli during passive presentation) aligned to visual stimulus onset (dashed line). Optogenetic light onset here and below is -0.1s to 1.5s from visual stimulus onset (red shading). Cells are sorted by their average response difference 0–1 s from stimulus onset. Left to right: VIP n = 85 cells, SOM n = 30 cells, PV n = 40 cells, PYR n = 1567 cells, all from 4 mice. **c)** Mean of each column of **b**, showing average change in activity with VIP activation, shading indicates SEM. **d)** Box plots of visual stimulus evoked activity with and without VIP photoactivation, averaged 0 to 1s from visual stimulus onset, for each cell class (Wilcoxon signed-rank tests for differences in activity: PYR, n = 1567 cells, $p = 4.52\times10^{-187}$; SOM, n = 30 cells, $p = 5.71\times10^{-04}$; VIP, n = 85 cells, $p = 1.17\times10^{-15}$; PV, n = 40 cells, $p = 3.57\times10^{-08}$, all from 4 mice.

The orientation tuning curves of each cell class were also modified in a similar pattern to their average activity, with PYR (High power: slope=1.452, intercept=0.042, n=472 cells) and PV cells (High power: slope=1.304, intercept=0.125, n=40 cells) largely enhanced and SOM (High power: slope=0.690, intercept=0.019, n=30 cells) largely inhibited at all orientations during VIP activation (High power: slope=1.489, intercept=0.567, n=85 cells)(Fig. 3.14). Collectively these results indicate that VIP interneuron activation drives multiplicative gain of PYR neuron responses through SOM mediated disinhibition and network-wide changes in activity of all cell classes molecularly identified here.

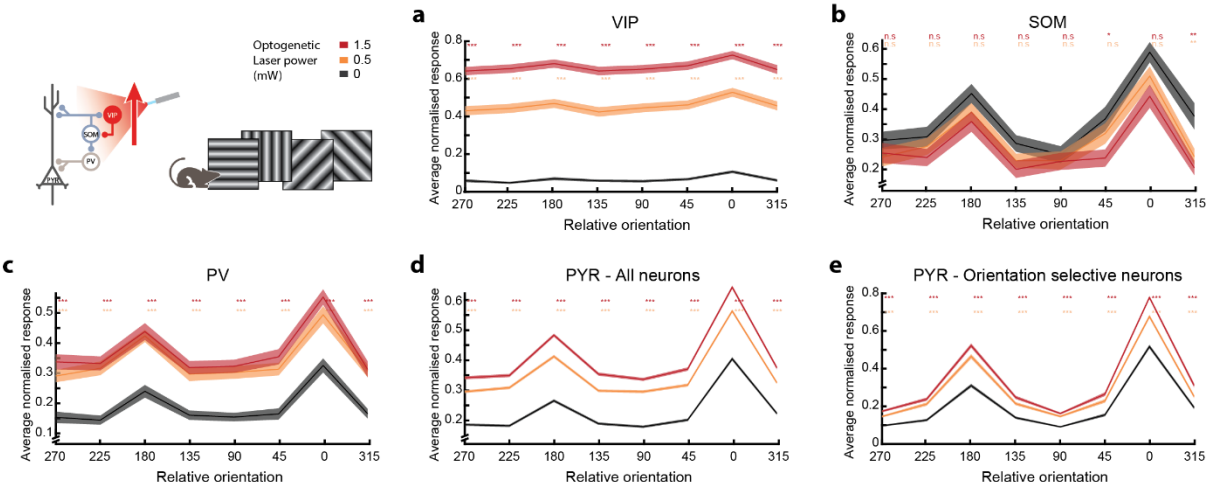

Figure 3.14: Effect of VIP activation on orientation tuning curves of distinct cell types.

a) Stimulus evoked normalised activity in response to different oriented gratings, averaged across all VIP interneurons (n = 85 cells, 3 mice) aligned to their preferred orientation. *, p<0.05, **, p<0.01, ***, p<0.001 Wilcoxon signed-rank test for photoactivation compared to non-photoactivation conditions at each orientation, corrected for multiple comparisons. Linear regression, low power, slope = 1.691, intercept = 0.347. High power, slope = 1.489, intercept = 0.567. **b)** Same as **a**, for SOM cells (n = 30 cells, 3 mice). Linear regression, slope = 0.858, intercept = -0.009. High power, slope = 0.690, intercept = 0.019. **c)** Same as a, for PV cells (n = 40 cells, 3 mice). Linear regression, slope = 1.158, intercept = 0.125. High power, slope = 1.304, intercept = 0.125. **d)** Same as **a**, for all PYR cells (n = 1567 cells, 3 mice). Linear regression, slope = 1.214, intercept = 0.074. High power, slope = 1.375, intercept = 0.092. **e)** Same as **a**, for orientation selective PYR cells (n = 472 cells, 3 mice). Linear regression, slope = 1.270, intercept = 0.034. High power, slope = 1.452, intercept = 0.042.

3.4.4 – VIP photoactivation alone produces heterogeneous changes in SOM interneurons

A slightly different pattern is seen when looking at activity changes in response to optogenetic excitation alone for the same post-hoc immunolabelled cell types with only a grey screen and no visual stimuli presented. In this case, the optogenetic laser led to an increase in the average activity of VIP, PYR and PV cells with increasing laser power (Fig. 3.15a). However, the population of SOM interneurons do not show a clear change in their average activity with VIP photoexcitation as they did when presented with visual gratings (Fig. 3.15c).

In all recordings the mice were head-fixed, but able to run freely on the Styrofoam wheel. Mice ran through significant portions of optogenetic only sessions despite the lack of any ongoing task. Potentially because of running's reported anxiolytic effect on mice (Duman et

al., 2008; Salam et al., 2009). VIP interneurons are activated by locomotor activity (Fu et al., 2014), one possibility is that the activation of VIP cells by running is already inhibiting SOM and we therefore see no additional change due to a flooring effect. In depth analysis of this is made difficult due to a dearth of trials on which the mice are still. However, when partitioning the data into running and non-running trials there is still no average inhibition of SOM (Data not shown) and there is the same pattern of changes in SOM activity for all trials pooled and when restricting to trials with locomotion. If SOM activity were simply being floored, then the increase in PYR activity with increasing VIP photoexcitation would be harder to explain. It seems more likely that either the subset of SOM interneurons that do show inhibition are mediating the effect, or I am witnessing an effect similar to (Pakan et al., 2016) and rapid dynamics (on a timescale I cannot observe here) are producing disinhibition before a new steady state is reached (Garcia Del Molino et al., 2017).

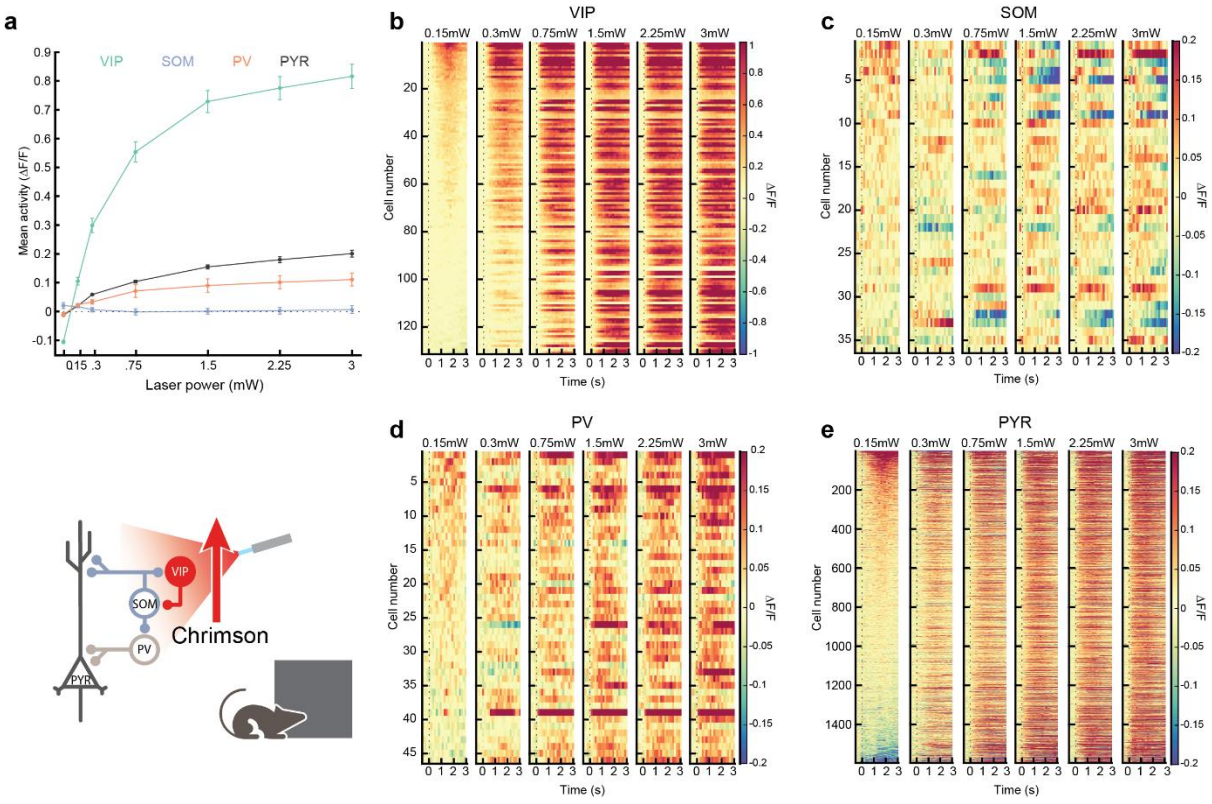

Figure 3.15: Changes in the activity of immunolabelled cell type induced by VIP photoactivation alone.

a) Average activity (0.5-1.5s) for all VIP, SOM, PV and PYR cells aligned to optogenetic light onset at each of 7 light powers. **b)** Average activity for VIP interneurons at each of 6 optogenetic light powers, increasing left to right, n= 4 mice. Responses are baseline subtracted and aligned to the onset of the optogenetic light (dashed

line). Cells sorted according to their mean activity in 0.5-1.5s in the no light condition. **c-e)** Same as **b**, for SOM, PV and PYR cells.

3.4.5 – Circuit changes with attention and VIP modulation suggest distinct mechanisms

If the modulations due to VIP interneurons and attention are actually orthogonal, we might expect that the changes they induce at the circuit-level would be distinct.

First, as reported earlier, the non-VIP cells that significantly increase their selectivity with attention do so through a combination of enhancement and suppression of their responses (Fig. 3.5d,e and Fig. 3.9d,e), an effect that has been previously published (Poort et al., 2022). In contrast, the activation of VIP interneurons overwhelmingly leads to increases in stimulus evoked responses (Fig 3.5d).

Second, noise correlations can provide an estimate of mutual connectivity and shared inputs. I measured noise correlations between the 4 simultaneously recorded cell-types just discussed. Attention significantly decreased the correlation between PYR and SOM, SOM and VIP and PV and SOM cell pairs and significantly increased noise correlation between VIP cells (Fig. 3.16a). Whereas the optogenetic activation of VIP interneurons significantly decreased noise correlation within PYR, VIP and PV cells as well as between PYR and VIP, PV and VIP and SOM and VIP cell pairs (Fig. 3.16b). P-values (without multiple comparisons correction, for unrewarded visual stimulus responses) for changes with attention are PYR-PYR: p=0.320, VIP-VIP: p=0.005, SOM-SOM: p=0.966, PV-PV: p=0.123, PV-VIP: p=0.278, PYR-PV: p=0.054, PYR-VIP: p=0.123, PV-SOM: p=0.014, PYR-SOM: p=0.019, SOM-VIP: p=0.005; for changes with VIP photoactivation, PYR-PYR: p=0.010, VIP-VIP: p=0.001, SOM-SOM: p=0.240, PV-PV: p=0.019, PV-VIP: p=0.010, PYR-PV: p=0.067, PYR-VIP: p=0.032, PV-SOM: p=0.083, PYR-SOM: p=0.278, SOM-VIP: p=0.003. Results were similar for responses to the rewarded stimulus.

Third, the activity changes of PYR, VIP, SOM and PV cells to stimulus evoked responses with attention and VIP photoexcitation are also distinct. In the absence of VIP photoexcitation, attention led to heterogenous changes with decreases in the average activity of all 4 classes of cells (Fig. 3.16c). However, VIP activation led to increased activity in PYR and PV cells and decreased activity in SOM interneurons (Fig. 3.16d). More detailed plots of the activity changes of VIP, SOM, PV and PYR cells with attention and VIP photoactivation can be found below in Fig. 3.17.

Finally, for each cell class I compared each cell's change in stimulus selectivity with attention to the change in its activity with VIP activation (Fig. 3.16e). I did not find a strong correlation in any cell class, indicating that a specific subset of cells is not driving both the changes with attention and with VIP photoexcitation (Pearson's correlation coefficients -0.05, 0.03, 0.05, -0.1 in VIP, SOM, PV and PYR cells respectively). PYR ($p = 3.4\times10^{-6}$) and VIP interneurons ($p = 0.015$, all other ps > 0.05) actually displayed a small but significant negative correlation, suggesting a slight segregation of attention and VIP modulations in these cell populations. Collectively, these results indicate that attention alters V1 stimulus processing through heterogeneous changes in activity and correlations across different cell classes, whereas activation of VIP interneurons produces relatively homogenous disinhibition of PYR and PV cells through SOM inhibition. These results agree with attention and VIP modulations working through separate mechanisms.

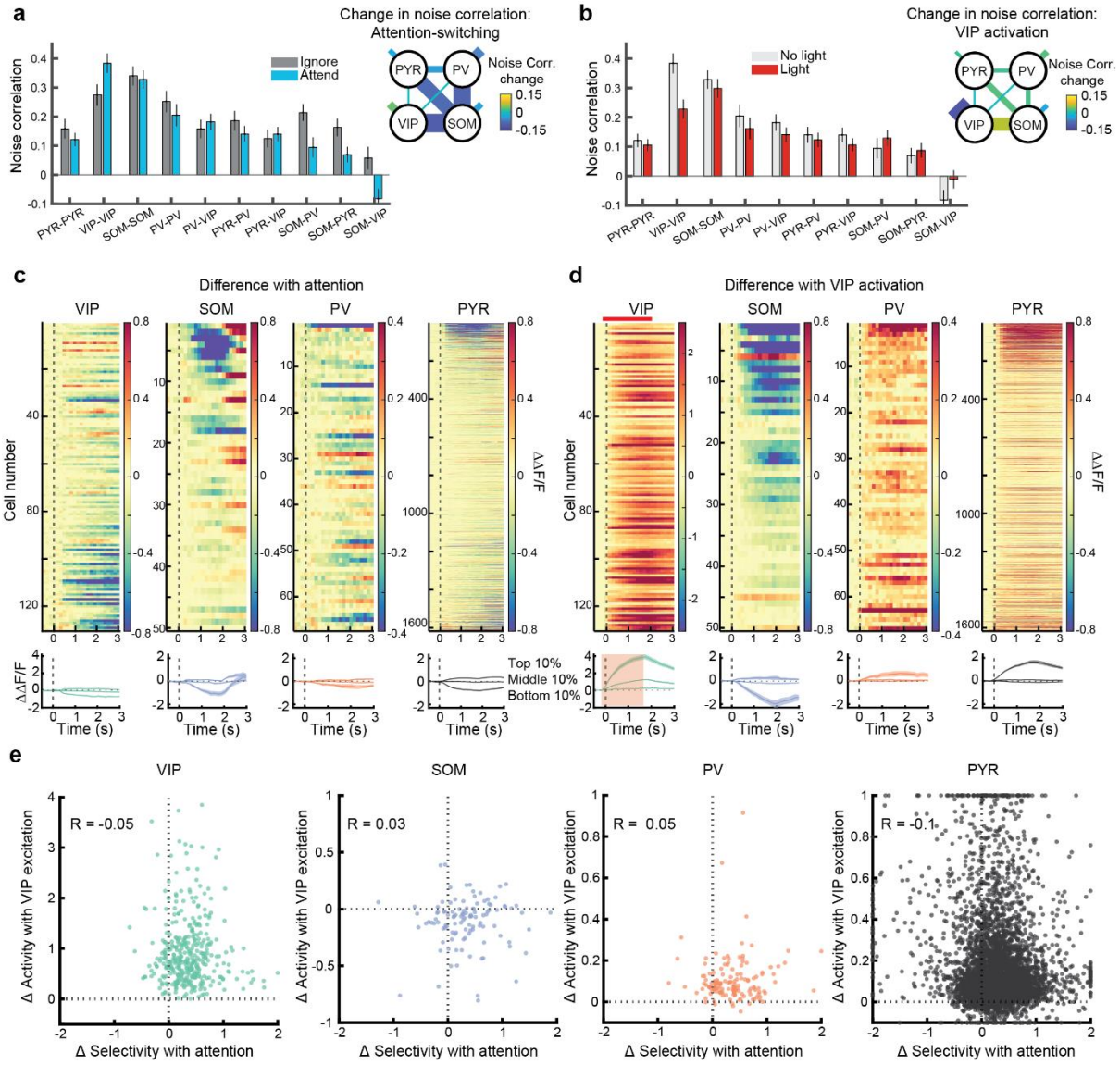

Figure 3.16: Simultaneous VIP, SOM, PV and pyramidal cell activity reveals distinct mechanisms of modulation with attention and VIP photoactivation.

a) Mean noise correlations between cell pairs belonging to the same or different cell classes, in the ignore and attend conditions, without photoactivation. Error bars represent SEM here and below (n = 11 sessions, 4 mice). Inset: Changes in noise correlations due to attention as indicated by line thickness and colour code. Shorter line segments indicate change in noise correlations between cells of the same type. **b)** Same as a, for noise correlations with and without VIP photoactivation in the attend condition. **c)** Top, difference in mean visual stimulus evoked response with attention (baseline subtracted, unrewarded grating), for each cell type, aligned to visual stimulus onset (dashed line). Cells are sorted by their average activity in the ignore condition (see also

Fig. 3.16). Bottom, average responses of cells from the top, middle and bottom 10th percentiles of the difference in responses (averaged 0-1s) with attention shown above. Shaded area indicates SEM. **d)** Same as **c** but for differences in mean visual stimulus evoked response with photoactivation of VIP interneurons (red bar and shading) compared to no photoactivation in the ignore condition. Top, cells are sorted the same as in **c**, by their average activity in the ignore condition. **e)** Relationship between ΔSelectivity with attention (positive values indicate increased stimulus selectivity with attention) and change in stimulus evoked activity with VIP photoactivation (mean 0-1s, baseline subtracted), for VIP (N = 130 cells), SOM (N = 50 cells), PV (N = 67 cells) and PYR cells (N = 1616 cells), all from 4 mice.. Cells with values greater than the axes limits were pegged to the axes. Significant negative correlations were present only in VIP and PYR cells.

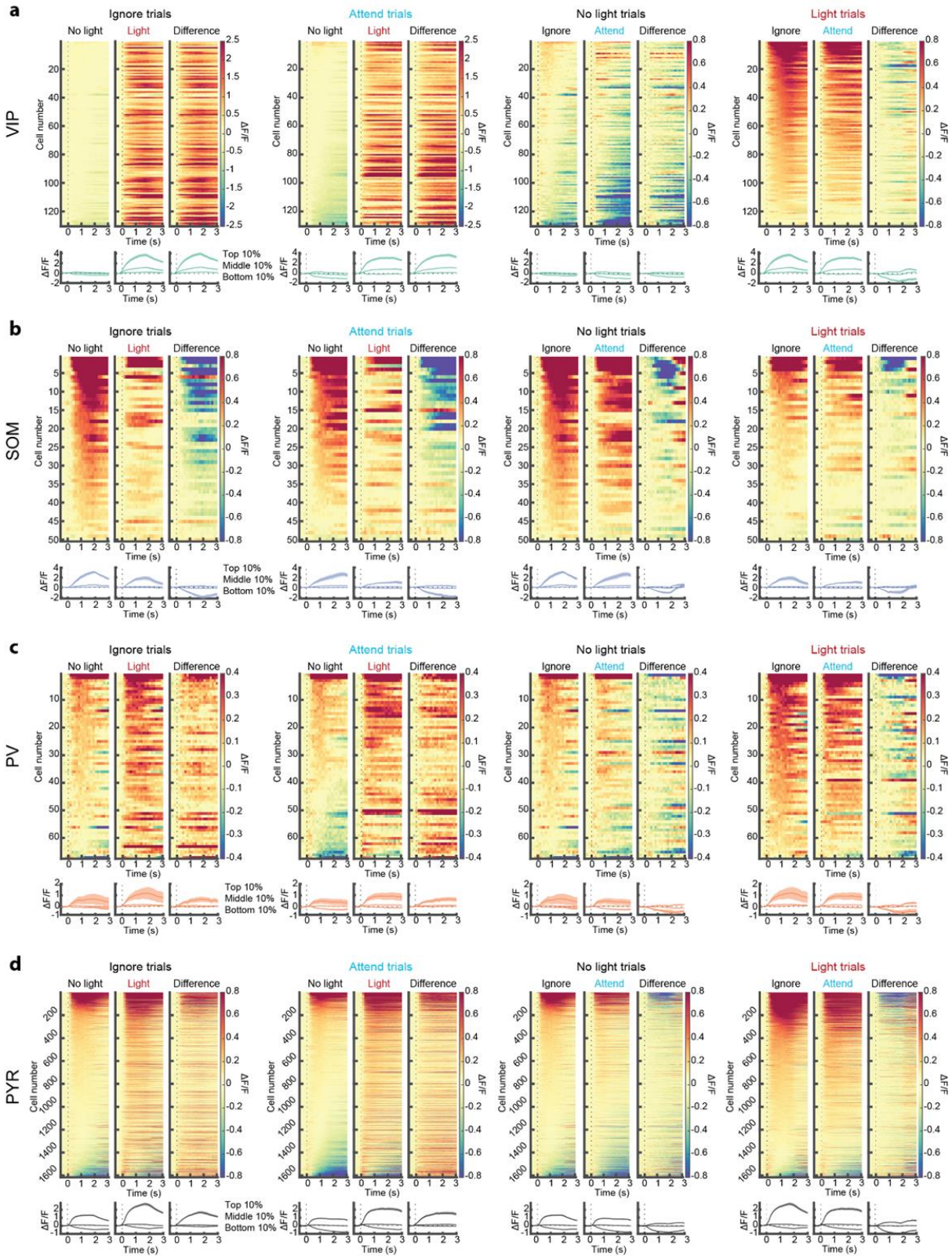

Figure 3.17: Changes in stimulus-evoked activity with attention and VIP photoactivation for multiple cell classes.

a) Top, average visual stimulus-evoked responses for all VIP interneurons (n = 130 cells, 4 mice, baseline

subtracted responses, average response to the unrewarded visual stimulus during the task) in two different conditions of no VIP photoactivation (No Light) and VIP photoactivation (Light) as indicated, and the difference of each pair of conditions. Cells are sorted according to their average activity (0-1.5s from stimulus onset) in the leftmost condition of each triplet. Bottom, average responses of cells from the top, middle and bottom 10th percentiles of activity for each condition. Shaded areas indicate SEM. **b-d)** Same as **a**, for SOM cells (n = 50 cells), PV cells (n = 67 cells), and PYR cells (n = 1616 cells), all from 4 mice.

3.5 - ACC and PL likely involved in rule maintenance and not attentional modulations

3.5.1 – ACC and PL inhibition disrupts ability to ignore visual stimuli

In addition to investigating the circuit mechanisms that might mediate attentional modulations in V1, I examined an area that could be the source of the top-down inputs that induce the attentional changes in V1. The medial prefrontal cortex is involved in rule guided behaviour (Ragozzino and Rozman, 2007; Powell and Redish, 2016; Marton et al., 2018), and one region - the anterior cingulate cortex (ACC) - has previously been shown both to project to V1 and to modulate activity in V1 in a behaviourally relevant manner (Zhang et al., 2014; Leinweber et al., 2017). The prelimbic cortex (PL) may be another source of attention modulations. Rats with lesions in PL were impaired when shifting attention between features of a stimulus, i.e. discriminating between bowls based on their odour instead of their texture (Birrell and Brown, 2000). PL may be necessary to ignore previously relevant stimuli (Floresco et al., 2008; Sharpe and Killcross, 2014).

I co-supervised a masters project conducted by Francesca Ruggeri, investigating whether ACC or PL might be the source for the attentional modulation seen in this attention switching task. Other work in the lab (Cole et al., 2022 BioRxiv) has found that the ACC has a role in the act of switching between odour and visual blocks, but not in steady state task performance. However, in those experiments the mice were discriminating between ±20° visual stimuli and achieve near perfect visual discrimination. Inhibition may not reveal an effect in these conditions because even with reduced attentional modulation the stimulus representations in V1 could still be clearly separable. We silenced ACC or neighbouring PL for alternating pairs of visual and odour blocks in the attention switching task using 3 different interleaved difficulties of visual stimulus (as described in chapter 2). If inhibiting the ACC or PL attenuates

the attentional modulation, and the enhancement from attention is required for successful behaviour, then a difficulty dependent impairment in performance might be expected; given that I found attentional modulation of stimulus selectivity to be difficulty depended in chapter 2 (Fig 2.9b).

As expected, performance in the task is higher when the mice are presented with more extreme orientation differences in the gratings (Fig. 3.18). ACC inhibition produced an increase in licking to all visual block trials, shown by a significant increase in the bias of fit psychometric curves ($p = 0.046$). ACC Inhibition also increased licking responses to the visual stimuli during the odour block when they should be ignored ($p < 0.0001$). The increased licking to irrelevant visual stimuli showed a preference for the stimulus that was otherwise rewarded during the visual block, suggesting that inhibition of ACC could be interfering with rule maintenance. Inhibition of PL significantly increased licking behaviour in response to the rewarded visual gratings in both the visual and odour blocks. The general increase in licking responses from ACC inhibition may be indicative of a role for the ACC in moderating impulsivity. The preferential responses to previously rewarded irrelevant gratings during ACC and PL inhibition align with medial prefrontal cortex's role in rule guided behaviour and could be failed suppression of the visual block response rules. The behavioural results from suppression of the ACC and PL do not indicate a role for these areas in the attention related modulation of V1.

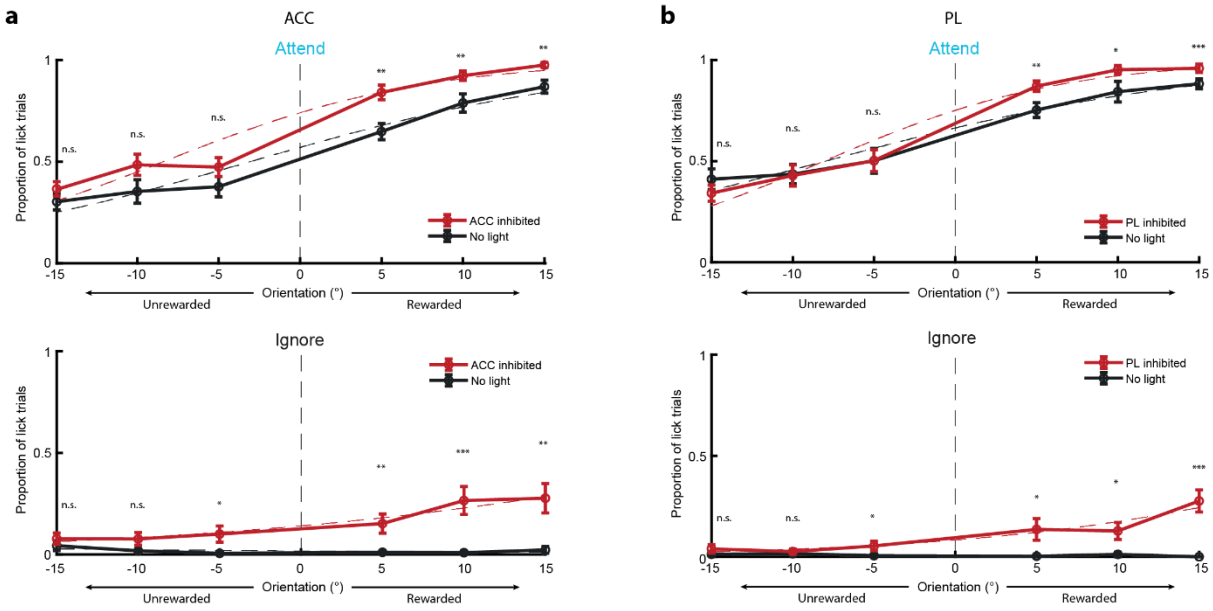

Figure 3.18: Inhibition of ACC or PL increases licking at rewarded orientations.

a) From sessions in which ACC was inhibited (n = 5 mice, 17 sessions) - the probability of the mouse responding by licking for each difficulty of visual trial with and without inhibition. Orientations further from 0 represent easier trials. Negative orientations are unrewarded gratings which in the visual block are punished with a timeout. Positive orientations are rewarded gratings, in the visual block licking in response to them releases a drop of soya milk. Top - trials from the visual block. Bottom - visual trials from the odour block. n.s. = $p > 0.05$, * = $p < 0.05$, ** = $p < 0.01$, *** = $p < 0.001$. **b)** Same as in **a**, but for sessions in which the PL was inhibited (n = 5 mice, 18 sessions).

3.5.2 – ACC and non-ACC projecting visual cortical neurons are similarly modulated by attention and behaviour

Although the experiments just presented indicate that the ACC is not involved in improving behaviour at difficult discriminations, it is still involved in representing distinct rules and its silencing affects behaviour. Long-range reciprocal connectivity links visual cortex and the ACC. The reciprocal connections between sensory and motor cortical areas can have a direction dependent preference for particular types of information (Itokazu et al., 2018). Therefore, I investigated the neurons in visual cortex that project to ACC, with the hypothesis that the ACC projecting population would be enriched for attentionally modulated neurons.

To test this possibility, I injected the retrograde tracer CTB-647 into ACC of the mice used for imaging higher visual areas described in chapter 2 (Fig. 3.19a). I was therefore able to identify which of the recorded neurons in L2/3 projected to ACC (Fig. 3.19b). Fewer neurons were labelled than expected. Most labelled neurons were in M (n=58 cells), with area PM (n = 22 cells) and (AM n = 13 cells) each having fewer. Further analysis will be focused on these 3 areas, as RL, AL, LM, and V1 each had fewer than 5 neurons labelled total across all mice. As a comparison, I used connectivity data from the Allen brain institute, taking one experiment per visual area. As a measure of the likelihood of labelling neurons, I took the ratio of the volume of visual cortex projections in ACC and the volume of the injection site in visual cortex (Fig. 3.19d). A comparison of this measure with the percentage of cells I recorded in each area that projected to the ACC (Fig. 3.19e) suggests that I am missing many ACC projecting neurons, most significantly in lateral visual cortical areas. All areas preferentially projected to ipsilateral ACC, and my injection of retrograde tracer was ipsilateral to my recording sites. However, the ACC is a long structure and my injections covered only a small portion. Different visual areas may project preferentially to different portions of the ACC, which could account for my missing connections.

For areas AM, PM and M, there was no significant difference between the ACC projecting and non-projecting populations of cells in their proportions of attentionally modulated and stimulus selective neurons (Fig. 3.19f, AM X^2=1.49, df = 3, p = 0.68, PM X^2=3.13, df = 3, p = 0.37, AM X^2=0.74, df = 3, p = 0.86). In terms of the changes with attention in the absolute stimulus selectivity of the populations of neurons, both ACC and non-ACC neurons in AM significantly enhanced their selectivity with attention. ACC projecting neurons in M and PM did not significantly change their selectivity with attention, despite non-ACC neurons in PM being enhanced. Given the small number of labelled neurons it is hard to establish the validity of this result.

Considering the involvement of VIP interneurons in locomotion induced gain, and the connectivity of ACC to VIP cells in V1 (Zhang et al., 2014), ACC projecting V1 neurons could be preferentially involved in processing information about the behaviour of the mouse. I fit the same ridge regression models used in figure 2.4 and compared the change in model R^2 with behaviour for ACC projecting cells to non-ACC projecting cells (Fig. 3.19h). A Wilcoxon rank

sum test between the two groups found no significant difference between ACC and non-ACC cells for AM (p = 0.353), PM (p = 0.829) or M (p = 0.086). This suggests that projections from the 3 visual areas tested to ACC are not enriched for behavioural information.

Neurons projecting to the prefrontal area ACC from the visual areas AM, PM, and M are not more likely to be selective for visual stimuli, preferentially modulated by attention, or preferentially modulated by behaviour using the metrics I have tested. The channel from visual areas directly to ACC may be specialised for something I have not measured such as reinforcement information from trial outcomes. Further experiments with effective labelling of neurons projecting to ACC will be required to investigate V1 and lateral visual areas.

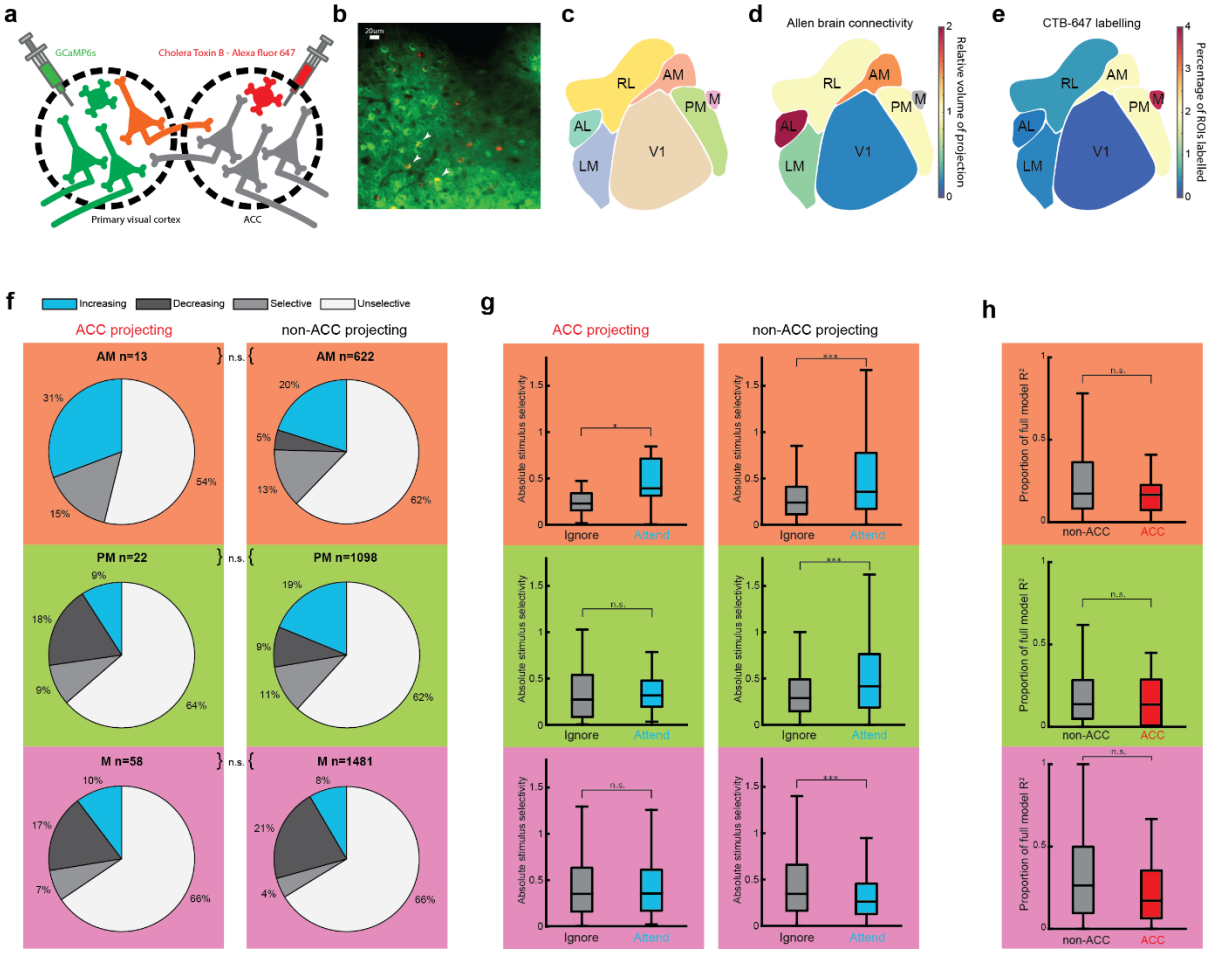

Figure 3.19: No differences between ACC and non-ACC projecting neurons in attention or behaviour modulation.

a) Schematic of viral injections used for imaging and retro-labelling. **b**) Example imaging site showing ACC projecting neurons in red and GCaMP6s in green. White arrowheads indicate 3 co-labelled neurons. **c**) Schematic

indicating colour coding of all HVA's for the in **f**, **g** and **h**. **d)** Heatmap indicating the relative intensity of projections from visual areas to the ACC using Allen brain observatory data, both dorsal and ventral ACC were included in the estimation. Values were obtained by dividing the total volume of projections (P) in the ipsilateral ACC by the injection volume (I). The values and experiment numbers (ID) are as follows. V1 - P = 0.148mm^3, I = 0.79mm^3, ID = 309113907. LM - P= 0.052mm^3, I = 0.10mm^3, ID = 479700629. AL - P = 0.0945mm^3, I = 0.04mm^3, ID = 524666904. RL - P = 0.172mm^3, I = 0.18mm^3, ID = 518606617. AM - P = 0.2502mm^3, I = 0.17mm^3, ID = 126861679. PM - P = 0.0628mm^3, I = 0.06mm^3, ID = 146077302. Area M is not in the Allen brain atlas and so was excluded. **e)** Heatmap showing the percentage of all recorded neurons in each visual area that were labelled as red and therefore projecting to ACC. **f)** Proportions of attentionally modulated ACC (left) and non-ACC neurons (right). Each colour-coded box displays information for one higher visual area. Expanded pie chart legend descriptions are as follows. Increasing - cells that significantly increase their selectivity with attention. Decreasing - cells that significantly decrease their selectivity with attention. Selective - cells that were significantly selective for one of the two visual stimuli, but which did not change significantly with attention. Unselective - cells that were not significantly selective. n.s. = not significant. **g)** Average absolute stimulus selectivity during the ignore and attend conditions ACC (left) and non-ACC (right) projecting neurons. Each colour-coded box displays information for one higher visual area. n.s. = not significant, * = p<0.05, *** = p<0.001. **h)** For ACC and non-ACC projecting cells, the reduction in R^2 when removing behavioural information (running and licking) from a ridge regression model predicting each neurons activity (1 - (no behaviour model R^2)/(full model R^2)), larger values indicate a greater proportion of the models predictive power was provided by behavioural information. Each colour-coded box displays information for one higher visual area.

3.6 – Discussion

In chapter 1 I showed that attention modulates the response properties of neurons in mouse V1 leading to increased stimulus selectivity. I demonstrate in this chapter that V1 stimulus response properties are also strongly modulated through VIP-SOM microcircuit mediated disinhibition. Critically, these modulations do not interact and appear orthogonal to one another at the population level. In support of this, attention and VIP modulations produce distinct patterns of changes, both in the activity of attentionally modulated cells and in the noise-correlations between molecularly distinct cell classes. Finally, Inhibition of VIP interneurons does not significantly perturb attentionally modulated selectivity changes, confirming that VIP interneurons are not necessary to produce the attentional modulation.

3.6.1 – Investigating the circuit basis of attentional modulation

Powerful genetic, molecular, viral and optical techniques are available when working with mice, and recent studies of visual attention using them have granted detailed insights into the circuitry underlying this cognitive phenomenon (Wang et al., 2018; McBride et al., 2019; Speed et al., 2020; You and Mysore, 2020; Hu and Dan, 2022), as well as key information on the part played by molecularly defined cell classes, and the targeting and influence of long range top-down projections on those cell classes (Wang et al., 2018; McBride et al., 2019; Speed et al., 2020; You and Mysore, 2020; Hu and Dan, 2022). However, investigation of the circuit mechanisms of cognitive phenomena like attention is difficult as it requires measurement and manipulation of the neural circuit components whilst animals perform a cognitive task. Here I have aimed to advance this approach by simultaneously measuring the activity of 4 cell classes while applying physiologically relevant manipulations to VIP interneurons as mice switched between distinct attentional states. Through this approach I demonstrate that VIP-SOM disinhibition is not the mechanism which top-down attentional signals use to alter V1 activity.

3.6.2 – Alternative circuit mechanisms of attention

A different explanation for the lack of interaction between VIP and attentional modulations could be that full-field excitation of all VIP interneurons is too coarse a manipulation, and that a precise pattern of VIP activity is played out by attentional modulation. However, if this were the case inhibition of VIP cells would be expected to disrupt the attentional modulation. Since VIP inhibition leaves the attentional modulation observed here unperturbed, what alternative local circuits could be implementing these changes?

It is possible that the attentional modulation of V1 excitatory neurons is mediated by another class of interneurons. SOM interneurons also receive direct top-down projections and attentional modulation could be inhibitory rather than disinhibitory in nature, skipping VIP (Shen et al., 2022). This seems unlikely, SOM responses were on average inhibited by attention, and if this were the case inhibition of SOM through VIP activation might also be expected to disrupt attentional modulations.

Alternatively, attention increases the selectivity of PV interneurons (Poort et al., 2022). Electrophysiological recordings in macaque V4 find that narrow-spiking (putative PV) neurons

are not only modulated by attention but are modulated more strongly than putative pyramidal neurons (Mitchell et al., 2007). Furthermore, optogenetic activation of PV interneurons, but not SOM or VIP interneurons, enhanced stimulus selectivity in mouse V1 and improved behavioural discrimination in a visual task (Lee et al., 2012). Collectively, making PV interneurons a promising candidate; I will discuss the potential role of PV interneurons in attentional modulation more in the following chapter.

As a third option, NDNF positive layer 1 interneurons display several properties similar to both VIP and SOM interneurons. They are implicated in disinhibitory control over the apical dendrites of pyramidal neurons (Abs et al., 2018), receive cholinergic inputs (Kepecs and Fishell, 2014; Poorthuis et al., 2018), and are targeted by various top-down projections (Wall et al., 2016; Abs et al., 2018).

Finally, the local mechanism of attentional modulation could initially bypass interneurons in V1 altogether; top-down inputs could instead directly synapse onto pyramidal neurons (Johnson and Burkhalter, 1997; Yang et al., 2013; Leinweber et al., 2017).

3.6.3 – What aspects of cortical function might VIP-SOM disinhibition be regulating if not attention?

VIP interneurons are clearly important for normal visual function, as their disruption during development led to visual impairments in mice (Batista-Brito et al., 2017), and their activation improved performance on a contrast detection task (Cone et al., 2019).

Locomotion induces a variety of changes to neural signalling in mice that resemble changes with attention for both mice and primates (Speed and Haider, 2021). Although their effects on the network are similar and there has been some expectation that locomotion and attention share common modulatory mechanisms, recent work indicates that they act on the network independently (McBride et al., 2019; Kanamori and Mrsic-Flogel, 2022). VIP interneurons in V1 are activated by locomotion and may mediate these changes via the VIP-SOM disinhibitory motif (Fu et al., 2014). VIP interneurons may be specifically recruited for behavioural state modulation rather than as a general mechanism for producing these sorts of changes in neural activity.

The VIP-SOM disinhibitory motif is found in other cortical areas (Lee et al., 2013; Pfeffer et al., 2013; Pi et al., 2013; Bigelow et al., 2019). In contrast to visual cortex, in mouse auditory cortex

the effects on stimulus processing of movement and VIP activation were separable (Bigelow et al., 2019). Further research will be required to identify whether VIP interneurons are processing distinct information but applying the same computation in different brain areas.

VIP-SOM disinhibition could be poised to gate plasticity onto pyramidal cells through its influence on the pyramidal apical dendrites (Williams and Holtmaat, 2019) controlling associative (Larkum, 2013) and motor learning (Chen et al., 2015). Although there are area specific differences in VIP activity, VIP interneurons across multiple brain areas have been shown to be activated by reward and punishment signals during the initial learning of the task (Szadai et al., 2022). Perhaps the function of VIP disinhibition is in all cases to facilitate plasticity of pyramidal inputs, but the information relevant to the regulation of plasticity can vary from region to region.

3.6.4 – Heterogeneity in the effects of VIP excitation

VIP activation produced robust changes in the stimulus responses of all other simultaneously measured cell classes, a reasonable outcome considering that excitatory and inhibitory cell types form a specific but richly interconnected recurrent network (Pfeffer et al., 2013). Consistent with a VIP-SOM disinhibitory motif the dominant change in SOM interneurons was inhibition and most pyramidal neurons were excited. PV interneurons also primarily increase their activity with VIP excitation, this could also be through SOM mediated disinhibition and/or due to changes in pyramidal neurons affecting their PV neighbours (Scholl et al., 2015). However, this pattern of modulation is not uniform, and optogenetic activation of VIP cells and attention expose heterogeneity within these molecular cell classes. This is to be expected as each cell class reported here contains multiple sub-classes with distinct morphology, connectivity, intrinsic properties and gene expression patterns (Tremblay et al., 2016; Bugeon et al., 2022; Condylis et al., 2022). For example, the responses of a small proportion of pyramidal neurons were inhibited by VIP photoactivation. It may be that this group represents a GABAergic population not covered by the immunohistochemical labels employed here, but it seems more likely that they represent the effect of CCK-positive VIP interneurons which directly inhibit pyramidal neurons (Tremblay et al., 2016).

Changes consistent with VIP activation disinhibiting PYR through inhibition of SOM occurred both during the attention switching task and when the mouse was passive and presented with

visual stimuli. However, a completely straightforward interpretation of this network activity runs into issues when expanding to the effects of VIP photoexcitation with no stimuli. In this scenario PYR and PV increased their activity with increasing optogenetic excitation of VIP interneurons while there was no concomitant change in the average SOM activity. These differences may be the same as Pakan et al., 2016 who found disagreement between running evoked disinhibition depending on whether the mouse was in the dark or had light (Pakan et al., 2016). A theoretical model incorporating a nonlinear input-output relationship for neurons was able to reconcile those data (Garcia Del Molino et al., 2017). In my experiments the luminance is matched across all conditions, but the network still has a different level of activity and SOM may be more active here when presented with stimuli. Caution is key when interpreting the effects of circuit manipulations, although interneurons may have clear subtractive or divisive inhibitory effects on an individual pyramidal neuron the effect can be much more complicated when placed into densely connected networks with ongoing activity (Scholl et al., 2015). However, in the data I have presented here multiple results point toward the same conclusion that the VIP and attentional modulations are independent: there is no interaction between attention and VIP activation on either firing rate or selectivity, VIP inhibition has no effect on firing rate or selectivity, and the axes of attentional and VIP modulations at the population level are orthogonal.

3.6.5 – Sources of the top-down attentional modulation

We investigated ACC and PL as potential sources of top-down inputs in this cross-modality attention switching task, because these areas are involved in rule guided behaviour (Ragozzino and Rozman, 2007; Powell and Redish, 2016; Marton et al., 2018). Although ACC projections into V1 enhance stimulus evoked activity and can affect mouse visual task behaviour (Zhang et al., 2014; Leinweber et al., 2017), there was no impairment in the ability of the mouse to discriminate between attended visual stimuli with ACC inhibition. Similarly, inhibition of the PL did not produce an attention related decrease in behavioural performance. Increased responses to the rewarded stimulus in visual blocks actually increased behavioural performance with PL inhibition. Both the ACC and PL have been implicated in regulating impulsivity (Dalley et al., 2011; Golchert et al., 2017), and so these results might be explained

by a disruption in the mouse's ability to withhold from responding to the visual stimuli.

In the odour blocks, both ACC and PL inhibition led to mice preferentially responding to the previously rewarded visual stimuli. This suggests that mice are failing to fully transition into ignoring the visual stimuli, or that inhibition of these areas is disrupting the maintenance of the current rule. This is supported by evidence showing that the ACC (Ragozzino and Rozman, 2007; Newman and McGaughy, 2011) and PL (Floresco et al., 2008; Sharpe and Killcross, 2014) are required to suppress responses to previously relevant stimuli.

An alternative possibility is that the effects presented here are not the result of ACC/PL inhibition but are instead artefactual results due to the mouse seeing the light from the optogenetic LED as it propagates through the brain. The light could distract the mouse and interfere with its maintenance of the rule of the current block. However, blue light (473nm) delivered at up to 10mW - in the absence of an opsin - has not been found to produce a significant difference in false alarm rate during a go/no-go task (Danskin et al., 2015). Blue light (470nm) of 1-4mW was used for this experiment, it therefore seems unlikely that the behavioural effects were caused by the presence of light rather than by optogenetic inhibition. Nonetheless, performing the same experiments with a light-only control would be required to confirm this position.

The results observed from ACC and PL inhibition are similar and so one concern is that the results observed are from a mixed inhibition of both areas. The same mice were used for both ACC and PL inhibition experiments with fibre optic cannulas implanted approximately 1mm apart. However, a recent pre-print measuring the spread of optogenetic light through neural tissue suggests that this effect will likely be minimal (Johnson et al., 2021). Future experiments could test this by concurrent measurement of PL and ACC activity with the inhibition. These experiments inhibiting ACC and PL suggest that they are not providing top-down inputs required for the attentional modulation of V1. Further experiments will be required to show conclusively that they are not involved.

If ACC is not the source, what other areas might be involved. The attentional modulation could come from thalamic areas. Silencing the pulvinar nucleus of the thalamus reduces attentional effects in monkey V4 (Zhou et al., 2016), and the mouse homolog of pulvinar the lateral posterior nucleus (LP) of the thalamus enhances stimulus selectivity in V1 via L1 interneuron

mediated subtractive inhibition (Fang et al., 2020). Other thalamic areas such as the mediodorsal thalamus also appear to be involved in attention (Schmitt et al., 2017; Hsiao et al., 2020). Alternatively, rather than higher thalamic areas like LP modifying V1 activity, the attentional modulation could be inherited from LGN (Casagrande et al., 2005). The reticular nucleus of the thalamus regulates the activity of other thalamic nuclei rather than projecting to cortex. Through the reticular nucleus the PFC could bias activity in thalamus to selectively enhance visual stimulus processing before it reaches cortex, allowing LGN to act as more than a relay for information from the retina (Wimmer et al., 2015).

Thirdly, the attentional modulation could route through an inferior-superior colliculus circuit. In a mouse visual spatial attention task, the motor layers of SCm were found to be attentionally modulated earlier than V1 (Hu and Dan, 2022). Moreover, an area in the inferior colliculus was required for the attentional modulation, although the specific circuit of connections found in this experiment may reflect the auditory information used to cue attention rather than a general mechanism. Further experiments will be required to investigate the potential involvement of these areas in this task.

The results presented here provide additional information on the part of VIP-SOM mediated disinhibition in top-down modulations. Activity in V1 is high-dimensional and stimulus and behavioural information can be simultaneously represented in the same neurons whilst remaining orthogonal at the population level (Stringer et al., 2019). In a similar fashion the cognitive computations served by VIP-mediated disinhibition and the modulation of V1 activity by attention appear orthogonal, allowing both to be simultaneously represented in the network without degrading the information they each carry.

Chapter 4 - PV photoexcitation impacts stimulus selectivity and has paradoxical effects on non-PV cells.

4.1 - Introduction

Parvalbumin expressing (PV) interneurons account for approximately 40% of cortical GABAergic interneurons making them a major source of cortical inhibition (Rudy et al., 2011; Kepecs and Fishell, 2014). Indeed, PV interneuron activation has been used as a method of silencing excitatory neurons (Lien and Scanziani, 2018). PV interneurons primarily contact the soma and proximal dendrites of pyramidal neurons, a connectivity pattern that is expected to produce divisive inhibition (Silver, 2010). Studies have indeed found that PV activation has divisive effects on neural responses, causing them to decrease but maintaining the neurons selectivity (Atallah et al., 2012; Wilson et al., 2012). However, at different stimulation intensities it appears PV can sharpen tuning through an 'iceberg' effect - where suppressing the inputs to a cell without changing its spiking threshold, causes many of its non-preferred inputs to drop below threshold (Lee et al., 2012, 2014b; Atallah et al., 2014; El-Boustani et al., 2014; Shapiro et al., 2022a). The effects of PV inteneuron activity may additionally vary depending on other network properties (Seybold et al., 2015; Phillips and Hasenstaub, 2016). PV interneurons have been found to reflect the average tuning of their network likely as a result of receiving input from nearby excitatory neurons with a broad range of orientation preferences (Kerlin et al., 2010; Bock et al., 2011; Scholl et al., 2015). It's also been shown that PV interneuron activity relates more to local network activity than to the features of visual stimuli (Hofer et al., 2011). PV interneurons can become more selective to visual stimuli with learning, and hence less reflective of the local average preferences (Khan et al., 2018). They can also affect the timing of the network as, PV interneurons have been shown to be involved in the production of gamma oscillations (Cardin et al., 2009; Sohal et al., 2009).

Some reported changes in neural responses with attention are in tension and PV interneuron activity could be part of the reconciling mechanism. Attention has been associated with multiplicative scaling of neural responses that maintains stimulus tuning (McAdams and Maunsell, 1999; Treue and Martínez-Trujillo, 1999; Ferguson and Cardin, 2020). Interestingly,

increases in neural tuning have also been reported, something that this simple gain modulation model cannot capture (Spitzer et al., 1988; Martinez-Trujillo and Treue, 2004; Maunsell, 2015). One possible reconciliation for these different modulations is the normalisation model of attention (Reynolds and Heeger, 2009). Normalisation involves neuron's responses being divided by a common factor which usually involves the summed activity of a group of neurons. In the neural circuit, the implementation of this computation could have several different biophysical mechanisms, potentially involving GABAergic inhibition from PV interneurons (Carandini and Heeger, 2012).

Indeed, PV interneurons have been found to be modulated by attention (Mitchell et al., 2007; Poort et al., 2022). Additionally, gamma oscillations - which PV activity can promote - have been associated with changes in attention (Fries et al., 2001; Börgers et al., 2005). It is possible that the attentional modulation of PV interneurons could be due to them reflecting changes in the local network with attention. Alternatively, PV interneurons might be mediating the attentional modulation of their surrounding cells.

A good way to understand how and if PV cells are involved in attentional effects is by manipulating their activity during an attention task. However, excitation of cortical interneurons has produced paradoxical effects. Photoexcitation of PV interneurons has been reported to produce an inhibition of both the stimulated PV interneurons and pyramidal neurons (Li et al., 2019). Conversely, PV photoexcitation has also been reported to enhance magnitude of stimulus-evoked responses in putative pyramidal neurons in auditory cortex (Aizenberg et al., 2015). While this behaviour might be counterintuitive, network models with high-gain excitatory neurons and recurrently connected inhibitory neurons can display this kind of behaviour after perturbations to the inhibitory units (Tsodyks et al., 1997; Ozeki et al., 2009; Rubin et al., 2015; Litwin-Kumar et al., 2016; Kato et al., 2017; Sadeh et al., 2017; Sanzeni et al., 2020).

Here I report that PV activation changes stimulus selectivity of non-PV neurons in mouse primary visual cortex during a cross-modal attention switching task, both when mice attended and ignored the visual stimuli. However, this change in stimulus selectivity is difficult to interpret for two reasons. First, while selectivity changed monotonically with PV activation, the underlying activity changes were non-monotonic. Second, the changes in activity were

paradoxical in nature, with an increase in non-PV cell activity caused by PV activation.

I also show that the manipulation of an interneuron can have opposite effects on the network based on the cognitive state of the animal. PV activation produced a clear inhibition of visually evoked activity in non-PV cells during calibration sessions, where the mouse does not have to switch between modalities. However, the same manipulation of PV interneurons produced no inhibition or even an excitation of non-PV visual responses whilst the mouse was engaged in an attention switching task with the same visual stimuli as in the calibration sessions. Further analysis, modelling and experiments are needed and later suggested to identify the causes and implications of these unexpected effects.

4.2 – Results

4.2.1 – PV interneuron photoactivation suppresses non-PV visually evoked activity during calibration sessions

To investigate the possibility that PV interneurons might be involved in the attentional modulation of neurons in V1, I used an all-optical approach like the one I employed in chapter 3. Using PV-cre transgenic mice, I expressed the excitatory opsin Chrimson selectively in PV cells and GCaMP7f non-selectively (Fig. 4.1a,b).

I first performed optogenetic calibration sessions to establish the efficacy of the photoexcitation of PV interneurons and to select the appropriate laser powers for use in the attention switching sessions. Chrimson is an excitatory opsin, so the light activates PV interneurons, and the expected impact of this manipulation is the inhibition of non-PV neuron activity. If the inhibition of the non-PV cell population were too severe it would have been difficult to identify whether (during the attention switching task) potential changes in selectivity were due to an actual interaction between PV cell activity and attentional modulation, or whether they were due to a flooring effect artificially shrinking the difference between the responses of stimulus selective cells to the visual stimuli. Therefore, calibration sessions are necessary to pick the laser powers that avoid this flooring effect. I conducted these calibrations while the mouse was engaged in behavioural conditions very similar to those in the attention switching task. Mice performed a session which was in effect a single extended odour block of the attention switching task introduced in chapter 2 (Fig. 4.1c). The

mice discriminated between the two odours, while they ignored visual gratings. The only difference between the calibration and attention switching sessions was that the relevance of visual stimuli did not change in the calibration sessions and the mice thus did not have to switch modalities. During these sessions I stimulated the PV interneurons with laser powers of up to 3mW.

Optogenetic activation of PV interneurons with increasing laser power produced a robust, monotonic increase in the activity of PV cells (Fig. 4.1d,f) and a decrease in the activity of non-PV neurons that were initially responsive to the grating stimulus (Fig. 4.1e,g). One mouse (M4) showed a counterintuitive increase in non-PV cell activity with increasing light power after an initial inhibition (Fig. 4.1g). This paradoxical enhancement is discussed in more detail below. There was no significant difference in the effect of PV photoexcitation on responses to the two different visual gratings, either for PV (two-way ANOVA, light p=~0, visual stimulus p=0.946, interaction $F(5,1344) = 0.18$ p=0.969) or non-PV cells (two-way ANOVA, light p=~0, visual stimulus p=0.655, interaction $F(5,4860) = 0.03$ p=0.999).

I inspected the plots for the individual mice and for each recording site selected one power ('low') that reduced - without flooring - the activity of non-PV cells (range 0.075 to 0.3mW). I then selected a second higher laser power ('high') which did not saturate the inhibition of previously active cells, but which caused greater inhibition than the first power (range 0.3mW to 0.75mW).

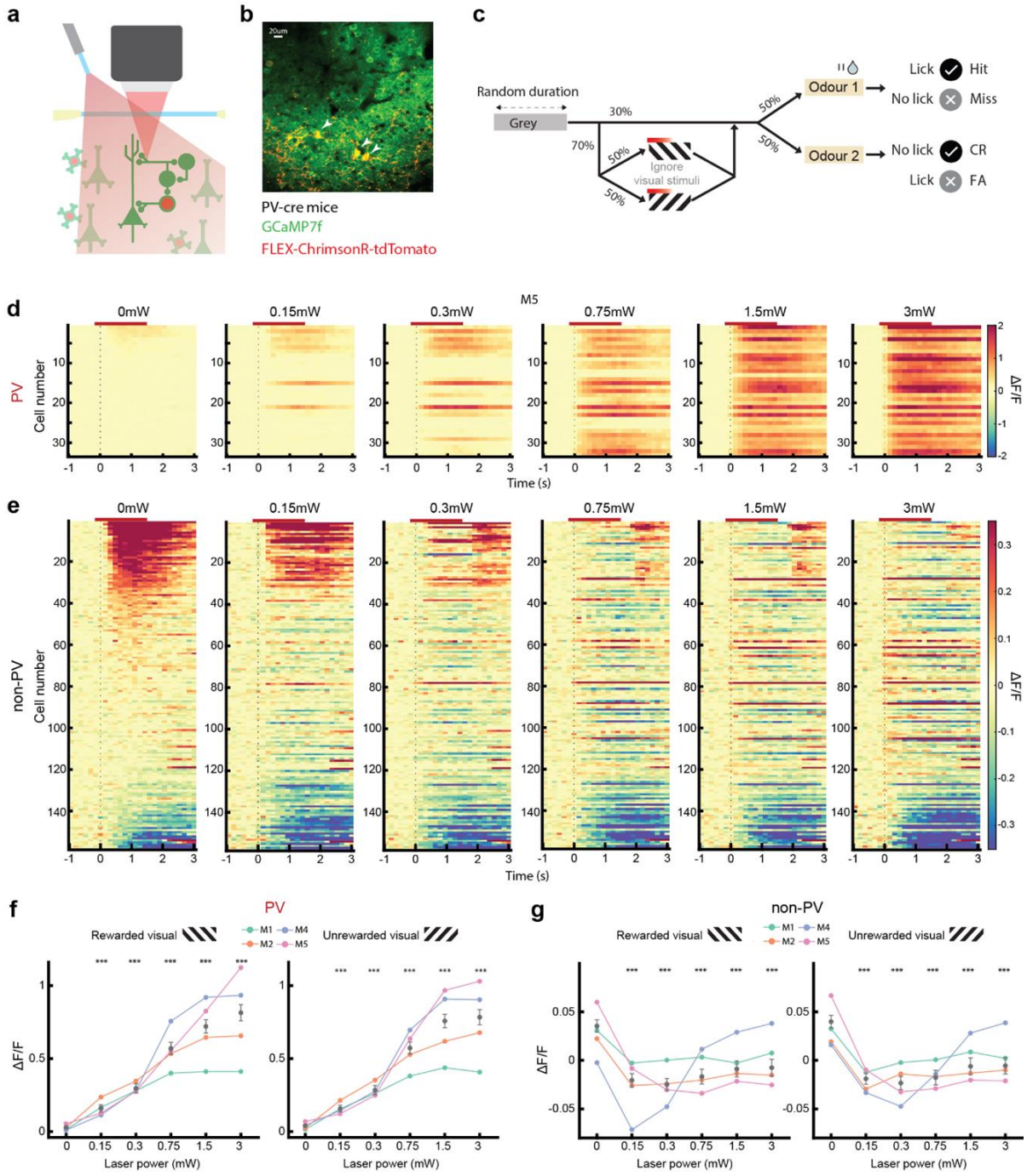

Figure 4.1: Optogenetic activation of PV interneurons suppresses non-PV responses to task irrelevant stimuli. **a)** Schematic of near-simultaneous imaging and optogenetic stimulation. **b)** Example region of an in vivo imaged plane showing non-specific expression of GCaMP7f and a PV interneuron (arrowhead) additionally expressing Chrimson-tdTomato. **c)** Schematic of the task structure used for optogenetic calibration. A continuous odour block. Mice perform go/no-go task with the odour stimuli, whilst ignoring the irrelevant visual stimuli which were paired with the optogenetic laser. **d)** Mean visual stimulus evoked activity (baseline subtracted, unrewarded grating) at each of 6 laser powers for all recorded PV interneurons from an example session. Sorted according to their average activity in the no laser condition. Responses are aligned to visual

stimulus onset (dashed line). **e)** Same as d, but for all recorded non-PV cells from the same session. **f)** Average activity in response to the previously rewarded (left) and unrewarded (right) - now irrelevant - visual stimuli (0-1.5s) for all PV cells at each of 6 optogenetic laser powers. Each coloured line indicates the responses for cells from one mouse (baseline subtracted) (n=4 mice). Grey points indicate average for all PV interneurons (n = 113 cells), error bars are s.e.m. *** = $p < 0.001$, paired t-test between no light condition and the indicated laser power. **g)** Same as in **f**, but for all non-PV cells in the same session (n = 406 cells).

4.2.2 – PV interneurons change stimulus selectivity with attention

Mice performed the same cross-modality attention switching task described in the previous two chapters (Fig. 4.2b) whilst I recorded activity in V1 through two-photon calcium imaging. Mice performed the task well, accurately discriminating between the visual grating stimuli in the visual blocks and the odour stimuli in the odour blocks, whilst ignoring the task irrelevant visual stimuli presented in the odour blocks (Fig. 4.2c).

The distribution of selectivity values in non-PV cells broadens when attending to the visual gratings (Fig. 4.2d). Cells became both more negatively and positively selective with attention, indicating an increased preference for either the unrewarded or rewarded grating respectively (Fig. 4.2e). As in chapter 2, these changes led to an increase in the absolute selectivity for the population (Fig. 4.2f). Similar to other recordings from V1 discussed in earlier chapters (Fig. 2.3b, 2.7a), the cells that enhanced their selectivity with attention constitute the majority of the significant selective cells (Fig. 4.2g). However, fewer cells were simply significantly selective without being attentionally modulated and a larger proportion of cells were unselective.

The pattern of selectivity changes similar for PV and non-PV cells, as might be expected from previous data (Mitchell et al., 2007; Poort et al., 2022). Interestingly, there was a clear bias towards negative selectivity values with attention (Fig. 4.2h), potentially a side effect of the smaller sample size in this study.

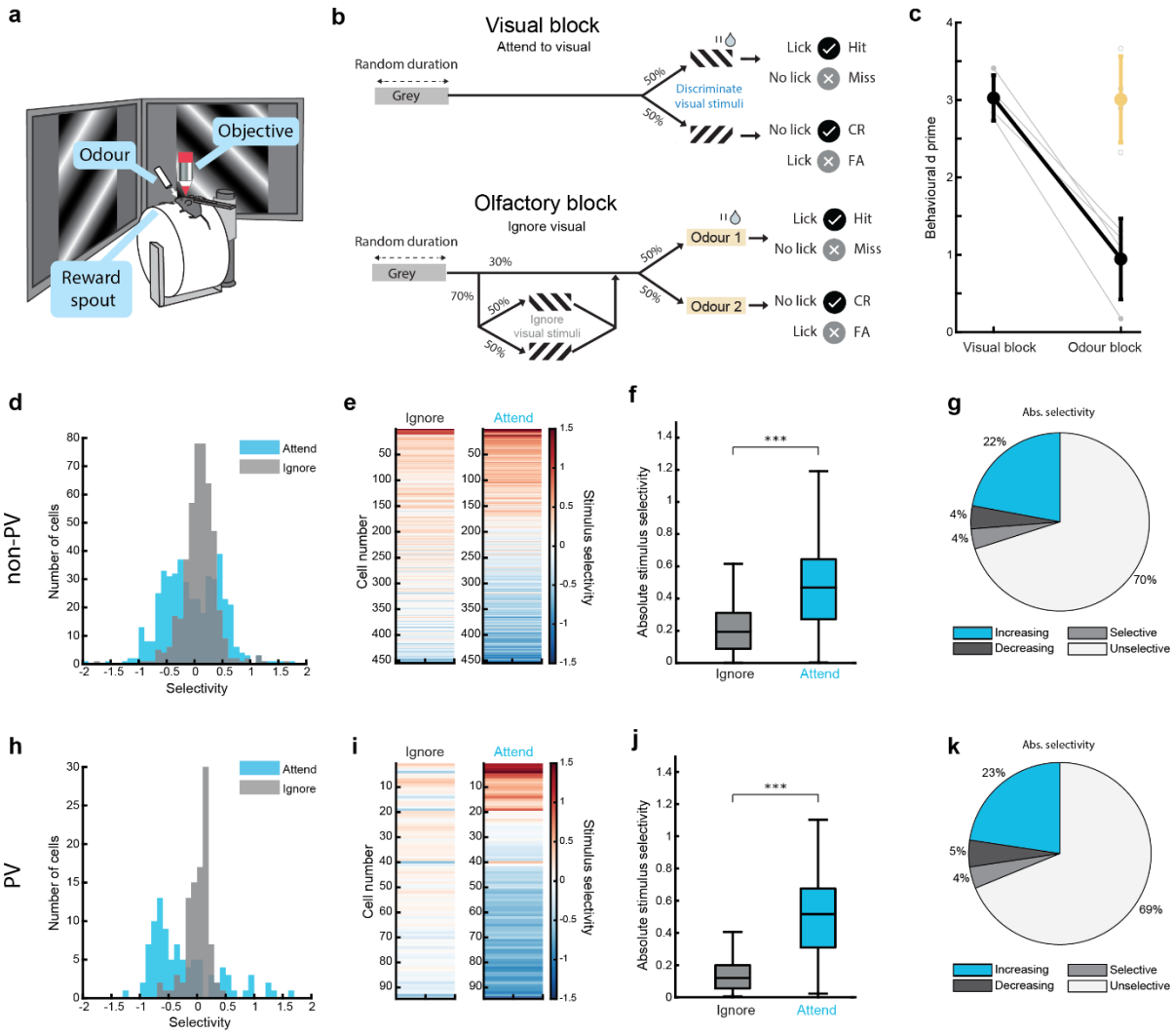

Figure 4.2: PV and non-PV cells display similar selectivity changes during the attention switching task.

a) Schematic of the experimental apparatus. **b)** Schematic of the behavioural task. Top, visual block: mice were rewarded for licking the reward spout when gratings of a specific orientation were presented (+15 degrees from vertical, rewarded grating) and not when gratings of a second orientation were presented (-15 degrees from vertical, unrewarded grating). Olfactory block: mice were rewarded for licking when odour 1 was presented and not when odour 2 or either visual grating was presented. **c)** Behavioural discrimination performance (behavioural d') across attention (n = 4 mice, t-test between attended visual trials and ignored visual trials, p = 0.003). Connected points indicate visual discrimination, individual points in the odour block represent olfactory discrimination. Grey lines and points are individual sessions, coloured lines show the average of all sessions, error bars indicate STD. **d)** Histograms of stimulus selectivity of non-PV cells when ignoring and attending the visual stimuli (n = 454 neurons, 4 mice). **e)** Stimulus selectivity of the same non-PV

cells in the attend and ignore conditions (columns). Cells were ordered by their mean selectivity across both contexts (n = 454 neurons, 4 mice). **f)** Box plots of absolute stimulus selectivity of non-PV cells during the ignore and attend conditions (n = 454 cells, 4 mice, $p = 1.20 \times 10^{-25}$, Wilcoxon signed-rank test). **g)** Proportions of selective and attentionally modulated non-PV neurons (n = 454 neurons, 4 mice). Increasing - cells that significantly increase their selectivity with attention. Decreasing - cells that significantly decrease their selectivity with attention. Selective - cells that were significantly selective for one of the two visual stimuli, but which did not change significantly with attention. Unselective - cells that were not significantly selective. **h-k)** Same as for **d-g** but for PV cells in the same sessions (n= 94 cells, 4 mice). In **j** $p = 1.28 \times 10^{-13}$, Wilcoxon signed-rank test).

4.2.3 – Activity of PV interneurons correlates with running and licking

I performed the same analysis as in the previous two chapters to determine if the changes in stimulus selectivity could be accounted for by changes in running and licking behaviour, fitting a cross-validated ridge regression model on each neuron's activity trace and evaluating the change in the model performance (R^2) with and without the behavioural predictors (for more details see chapter 2 or the methods). Similar to what I report for non-VIP cells and excitatory neurons in previous chapters, a greater change in selectivity with attention of non-PV cells was correlated with less influence from behaviour on model performance - a significant negative correlation ($r(452) = -0.168$, $p = 3.24 \times 10^{-4}$) (Fig. 4.3a). However, PV interneurons had a significant positive correlation between change in selectivity and change in model performance with behaviour, suggesting that their activity is influenced by mouse behaviour ($r(92) = 0.378$, $p = 1.73 \times 10^{-4}$) (Fig. 4.3b). This is surprising given that PV cells have been reported to reflect the tuning of their neighbouring pyramidal neurons (Kerlin et al., 2010; Bock et al., 2011; Scholl et al., 2015). However, when selecting PV cells with the least influence of running and licking (bottom 50^{th} percentile) I found that there was still a significant modulation from attention (Wilcoxon signed-rank test, n = 47 cells, $p = 2.10 \times 10^{-5}$) suggesting that these cells are both affected by behaviour and attention.

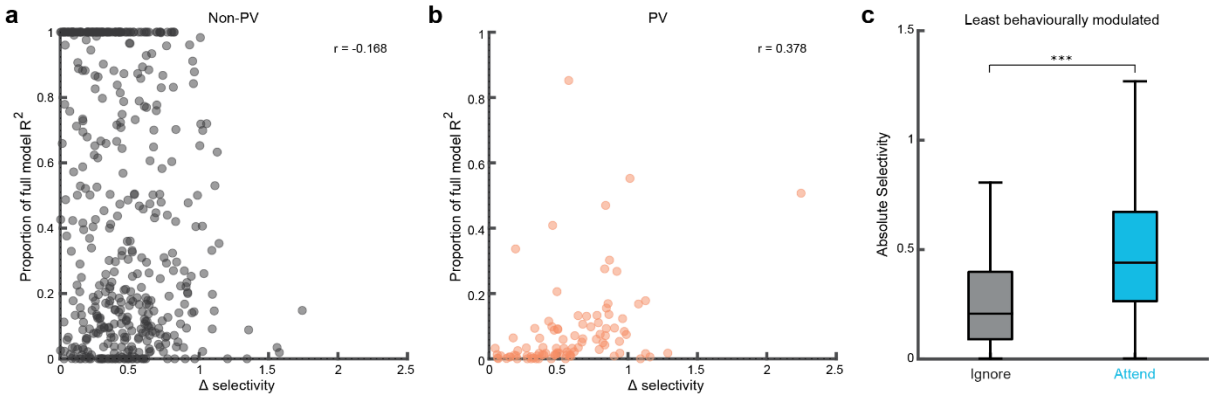

Figure 4.3: Changes in PV interneuron stimulus selectivity correlates with changes in behaviour.

a) Non-PV cells with stronger influence of running and licking do not account for attentional modulation. Relationship between absolute change in selectivity for the visual stimuli with attention (ΔSelectivity) and the reduction in R^2 when removing running and licking behaviour information from a ridge regression model predicting the activity of each neuron: 1 - (no-behaviour model R^2)/(full model R^2). Larger values indicate a greater influence of running and licking. **b)** Same as **a**, but for PV cells. Although the change in PV cell selectivity is positively correlated with model changes when removing running. **c)** Average absolute stimulus selectivity during the ignore and attend conditions (n = 190 cells, 4 mice, non-PV neurons) when selecting only neurons whose activity is least influenced by running and licking behaviour (bottom 50% of the median change in model R^2, Wilcoxon signed-rank test, $p = 3.28 \times 10^{-14}$).

4.2.4 – Increasing PV photoexcitation during the attention switching task increases non-PV cell activity

The optogenetic laser powers used in the attention switching task were chosen based on the inhibition of non-PV responses in the calibration sessions under very similar conditions. I therefore expected that average activity of non-PV cells in response to visual stimuli would also be reduced at both the low and high laser powers when attention switching. While PV interneurons showed monotonic increases in their activity with increasing light power (Fig. 4.4e, g), the effects on average non-PV responses are heterogeneous (Fig. 4.4f, h).

When comparing the conditions of no light to low light power, the effects of PV photoexcitation in the attention switching task led to a significant reduction in the visually evoked responses of non-PV cells to the ignored visual stimuli (Mean baseline corrected

activity - no light = 0.047 ΔF/F, low light = -0.013 ΔF/F. Paired t-test p = 3.21x10-12, n = 454). This is similar to the effect of light in the calibration sessions at similar light powers shown (Fig. 4.4h). However, when comparing the conditions of low and high light power, the effects of PV photoactivation differ between the attention switching task and the calibration sessions. For the attention task, there is a significant increase in non-PV cell activity from low to high light power (Mean baseline corrected activity - low = -0.013 ΔF/F, high = 0.078 ΔF/F. Paired t-test p = 4.11x10-12, n = 454 cells), returning average activity to unperturbed levels (no vs high light, paired t-test = 0.057, n = 454 cells). For the calibration session at similar powers, the average activity remained inhibited from low to high powers, with no significant difference (Mean baseline corrected activity - low = -0.020 ΔF/F, high = -0.017 ΔF/F. Paired t-test p = 0.626, n = 406 cells). As a result, a monotonic increase in PV interneuron activity with photoexcitation produced non-monotonic changes in the average activity of non-PV cells, with a decrease from no light to low laser power and increase from low to high laser power. Changes in mean activity with the optogenetic laser were similar both when ignoring and attending to the gratings.

It is unlikely that the difference between calibration and attention sessions is due to behaviour. Mice responded similarly to the visual stimuli in calibration session (Behavioural d', mean = 0.88, individual mice = 1.15, 0.44, 0.47, 1.45) and in the odour block of the attention switching session (Behavioural d', mean = 0.94, individual mice = 1.31, 1.21, 0.17, 1.08). Additionally, the effects are unlikely to be due to an artefactual effect of light, both because much lower powers are used here than those in the opsin free control mice presented in chapter 3, and because the difference of effect here occurs despite the visual stimuli, imaging site, laser power and task requirements being the same. The only differences between the calibration and the attention switching task sessions are: (1) time spent performing the task and (2) the requirement that the mouse must alternate between visual and odour blocks, rather than performing a single continuous odour block. These results suggest that subtle changes in the cognitive state of the animal can impact the effect that PV activation has on the average activity in the local network.

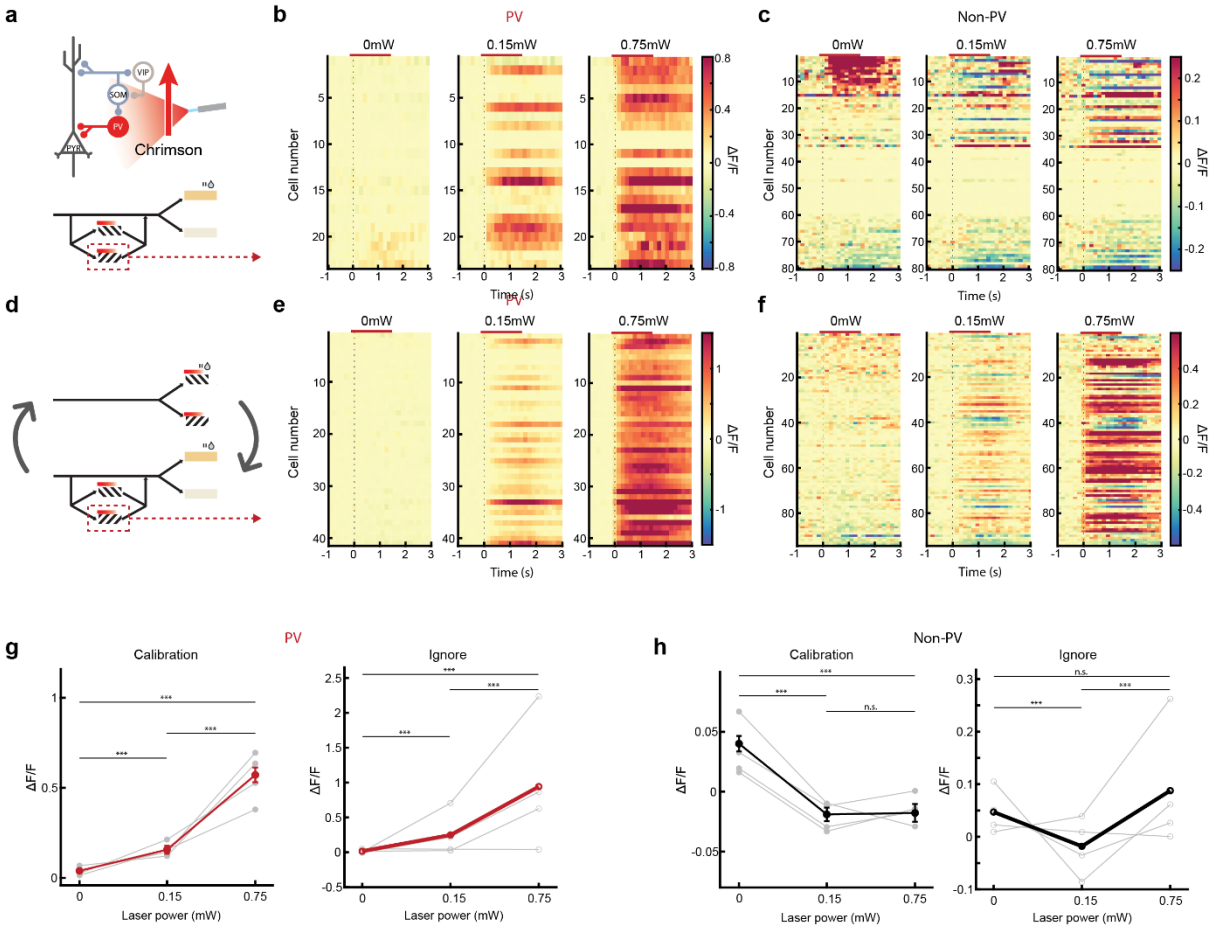

Figure 4.4: Effect of PV activation differs depending on behavioural task and laser power.

a) Schematic of the task used in figure 4.1. **b)** Data from an optogenetic calibration session, as in figure 4.1, task in **a**. Mean visual stimulus evoked activity (baseline subtracted, unrewarded grating) at each of 3 laser powers for all recorded PV interneurons from one mouse. Responses are aligned to visual stimulus onset (dashed line). Sorted according to their average activity in the no laser condition. **c)** Same as for **b**, but for all recorded non-PV cells from the same session. **d)** Schematic of the attention task used in figure 4.2. **e)** Data from odour block of the attention switching task, as in figure 4.2, task in **d**. Mean visual stimulus evoked activity (baseline subtracted, unrewarded grating) at each of 3 laser powers, for PV cells. For the same mouse as in **b** and **c. f)** Same as for **e**, but for all recorded non-PV cells from the same session. **g)** Mean visual stimulus evoked activity of PV interneurons with increasing PV photoactivation. Left, during the optogenetic calibration session (n=113 cells, 4 mice). Right, ignored visual stimuli during the attention switching task (n = 94 cells, 4 mice). Gray lines indicate individual mouse averages, coloured lines indicate overall average of all cells. *** = p<0.001 for paired t-tests. **h)** Same as in **g**, but for non-PV cells. Left, calibration session (n = 406 cells, 4 mice). Right, attention switching task ignored visual stimuli (n = 454 cells, 4 mice).

4.2.5 – PV photoexcitation affects cells differently depending upon their stimulus selectivity

The PV interneurons recorded here displayed a preference for the unrewarded grating in the attention switching task. The tuning of these PV cells could be reflective of which neurons they are connected to. I therefore examined whether the effect of PV photoexcitation on non-PV cell activity in the attention switching task differed depending on visual stimulus preference and attentional modulation. Negatively selective non-PV cells that significantly increased their selectivity with attention (Fig. 4.5b) were on average inhibited during both the low and high power optogenetic laser, reducing the response to both visual stimuli when they were attended and ignored (see the table below for the results of a two-way ANOVA on mean responses). A different pattern was observed in the responses of positively selective non-PV cells that become more selective with attention. Their activity was unperturbed during the low laser power and increased significantly for high laser power for both stimuli and with and without attention (see table below for ANOVA results).

As might be expected given that they were a majority of recorded neurons, the responses of non-PV cells that did not significantly change their selectivity with attention more closely reflected the population average presented in Fig. 4.4h (Fig. 4.5c). For these cells the low light power significantly inhibited responses, but paradoxically the high light power significantly enhanced responses compared to the no light condition. This pattern was true for both visual stimuli when the mouse was attending or ignoring (see table below for ANOVA results). This demonstrates that non-PV cells can be influenced differently by PV activation depending on their stimulus selectivity and whether their activity is modulated by attention, suggesting that these neurons are connected differently into the local network. Further analysis will be required to explicitly test which features of a cell's activity are predictive of the effect that PV activation will have on its responses, but these experiments indicate that stimulus selectivity may be an important factor.

Table 4.1: Two-way ANOVA with multiple comparisons for effects of attention and PV photoexcitation on mean response to visual stimuli.

Cell group	Visual stimulus	Attention effect	Laser effect	Interaction	No vs low light	No vs high light	Low vs high light

Negatively selective	Preferred	p=0.770	$p=2.48x10^{-4}$	F(2, 336) = 0.528, p=0.590	$p=1x10^{-4}$	p=0.020	p=0.351
Negatively selective	Non-preferred	$p=4.93x10^{-4}$	p=0.046	F(2, 336) = 0.128, p=0.880	p=0.034	p=0.364	p=0.493
Positively selective	Preferred	p=0.214	p=0.006	F(2, 60) = 0.072, p=0.931	p=0.977	p=0.018	p=0.011
Positively selective	Non-preferred	p=0.889	$p=6.58x10^{-4}$	F(2, 60) = 0.021, p=0.979	p=0.998	p=0.003	p=0.002
Unmodulated	Preferred	p=0.645	$p=7.17x10^{-12}$	F(2, 2088) = 0.120, p=0.887	$p=2x10^{-4}$	p=0.005	$p < 1x10^{-4}$
Unmodulated	Non-preferred	p=0.207	$p=1.54x10^{-12}$	F(2, 2088) = 0.232, p=0.793	p=0.014	$p < 1x10^{-4}$	$p < 1x10^{-4}$

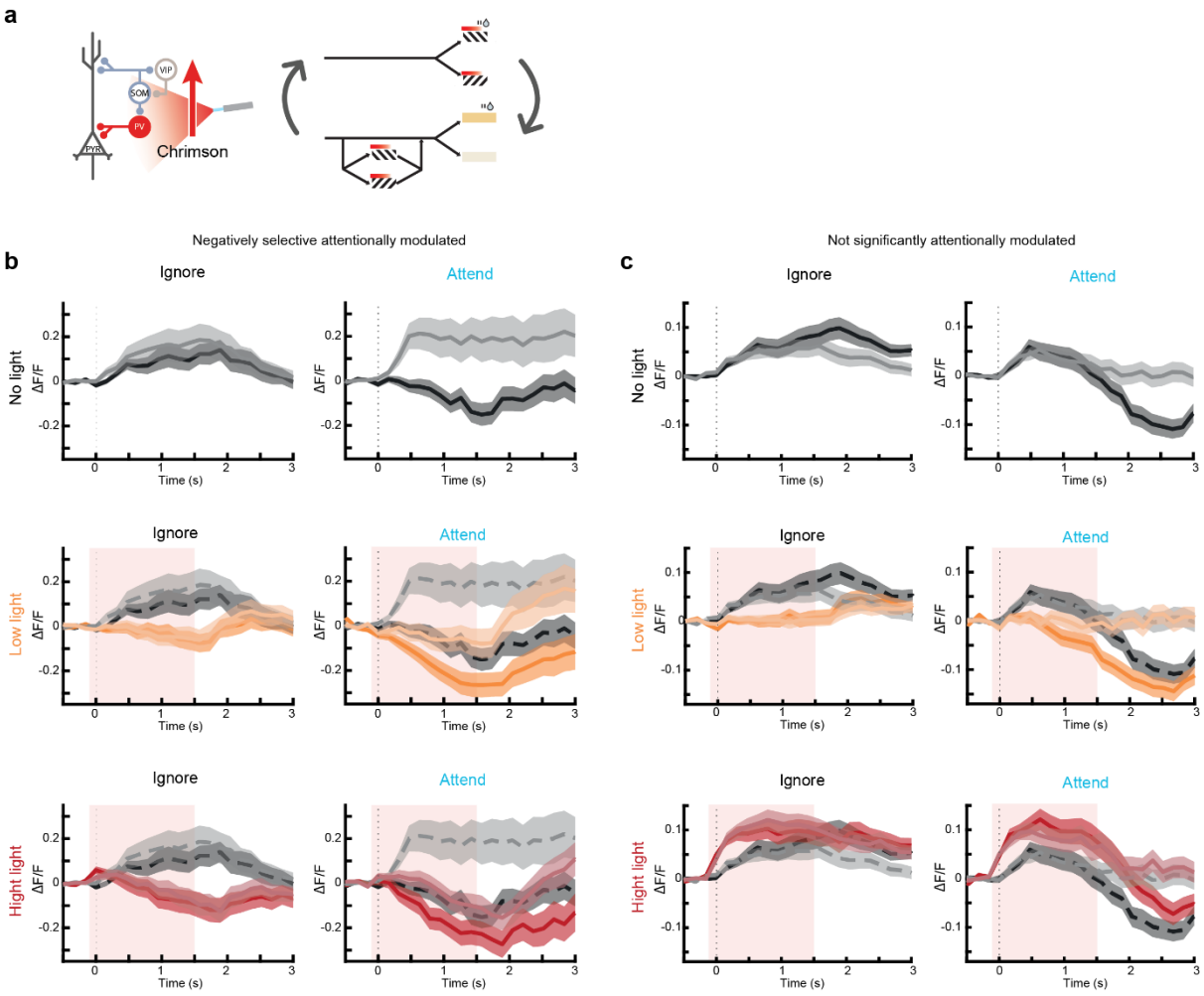

Figure 4.5: PV photoactivation affects the mean responses of different non-PV cell groups differently.

a) Schematic showing PV photoactivation during the attention switching task. Light onset (red bars) was from -0.1s to 1.5s relative to visual stimulus onset. Light was ramped off over 0.2s. **b)** Top - mean visual stimulus evoked activity for all non-PV cells with preference for the unrewarded stimulus that significantly increased their selectivity with attention (mean of n = 57 cells, 4 mice, shading indicates SEM). Middle - same sessions, responses with low PV photoactivation (orange). Responses from top are superimposed for comparison (grey dashed lines, light red shading indicates light onset). Bottom - Same as middle, but with high PV photoactivation (red). **c)** Same as in **b**, but for all non-PV cells whose stimulus selectivity was not significantly modulated by attention (n = 349 cells, 4 mice).

4.2.6 – Average prestimulus activity differs between calibration sessions and the attention switching task

A subtle shift in top-down inputs or baseline activity may play a role in the difference in effect that PV activation has on non-PV neuron visual evoked activity between calibration and

attention switching sessions. To investigate this possibility, I compared the mean activity in the period before visual stimulus onset for the calibration sessions and for the odour block of the attention switching sessions (1s to 0.1s before visual stimulus onset). Baseline activity was significantly higher during attention switching sessions than in calibration sessions for both PV cells ($p = 2.66x10^{-18}$ Wilcoxon rank sum test, calibration – n = 113 cells, attention switching – n = 94 cells) and non-PV cells (p = ~0 - *within MATLAB precision* - Wilcoxon rank sum test, calibration – n = 406 cells, attention switching – n = 454 cells). For non-PV cells this effect was consistent when averaging cells from each mouse separately (Fig. 4.6b). This difference in baseline activity may be involved in the paradoxical responses seen here, but further research will be required to identify any specific mechanism.

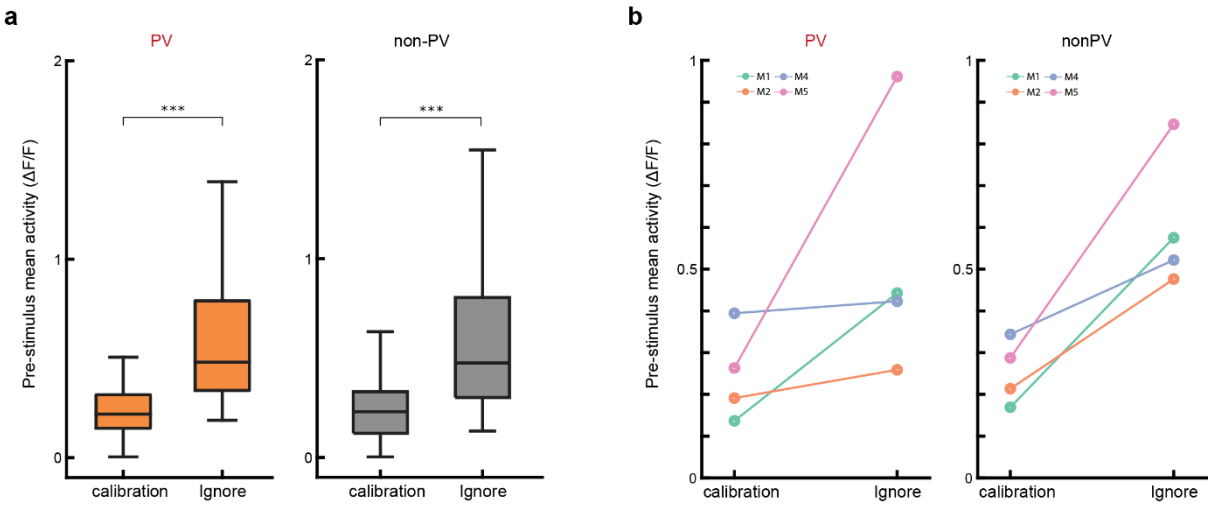

Figure 4.6: Prestimulus activity is higher when mice are attention switching than during optogenetic calibration sessions.

a) Mean activity from 1s to 0.1s before visual stimulus onset during optogenetic calibration sessions or the odour block of attention switching sessions. Left – for all PV cells (Calibration – n = 113 cells, Ignore – n = 94 cells), right – for all non-PV cells (Calibration – n = 406 cells, Ignore – n = 454 cells). Wilcoxon rank sum test *** = p <0.001. **b)** The same data as in **a** but averaged for across neurons for each mouse (n = 4 mice). Left – averages of all PV cells, right – averages of all non-PV cells.

4.2.7 – PV photoexcitation impacts selectivity changes with attention

I next examined the effect that PV photoexcitation had on stimulus selectivity. Given the non-monotonic change in average responses, one might expect that selectivity changes would also be non-monotonic. PV interneuron photoactivation differentially affects the selectivity of

neurons when the mice are attending to versus ignoring the visual stimuli. For both non-PV (Fig. 4.7b) and PV cells (Fig. 4.7c) there is a significant effect of attention on the absolute selectivity of the population. Importantly, with increasing laser power, PV photoexcitation increases selectivity when ignoring the visual stimuli and decreases selectivity when attending to the visual stimuli. When restricting the analysis to attentionally modulated non-PV cells (Fig. 4.7d), stimulus selectivity was not statistically significantly affected by PV photoexcitation, but a trend resembling the PV and non-PV populations overall can be seen - see the table below for the statistical results. These changes in selectivity do not seem to be due to changes in the variation of responses with PV photoexcitation because a different selectivity index using only the mean responses ((Attend - ignore) / (Attend + Ignore)) produces - if anything - more extreme results following the same pattern - statistics summarised in the table below. Using this simpler selectivity index, the pattern of stimulus selectivity changes with PV photoexcitation for attentionally modulated non-PV cells matches the pattern described above for all non-PV cells.

Given that monotonic changes in stimulus selectivity occur due to non-monotonic paradoxical changes in mean activity with PV photoexcitation, it is difficult to interpret the role of PV interneurons in stimulus selectivity changes with attention. Further analysis and modelling of the data may help to clarify the results. Matching recorded neurons across recordings will identify whether individual non-PV cells are consistent in their changes with PV photoexcitation or whether different ensembles dominate under different task conditions. Post-hoc immunolabelling of cell types as in chapter 3 could clarify whether the paradoxical changes were due to the activity of a different interneuron population. Additionally, I am currently collaborating with Katharina Wilmes and Claudia Clopath to extend the circuit model used in (Poort et al., 2022) to gain insight into the changes happening with VIP photoexcitation in chapter 3. Application of models like this may help the interpretation of the effects of PV photoexcitation presented here.

Table 4.2: Two-way ANOVA results for the effects of attention and PV photoexcitation on selectivity.

Cell group	Attention effect	Laser effect	Interaction
All non-PV	$p=2.93\times10^{-9}$	p=0.026	$F(1,1812) = 58.830$, $p=2.79\times10^{-14}$
Increasing with attention	$p=3.02\times10^{-4}$	p=0.202	F(1,264) = 3.835, p=0.051
PV	$p=1.05\times10^{-10}$	p=0.020	$F(1,372) = 102.670$, $p=1.81\times10^{-21}$

Table 4.3: Two-way ANOVA results for the effects of attention and PV photoexcitation on simpler selectivity measure (A-B)/(A+B).

Cell group	Attention effect	Laser effect	Interaction
All non-PV	P=0.004	$P=1.06\times10^{-4}$	$F(1,1812) = 136.770$, $p=1.64\times10^{-30}$
Increasing with attention	$P=5.42\times10^{-6}$	P=0.007	$F(1,252) = 22.993$, $p=2.78\times10^{-6}$
PV	$P=5.05\times10^{-7}$	$P=3.27\times10^{-6}$	$F(1,372) = 154.700$, $p=6.16\times10^{-30}$

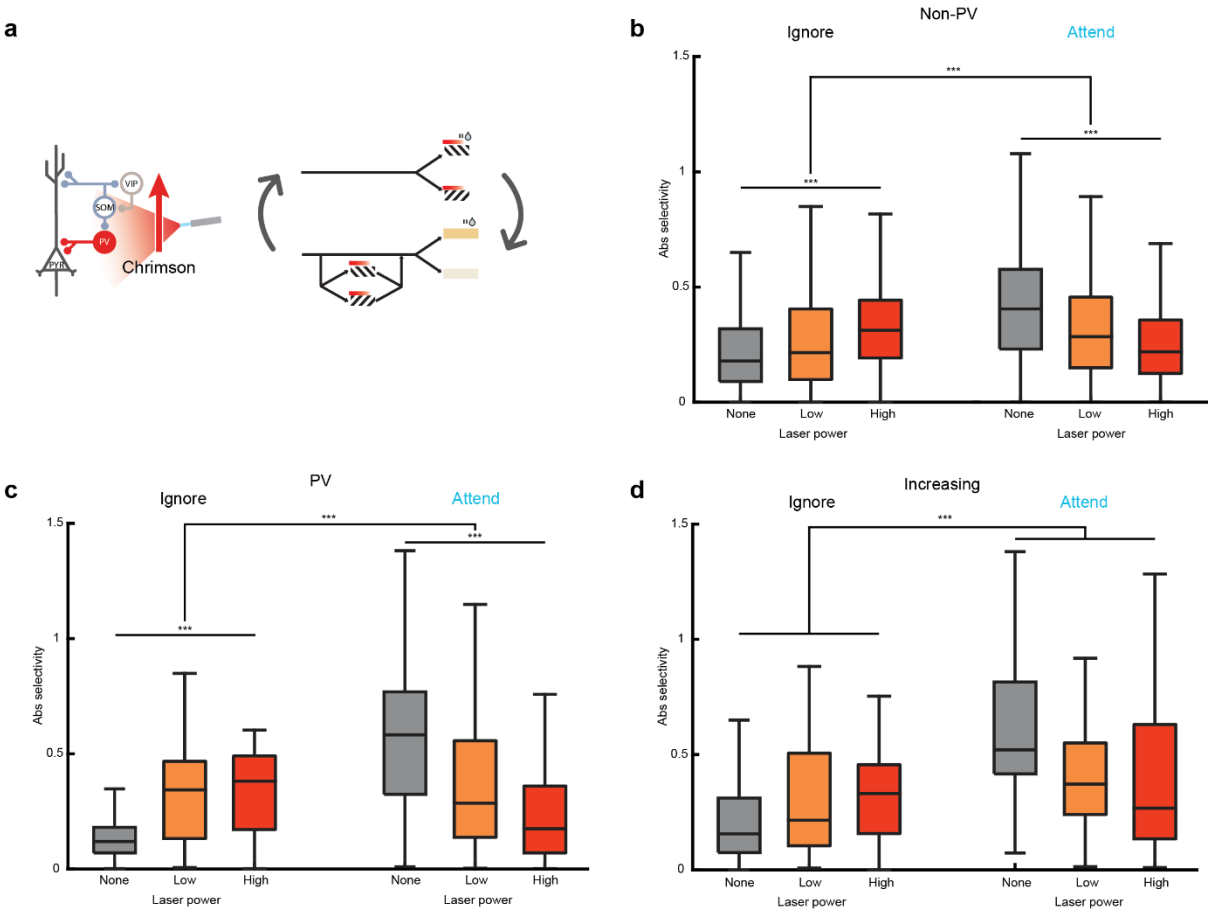

Figure 4.7: Non-monotonic changes in activity with PV photoactivation induce monotonic changes in selectivity both when attending and ignoring visual stimuli.

a) Schematic showing PV photoinhibition during the attention switching task. Light onset (red bars) was from -0.1s to 1.5s relative to visual stimulus onset. Light was ramped off over 0.2s. **b)** Absolute stimulus selectivity without and with PV photoinhibition for all non-PV cells which significantly increased their selectivity with attention (n = 68 cells, 4 mice). Stimulus selectivity measured when ignoring the visual stimuli (left) and attending the same stimuli (right). See text for results of 2-way ANOVA. **c)** Same as in **b**, but for all non-PV cells (n= 454 cells, 4 mice). **d)** Same as in **b**, but for all PV interneurons (n = 94 cells, 4 mice).

4.3 – Discussion

4.3.1 – PV photoexcitation interacts with the modulation of stimulus selectivity by attention

PV interneurons form a major component of the network of GABAergic interneurons and are modulated by attention (Mitchell et al., 2007; Poort et al., 2022). I investigated the effect of PV photoactivation on a neural correlate of attention in mouse V1. In this task attending to the visual stimuli increases the stimulus selectivity of both individual neurons and the neural population as a whole. PV photoactivation decreased stimulus selectivity when the mice were attending to the visual stimuli and enhanced selectivity when the visual stimuli were ignored, for both PV and non-PV cells alike. Crucially, these changes occurred with non-monotonic and paradoxical changes in non-PV neuron activity as a result of increasing PV photoactivation, making interpretation of these results difficult. Further analysis may help to resolve this picture. Post-hoc identification of the molecularly defined cell types of the recorded neurons may attribute some of the paradoxical effect to interneuron populations and help to constrain the pyramidal cell population. Additionally, circuit models such as those in (Poort et al., 2022) may produce plausible and testable explanations for how non-monotonic activity changes can lead to monotonic changes in selectivity.

It is also possible that selectivity changes may not necessarily be due only to the direct effect of manipulations on V1 activity. Circuit manipulations could be echoing through and feeding back from downstream regions. For example, mouse anterior lateral motor cortex (ALM) and thalamus are bidirectionally connected; inhibition of activity in thalamus caused a collapse of ALM activity, and photostimulation of PV interneurons in ALM similarly caused a reduction in thalamic activity (Guo et al., 2017) (see also (Reinhold et al., 2015)). Equally, the activity

reciprocally connected areas could be robust to the changes in V1 (Li et al., 2016). Further experiments will be needed to identify whether the effects of PV photostimulation on selectivity are robust, and experiments inhibiting PV interneuron activity during attention tasks may help resolve the role of these interneurons in the modulation of visual activity by attention.

In the process of investigating the role of PV interneurons in attentional modulation, I discovered that the effect of PV activation changes dramatically based on a subtle change in cognitive state of the animal, to the extent that the same non-PV cells can be either inhibited or paradoxically excited at the same light powers. It is important to first understand how and why these paradoxical effects occur.

4.3.2 – Paradoxical activity changes with PV photoexcitation

Optogenetic activation of PV interneurons has been shown to reduce network activity in response to visual stimuli (Kaplan et al., 2016). Excitation of PV interneurons with channelrhodopsin-2 (ChR2) has been used as a method of inhibitory investigation of excitatory neurons (Lien and Scanziani, 2018). Activation of PV interneurons has even been reported to be more effective at silencing the excitatory neuron population than the direct effect of inhibitory opsins expressed in pyramidal neurons at low laser powers (Li et al., 2019). It is therefore surprising that the same laser powers produced distinct effects on non-PV cells in calibration vs. attention switching task sessions, despite being applied to the same recording sites in the same mice, with the same visual stimuli and the same behavioural task.

The preferential inhibition of negatively selective non-PV cells (Fig. 4.5b) and excitation of unselective cells (Fig. 4.5c) could be associated with PV interneurons in these recorded sites being predominantly negatively selective when the mice were attending to the visual stimuli (Fig. 4.2h). However, further analysis will be required to establish whether there is another metric which more accurately predicts the effect of PV photoexcitation on these cells, and whether the negatively selective bias represents a scientifically relevant finding or if it is simply a feature of the sample I have collected.

Other changes in context have also been found to influence the interaction of interneuron populations. Locomotion has been shown to inhibit the activity of SOM interneurons when

mice were in the dark, consistent with a VIP-SOM disinhibitory motif (Fu et al., 2014; Pakan et al., 2016). However, when the mice were presented with visual stimuli, the activity of both SOM and VIP interneurons was positively modulated by locomotion (Polack et al., 2013; Pakan et al., 2016). One explanation for these results is offered by a theoretical model using excitatory, PV, SOM and VIP neural populations and a nonlinear neuronal input-output relationship (Garcia Del Molino et al., 2017). Under these conditions the activity of SOM interneurons in response to top-down modulation is reversed depending on the baseline network activity. As seen in chapter 3, attention switching elicits changes in the activity of all recorded populations and an increase in baseline activity from calibration to attention switching sessions was observed for both PV and non-PV cells, so it is possible that this difference in baseline activity could be involved in the reversal of PV interneuron effects seen here. A prediction of the model is that even when the overall effect is excitatory, the initial response of SOM interneurons would be inhibitory (aligned with a VIP-SOM disinhibitory motif) (Garcia Del Molino et al., 2017). Unfortunately, the rate at which brain volumes were imaged in my experiments (6.33Hz) is not rapid enough to resolve fast early activity changes. Paradoxical responses to photoexcitation of PV interneurons have been observed before (Aizenberg et al., 2015; Li et al., 2019). This paradoxical result might be explained by strong recurrent excitation, such as in inhibition stabilised networks (Tsodyks et al., 1997; Ozeki et al., 2009; Rubin et al., 2015; Litwin-Kumar et al., 2016; Kato et al., 2017; Sadeh et al., 2017; Sanzeni et al., 2020). Other studies have manipulated PV interneurons and found no paradoxical effects (Atallah et al., 2012; Yu et al., 2016; Gutnisky et al., 2017). The difference between the different studies could be methodological, for example in the proportion of interneurons that are activated. In general, cell-specific manipulations must be considered in the context of the circuit as a whole. As an additional example of an initially surprising results of cell type manipulations, subtle excitation of pyramidal neurons produces a net inhibitory effect on the response of the population to visual stimuli (Chettih and Harvey, 2019).

Beyond a repeat of these experiments, other further experiments and analyses that might help clarify the results presented here include:

- An identification of recorded neurons across days. Are the inhibited cells in the calibration sessions and the excited cells in attention switching sessions the same?

Since these experiments were conducted on different days, cell matching across days would allow me to answer this question. By the time of writing this thesis I was unable to complete this step.

- Are the cells activated by PV photoexcitation actually pyramidal neurons? I will be able to extract much more about the circuit dynamics and what is causing this reversal if these brains can be post-hoc immunolabelled and matched (similar to the VIP-cre mice in chapter 3). This would allow the application of modelling techniques that could help explain the effects observed. Is the paradoxical effect replicable across successive transitions between a go/no-go task with irrelevant visual stimuli and the full cross-modal attention task? Are there other task parameters, such as the contrast of the stimuli, or behavioural parameters such as locomotion, that are involved in the transition from inhibition to excitation of non-PV cells by PV photoexcitation.
- Performing similar experiments using recording techniques with greater temporal resolution, such as electrophysiological probes, would resolve whether there is an initially non-paradoxical change in activity happening before the network arrives at a new steady state.

Chapter 5 - Materials and Methods

All experimental procedures were carried out in accordance with the institutional animal welfare guidelines and licensed by the UK Home Office.

5.1 – Surgical procedures

All experiments used both male and female mice with a C57Bl/6 background (P70-P84). Mice were anaesthetised using isoflurane, at 4% concentration for induction and at 1-1.5% for maintenance. At the start of the surgery additional drugs were given to provide analgesia (Metacam 5mg/kg), anti-inflammatory effects (dexamethasone 3.8mg/kg), and to reduce mucus secretions (Atropine 0.08mg/kg). Eye-cream (Maxitrol) was applied to the eyes to prevent drying and body temperature was maintained at 37°C using a heating mat and rectal temperature probe (Harvard Apparatus).

A circular piece of scalp was removed and the skull beneath was cleaned and dried. A custom machined aluminum head-plate was cemented onto the skull using dental cement (C&B Superbond). Using stereotaxic coordinates, a circular craniotomy (3-5 mm diameter) was made over the right primary visual cortex (V1) (2.7mm ML, +0.6mm AP to lamda). A small incision was made in the dura and viruses were injected into the brain underneath using glass pipettes and a pressure micro-injection system (Picospritzer III, Parker). The details of the viruses used for each cohort can be found below. The craniotomy was then sealed with a glass coverslip and cyano-acrylic glue (Loctite).

Before the removal of anaesthesia mice were injected with antibiotic (Betamox 120mg/kg) and analgesia (methadone hydrochloride 10mg/kg). Mice were closely monitored for 4 days after surgery and further analgesia was given daily for 1-2 days during recovery of the animal. Imaging and behavioural training were not started until at least one week after surgery.

The mice and viruses used per chapter are as follows:

Chapter 2 - Transgenic GCaMP6s mice (Camk2a-tTA;tetO-G6s)

- To identify neurons in visual areas which project to anterior cingulate cortex (ACC), in addition to the main surgical protocol above, the retrograde tracer cholera toxin subunit B conjugated to Alexa Fluor 647 was injected into ACC using glass pipettes and a pressure micro-injection system (Picospritzer III, Parker). To do this the skull was levelled, and using stereotactic coordinates, a single hole drilled in the skull at +0.7mm AP, 0.5mm ML, 1.0-1.5mm DV relative to bregma.
- 9 mice underwent surgery, 4 included in analysis after exclusion based on imaging site quality and behaviour.

Chapter 3 - C57BL/6-VIP-Cre mice (Viruses injected into V1)

- Photoactivation experiments: AAV2/1-hSyn-GCaMP7f and AAV5-hSyn-FLEX-ChrimsonR-tdTomato. 17 mice, 8 included after quality control for imaging site and behaviour.
- Photoinhibition experiments: AAV2/1-hSyn-GCaMP7f and AAV5-hSyn-FLEX-ArchT-tdTomato. 10 mice, 6 included after quality control for imaging site and behaviour.
- No-opsin control experiments: AAV2/1-hSyn-GCaMP7f and AAV1-FLEX-tdTomato. 5 mice, 3 included after quality control for imaging site and behaviour.
- Passive viewing experiments at different contrasts. ssAAV-8/2-hEF1a-jGCaMP7f-WPRE-bGHp(A) (1x10^12vg/ml) and AAV5-hSyn-FLEX-ArchT-tdTomato. 5 mice, 4 after quality control for imaging site.

Chapter 4 - C57BL/6-PV-Cre mice

- ssAAV-8/2-hEF1a-jGCaMP7f-WPRE-bGHp(A) and AAV5-hSyn-FLEX-ChrimsonR-tdTomato

After discussion with Filipe Ferreira (PhD student in the lab), who had previous experience using viral vectors in PV-cre mice, I supplemented the injected viruses with a cre-dependent GCaMP7f (AAV-hsyn_FLEX-jGCaMP7f). Whether due to viral tropism or some other unknown factor, the viruses we were using provided relatively low infection rate of PV interneurons (Unpublished communication). 7 mice, 4 included after quality control for imaging site and behaviour.

5.2 – Immunohistochemistry and ex vivo imaging

Brains were fixed by transcardial perfusion with 4% paraformaldehyde in phosphate buffer 0.1 M, followed by 24h of post-fixation in the same solution at 4°C. The whole brains were incubated successively in 15% and 30% sucrose in phosphate-buffered saline (PBS) at 4°C for 2 and 12h respectively. Brains were sectioned tangentially to the surface of visual cortex at 80µm thickness on a microtome (Leica). Slides were washed and permeabilized with 0.4% Triton X-100 in PBS for 4 × 15 minutes and then incubated with blocking buffer (0.3% Triton X-100 + 5% BSA + 10% Normal Donkey Serum and 10% Normal Goat Serum in PBS) for 3h at room temperature. Primary antibodies were incubated with blocking buffer (0.3% Triton X-100 + 1% BSA + 5% Normal Donkey Serum and 5% Normal Goat Serum in PBS) overnight at 4°C. The next day, slides were washed and incubated for 2h with secondary antibodies, then mounted in DABCO-PVA (2.5% DABCO, 10% polyvinyl alcohol (Sigma; Type II), 5% glycerol and 25 mM Tris buffer at pH 8.7).

The slides were imaged with a confocal microscope (Zeiss LSM 800), and confocal z-stacks were compared with the previously acquired in vivo imaging planes and z-stacks of the recording sites. We determined the approximate location of the injection site using GCaMP7f fluorescence and then used blood vessel patterns and cellular morphology to identify the imaging site. We matched at least three points in the confocal z-stack to points in the in vivo imaging plane to obtain a three-dimensional transformation matrix that was applied to the entire confocal z-stack. Cells were then manually identified and assigned to cell classes based on immunostaining.

Primary antibodies and dilutions used: Rat anti-Somatostatin, 1:200 (Millipore MAB354); Mouse anti-Parvalbumin, 1:5000, (Swant PV235); Rabbit anti-Vasoactive Intestinal Peptide (VIP), 1:500 (Immunostar #20077). Secondary antibodies and dilutions used: Goat anti-Rat Alexa 647, 1:500 (Thermo Fisher #A21247); Donkey anti-Mouse Dylight 405, 1:500 (Jackson Immunoresearch #715-475-150); Goat anti-Rabbit Alexa 594, 1:500 (Thermo Fisher #A11012)

5.3 – Two-photon imaging

Two-photon imaging was performed using a custom-built resonant scanning two-photon microscope (Cosys) and a Chameleon Vision S laser (Coherent) at 930nm using a 16X, .8NA objective (Nikon). Images were acquired using a 12 KHz resonant scanner (Cambridge Technology) and an FPGA module (PXIe-7965R FlexRIO, National Instruments). Multi-plane imaging was performed using a piezoelectric objective scanner (Physik Instrumente). Injection coordinates and depth indicated that all recordings were made of neurons in L2/3 (generally 150-250um below the surface). For all experiments, imaging power on sample was between 25 and 40mW for the uppermost plane of the imaging volume. Power increase with depth was calculated using Scanimage's "default exponential" power vs depth adjustment function ($P = P0 * \exp^{((z-z0)/Lz)}$) with an Lz value of 350-400um. Each imaging volume consisted of 6 planes, 20µm apart, approximately 450x450um, 512x512 pixels in size. Images were captured at a framerate of 44Hz, an effective framerate of 6.33Hz per volume.

At the beginning of each session anatomical landmarks were used to find and record from the same imaging site as on previous days. Mice which were found to have bone regrowth under the window, poor viral expression or many brightly labelled cells with nuclear GCaMP7f expression were excluded.

The approximate receptive field positions of the recorded sites were determined at the beginning of each imaging session while mice ran freely on the cylinder. The monitor in front of the contralateral eye (covering ~100x60 degrees of visual space) was divided into a 4x3 grid and rectangles alternating between black and white at 2Hz were presented at each grid position on a grey background in randomized order (10 repetitions). Stimuli were generated using Psychtoolbox-3 in MATLAB.

At the end of in-vivo imaging data collection, a high-quality image stack of all recording sites was acquired under anaesthesia to allow registration of immunohistochemically labelled brain slices and in-vivo data. Anaesthesia was induced with subcutaneous injections of ketamine (100mg/kg) and xylazine (16mg/kg), and further injections of ketamine were used to maintain anaesthesia if necessary. In some mice isoflurane anaesthesia was used instead for these recordings, 4% concentration for induction and 1% for maintenance. Eye-cream (Maxitrol) was used to prevent drying, and body temperature was maintained using a heating pad.

5.4 – Behaviour task

The hardware and method used for behavioural training was similar to previous studies (Poort et al., 2015; Khan et al., 2018). Mice were trained on a visual discrimination go-nogo task for up to two weeks, until they reached a discrimination performance threshold. After reaching this threshold mice were moved onto the full switching task described below. Mice were food restricted to maintain at least 85% of their free-feeding body weight (typically 85-90%, 2-3g of standard food pellets per animal per day) but had free access to water. A 10% solution of soy milk powder (SMA Wysoy) was used as reward during the task and delivered through a spout positioned near the snout of the mouse. Licks to this spout were detected through a piezo disc sensor and reward was released by opening a pinch valve (NResearch), both controlled by custom electronics. The visual stimuli were presented on two luminance-corrected monitors (luminance meter LS-100, Konica Minolta) positioned at 45° angles and 25cm distance relative to the mouse. Visual stimuli were generated using psychtoolbox-3 and all behavioural tasks were controlled using custom scripts written in MATLAB and with a teensy microcontroller board.

Mice were first habituated to handling and gentle restraint over two to three days, they were then head-fixed and trained to run on a polystyrene cylinder (20cm diameter) for a further one to four days. Mice were free to run on the polystyrene cylinder during all awake recordings and their running speed on this cylinder was measured using an incremental rotary encoder (Kübler).

Once mice were running smoothly on the wheel, they performed one ‘closed-loop’ visual discrimination behavioural session during which the movement of the mouse on the wheel controlled the movement of the visual gratings on the screen. During the task mice self-initiate trials through sustained running on the wheel, after the ’closed-loop’ session mice were trained to run for longer periods to initiate trials - at least 2.8s with an added random duration drawn from an exponential distribution (mean 0.4s).

The stimuli used for visual discrimination were two sinusoidal gratings drifting in the opposite

direction to the direction of running, with a fixed spatial and temporal frequency of 0.1 cycles per degree and 2Hz respectively. Unless otherwise specified the rewarded and unrewarded gratings were oriented +/-15° relative to vertical, symmetrically on both screens. The stimulus presented on a given trial was selected at random.

The mouse could trigger the release of a drop of soya milk when the rewarded grating was display by licking the reward spout during the 'reward period'. The reward period started 1.5s (with added random duration, mean 0.2s) after rewarded visual stimulus onset and lasted until the offset of the stimulus 1s later. If the mouse licked during the 'reward period' the trial was recorded as a 'hit', if the mouse did not it was recorded as a 'miss' and a drop of soya milk was dispensed automatically shortly before the disappearance of the visual stimulus.

A lick at any time when the unrewarded grating was displayed was recorded as a 'false alarm' and the mouse was punished with a 4s time-out period, during which the unrewarded grating persisted on the screen and any more licks reset the time-out duration. Ignoring the unrewarded visual stimulus by not licking was recorded as a 'correct rejection'. In the initial stages of training, to discourage incorrect licking the probability of unrewarded trials was sometimes temporarily increased from 0.5 to 0.7. Mice typically learned the visual discrimination task in 5-10 days, with the threshold for learning defined as three consecutive days of discrimination with a behavioural d-prime score of 2 or above. Behavioural d-prime was calculated as: $bd' = \Phi^{-1}(H) - \Phi^{-1}(F)$, where Φ^{-1} is the normal inverse cumulative distribution function, H is the rate of hit trials, and F is the rate of false alarm trials.

After learning the visual discrimination task, mice were trained to perform odour discrimination. The odour discrimination task was identical in structure to the visual discrimination task except that instead of visual stimuli one of two odour stimuli were presented to the mouse via a polyethylene tubing positioned above the snout of the mouse. A custom-built flow dilution olfactometer calibrated with a mini PID (Aurora) delivered 10-20% saturated vapour concentration of two solutions, 10% soy milk (rewarded odour) and 10% soy milk with 0.1% p-Cymene mixture (unrewarded odour). Mice typically started accurately discriminating between the odours after 30-40 trials, after which they were trained to switch between blocks of the olfactory and visual discrimination task.

Mice usually learned to perform the full switching task in a further 1-3 days. In the olfactory

blocks, 70% of odour stimuli were preceded by one of the two visual gratings presented in the visual discrimination task The visual stimuli were displayed for a fixed duration of 1.8s, with an onset delay distribution identical to the visual block, neither grating was rewarded or punished. Mice learned to accurately discriminate between the odours while ignoring the irrelevant gratings. Odours followed the irrelevant visual gratings with a delay of 1.5s, plus an added random duration drawn from an exponential distribution with mean 0.2s.

5.5 – Functional mapping of higher visual areas

Widefield Calcium Imaging:

Widefield imaging was performed on a custom built inverted tandem lens macroscope (Cosys), with two photographic lenses (AF-S NIKKOR 85mm f/1.8G lens and AF NIKKOR 50mm f/1.4D Lens). The brain was illuminated with interleaved collimated blue (470nm, Thorlabs M470L4) and violet light (405nm, Thorlabs M405L4) at an irradiance of ~0.03mW/mm2. Images were recorded with a CMOS camera (Point Grey Research Grasshopper3) at frame rate of 54Hz. LEDs and camera frame acquisition were triggered using a digital microprocessor (Teensy 3.2).

Widefield Pre-processing:

The widefield video underwent motion correction and the brain images were aligned within and across mice by manual rigid alignment to several anatomical landmarks. The ΔF/F was computed for each pixel by taking the difference between F and F0, and dividing by F0, where F0 was the mean value across the entire session. Traces were filtered with a 0.0033 Hz high-pass second order Butterworth filter, and an additional 7Hz lowpass filter was applied to the violet trace. To correct for haemodynamic artefacts, a scaled version of the violet illumination trace was subtracted from the blue illumination trace for each pixel. This scaling factor was found by regressing the violet trace onto the blue trace.

Visual stimuli for retinotopic mapping

Stimulus presentation code was written using psychtoolbox-3 to mimic the visual stimuli presented in (Zhuang et al., 2017). A bar containing a flickering black-and-white checkerboard

pattern was swept horizontally and vertically across the screen in front of the mouse's eye contralateral to the imaging site. The bar was spherically corrected to stimulate in spherical visual coordinates using a planar monitor (Marshel et al., 2011; Garrett et al., 2014); Videos 2 and 3). The bar subtended 20 degrees in its direction of movement and spanned the monitor in the perpendicular direction. Each checkerboard square within the bar was 25 degrees wide and alternated colour at 6Hz. The bar was moved across the screen 10 times in each of the cardinal directions, with a minimum time of 5s between each sweep.

Identification of visual areas:

Retinotopic maps were created using the method of Zhuang et al. 2017 and Garrett et al. 2014. First stimulus aligned average delta F movies were created, by averaging all the trials of a certain direction, aligned to the onset of the drifting bar. Next, we performed Fourier decomposition and at each pixel extracted the phase and magnitude for the frequency of the drifting grating. This was done using the numpy.fft function. Following this we calculated the local gradient of the vertical and horizonal phase maps at each pixel using the numpy.gradient function. The visual sign was then calculated as the sine of the angle between the local horizonal and vertical gradients at each pixel. The visual sign maps where then smoothed with a gaussian filter with a standard deviation of 3 pixels. Maps were then subsequently thresholded, using a threshold of 1.5 times the standard deviation of the entire sign map, any pixel with an absolute value below this threshold was set to zero. This process produced continuous sign maps organised into distinct clusters. The boundaries of these regions were then found using the sklearn.find_contours function.

5.6 – Optogenetic manipulations

Expression of the tdTomato conjugated opsin (Chrimson or ArchT) was first verified in each imaging site through two-photon imaging at 1030nm excitation wavelength. Optogenetic light was delivered using a digitally triggered 637nm laser (OBIS 637nm LX, Coherent), through a 200µm diameter 0.39 NA optic fibre (Thorlabs) positioned above the cranial window. To allow for quasi-simultaneous two-photon imaging and optogenetic activation, the laser and stimulus monitors were blanked during the linear phase of the resonant scanner. Powers

detailed below were measured using a power meter positioned in the same location as the cranial window of the mouse – integrating power over the whole scan. However, as the optogenetic laser was only on during the turnaround times of the resonant scanner the duty cycle was approximately 11%.

For each two-photon imaging site an optogenetic calibration session was performed. During these calibration sessions the screens were grey, and 8 light powers (including 0%) were applied in pseudorandom sequence to the imaging window for 1.5s with 5s intervals. The effective maximum output used in mice expressing ArchT was 9mW, and in mice expressing Chrimson was 3mW. The average activity of each ROI in the 1s before the optogenetic laser onset was subtracted from the light period and the resulting baseline corrected activity was used for the calibration plots. Based on the shape of these calibration curves, 2 powers were chosen for the behavioural task for each imaging site: the lowest power producing a saturated or just below saturated response, and a second power with approximately half of this effect.

To select optogenetic laser powers for the PV-cre mice in chapter 4 ongoing activity was required to detect inhibition through activation of PV interneurons. To this end calibration was performed in session which was a single extended odour block. The irrelevant visual gratings were presented as normal but were paired with one of six laser powers (including 0mW). The maximum power output for these sessions was 3mW.

Optogenetic stimulation during attention-switching

Application of the optogenetic light during attention switching sessions was similar to the orientation mapping sessions. Optogenetic laser powers were interleaved and randomly selected on each trial from 1 of 3 powers (No laser, low power, high power) with equal probability. The optogenetic laser was on from 100ms before stimulus presentation to 1.5s after visual stimulus onset. The optogenetic laser was delivered only during presentation of the visual stimuli in both the visual and odour blocks.

Silencing of the ACC during the attention switching task - Chapter 2.4

To inhibit either ACC or PL cortex mice expressed the excitatory opsin Channelrhodopsin in PV-positive interneurons and blue light was delivered through an optic fibre cannulae

connected to an LED (470nm, Thorlabs). Each optic fibre was confirmed to have an effective power output of >1mW before implantation.

Light alternated between being delivered continuously (pulsed at 40Hz(Li et al., 2019)) for the whole of one visual block and the following odour block, and being off for the next visual and odour block. The optogenetic LED started off for the first visual and odour block of each session. In half of the sessions for each mouse silencing began in the 2nd visual block of the session, for the other half silencing began in the 3rd - to account for within-session performance variation. Optogenetic sessions were only included in analysis if the mouse completed 3 or more visual and odour blocks (≥6 blocks total). Each mouse performed 4 optogenetic sessions in which the PL was silenced and 4 sessions in which the ACC was silenced.

5.7 – Direction tuning

To examine the effect of the optogenetic light on visual processing in mice passively viewing stimuli, two-photon imaging sessions were conducted while head-fixed mice (free to run on a polystyrene wheel) were shown sinusoidal visual gratings drifting in one of 8 directions separated by 45°, with a spatial frequency of 0.1 cycles per degree and temporal frequency of 2Hz. These visual stimuli were randomly interleaved and one of three laser powers (including 0%, the same as those used in the attention switching task) was selected with equal probability for each visual stimulus presentation. The visual gratings were presented for 2s and the optogenetic laser lasted from 100ms before the stimulus onset to 1.5s after the start of stimulus presentation. There was a 5s interval before the start of the next visual stimulus presentation.

Direction tuning curves were constructed for each cell using their mean responses to each direction after baseline correction. The activity of each neuron was ‘soft’ normalized (Elsayed et al., 2016) so that neurons with strong responses had approximately unity firing rate range (normalization factor = firing rate range + 0.2).

When aligning direction tuning curves across neurons to each neuron’s preferred direction, the preferred direction was determined by taking the greatest response after pooling all light power and no light conditions. This prevented artefactual results which would occur from

selecting the maximum firing rate in one condition (e.g. no light) and comparing this to other conditions (e.g. optogenetic stimulation). An orientation selectivity index was calculated as

OSI = (Rpref - Rorth)/(Rpref + Rorth)

Where Rpref and Rorth are the average responses to the preferred and orthogonal directions respectively (Mazurek et al., 2014). Neurons were considered orientation selective if their OSI was greater than 0.33, such that the response at the preferred direction was twice as large as it's response to the orthogonal direction.

5.8 - Two-photon imaging data pre-processing

Pre-processing of two-photon calcium imaging data was performed using the software Suite2p (https://github.com/MouseLand/suite2p) to correct for motion, detect regions of interest (ROIs) and extract the raw fluorescence time series of those ROIs, F(t). Each site yielded between 164 and 688 cells, median = 432 cells. We corrected the calcium traces for out of focus neuropil fluorescence using the neuropil masks identified by suite2p. For each frame we subtracted 0.7 * (neuropil - median neuropil fluorescence). Subsequent analysis unless otherwise specified was done with custom code in MATLAB and Python. Baseline fluorescence F0(t) was computed by smoothing F(t) (causal moving average of 0.75s) and taking the 2.5th percentile of the smoothed data. The change in fluorescence relative to baseline, ΔF/F, was computed by taking the difference between F and F0 and dividing by F0. Video recording (The Imaging Source) of the eye contralateral to the imaging site was performed during all sessions, and the time-points of saccades and blinks identified. Frames in which the mouse made a saccade or blinked were removed from further analysis.

5.9 – Red-cell labelling

To identify VIP or PV interneurons labelled with tdTomato, a brief two channel recording of the imaging planes was taken before each imaging session at an excitation wavelength of 1020nm. After image registration and ROI identification, neurons that co-expressed tdTomato and GCaMP were labelled using this recording. A similar process was used for identification of ACC projecting cells. However, as the fluorophore used was Alexa-647 the excitation wavelength was 830nm.

5.10 – Selectivity

We computed a selectivity index for individual ROIs as the difference between the mean response to each of the two gratings divided by the pooled standard deviation of that ROIs responses. Unless otherwise specified, all selectivity values presented here are from an analysis of the activity in the first 1s of visual stimulus presentation. To calculate ΔSelectivity we took the difference selectivity(attend) - selectivity(ignore). For cells that were negatively selective in the attend condition we multiplied the resultant values by –1, to ensure that cells that became more selective with attention had positive values.

To test if an ROI was significantly selective within a certain time window, a two-sided Wilcoxon rank sum test was performed comparing the activity on trials for the two visual stimuli. ROIs were excluded from further analysis if they displayed selectivity in the period before visual stimuli were presented.

To find ROIs that significantly changed their selectivity with attention, an ROI's selectivity in the attend condition was compared to a distribution produced through bootstrapping using the data in the ignore condition (1000 repeats). If the attend selectivity was below or above the 2.5th or 97.5th percentiles respectively of the bootstrapped distribution, then the ROI was considered to have significantly changed its selectivity with attention. To avoid artefactual effects from selecting cells in one condition and testing in another, the test for significance was performed with no light and all light powers pooled.

After each behavioural block transition, transient periods of less accurate behaviour were discarded by identifying the trial in each block beyond which behaviour was stably accurate, that is, where mice displayed greater than 75% accuracy on both the go and no-go stimuli for the remainder of the block, and for the odour block, where mice licked in response to fewer than 25% of either of the irrelevant visual gratings for the remainder of the block. Light and no light trials were pooled to identify this point to avoid artefactual results

5.11 – Behavioural controls

To assess the proportion of neural activity which was attributable to overt behaviour recorded during our task, a linear model was fit using ridge regression to predict neural activity. The

model was constructed by combining multiple sets of variables into a design matrix, to capture signal modulation by the following different task or behavioural events: 2 visual stimuli, 2 odour stimuli, reward delivery, licks, running speed, block type, and an interaction term for visual stimuli and block type. Each stimulus/event variable was structured to capture a time-varying event kernel. Variables therefore consisted of a vector of the relevant stimulus/event, and copies of this vector, each shifted in time by one frame for specific durations. For sensory stimuli, the time-shifted copies ranged up to 2s after the original. For motor events (running and licking) the time-shifted copies spanned the frames from 0.5s before until 2s after the original. The model was fit with 5-fold cross validation and the coefficient of determination (R^2) was calculated based on the predictions of the model on held out data not used during training. We then assessed the predictive power of the behavioural model variables by comparing the R^2 value for the full model to a model without the running and licking predictors, taking the proportion 1-(no behaviour model R^2)/(full model R^2).

To decode block type based on neural activity or running speed the neural decoding toolbox readout.info was used with the max_correlation_coefficient_CL classifier. To separate sessions according to their timepoint of divergence in running speed the pre-stimulus baseline speed was subtracted and the first timepoint found at which there was a significant difference in running speed between the attended and ignored rewarded visual stimulus trials using Wilcoxon rank sum tests at each time-point.

5.12 – Orthogonality

Visualisation of the LDA transformation of neural activity was done using the Python library scikit-learn. All other analysis for testing orthogonality was done on axes found in MATLAB using the fitcdiscr function. The alignment of the axes best separating the optogenetic modulation and attentional modulation were found through the cosine similarity of the coefficients of two linear discriminant analysis models. One model separated visual stimulus trials in the odour block from visual stimulus trials in the visual block, both sets of trials without the optogenetic perturbation. The second model separated visual stimulus trials in the odour block without optogenetic perturbation from visual stimulus trials in the odour

block with optogenetic perturbation.

The cosine similarity for the split data control was found using a similar approach. In the visual block, the rewarded and unrewarded visual stimulus trials were separated into two halves and the coefficients used to calculate cosine similarity were for two models separating the rewarded and unrewarded trials using non-overlapping halves of the data. This process was repeated 50 times for each session and the resulting values were averaged to produce one value for cosine similarity for split data for each session.

To ensure that we do not obtain orthogonal axes simply because they lie within a high-dimensional neural subspace, random axes were found using the method from (Elsayed et al., 2016). The neural covariance was estimated from each session and a Monte Carlo analysis used to sample pairs of random axes (10,000 samples) that were then used to calculate an expectation of cosine similarity based only on the dimensionality of the data.

5.13 – Noise correlations

To calculate noise correlation, the average stimulus evoked response across all trials of a particular type was taken for each cell and subtracted from each trial of the corresponding type. There were 14 trial types in total, rewarded and unrewarded odour stimuli, and rewarded and unrewarded visual stimuli in the visual and odour blocks, all at multiple laser powers. The Pearson correlation coefficient was then used to quantify the correlation between responses of pairs of cells for each trial type. Changes in noise correlations between different cell types with attention or optogenetic modulation were tested using a Wilcoxon signed-rank test on all sessions for which the post-hoc immunomatching had been successful (n = 4 mice).

5.14 – Population sparseness

Population sparseness was calculated using a modified version of the Treves-Rolls formula as described in Tolhurst et al., 2009 (See below). Which ensures that sparser response distributions have larger values, and which can respond appropriately for distributions with a mean of zero, such as may be the case in baseline corrected visual cortex responses.

$$\mathrm{TR} = 1 - \left(\sum_{i=1}^{n} |r_i| / n \right)^2 \Big/ \left(\sum_{i=1}^{n} r_i^2 / n \right).$$

5.15 – Immunolabeling image registration and cell matching across days

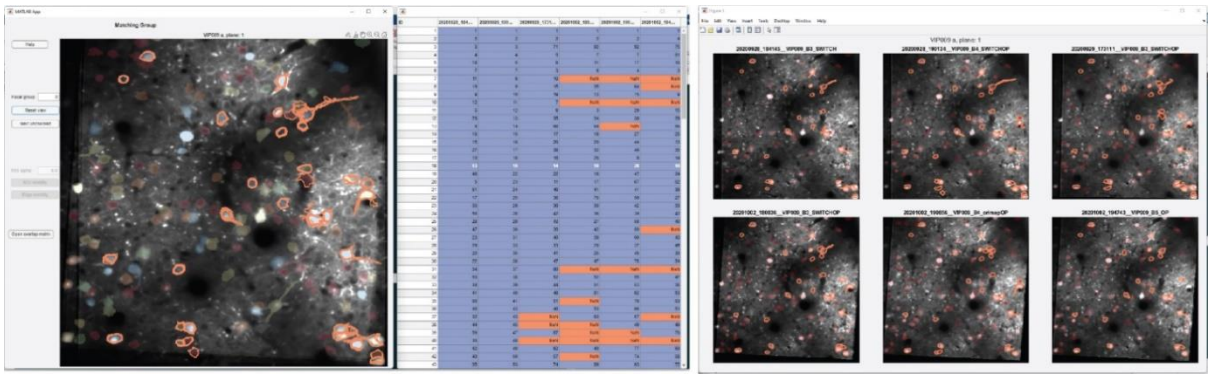

Figure 5.1: Example images from the across day image registration GUI.

Left – the average image produced from registering 6 recording sessions. ROIs are overlayed and colour coded based on the number of sessions they appeared in. Orange outlines indicate ROIs that have been manually inspected for quality control. Next to the average image is the overlap matrix, where the local ID of ROIs in individual sessions is associated with a global ID for each unique recorded ROI. Right – the individual planes from each of the recorded sessions after transformation to align them, with the ROIs recorded in that session overlayed.

To facilitate data analysis, I wrote code which coordinated the input and output of recorded sessions between MATLAB and suite2p run in python. This code also performed several data analysis steps to produce intermediate data structures that are used by downstream functions for analysing the data.

To allow the identification of the same cell on multiple days I made a tool which works off these intermediate data structures. It performs an affine transformation to register the recordings from multiple days to one another, automatically identifies ROIs that are present on multiple days, and allows the user to perform quality control for mistaken or missed matches between ROIs. The map of unique cells made using this tool is then stored for further analysis.

For the registration of the *in vivo* and immunolabeled confocal images, MIJI (a java package that allows MATLAB to communicate with imageJ) was used to register the two sets of images based on anatomical landmarks found by the user. I wrote a similar GUI to the one used for

matching across days to support labelling of the different cell types and integration of those labels into the intermediate data structures and the map of ROIs identified across days. Immunohistochemical labels from one session were replicated onto all other instances of that cell using the information from matching across days.

Chapter 6 – Discussion

In this thesis I have presented the results of experiments I conducted investigating the neural circuit basis of attentional modulation in visual cortex. I used an all-optical experimental setup to record and manipulate the activity of mouse visual cortex as mice performed a cross-modal attention switching task. After surveying 7 mouse visual cortical areas, I found that activity in V1 and the two higher visual areas AM and PM was modulated by attention. Contrary to a hypothesis based on primate data, V1 was the area most strongly effected by attention. To gain further insight into how visually evoked activity in V1 is modified by attention, I perturbed the activity of VIP and PV interneurons in V1.

Neither inhibition nor excitation of VIP interneurons interacted with the attentional modulation of stimulus selectivity of non-VIP cells. However, VIP photoactivation did strongly modulate visually evoked activity and this modulation was found to be orthogonal to the modulation of activity by attention.

In contrast, excitation of PV interneurons altered the stimulus selectivity of non-PV interneurons in an attention dependent manner. However, these changes in stimulus selectivity occurred on top of paradoxical changes in non-PV activity with increasing PV photoexcitation, making interpretation difficult. The excitation of PV interneurons affected the visually evoked activity of non-PV cells differently depending on the task the mouse was engaged in. In the calibration sessions, PV photoexcitation caused an inhibition of non-PV activity at both laser powers, whereas in the attention-switching task the low power caused an inhibition of non-PV and the high power produced no-change or even an excitation of non-PV.

The results summarised above are discussed in greater detail in the discussion in the previous chapters. Below I want to highlight and discuss more general points and proposed further experiments.

6.1 – Is the attentional modulation in mouse higher visual areas inherited from V1?

Although AM and PM were the only areas aside from V1 whose neural population displayed a significant overall modulation with attention, I observed a substantial portion of attentionally modulated neurons in almost all the HVAs I recorded from. Different HVAs

exhibit a preference for different visual stimulus properties (Andermann et al., 2011; Marshel et al., 2011; Roth et al., 2012; de Vries et al., 2020). Potentially, the primary site of attentional modulation is in V1 and mouse HVAs inherit the changes in stimulus processing from V1. Different sets of HVAs would then be attentionally modulated depending on the task and the visual stimuli used. If this is the case, it might highlight a significant discrepancy in attentional modulation between mice and non-human primates – in which the intensity of attentional modulation increases up the cortical hierarchy.

Further experiments could clarify this by recording from HVAs in mice performing attention tasks, where the structure of the task remains the same but the properties of the visual stimuli that must be attended to are systematically varied. In this way the requirement for attention could be held constant while the stimuli are changed to target the preferences of particular visual areas.

6.2 – Are locomotion and attention truly separate?

If VIP interneurons are not involved in attention, what are VIP interneurons doing? VIP interneurons may be specifically involved in mediating the modulation of visual responses by locomotion. Despite broad similarities between the effects of locomotion and attention on cortical circuits (Mineault et al., 2016; Dadarlat and Stryker, 2017; Speed and Haider, 2021), they do not appear to use the same mechanisms. A recent paper using a spatial attention task in mice found that running and attention modulated individual neurons independently (Kanamori and Mrsic-Flogel, 2022). Likewise, arousal and locomotion have been found to alter the activity in visual cortex in distinct ways (Vinck et al., 2015).

I found that VIP photoactivation multiplicatively scaled the visually evoked responses of non-VIP cells when mice passively viewed visual stimuli. This is similar to what was found in macaques, where recordings in the higher visual area IT showed that when properties of a visual object needed to be decoded separately (such as object identity and attributes like size or location) they were combined multiplicatively. However, when the encoded information needed to be integrated (such as parts of an object) they were combined additively (Ratan Murty and Arun, 2018). The multiplicative gain of neural responses from VIP photoactivation in my experiments may be indicative of the independent encoding of locomotion into network

activity. This is supported by the finding that the high dimensionality of activity in mouse V1 allows motor related activity and stimulus evoked activity to co-exist without perturbing one another (Stringer et al., 2019).

There is still some unresolved overlap between motor and attention related modulations. For example, cholinergic signalling has been associated with both attention (Everitt and Robbins, 1997; Sarter et al., 2005, 2009) and VIP activity (Alitto and Dan, 2013; Gasselin et al., 2021). Are there therefore distinct cholinergic circuits to mediate the effects of locomotion and attention?

6.3 – Are VIP interneurons involved in a different form of attention?

There are similarities between the neural correlates of different forms of attention. Additionally, models have been proposed which can parsimoniously explain different forms of attention as applications of the same mechanism (Reynolds and Heeger, 2009). Despite this, they may utilise distinct neural substrates to perform the same computations (Maunsell, 2015).

VIP-SOM disinhibition can release excitatory activity within a localised patch of cortex (Karnani et al., 2016a). Given the retinotopic arrangement of visual cortex, spatial attention could be mediated by the activation of specific VIP interneurons, which would increase the gain of neural activity at particular locations in visual space. This VIP activation could come through input from prefrontal cortex (Zhang et al., 2014). In support of this, the VIP-SOM disinhibitory motif contributes to another function in which spatial location is relevant; the modification of stimulus responses by the surrounding visual scene (Keller et al., 2020). It would be interesting to see whether stimulation of spatially restricted ensembles of VIP interneurons interacts with the neural correlates of spatial attention in mice, or whether it can even direct the spotlight of attention towards the stimulated location.

6.4 – Are neural correlates of attention actually required for attention related improvements in behaviour?

V1 is required to perform the visual discrimination in the cross-modal attention task employed here (Poort et al., 2015). The perturbations of VIP activity I have performed indicate that VIP interneuron activity is not required for the modulation of visually evoked activity by attention.

However, these experiments do not investigate whether the attentional modulation of stimulus evoked activity in V1 (neural correlates of attention) is required for behavioural correlates of attention.

An improvement in behavioural performance with attention cannot be measured with the task I have used in this thesis, because by design no task is performed with the visual stimuli when they are presented in the odour block. It is assumed that the mouse's voluntary lack of response to the visual stimuli in the odour block means that they are being ignored. Task relevance is likely an effective way of controlling attention. The mice are not motivated to engage with the visual stimuli in the odour block and experiments have shown that reward expectation and attention produce equivalent effects (Stănişor et al., 2013). Indeed, there is cause to question whether reward expectation and attention can be separated (Maunsell, 2015).

A redesign of the task would be required to investigate the effect of VIP perturbations on the enhancement of behaviour with attention. One option is to present visual and odour stimuli that are always task relevant in a continuous interleaved stream. Attention to either the visual or odour modality could then be controlled by varying the proportion of visual or odour stimuli presented over blocks of trials - similar to the structure of an "oddball" task. In this way the mice may develop an expectation of stimuli of one modality and attend to that modality in preparation for the presentation of the stimulus. A difference in reaction time or percentage of correct trials could then be measured and compared for both visual and odour stimuli in either majority visual or majority odour blocks of trials.

Attention may not be a unitary phenomenon. Neural correlates of attention and behavioural enhancements with attention may be separable. The role of the superior colliculus (SC) in the control of saccades and other orienting movements suggests SC might be downstream of cortex (Sparks, 1999). SC also plays a role in attention. By separating covert attention from saccadic eye movements Lovejoy & Krauzlis (2010) found that pharmacological inactivation of macaque SC impaired attention for stimuli in the affected portion of visual space. However, subsequent experiments showed that attentional modulations MT and MST were intact during inhibition of SC despite an attention related impairment in behaviour (Zénon and Krauzlis, 2012). One possible explanation is that attention could be composed of multiple

distinct processes mediated by distinct circuits across different brain regions, rather than a unitary process (Krauzlis et al., 2013; Maunsell, 2015).

The experimental tools available in mice could be used to investigate whether the enhancement in stimulus selectivity in V1 with attention is involved in behavioural enhancements with attention. By an all-optical experimental setup capable of holographic optogenetic stimulation, one could bidirectionally manipulate the activity of groups of specific neurons (Packer et al., 2015; Marshel et al., 2019). Small uni-laterally presented visual stimuli could be used to restrict relevant visual information to a small patch of cortex. The neural correlates of attention could be observed in the patch of recorded V1 as the mouse performs the task, to identify which cells have their visually evoked activity modulated by attention. The changes in response amplitude recorded with attention of ensembles of attentionally modulated cells could then be subtly suppressed or played back into the network to see if it elicits an associated behavioural change. Any changes could then be compared to similar magnitude manipulations of similarly stimulus selective, but non-attention modulated neurons.

When rats were required to switch back and forth between rules in a single session, different patterns of population activity in prefrontal cortex were found to represent the same task strategies (Malagon-Vina et al., 2018). It is possible that no behavioural change would be seen from the manipulations I just proposed because across switches in attention the patterns of top-down inputs that influence V1 activity may not be the same. Therefore, a different set of V1 cells would be attentionally modulated despite task conditions remaining the same and the recordings which identified the attentionally modulated neurons that should be manipulated would be inaccurate by the time it was ready to be used.

Indeed, recent work shows that the neurons recruited by attention in mouse V1 are not reliable over time (Kanamori and Mrsic-Flogel, 2022). This is in accord with preliminary analysis from my own work. When tracking the same neurons across days I find a low correlation between the modulation of stimulus selectivity with attention on one day and the next. It may be that the activity of the population has high dimensionality, as in prefrontal cortex, and that it is the population of neurons that is important rather than their individual tuning (Rigotti et al., 2013; Fusi et al., 2016).

6.5 – Are on-off manipulations of cell-types too simplistic?

I observed different effects of PV interneuron photoexcitation depending on the task the mouse was engaged in. If this paradoxical effect holds true in other conditions it will have significant consequences for the interpretation of interneuron manipulation during behavioural tasks, especially considering the use of PV activation as a method of suppressing cortical activity. Previous studies have observed paradoxical inhibition of PV cell activity with PV photoexcitation, an effect that was interestingly only present at low laser powers (Li et al., 2019). It is possible that at higher laser powers the paradoxical effect of PV activation I observe might revert back to net inhibition of activity, although the experiments I conducted do not allow me to check this.

General caution is required in experiments perturbing the activity of molecularly defined cell classes as there is heterogeneity in the responses of cells of the same class - such as the changes with attention observed in this task (Fig. 3.15c). This heterogeneity could arise from a plurality of sub-types (Harris et al., 2018). However, cell identity is not the only dimension to be cautious about - differences in the temporal patterns of neural activity will also be important to consider.

In this experiment I considered the effect of the timing of applied perturbations in minor ways, such as the relative onset of the optogenetic light and ramping the offset of optogenetic light to avoid rebound effects. This may be insufficient. Different interneurons play different temporal roles in visual processing and their responses and synaptic dynamics have different temporal profiles (Cardin, 2018). For example, changing the duration of SOM inhibition can result in distinct effects on stimulus tuning (El-Boustani et al., 2014).

Simple photoactivation experiments may not be able to reproduce complex cognitive phenomena, because they are unable to replicate the way these phenomena evolve over time. Holding an interneuron at a particular level of activity may destroy temporal information which could be key to the process or produce un-physiological dynamics that echo within the recurrently connected circuit - the element of interest is not being changed in isolation. Simply activating interneurons to mimic physiological levels of activity - as I have done here - may not be enough. Perhaps temporal patterns or the activation of specific ensembles of interneurons

will be required.

One option is that instead of manipulating individual cell types, investigation should instead proceed top-down as the attentional inputs do. First, candidate areas for the source of the attentional modulation should be tested for their involvement in the behaviour and the neural correlates of attention in V1. The activity of V1 neurons that those source areas influence could then be investigated and later replayed back into the network to try to induce attention-related changes.

In line with the above suggestion that the top-down sources should be investigated directly, I attempted to investigate whether projections from ACC are involved in the neural correlates of attention observed in this task. The aim was to inhibit projections from regions of the PFC (starting with ACC) in V1 whilst recording the activity of V1 neurons. I aimed to begin these experiments through simultaneous two-photon calcium imaging and optogenetic silencing of ACC boutons in V1. I tested GCaMP7b (pGP-AAV-syn-jGCaMP7b-WPRE (AAV1)), GCaMP7f (ssAAV-8/2-hEF1a-jGCaMP7f-WPRE-bGHp(A)), and synaptophysin-GCaMP6s (PAAV-Ef1a-DIO-Synaptophysin-GCaMP6s) at different concentrations in combination with either the opsin eOPN3 (ssAAV-1/2-mCaMKIIα(short)-eOPN3_mScarlet-WPRE-synp(A)) or ArchT. All pilot experiments were unsuccessful with blebbing of the ACC projections visible in V1. Given the time constraints of the PhD I did not continue with this line of experiments, but I believe this would be an interesting future route for investigation.

6.6 – Can results from mice be translated to primates?

Of the cortical visual areas I recorded, V1 was the most strongly modulated by attention, an inversion of what might be expected given primate attention research. Perhaps because mice rely less on vision than primates, the selective enhancement of visual information may be less full featured in mice and exhibit fewer specialisations.

If mouse higher visual areas are also found to be less effected by attention in spatial and feature-based attention tasks, this difference may add a serious caveat to the translatability of research on attention between the primate and the mouse. However, an investigation of the circuit mechanisms of attention in mouse V1 will likely still prove useful. There is homology in the arrangements and connections of the cortical circuit across areas and species from

which we may be able to extract general mechanisms (Harris and Shepherd, 2015).

It is possible that the effects of attention are similar between primates and mice in metrics that I have not recorded here. For example, attention modulations could still backpropagate down the visual hierarchy. Using a system of electrophysiological recording such as in (Siegle et al., 2021) the latency to attentional modulation could be measured because of the higher temporal resolution of these techniques compared to the calcium imaging used. This might provide insights such as from Hu and Dan (2022) that responses in SC may be attentionally modulated before V1 in a mouse spatial attention task. Attentional modulation of stimulus evoked responses in non-human primates has been found to arrive hundreds of milliseconds later than the latency to the earliest visual evoked response (Buffalo et al., 2010) - potentially due to the greater distances of information transmission. However, any temporal separation between top-down attentional modulation and first visually evoked response will likely be much smaller in rodents, and therefore an analysis of the latency to attentional modulation may be more difficult in mice.

In this thesis I have attempted to investigate the mechanisms underlying cross-modal attention switching in mice. To do so I have manipulated the activity of VIP and PV interneurons. Contrary to expectations, VIP interneurons – rather than mediating the attentional modulation – affected the activity of the population of non-VIP cells in a way that was orthogonal to attention. The results of PV cell optogenetic manipulations during attention switching were more promising as a candidate mechanism for mediating attentional modulation, however the manipulation produced paradoxical effects on the network activity potentially limiting the interpretation of results. It may be the case that for a complex cognitive phenomenon like attention, the search for a single linchpin pivotal for its manifestation in the network is too simplistic and yet more sophisticated techniques will be required to more subtly interrogate the network.

References:

Abs E, Poorthuis RB, Apelblat D, Muhammad K, Pardi MB, Enke L, Kushinsky D, Pu DL, Eizinger MF, Conzelmann KK, Spiegel I, Letzkus JJ (2018) Learning-Related Plasticity in Dendrite-Targeting Layer 1 Interneurons. Neuron.

Adesnik H, Bruns W, Taniguchi H, Huang ZJ, Scanziani M (2012) A neural circuit for spatial summation in visual cortex. Nature 490:226–231.

Aizenberg M, Mwilambwe-Tshilobo L, Briguglio JJ, Natan RG, Geffen MN (2015) Bidirectional Regulation of Innate and Learned Behaviors That Rely on Frequency Discrimination by Cortical Inhibitory Neurons. PLOS Biology 13:e1002308.

Alho K, Woods DL, Algazi A, Näätänen R (1992) Intermodal selective attention. II. Effects of attentional load on processing of auditory and visual stimuli in central space. Electroencephalography and Clinical Neurophysiology 82:356–368.

Alitto H, Dan Y (2013) Cell-type-specific modulation of neocortical activity by basal forebrain input. Frontiers in Systems Neuroscience 6 Available at: https://www.frontiersin.org/articles/10.3389/fnsys.2012.00079 [Accessed December 5, 2022].

Alitto HJ, Moore BD, Rathbun DL, Usrey WM (2011) A comparison of visual responses in the lateral geniculate nucleus of alert and anaesthetized macaque monkeys. J Physiol 589:87–99.

Andermann ML, Kerlin AM, Roumis DK, Glickfeld LL, Reid RC (2011) Functional Specialization of Mouse Higher Visual Cortical Areas. Neuron 72:1025–1039.

Ascoli GA et al. (2008) Petilla terminology: nomenclature of features of GABAergic interneurons of the cerebral cortex. Nat Rev Neurosci 9:557–568.

Atallah BV, Bruns W, Carandini M, Scanziani M (2012) Parvalbumin-Expressing Interneurons Linearly Transform Cortical Responses to Visual Stimuli. Neuron 73:159–170.

Atallah BV, Scanziani M, Carandini M (2014) Atallah et al. reply. Nature 508:E3–E3.

Ayaz A, Saleem AB, Schölvinck ML, Carandini M (2013) Locomotion Controls Spatial Integration in Mouse Visual Cortex. Current Biology 23:890–894.

Ayzenshtat I, Karnani MM, Jackson J, Yuste R (2016) Cortical Control of Spatial Resolution by VIP+ Interneurons. J Neurosci 36:11498–11509.

Bacci A, Huguenard JR, Prince DA (2005) Modulation of neocortical interneurons: extrinsic influences and exercises in self-control. Trends in Neurosciences 28:602–610.

Bakken TE et al. (2021) Comparative cellular analysis of motor cortex in human, marmoset and mouse. Nature 598:111–119.

Bargmann CI, Marder E (2013) From the connectome to brain function. Nat Methods 10:483–490.

Batista-Brito R, Vinck M, Ferguson KA, Chang JT, Laubender D, Lur G, Mossner JM, Hernandez VG, Ramakrishnan C, Deisseroth K, Higley MJ, Cardin JA (2017) Developmental Dysfunction of VIP Interneurons Impairs Cortical Circuits. Neuron 95:884-895.e9.

Batista-Brito R, Zagha E, Ratliff JM, Vinck M (2018) Modulation of cortical circuits by top-down processing and arousal state in health and disease. Current Opinion in Neurobiology 52:172–181.

Beauchamp A, Yee Y, Darwin BC, Raznahan A, Mars RB, Lerch JP (2022) Whole-brain comparison of rodent and human brains using spatial transcriptomics Fornito A, Wassum KM, Misic B, eds. eLife 11:e79418.

Beierlein M, Gibson JR, Connors BW (2003) Two Dynamically Distinct Inhibitory Networks in Layer 4 of the Neocortex. Journal of Neurophysiology 90:2987–3000.

Bennett C, Gale SD, Garrett ME, Newton ML, Callaway EM, Murphy GJ, Olsen SR (2019) Higher-Order Thalamic Circuits Channel Parallel Streams of Visual Information in Mice. Neuron 102:477-492.e5.

Bichot NP, Heard MT, DeGennaro EM, Desimone R (2015) A Source for Feature-Based Attention in the Prefrontal Cortex. Neuron 88:832–844.

Bichot NP, Rossi AF, Desimone R (2005) Parallel and Serial Neural Mechanisms for Visual Search in Macaque Area V4. Science 308:529–534.

Bichot NP, Schall JD (1999) Effects of similarity and history on neural mechanisms of visual selection. Nat Neurosci 2:549–554.

Bigelow J, Morrill RJ, Dekloe J, Hasenstaub AR (2019) Movement and VIP Interneuron Activation Differentially Modulate Encoding in Mouse Auditory Cortex. eNeuro 6 Available at: https://www.eneuro.org/content/6/5/ENEURO.0164-19.2019 [Accessed October 28, 2022].

Birrell JM, Brown VJ (2000) Medial Frontal Cortex Mediates Perceptual Attentional Set Shifting in the Rat. J Neurosci 20:4320–4324.

Blomfield S (1974) Arithmetical operations performed by nerve cells. Brain Research 69:115–124.

Bock DD, Lee W-CA, Kerlin AM, Andermann ML, Hood G, Wetzel AW, Yurgenson S, Soucy ER, Kim HS, Reid RC (2011) Network anatomy and in vivo physiology of visual cortical neurons. Nature 471:177–182.

Börgers C, Epstein S, Kopell NJ (2005) Background gamma rhythmicity and attention in

cortical local circuits: A computational study. Proceedings of the National Academy of Sciences 102:7002–7007.

Brecht M, Krauss A, Muhammad S, Sinai-Esfahani L, Bellanca S, Margrie TW (2004) Organization of rat vibrissa motor cortex and adjacent areas according to cytoarchitectonics, microstimulation, and intracellular stimulation of identified cells. Journal of Comparative Neurology 479:360–373.

Buffalo EA, Fries P, Landman R, Liang H, Desimone R (2010) A backward progression of attentional effects in the ventral stream. Proceedings of the National Academy of Sciences of the United States of America 107:361–365.

Bugeon S, Duffield J, Dipoppa M, Ritoux A, Prankerd I, Nicoloutsopoulos D, Orme D, Shinn M, Peng H, Forrest H, Viduolyte A, Reddy CB, Isogai Y, Carandini M, Harris KD (2022) A transcriptomic axis predicts state modulation of cortical interneurons. Nature 607:330–338.

Burwell RD, Amaral DG (1998) Cortical afferents of the perirhinal, postrhinal, and entorhinal cortices of the rat. Journal of Comparative Neurology 398:179–205.

Campagnola L et al. (2022) Local connectivity and synaptic dynamics in mouse and human neocortex. Science 375:eabj5861.

Carandini M, Heeger DJ (2012) Normalization as a canonical neural computation. Nat Rev Neurosci 13:51–62.

Carcea I, Froemke RC (2013) Chapter 3 - Cortical Plasticity, Excitatory–Inhibitory Balance, and Sensory Perception. In: Progress in Brain Research (Merzenich MM, Nahum M, Van Vleet TM, eds), pp 65–90 Changing Brains. Elsevier. Available at: https://www.sciencedirect.com/science/article/pii/B9780444633279000035 [Accessed October 20, 2022].

Cardin JA (2018) Inhibitory Interneurons Regulate Temporal Precision and Correlations in Cortical Circuits. Trends in Neurosciences 41:689–700.

Cardin JA, Carlén M, Meletis K, Knoblich U, Zhang F, Deisseroth K, Tsai L-H, Moore CI (2009) Driving fast-spiking cells induces gamma rhythm and controls sensory responses. Nature 459:663–667.

Cardin JA, Kumbhani RD, Contreras D, Palmer LA (2010) Cellular Mechanisms of Temporal Sensitivity in Visual Cortex Neurons. J Neurosci 30:3652–3662.

Carrasco M (2011) Visual attention: The past 25 years. Vision Research 51:1484–1525.

Casagrande VivienA, Sáry G, Royal D, Ruiz O (2005) On the impact of attention and motor planning on the lateral geniculate nucleus. In: Progress in Brain Research, pp 11–29 Cortical Function: a View from the Thalamus. Elsevier. Available at:

https://www.sciencedirect.com/science/article/pii/S0079612305490020 [Accessed November 9, 2022].

Caviness VS (1975) Architectonic map of neocortex of the normal mouse. J Comp Neurol 164:247–263.

Chadwick A, Khan AG, Poort J, Blot A, Hofer SB, Mrsic-Flogel TD, Sahani M (2023) Learning shapes cortical dynamics to enhance integration of relevant sensory input. Neuron 111:106-120.e10.

Challis C, Beck SG, Berton O (2014) Optogenetic modulation of descending prefrontocortical inputs to the dorsal raphe bidirectionally bias socioaffective choices after social defeat. Frontiers in Behavioral Neuroscience 8:1–14.

Charbonneau V, Laramée M-E, Boucher V, Bronchti G, Boire D (2012) Cortical and subcortical projections to primary visual cortex in anophthalmic, enucleated and sighted mice. European Journal of Neuroscience 36:2949–2963.

Chelazzi L, Miller EK, Duncan J, Desimone R (1993) A neural basis for visual search in inferior temporal cortex. Nature 363:345–347.

Chen G, Zhang Y, Li X, Zhao X, Ye Q, Lin Y, Tao HW, Rasch MJ, Zhang X (2017) Distinct Inhibitory Circuits Orchestrate Cortical beta and gamma Band Oscillations. Neuron 96:1403-1418.e6.

Chen JL, Lin WC, Cha JW, So PT, Kubota Y, Nedivi E (2011) Structural basis for the role of inhibition in facilitating adult brain plasticity. Nat Neurosci 14:587–594.

Chen SX, Kim AN, Peters AJ, Komiyama T (2015) Subtype-specific plasticity of inhibitory circuits in motor cortex during motor learning. Nat Neurosci 18:1109–1115.

Chettih SN, Harvey CD (2019) Single-neuron perturbations reveal feature-specific competition in V1. Nature 567:334–340.

Chung JE, Sellers KK, Leonard MK, Gwilliams L, Xu D, Dougherty ME, Kharazia V, Metzger SL, Welkenhuysen M, Dutta B, Chang EF (2022) High-density single-unit human cortical recordings using the Neuropixels probe. Neuron 110:2409-2421.e3.

Clavagnier S, Falchier A, Kennedy H (2004) Long-distance feedback projections to area V1: Implications for multisensory integration, spatial awareness, and visual consciousness. Cognitive, Affective, & Behavioral Neuroscience 4:117–126.

Cohen MR, Maunsell JHR (2009a) Attention improves performance primarily by reducing interneuronal correlations. Nature Neuroscience 12:1594–1600.

Cohen MR, Maunsell JHR (2011) Using neuronal populations to study the mechanisms underlying spatial and feature attention. Neuron 70:1192–1204.

Cole N, Harvey M, Myers-Joseph D, Gilra A, Khan AG (2022) Prediction error signals in anterior cingulate cortex drive task-switching. :2022.11.27.518096 Available at: https://www.biorxiv.org/content/10.1101/2022.11.27.518096v1 [Accessed December 26, 2022].

Condylis C, Ghanbari A, Manjrekar N, Bistrong K, Yao S, Yao Z, Nguyen TN, Zeng H, Tasic B, Chen JL (2022) Dense functional and molecular readout of a circuit hub in sensory cortex. Science 375:eabl5981.

Cone JJ, Scantlen MD, Histed MH, Maunsell JHR (2019) Different Inhibitory Interneuron Cell Classes Make Distinct Contributions to Visual Contrast Perception. eNeuro 6 Available at: https://www.eneuro.org/content/6/1/ENEURO.0337-18.2019 [Accessed December 13, 2022].

Coogan TA, Burkhalter A (1993) Hierarchical organization of areas in rat visual cortex. J Neurosci 13:3749–3772.

Cook EP, Maunsell JHR (2002) Attentional Modulation of Behavioral Performance and Neuronal Responses in Middle Temporal and Ventral Intraparietal Areas of Macaque Monkey. J Neurosci 22:1994–2004.

Cottam JCH, Smith SL, Häusser M (2013) Target-Specific Effects of Somatostatin-Expressing Interneurons on Neocortical Visual Processing. J Neurosci 33:19567–19578.

Cruikshank SJ, Lewis TJ, Connors BW (2007) Synaptic basis for intense thalamocortical activation of feedforward inhibitory cells in neocortex. Nat Neurosci 10:462–468.

Dadarlat MC, Stryker MP (2017) Locomotion enhances neural encoding of visual stimuli in mouse V1. Journal of Neuroscience 37:3764–3775.

Dalley JW, Everitt BJ, Robbins TW (2011) Impulsivity, Compulsivity, and Top-Down Cognitive Control. Neuron 69:680–694.

Danskin B, Denman D, Valley M, Ollerenshaw D, Williams D, Groblewski P, Reid C, Olsen S, Waters J (2015) Optogenetics in mice performing a visual discrimination task: Measurement and suppression of retinal activation and the resulting behavioral artifact. PLoS ONE 10:e0144760.

de Vries SEJ et al. (2020) A large-scale standardized physiological survey reveals functional organization of the mouse visual cortex. Nat Neurosci 23:138–151.

Disney AA, Aoki C, Hawken MJ (2007) Gain Modulation by Nicotine in Macaque V1. Neuron 56:701.

Donato F, Rompani SB, Caroni P (2013) Parvalbumin-expressing basket-cell network plasticity induced by experience regulates adult learning. Nature 504:272–276.

D'Souza RD, Wang Q, Ji W, Meier AM, Kennedy H, Knoblauch K, Burkhalter A (2020)

Canonical and noncanonical features of the mouse visual cortical hierarchy. :2020.03.30.016303 Available at: https://www.biorxiv.org/content/10.1101/2020.03.30.016303v1 [Accessed October 23, 2022].

Duman CH, Schlesinger L, Russell DS, Duman RS (2008) Voluntary Exercise Produces Antidepressant and Anxiolytic Behavioral Effects in Mice. Brain Res 1199:148–158.

Durstewitz D, Vittoz NM, Floresco SB, Seamans JK (2010) Abrupt transitions between prefrontal neural ensemble states accompany behavioral transitions during rule learning. Neuron 66:438–448.

El-Boustani S, Sur M (2014) Response-dependent dynamics of cell-specific inhibition in cortical networks in vivo. Nat Commun 5:5689.

El-Boustani S, Wilson NR, Runyan CA, Sur M (2014) El-Boustani et al. reply. Nature 508:E3–E4.

Elsayed GF, Lara AH, Kaufman MT, Churchland MM, Cunningham JP (2016) Reorganization between preparatory and movement population responses in motor cortex. Nature Communications 2016 7:1 7:1–15.

Erisken S, Vaiceliunaite A, Jurjut O, Fiorini M, Katzner S, Busse L (2014) Effects of Locomotion Extend throughout the Mouse Early Visual System. Current Biology 24:2899–2907.

Everitt BJ, Robbins TW (1997) Central cholinergic systems and cognition. Annual Review of Psychology 48:649–684.

Fagiolini M, Hensch TK (2000) Inhibitory threshold for critical-period activation in primary visual cortex. Nature 404:183–186.

Failor SW, Carandini M, Harris KD (2022) Visuomotor association orthogonalizes visual cortical population codes. :2021.05.23.445338 Available at: https://www.biorxiv.org/content/10.1101/2021.05.23.445338v3 [Accessed May 11, 2023].

Fang Q, Chou X, Peng B, Zhong W, Zhang LI, Tao HW (2020) A Differential Circuit via Retino-Colliculo-Pulvinar Pathway Enhances Feature Selectivity in Visual Cortex through Surround Suppression. Neuron 105:355-369.e6.

Fehérvári TD, Yagi T (2016) Population Response Propagation to Extrastriate Areas Evoked by Intracortical Electrical Stimulation in V1. Frontiers in Neural Circuits 10 Available at: https://www.frontiersin.org/articles/10.3389/fncir.2016.00006 [Accessed October 21, 2022].

Felleman DJ, Van Essen DC (1991) Distributed Hierarchical Processing in the Primate Cerebral Cortex. Cerebral Cortex 1:1–47.

Ferguson KA, Cardin JA (2020) Mechanisms underlying gain modulation in the cortex. Nat Rev Neurosci 21:80–92.

Floresco SB, Block AE, Tse MTL (2008) Inactivation of the medial prefrontal cortex of the rat impairs strategy set-shifting, but not reversal learning, using a novel, automated procedure. Behavioural Brain Research 190:85–96.

Franke K, Berens P, Schubert T, Bethge M, Euler T, Baden T (2017) Inhibition decorrelates visual feature representations in the inner retina. Nature 542:439–444.

Fries P, Reynolds JH, Rorie AE, Desimone R (2001) Modulation of Oscillatory Neuronal Synchronization by Selective Visual Attention. Science 291:1560–1563.

Froemke RC, Merzenich MM, Schreiner CE (2007) A synaptic memory trace for cortical receptive field plasticity. Nature 450:425–429.

Froudarakis E, Fahey PG, Reimer J, Smirnakis SM, Tehovnik EJ, Tolias AS (2019) The Visual Cortex in Context. Annual Review of Vision Science 5:317–339.

Fu Y, Tucciarone JM, Espinosa JS, Sheng N, Darcy DP, Nicoll RA, Huang ZJ, Stryker MP (2014) A Cortical Circuit for Gain Control by Behavioral State. Cell 156:1139–1152.

Fusi S, Miller EK, Rigotti M (2016) Why neurons mix: high dimensionality for higher cognition. Current Opinion in Neurobiology 37:66–74.

Galletti C, Fattori P (2018) The dorsal visual stream revisited: Stable circuits or dynamic pathways? Cortex 98:203–217.

Gămănuţ R, Kennedy H, Toroczkai Z, Ercsey-Ravasz M, Van Essen D, Knoblauch K, Burkhalter A (2018) The Mouse Cortical Connectome Characterized by an Ultra Dense Cortical Graph Maintains Specificity by Distinct Connectivity Profiles. Neuron 97:698-715.e10.

Gao W-J, Wang Y, Goldman-Rakic PS (2003) Dopamine Modulation of Perisomatic and Peridendritic Inhibition in Prefrontal Cortex. J Neurosci 23:1622–1630.

Garcia Del Molino LC, Yang GR, Mejias JF, Wang XJ (2017) Paradoxical response reversal of top- down modulation in cortical circuits with three interneuron types. eLife 6:1–15.

Garcia-Junco-Clemente P, Ikrar T, Tring E, Xu X, Ringach DL, Trachtenberg JT (2017) An inhibitory pull–push circuit in frontal cortex. Nat Neurosci 20:389–392.

Garrett ME, Nauhaus I, Marshel JH, Callaway EM, Garrett ME, Marshel JH, Nauhaus I, Garrett ME (2014) Topography and areal organization of mouse visual cortex. Journal of Neuroscience 34:12587–12600.

Gasselin C, Hohl B, Vernet A, Crochet S, Petersen CCH (2021) Cell-type-specific nicotinic input disinhibits mouse barrel cortex during active sensing. Neuron 109:778-787.e3.

Gentet LJ, Avermann M, Matyas F, Staiger JF, Petersen CCH (2010) Membrane Potential Dynamics of GABAergic Neurons in the Barrel Cortex of Behaving Mice. Neuron 65:422–435.

Gentet LJ, Kremer Y, Taniguchi H, Huang ZJ, Staiger JF, Petersen CCH (2012) Unique functional properties of somatostatin-expressing GABAergic neurons in mouse barrel cortex. Nat Neurosci 15:607–612.

Glickfeld LL, Andermann ML, Bonin V, Reid RC (2013) Cortico-cortical projections in mouse visual cortex are functionally target specific. Nat Neurosci 16:219–226.

Glickfeld LL, Olsen SR (2017) Higher-Order Areas of the Mouse Visual Cortex. Annual Review of Vision Science 3:251–273.

Golchert J, Smallwood J, Jefferies E, Liem F, Huntenburg JM, Falkiewicz M, Lauckner ME, Oligschläger S, Villringer A, Margulies DS (2017) In need of constraint: Understanding the role of the cingulate cortex in the impulsive mind. NeuroImage 146:804–813.

Graupner M, Reyes AD (2013) Synaptic Input Correlations Leading to Membrane Potential Decorrelation of Spontaneous Activity in Cortex. J Neurosci 33:15075–15085.

Gregoriou GG, Rossi AF, Ungerleider LG, Desimone R (2014) Lesions of prefrontal cortex reduce attentional modulation of neuronal responses and synchrony in V4. Nat Neurosci 17:1003–1011.

Grinband J, Hirsch J, Ferrera VP (2006) A Neural Representation of Categorization Uncertainty in the Human Brain. Neuron 49:757–763.

Guet-McCreight A, Skinner FK, Topolnik L (2020) Common Principles in Functional Organization of VIP/Calretinin Cell-Driven Disinhibitory Circuits Across Cortical Areas. Frontiers in Neural Circuits 14 Available at: https://www.frontiersin.org/articles/10.3389/fncir.2020.00032 [Accessed November 10, 2022].

Guo ZV, Inagaki HK, Daie K, Druckmann S, Gerfen CR, Svoboda K (2017) Maintenance of persistent activity in a frontal thalamocortical loop. Nature 545:181–186.

Guo ZV, Li N, Huber D, Ophir E, Gutnisky D, Ting JT, Feng G, Svoboda K (2014) Flow of Cortical Activity Underlying a Tactile Decision in Mice. Neuron 81:179–194.

Gutnisky DA, Yu J, Hires SA, To M-S, Bale MR, Svoboda K, Golomb D (2017) Mechanisms underlying a thalamocortical transformation during active tactile sensation. PLOS Computational Biology 13:e1005576.

Hackley SA, Woldorff M, Hillyard SA (1990) Cross-Modal Selective Attention Effects on Retinal, Myogenic, Brainstem, and Cerebral Evoked Potentials. Psychophysiology 27:195–208.

Haider B, McCormick DA (2009) Rapid Neocortical Dynamics: Cellular and Network Mechanisms. Neuron 62:171–189.

Hajós F, Zilles K, Schleicher A, Kálmán M (1988) Types and spatial distribution of vasoactive intestinal polypeptide (VIP)-containing synapses in the rat visual cortex. Anat Embryol (Berl) 178:207–217.

Han X, Vermaercke B, Bonin V (2022) Diversity of spatiotemporal coding reveals specialized visual processing streams in the mouse cortex. Nat Commun 13:3249.

Han Y, Kebschull JM, Campbell RAA, Cowan D, Imhof F, Zador AM, Mrsic-Flogel TD (2018) The logic of single-cell projections from visual cortex. Nature 556:51–56.

Hangya B, Pi H-J, Kvitsiani D, Ranade SP, Kepecs A (2014) From circuit motifs to computations: mapping the behavioral repertoire of cortical interneurons. Current Opinion in Neurobiology 26:117–124.

Harris KD, Hochgerner H, Skene NG, Magno L, Katona L, Bengtsson Gonzales C, Somogyi P, Kessaris N, Linnarsson S, Hjerling-Leffler J (2018) Classes and continua of hippocampal CA1 inhibitory neurons revealed by single-cell transcriptomics Jonas P, ed. PLOS Biology 16:e2006387.

Harris KD, Shepherd GMG (2015) The neocortical circuit: themes and variations. Nature Neuroscience 18:170–181.

Harvey CD, Coen P, Tank DW (2012) Choice-specific sequences in parietal cortex during a virtual-navigation decision task. Nature 484:62–68.

Hasenstaub A, Shu Y, Haider B, Kraushaar U, Duque A, McCormick DA (2005) Inhibitory Postsynaptic Potentials Carry Synchronized Frequency Information in Active Cortical Networks. Neuron 47:423–435.

Hasselmo ME, Sarter M (2011) Modes and Models of Forebrain Cholinergic Neuromodulation of Cognition. Neuropsychopharmacol 36:52–73.

Helias M, Tetzlaff T, Diesmann M (2014) The Correlation Structure of Local Neuronal Networks Intrinsically Results from Recurrent Dynamics. PLOS Computational Biology 10:e1003428.

Herrero JL, Roberts MJ, Delicato LS, Gieselmann MA, Dayan P, Thiele A (2008) Acetylcholine contributes through muscarinic receptors to attentional modulation in V1. Nature 454:1110–1114.

Higley MJ, Contreras D (2006) Balanced Excitation and Inhibition Determine Spike Timing during Frequency Adaptation. J Neurosci 26:448–457.

Hodge RD et al. (2019) Conserved cell types with divergent features in human versus mouse cortex. Nature 573:61–68.

Hofer SB, Ko H, Pichler B, Vogelstein J, Ros H, Zeng H, Lein E, Lesica NA, Mrsic-Flogel TD (2011) Differential connectivity and response dynamics of excitatory and inhibitory neurons in visual cortex. Nat Neurosci 14:1045–1052.

Holt GR, Koch C (1997) Shunting inhibition does not have a divisive effect on firing rates. Neural Comput 9:1001–1013.

Hong YK, Lacefield CO, Rodgers CC, Bruno RM (2018) Sensation, movement and learning in the absence of barrel cortex. Nature 561:542–546.

Hsiao K, Noble C, Pitman W, Yadav N, Kumar S, Keele GR, Terceros A, Kanke M, Conniff T, Cheleuitte-Nieves C, Tolwani R, Sethupathy P, Rajasethupathy P (2020) A Thalamic Orphan Receptor Drives Variability in Short-Term Memory. Cell 183:522-536.e19.

Hu F, Dan Y (2022) An inferior-superior colliculus circuit controls auditory cue-directed visual spatial attention. Neuron 110:109-119.e3.

Huberman AD, Niell CM (2011) What can mice tell us about how vision works? Trends in Neurosciences 34:464–473.

Huh CYL, Peach JP, Bennett C, Vega RM, Hestrin S (2018) Feature-Specific Organization of Feedback Pathways in Mouse Visual Cortex. Current Biology 28:114-120.e5.

Itokazu T, Hasegawa M, Kimura R, Osaki H, Albrecht U-R, Sohya K, Chakrabarti S, Itoh H, Ito T, Sato TK, Sato TR (2018) Streamlined sensory motor communication through cortical reciprocal connectivity in a visually guided eye movement task. Nat Commun 9:338.

Jackson J, Ayzenshtat I, Karnani MM, Yuste R (2016) VIP+ interneurons control neocortical activity across brain states. Journal of Neurophysiology 115:3008–3017.

Ji X, Zingg B, Mesik L, Xiao Z, Zhang LI, Tao HW (2016) Thalamocortical Innervation Pattern in Mouse Auditory and Visual Cortex: Laminar and Cell-Type Specificity. Cereb Cortex 26:2612–2625.

Jin M, Beck JM, Glickfeld LL (2019) Neuronal Adaptation Reveals a Suboptimal Decoding of Orientation Tuned Populations in the Mouse Visual Cortex. J Neurosci 39:3867–3881.

Jin M, Glickfeld LL (2020) Mouse Higher Visual Areas Provide Both Distributed and Specialized Contributions to Visually Guided Behaviors. Current Biology 30:4682-4692.e7.

Johnson EL, Walsh D, Hutchings F, Palmini RB, Ponon N, O'Neill A, Jackson A, Degenaar P, Trevelyan AJ (2021) Characterization of light penetration through brain tissue, for optogenetic stimulation. :2021.04.08.438932 Available at: https://www.biorxiv.org/content/10.1101/2021.04.08.438932v1 [Accessed December 19, 2022].

Johnson RR, Burkhalter A (1997) A Polysynaptic Feedback Circuit in Rat Visual Cortex. J

Neurosci 17:7129–7140.

Kamigaki T, Dan Y (2017) Delay activity of specific prefrontal interneuron subtypes modulates memory-guided behavior. Nat Neurosci 20:854–863.

Kanamori T, Mrsic-Flogel TD (2022) Independent response modulation of visual cortical neurons by attentional and behavioral states. Neuron Available at: https://www.sciencedirect.com/science/article/pii/S0896627322008030 [Accessed November 9, 2022].

Kanashiro T, Ocker GK, Cohen MR, Doiron B (2017) Attentional modulation of neuronal variability in circuit models of cortex Latham P, ed. eLife 6:e23978.

Kapfer C, Glickfeld LL, Atallah BV, Scanziani M (2007) Supralinear increase of recurrent inhibition during sparse activity in the somatosensory cortex. Nat Neurosci 10:743–753.

Kaplan ES, Cooke SF, Komorowski RW, Chubykin AA, Thomazeau A, Khibnik LA, Gavornik JP, Bear MF (2016) Contrasting roles for parvalbumin-expressing inhibitory neurons in two forms of adult visual cortical plasticity Mrsic-Flogel TD, ed. eLife 5:e11450.

Karlsson MP, Tervo DGR, Karpova AY (2012) Network Resets in Medial Prefrontal Cortex Mark the Onset of Behavioral Uncertainty. Science 338:135–139.

Karnani MM, Jackson J, Ayzenshtat I, Sichani AH, Manoocheri K, Kim S, Yuste R (2016a) Opening Holes in the Blanket of Inhibition: Localized Lateral Disinhibition by VIP Interneurons. J Neurosci 36:3471–3480.

Karnani MM, Jackson J, Ayzenshtat I, Tucciarone J, Manoocheri K, Snider WG, Yuste R (2016b) Cooperative Subnetworks of Molecularly Similar Interneurons in Mouse Neocortex. Neuron 90:86–100.

Kastner S, Ungerleider L (2000) Mechanisms of Visual Attention in the Human Cortex. Annual Review of Neuroscience 23:315–341.

Kato HK, Asinof SK, Isaacson JS (2017) Network-Level Control of Frequency Tuning in Auditory Cortex. Neuron 95:412-423.e4.

Kato HK, Gillet SN, Isaacson JS (2015) Flexible Sensory Representations in Auditory Cortex Driven by Behavioral Relevance. Neuron 88:1027–1039.

Kawaguchi Y (1997) Selective Cholinergic Modulation of Cortical GABAergic Cell Subtypes. Journal of Neurophysiology 78:1743–1747.

Kawaguchi Y, Katsumaru H, Kosaka T, Heizmann CW, Hama K (1987) Fast spiking cells in rat hippocampus (CA1 region) contain the calcium-binding protein parvalbumin. Brain Res 416:369–374.

Kawaguchi Y, Kubota Y (1997) GABAergic cell subtypes and their synaptic connections in rat frontal cortex. Cerebral Cortex 7:476–486.

Keller AJ, Dipoppa M, Roth MM, Caudill MS, Ingrosso A, Miller KD, Scanziani M (2020) A Disinhibitory Circuit for Contextual Modulation in Primary Visual Cortex. Neuron 108:1181-1193.e8.

Keller GB, Bonhoeffer T, Hübener M (2012) Sensorimotor Mismatch Signals in Primary Visual Cortex of the Behaving Mouse. Neuron 74:809–815.

Kepecs A, Fishell G (2014) Interneuron cell types are fit to function. Nature 505:318–326.

Kepecs A, Uchida N, Zariwala HA, Mainen ZF (2008) Neural correlates, computation and behavioural impact of decision confidence. Nature 455:227–231.

Kerlin AM, Andermann ML, Berezovskii VK, Reid RC (2010) Broadly Tuned Response Properties of Diverse Inhibitory Neuron Subtypes in Mouse Visual Cortex. Neuron 67:858–871.

Khan AG, Poort J, Chadwick A, Blot A, Sahani M, Mrsic-Flogel TD, Hofer SB (2018) Distinct learning-induced changes in stimulus selectivity and interactions of {GABAergic} interneuron classes in visual cortex. Nature Neuroscience 21:851–859.

Khibnik LA, Tritsch NX, Sabatini BL (2014) A Direct Projection from Mouse Primary Visual Cortex to Dorsomedial Striatum. PLoS ONE 9:104501.

Kim J, Connors B (2012) High temperatures alter physiological properties of pyramidal cells and inhibitory interneurons in hippocampus. Front Cell Neurosci 0 Available at: https://www.frontiersin.org/articles/10.3389/fncel.2012.00027/full [Accessed November 14, 2022].

Kim M-H, Znamenskiy P, Iacaruso MF, Mrsic-Flogel TD (2018) Segregated Subnetworks of Intracortical Projection Neurons in Primary Visual Cortex. Neuron 100:1313-1321.e6.

Klein BP, Harvey BM, Dumoulin SO (2014) Attraction of Position Preference by Spatial Attention throughout Human Visual Cortex. Neuron 84:227–237.

Knoblich U, Huang L, Zeng H, Li L (2019) Neuronal cell-subtype specificity of neural synchronization in mouse primary visual cortex. Nat Commun 10:2533.

Krabbe S, Paradiso E, d'Aquin S, Bitterman Y, Courtin J, Xu C, Yonehara K, Markovic M, Müller C, Eichlisberger T, Gründemann J, Ferraguti F, Lüthi A (2019) Adaptive disinhibitory gating by VIP interneurons permits associative learning. Nat Neurosci 22:1834–1843.

Krauzlis RJ, Lovejoy LP, Zénon A (2013) Superior Colliculus and Visual Spatial Attention. Annual Review of Neuroscience 36:165–182.

Kravitz DJ, Saleem KS, Baker CI, Mishkin M (2011) A new neural framework for visuospatial

processing. Nat Rev Neurosci 12:217–230.

Krienen FM et al. (2020) Innovations present in the primate interneuron repertoire. Nature 586:262–269.

Kruglikov I, Rudy B (2008) Perisomatic GABA Release and Thalamocortical Integration onto Neocortical Excitatory Cells Are Regulated by Neuromodulators. Neuron 58:911–924.

Kuchibhotla KV, Gill JV, Lindsay GW, Papadoyannis ES, Field RE, Sten TAH, Miller KD, Froemke RC (2017) Parallel processing by cortical inhibition enables context-dependent behavior. Nature Neuroscience 20:62–71.

Kuhlman SJ, Olivas ND, Tring E, Ikrar T, Xu X, Trachtenberg JT (2013) A disinhibitory microcircuit initiates critical-period plasticity in the visual cortex. Nature 501:543–546.

Kvitsiani D, Ranade S, Hangya B, Taniguchi H, Huang JZ, Kepecs A (2013) Distinct behavioural and network correlates of two interneuron types in prefrontal cortex. Nature 498:363–366.

Laramée M-E, Boire D (2015) Visual cortical areas of the mouse: comparison of parcellation and network structure with primates. Front Neural Circuits 8:149.

Larkum M (2013) A cellular mechanism for cortical associations: an organizing principle for the cerebral cortex. Trends in Neurosciences 36:141–151.

Lee AT, Cunniff MM, See JZ, Wilke SA, Luongo FJ, Ellwood IT, Ponnavolu S, Sohal VS (2019) VIP Interneurons Contribute to Avoidance Behavior by Regulating Information Flow across Hippocampal-Prefrontal Networks. Neuron 102:1223-1234.e4.

Lee AT, Vogt D, Rubenstein JL, Sohal VS (2014a) A Class of GABAergic Neurons in the Prefrontal Cortex Sends Long-Range Projections to the Nucleus Accumbens and Elicits Acute Avoidance Behavior. Journal of Neuroscience 34:11519–11525.

Lee S, Hjerling-Leffler J, Zagha E, Fishell G, Rudy B (2010) The Largest Group of Superficial Neocortical GABAergic Interneurons Expresses Ionotropic Serotonin Receptors. J Neurosci 30:16796–16808.

Lee S, Kruglikov I, Huang ZJ, Fishell G, Rudy B (2013) A disinhibitory circuit mediates motor integration in the somatosensory cortex. Nature Neuroscience 16:1662–1670.

Lee S-H, Kwan AC, Dan Y (2014b) Interneuron subtypes and orientation tuning. Nature 508:E1–E2.

Lee S-H, Kwan AC, Zhang S, Phoumthipphavong V, Flannery JG, Masmanidis SC, Taniguchi H, Huang ZJ, Zhang F, Boyden ES, Deisseroth K, Dan Y (2012) Activation of specific interneurons improves V1 feature selectivity and visual perception. Nature 488:379–383.

Leinweber M, Ward DR, Sobczak JM, Attinger A, Keller GB (2017) A Sensorimotor Circuit in Mouse Cortex for Visual Flow Predictions. Neuron 95:1420-1432.e5.

Letzkus JJ, Wolff SBE, Lüthi A (2015) Disinhibition, a Circuit Mechanism for Associative Learning and Memory. Neuron 88:264–276.

Letzkus JJ, Wolff SBE, Meyer EMM, Tovote P, Courtin J, Herry C, Lüthi A (2011) A disinhibitory microcircuit for associative fear learning in the auditory cortex. Nature 480:331–335.

Li L, Ji X, Liang F, Li Y, Xiao Z, Tao HW, Zhang LI (2014) A Feedforward Inhibitory Circuit Mediates Lateral Refinement of Sensory Representation in Upper Layer 2/3 of Mouse Primary Auditory Cortex. J Neurosci 34:13670–13683.

Li N, Chen S, Guo ZV, Chen H, Huo Y, Inagaki HK, Chen G, Davis C, Hansel D, Guo C, Svoboda K (2019) Spatiotemporal constraints on optogenetic inactivation in cortical circuits Huguenard J, Marder E, Petersen CC, eds. eLife 8:e48622.

Li N, Daie K, Svoboda K, Druckmann S (2016) Robust neuronal dynamics in premotor cortex during motor planning. Nature 532:459–464.

Lien AD, Scanziani M (2018) Cortical direction selectivity emerges at convergence of thalamic synapses. Nature 558:80–86.

Litwin-Kumar A, Rosenbaum R, Doiron B (2016) Inhibitory stabilization and visual coding in cortical circuits with multiple interneuron subtypes. Journal of Neurophysiology 115:1399–1409.

Liu Y, Xin Y, Xu N-L (2021) A cortical circuit mechanism for structural knowledge-based flexible sensorimotor decision-making. Neuron Available at: http://www.ncbi.nlm.nih.gov/pubmed/33957065 [Accessed May 17, 2021].

Long MA, Fee MS (2008) Using temperature to analyse temporal dynamics in the songbird motor pathway. Nature 456:189–194.

Loomba S, Straehle J, Gangadharan V, Heike N, Khalifa A, Motta A, Ju N, Sievers M, Gempt J, Meyer HS, Helmstaedter M (2022) Connectomic comparison of mouse and human cortex. Science 377:eabo0924.

Lovejoy LP, Krauzlis RJ (2010) Inactivation of primate superior colliculus impairs covert selection of signals for perceptual judgments. Nat Neurosci 13:261–266.

Lovett-Barron M, Turi GF, Kaifosh P, Lee PH, Bolze F, Sun X-H, Nicoud J-F, Zemelman BV, Sternson SM, Losonczy A (2012) Regulation of neuronal input transformations by tunable dendritic inhibition. Nat Neurosci 15:423–430.

Luck SJ, Chelazzi L, Hillyard SA, Desimone R (1997) Neural Mechanisms of Spatial Selective Attention in Areas V1, V2, and V4 of Macaque Visual Cortex. Journal of Neurophysiology 77:24–42.

Luo TZ, Maunsell JHR (2019) Attention can be subdivided into neurobiological components corresponding to distinct behavioral effects. Proceedings of the National Academy of Sciences 116:26187–26194.

Ly C, Middleton J, Doiron B (2012) Cellular and Circuit Mechanisms Maintain Low Spike Co-Variability and Enhance Population Coding in Somatosensory Cortex. Frontiers in Computational Neuroscience 6 Available at: https://www.frontiersin.org/articles/10.3389/fncom.2012.00007 [Accessed December 9, 2022].

Ma Y, Hu H, Berrebi AS, Mathers PH, Agmon A (2006) Distinct Subtypes of Somatostatin-Containing Neocortical Interneurons Revealed in Transgenic Mice. J Neurosci 26:5069–5082.

Mahn M, Prigge M, Ron S, Levy R, Yizhar O (2016) Biophysical constraints of optogenetic inhibition at presynaptic terminals. Nature Neuroscience 19:554–556.

Malagon-Vina H, Ciocchi S, Passecker J, Dorffner G, Klausberger T (2018) Fluid network dynamics in the prefrontal cortex during multiple strategy switching. Nature Communications 9:1–13.

Mante V, Sussillo D, Shenoy KV, Newsome WT (2013) Context-dependent computation by recurrent dynamics in prefrontal cortex. Nature 503:78–84.

Markram H, Toledo-Rodriguez M, Wang Y, Gupta A, Silberberg G, Wu C (2004) Interneurons of the neocortical inhibitory system. Nat Rev Neurosci 5:793–807.

Marshel JH, Garrett ME, Nauhaus I, Callaway EM (2011) Functional Specialization of Seven Mouse Visual Cortical Areas. Neuron 72:1040–1054.

Marshel JH, Kim YS, Machado TA, Quirin S, Benson B, Kadmon J, Raja C, Chibukhchyan A, Ramakrishnan C, Inoue M, Shane JC, McKnight DJ, Yoshizawa S, Kato HE, Ganguli S, Deisseroth K (2019) Cortical layer–specific critical dynamics triggering perception. Science 365:eaaw5202.

Martin AB, Yang X, Saalmann YB, Wang L, Shestyuk A, Lin JJ, Parvizi J, Knight RT, Kastner S (2019) Temporal dynamics and response modulation across the human visual system in a spatial attention task: An ECoG study. Journal of Neuroscience 39:333–352.

Martinez-Trujillo JC, Treue S (2004) Feature-Based Attention Increases the Selectivity of Population Responses in Primate Visual Cortex. Current Biology 14:744–751.

Martínez-Trujillo JC, Treue S (2002) Attentional Modulation Strength in Cortical Area MT Depends on Stimulus Contrast. Neuron 35:365–370.

Marton TF, Seifikar H, Luongo FJ, Lee AT, Sohal VS (2018) Roles of Prefrontal Cortex and Mediodorsal Thalamus in Task Engagement and Behavioral Flexibility. J Neurosci

38:2569–2578.

Matsui T, Ohki K (2013) Target dependence of orientation and direction selectivity of corticocortical projection neurons in the mouse V1. Frontiers in Neural Circuits 7 Available at: https://www.frontiersin.org/articles/10.3389/fncir.2013.00143 [Accessed October 20, 2022].

Maunsell JH (1992) Functional visual streams. Curr Opin Neurobiol 2:506–510.

Maunsell JHR (2015) Neuronal Mechanisms of Visual Attention. Annual Review of Vision Science 1:373–391.

Maunsell JHR, Treue S (2006) Feature-based attention in visual cortex. Trends in Neurosciences 29:317–322.

Mazurek M, Kager M, Van Hooser SD (2014) Robust quantification of orientation selectivity and direction selectivity. Frontiers in Neural Circuits 8 Available at: https://www.frontiersin.org/articles/10.3389/fncir.2014.00092 [Accessed November 6, 2022].

McAdams CJ, Maunsell JH (1999) Effects of attention on orientation-tuning functions of single neurons in macaque cortical area V4. The Journal of neuroscience : the official journal of the Society for Neuroscience 19:431–441.

McBride EG, Lee S-YJ, Callaway EM (2019) Local and Global Influences of Visual Spatial Selection and Locomotion in Mouse Primary Visual Cortex. Current Biology 29:1592-1605.e5.

McGarry L, Packer A, Fino E, Nikolenko V, Sippy T, Yuste R (2010) Quantitative classification of somatostatin-positive neocortical interneurons identifies three interneuron subtypes. Frontiers in Neural Circuits 4 Available at: https://www.frontiersin.org/articles/10.3389/fncir.2010.00012 [Accessed December 8, 2022].

McGaughy J, Everitt BJ, Robbins TW, Sarter M (2000) The role of cortical cholinergic afferent projections in cognition: impact of new selective immunotoxins. Behavioural Brain Research 115:251–263.

Mehta AD, Ulbert I, Schroeder CE (2000a) Intermodal selective attention in monkeys I: Distribution and timing of effects across visual areas. Cerebral Cortex 10:343–358.

Mehta AD, Ulbert I, Schroeder CE (2000b) Intermodal Selective Attention in Monkeys. II: Physiological Mechanisms of Modulation. Cerebral Cortex 10:359–370.

Mesik L, Ma W, Li L, Ibrahim LA, Huang ZJ, Zhang LI, Tao HW (2015) Functional response properties of VIP-expressing inhibitory neurons in mouse visual and auditory cortex. Frontiers in Neural Circuits 9 Available at:

https://www.frontiersin.org/articles/10.3389/fncir.2015.00022 [Accessed December 9, 2022].

Meyer AF, O'Keefe J, Poort J (2020) Two Distinct Types of Eye-Head Coupling in Freely Moving Mice. Current Biology 30:2116-2130.e6.

Michaiel AM, Abe ET, Niell CM (2020) Dynamics of gaze control during prey capture in freely moving mice Spering M, Colgin LL, Isa T, Leonardo A, Churchland AK, eds. eLife 9:e57458.

Middleton JW, Omar C, Doiron B, Simons DJ (2012) Neural Correlation Is Stimulus Modulated by Feedforward Inhibitory Circuitry. J Neurosci 32:506–518.

Miller EK, Cohen JD (2001) An Integrative Theory of Prefrontal Cortex Function. Annual Review of Neuroscience 24:167–202.

Miller MW, Vogt BA (1984) Direct connections of rat visual cortex with sensory, motor, and association cortices. Journal of Comparative Neurology 226:184–202.

Millman DJ, Ocker GK, Caldejon S, Kato I, Larkin JD, Lee EK, Luviano J, Nayan C, Nguyen TV, North K, Seid S, White C, Lecoq J, Reid C, Buice MA, de Vries SEJ (2020) VIP interneurons in mouse primary visual cortex selectively enhance responses to weak but specific stimuli. eLife 9:1–22.

Mineault PJ, Tring E, Trachtenberg JT, Ringach DL (2016) Enhanced spatial resolution during locomotion and heightened attention in mouse primary visual cortex. Journal of Neuroscience 36:6382–6392.

Mishkin M, Ungerleider LG, Macko KA (1983) Object vision and spatial vision: two cortical pathways. Trends in Neurosciences 6:414–417.

Mitchell JF, Sundberg KA, Reynolds JH (2007) Differential Attention-Dependent Response Modulation across Cell Classes in Macaque Visual Area V4. Neuron 55:131–141.

Mitchell JF, Sundberg KA, Reynolds JH (2009) Spatial Attention Decorrelates Intrinsic Activity Fluctuations in Macaque Area V4. Neuron 63:879–888.

Montijn J, Klink P, Van Wezel R (2012) Divisive Normalization and Neuronal Oscillations in a Single Hierarchical Framework of Selective Visual Attention. Frontiers in Neural Circuits 6 Available at: https://www.frontiersin.org/articles/10.3389/fncir.2012.00022 [Accessed November 18, 2022].

Moore T, Armstrong KM (2003) Selective gating of visual signals by microstimulation of frontal cortex. Nature 421:370–373.

Moore T, Fallah M (2001) Control of eye movements and spatial attention. Proceedings of the National Academy of Sciences 98:1273–1276.

Moore T, Zirnsak M (2017) Neural Mechanisms of Selective Visual Attention. Annual Review of Psychology 68:47–72.

Moran J, Desimone R (1985) Selective Attention Gates Visual Processing in the Extrastriate Cortex. Science 229:782–784.

Morris AP, Krekelberg B (2019) A Stable Visual World in Primate Primary Visual Cortex. Current Biology 29:1471-1480.e6.

Muir JL, Dunnett SB, Robbins TW, Everitt BJ (1992) Attentional functions of the forebrain cholinergic systems: effects of intraventricular hemicholinium, physostigmine, basal forebrain lesions and intracortical grafts on a multiple-choice serial reaction time task. Exp Brain Res 89:611–622.

Murakami T, Matsui T, Ohki K (2017) Functional Segregation and Development of Mouse Higher Visual Areas. J Neurosci 37:9424–9437.

Murayama M, Pérez-Garci E, Nevian T, Bock T, Senn W, Larkum ME (2009) Dendritic encoding of sensory stimuli controlled by deep cortical interneurons. Nature 457:1137–1141.

Narayanan NS, Cavanagh JF, Frank MJ, Laubach M (2013) Common medial frontal mechanisms of adaptive control in humans and rodents. Nat Neurosci 16:1888–1895.

Nelson CL, Sarter M, Bruno JP (2005) Prefrontal cortical modulation of acetylcholine release in posterior parietal cortex. Neuroscience 132:347–359.

Newman LA, McGaughy J (2011) Attentional effects of lesions to the anterior cingulate cortex: how prior reinforcement influences distractibility. Behav Neurosci 125:360–371.

Niell CM, Stryker MP (2010) Modulation of Visual Responses by Behavioral State in Mouse Visual Cortex. Neuron 65:472–479.

Niklaus S, Albertini S, Schnitzer TK, Denk N (2020) Challenging a Myth and Misconception: Red-Light Vision in Rats. Animals (Basel) 10:422.

Norman KJ, Bateh J, Maccario P, Cho C, Caro K, Nishioka T, Koike H, Morishita H (2022) Frontal-Sensory Cortical Projections Become Dispensable for Attentional Performance Upon a Reduction of Task Demand in Mice. Front Neurosci 15:775256.

O'Connor DH, Fukui MM, Pinsk MA, Kastner S (2002) Attention modulates responses in the human lateral geniculate nucleus. Nat Neurosci 5:1203–1209.

Olavarria J, Montero VM (1984) Relation of callosal and striate-extrastriate cortical connections in the rat: morphological definition of extrastriate visual areas. Exp Brain Res 54:240–252.

Olavarria J, Montero VM (1989) Organization of visual cortex in the mouse revealed by

correlating callosal and striate-extrastriate connections. Vis Neurosci 3:59–69.

Olcese U, Iurilli G, Medini P (2013) Cellular and Synaptic Architecture of Multisensory Integration in the Mouse Neocortex. Neuron 79:579–593.

Otchy TM, Wolff SBE, Rhee JY, Pehlevan C, Kawai R, Kempf A, Gobes SMH, Ölveczky BP (2015) Acute off-target effects of neural circuit manipulations. Nature 528:358–363.

Otis JM, Namboodiri VMK, Matan AM, Voets ES, Mohorn EP, Kosyk O, McHenry JA, Robinson JE, Resendez SL, Rossi MA, Stuber GD (2017) Prefrontal cortex output circuits guide reward seeking through divergent cue encoding. Nature 543:103–107.

Ozeki H, Finn IM, Schaffer ES, Miller KD, Ferster D (2009) Inhibitory Stabilization of the Cortical Network Underlies Visual Surround Suppression. Neuron 62:578–592.

Packer AM, Russell LE, Dalgleish HWP, Häusser M (2015) Simultaneous all-optical manipulation and recording of neural circuit activity with cellular resolution in vivo. Nat Methods 12:140–146.

Pakan JM, Lowe SC, Dylda E, Keemink SW, Currie SP, Coutts CA, Rochefort NL (2016) Behavioral-state modulation of inhibition is context-dependent and cell type specific in mouse visual cortex. eLife 5 Available at: https://elifesciences.org/articles/14985 [Accessed July 12, 2019].

Panzeri S, Petersen RS, Schultz SR, Lebedev M, Diamond ME (2001) The Role of Spike Timing in the Coding of Stimulus Location in Rat Somatosensory Cortex. Neuron 29:769–777.

Parikh V, Kozak R, Martinez V, Sarter M (2007) Prefrontal Acetylcholine Release Controls Cue Detection on Multiple Timescales. Neuron 56:141–154.

Paspalas CD, Papadopoulos GC (2001) Serotoninergic afferents preferentially innervate distinct subclasses of peptidergic interneurons in the rat visual cortex. Brain Research 891:158–167.

Paulk AC, Kfir Y, Khanna AR, Mustroph ML, Trautmann EM, Soper DJ, Stavisky SD, Welkenhuysen M, Dutta B, Shenoy KV, Hochberg LR, Richardson RM, Williams ZM, Cash SS (2022) Large-scale neural recordings with single neuron resolution using Neuropixels probes in human cortex. Nat Neurosci 25:252–263.

Pfeffer CK, Xue M, He M, Huang ZJ, Scanziani M (2013) Inhibition of inhibition in visual cortex: the logic of connections between molecularly distinct interneurons. Nature Neuroscience 16:1068–1076.

Phillips EAK, Hasenstaub AR (2016) Asymmetric effects of activating and inactivating cortical interneurons. eLife 5.

Pi H-J, Hangya B, Kvitsiani D, Sanders JI, Huang ZJ, Kepecs A (2013) Cortical interneurons that specialize in disinhibitory control. Nature 503:521–524.

Pinto L, Dan Y (2015) Cell-{Type}-{Specific} {Activity} in {Prefrontal} {Cortex} during {Goal}-{Directed} {Behavior}. Neuron 87:437–450.

Pinto L, Goard MJ, Estandian D, Xu M, Kwan AC, Lee S-H, Harrison TC, Feng G, Dan Y (2013) Fast modulation of visual perception by basal forebrain cholinergic neurons. Nat Neurosci 16:1857–1863.

Polack P-O, Friedman J, Golshani P (2013) Cellular mechanisms of brain state–dependent gain modulation in visual cortex. Nat Neurosci 16:1331–1339.

Poort J, Khan AG, Pachitariu M, Nemri A, Orsolic I, Krupic J, Bauza M, Sahani M, Keller GB, Mrsic-Flogel TD, Hofer SB (2015) Learning Enhances Sensory and Multiple Non-sensory Representations in Primary Visual Cortex. Neuron 86:1478–1490.

Poort J, Wilmes KA, Blot A, Chadwick A, Sahani M, Clopath C, Mrsic-Flogel TD, Hofer SB, Khan AG (2022) Learning and attention increase visual response selectivity through distinct mechanisms. Neuron 110:686-697.e6.

Poorthuis RB, Enke L, Letzkus JJ (2014) Cholinergic circuit modulation through differential recruitment of neocortical interneuron types during behaviour. The Journal of Physiology 592:4155–4164.

Poorthuis RB, Muhammad K, Wang M, Verhoog MB, Junek S, Wrana A, Mansvelder HD, Letzkus JJ (2018) Rapid Neuromodulation of Layer 1 Interneurons in Human Neocortex. Cell Reports 23:951–958.

Porter JT, Cauli B, Tsuzuki K, Lambolez B, Rossier J, Audinat E (1999) Selective Excitation of Subtypes of Neocortical Interneurons by Nicotinic Receptors. J Neurosci 19:5228–5235.

Posner MI, Rothbart MK (2007) Research on Attention Networks as a Model for the Integration of Psychological Science. Annual Review of Psychology 58:1–23.

Posner MI, Snyder CR, Davidson BJ (1980) Attention and the detection of signals. J Exp Psychol 109:160–174.

Pouille F, Scanziani M (2001) Enforcement of Temporal Fidelity in Pyramidal Cells by Somatic Feed-Forward Inhibition. Science 293:1159–1163.

Powell NJ, Redish AD (2016) Representational changes of latent strategies in rat medial prefrontal cortex precede changes in behaviour. Nat Commun 7:12830.

Prönneke A, Witte M, Möck M, Staiger JF (2020) Neuromodulation Leads to a Burst-Tonic Switch in a Subset of VIP Neurons in Mouse Primary Somatosensory (Barrel) Cortex. Cerebral Cortex 30:488–504.

Ragozzino ME, Rozman S (2007) The effect of rat anterior cingulate inactivation on cognitive flexibility. Behavioral Neuroscience 121:698–706.

Ratan Murty NA, Arun SP (2018) Multiplicative mixing of object identity and image attributes in single inferior temporal neurons. Proceedings of the National Academy of Sciences 115:E3276–E3285.

Reep RL, Chandler HC, King V, Corwin JV (1994) Rat posterior parietal cortex: topography of corticocortical and thalamic connections. Exp Brain Res 100:67–84.

Reep RL, Corwin JV, King V (1996) Neuronal connections of orbital cortex in rats: topography of cortical and thalamic afferents. Exp Brain Res 111:215–232.

Reimer J, McGinley MJ, Liu Y, Rodenkirch C, Wang Q, McCormick DA, Tolias AS (2016) Pupil fluctuations track rapid changes in adrenergic and cholinergic activity in cortex. Nature Communications 7.

Reinhold K, Lien AD, Scanziani M (2015) Distinct recurrent versus afferent dynamics in cortical visual processing. Nat Neurosci 18:1789–1797.

Renart A, de la Rocha J, Bartho P, Hollender L, Parga N, Reyes A, Harris KD (2010) The Asynchronous State in Cortical Circuits. Science 327:587–590.

Resulaj A, Ruediger S, Olsen SR, Scanziani M (2018) First spikes in visual cortex enable perceptual discrimination Slutsky I, ed. eLife 7:e34044.

Reynolds JH, Chelazzi L (2004) ATTENTIONAL MODULATION OF VISUAL PROCESSING. Annu Rev Neurosci 27:611–658.

Reynolds JH, Chelazzi L, Desimone R (1999) Competitive Mechanisms Subserve Attention in Macaque Areas V2 and V4. J Neurosci 19:1736–1753.

Reynolds JH, Heeger DJ (2009) The Normalization Model of Attention. Neuron 61:168–185.

Reynolds JH, Pasternak T, Desimone R (2000) Attention Increases Sensitivity of V4 Neurons. Neuron 26:703–714.

Rich EL, Shapiro M (2009) Rat Prefrontal Cortical Neurons Selectively Code Strategy Switches. Journal of Neuroscience 29:7208–7219.

Ridderinkhof KR, Ullsperger M, Crone EA, Nieuwenhuis S (2004) The Role of the Medial Frontal Cortex in Cognitive Control. Science 306:443–447.

Rigotti M, Barak O, Warden MR, Wang X-J, Daw ND, Miller EK, Fusi S (2013) The importance of mixed selectivity in complex cognitive tasks. Nature 497:585–590.

Rikhye RV, Gilra A, Halassa MM (2018) Thalamic regulation of switching between cortical representations enables cognitive flexibility. Nat Neurosci 21:1753–1763.

Rossi AF, Paradiso MA (1995) Feature-specific effects of selective visual attention. Vision Research 35:621–634.

Roth MM, Dahmen JC, Muir DR, Imhof F, Martini FJ, Hofer SB (2016) Thalamic nuclei convey diverse contextual information to layer 1 of visual cortex. Nature Neuroscience 19:299–307.

Roth MM, Helmchen F, Kampa BM (2012) Distinct Functional Properties of Primary and Posteromedial Visual Area of Mouse Neocortex. J Neurosci 32:9716–9726.

Rubin DB, Van Hooser SD, Miller KD (2015) The Stabilized Supralinear Network: A Unifying Circuit Motif Underlying Multi-Input Integration in Sensory Cortex. Neuron 85:402–417.

Rudy B, Fishell G, Lee S, Hjerling-Leffler J (2011) Three Groups of Interneurons Account for Nearly 100% of Neocortical GABAergic Neurons. Dev Neurobiol 71:45–61.

Ruff DA, Cohen MR (2019) Simultaneous multi-area recordings suggest that attention improves performance by reshaping stimulus representations. Nat Neurosci 22:1669–1676.

Ruff DA, Xue C, Kramer LE, Baqai F, Cohen MR (2020) Low rank mechanisms underlying flexible visual representations. Proceedings of the National Academy of Sciences 117:29321–29329.

Sadeh S, Silver RA, Mrsic-Flogel TD, Muir DR (2017) Assessing the Role of Inhibition in Stabilizing Neocortical Networks Requires Large-Scale Perturbation of the Inhibitory Population. J Neurosci 37:12050–12067.

Sàenz M, Buraĉas GT, Boynton GM (2003) Global feature-based attention for motion and color. Vision Research 43:629–637.

Salam JN, Fox JH, DeTroy EM, Guignon MH, Wohl DF, Falls WA (2009) Voluntary exercise in C57 mice is anxiolytic across several measures of anxiety. Behavioural Brain Research 197:31–40.

Saleem AB, Lien AD, Krumin M, Haider B, Rosón MR, Ayaz A, Reinhold K, Busse L, Carandini M, Harris KD (2017) Subcortical Source and Modulation of the Narrowband Gamma Oscillation in Mouse Visual Cortex. Neuron 93:315–322.

Salinas E, Sejinowski TJ (2001) Gain Modulation in the Central Nervous System: Where Behavior, Neurophysiology, and Computation Meet. Neuroscientist 7:430–440.

Salinas E, Thier P (2000) Gain Modulation: A Major Computational Principle of the Central Nervous System. Neuron 27:15–21.

Sanzeni A, Akitake B, Goldbach HC, Leedy CE, Brunel N, Histed MH (2020) Inhibition stabilization is a widespread property of cortical networks O'Leary T, Huguenard J, Adesnik H, eds. eLife 9:e54875.

Sarter M, Hasselmo ME, Bruno JP, Givens B (2005) Unraveling the attentional functions of

cortical cholinergic inputs: interactions between signal-driven and cognitive modulation of signal detection. Brain Research Reviews 48:98–111.

Sarter M, Parikh V, Howe WM (2009) Phasic acetylcholine release and the volume transmission hypothesis: time to move on. Nat Rev Neurosci 10:383–390.

Schall JD, Stuphorn V, Brown JW (2002) Monitoring and Control of Action by the Frontal Lobes. Neuron 36:309–322.

Schmitt LI, Wimmer RD, Nakajima M, Happ M, Mofakham S, Halassa MM (2017) Thalamic amplification of cortical connectivity sustains attentional control. Nature 545:219–223.

Scholl B, Pattadkal JJ, Dilly GA, Priebe NJ, Zemelman BV (2015) Local integration accounts for weak selectivity of mouse neocortical parvalbumin interneurons. Neuron 87:424–436.

Seybold BA, Phillips EAK, Schreiner CE, Hasenstaub AR (2015) Inhibitory Actions Unified by Network Integration. Neuron 87:1181–1192.

Shapiro JT, Gosselin EAR, Michaud NM, Crowder NA (2022a) Activating parvalbumin-expressing interneurons produces iceberg effects in mouse primary visual cortex neurons. Neuroscience Letters 786:136804.

Shapiro JT, Michaud NM, King JL, Crowder NA (2022b) Optogenetic Activation of Interneuron Subtypes Modulates Visual Contrast Responses of Mouse V1 Neurons. Cerebral Cortex 32:1110–1124.

Sharpe MJ, Killcross S (2014) The Prelimbic Cortex Contributes to the Down-Regulation of Attention Toward Redundant Cues. Cerebral Cortex 24:1066–1074.

Sheinberg DL, Logothetis NK (2001) Noticing Familiar Objects in Real World Scenes: The Role of Temporal Cortical Neurons in Natural Vision. J Neurosci 21:1340–1350.

Shen S, Jiang X, Scala F, Fu J, Fahey P, Kobak D, Tan Z, Zhou N, Reimer J, Sinz F, Tolias AS (2022) Distinct organization of two cortico-cortical feedback pathways. Nat Commun 13:6389.

Siegle JH et al. (2021) Survey of spiking in the mouse visual system reveals functional hierarchy. Nature 592:86–92.

Silberberg G, Markram H (2007) Disynaptic Inhibition between Neocortical Pyramidal Cells Mediated by Martinotti Cells. Neuron 53:735–746.

Silver RA (2010) Neuronal arithmetic. Nat Rev Neurosci 11:474–489.

Sippy T, Yuste R (2013) Decorrelating Action of Inhibition in Neocortical Networks. J Neurosci 33:9813–9830.

Smith IT, Townsend LB, Huh R, Zhu H, Smith SL (2017) Stream-dependent development of higher visual cortical areas. Nat Neurosci 20:200–208.

Sohal VS, Zhang F, Yizhar O, Deisseroth K (2009) Parvalbumin neurons and gamma rhythms enhance cortical circuit performance. Nature 459:698–702.

Sparks DL (1999) Conceptual issues related to the role of the superior colliculus in the control of gaze. Current Opinion in Neurobiology 9:698–707.

Speed A, Del Rosario J, Mikail N, Haider B (2020) Spatial attention enhances network, cellular and subthreshold responses in mouse visual cortex. Nature Communications 11:1–11.

Speed A, Haider B (2021) Probing mechanisms of visual spatial attention in mice. Trends in Neurosciences 44:822–836.

Spitzer H, Desimone R, Moran J (1988) Increased Attention Enhances Both Behavioral and Neuronal Performance. Science 240:338–340.

Sridharan D, Knudsen EI (2015) Selective disinhibition: A unified neural mechanism for predictive and post hoc attentional selection. Vision Research 116:194–209.

Stănişor L, van der Togt C, Pennartz CMA, Roelfsema PR (2013) A unified selection signal for attention and reward in primary visual cortex. Proceedings of the National Academy of Sciences 110:9136–9141.

Steinmetz NA, Koch C, Harris KD, Carandini M (2018) Challenges and opportunities for large-scale electrophysiology with Neuropixels probes. Current Opinion in Neurobiology 50:92–100.

Stringer C, Michaelos M, Tsyboulski D, Lindo SE, Pachitariu M (2021) High-precision coding in visual cortex. Cell 184:2767-2778.e15.

Stringer C, Pachitariu M, Steinmetz N, Reddy CB, Carandini M, Harris KD (2019) Spontaneous behaviors drive multidimensional, brainwide activity. Science 364:eaav7893.

Stujenske JM, Spellman T, Gordon JA (2015) Modeling the Spatiotemporal Dynamics of Light and Heat Propagation for InVivo Optogenetics. Cell Reports 12:525–534.

Sundberg KA, Mitchell JF, Reynolds JH (2009) Spatial Attention Modulates Center-Surround Interactions in Macaque Visual Area V4. Neuron 61:952–963.

Szadai Z, Pi H-J, Chevy Q, Ócsai K, Albeanu DF, Chiovini B, Szalay G, Katona G, Kepecs A, Rózsa B (2022) Cortex-wide response mode of VIP-expressing inhibitory neurons by reward and punishment Capogna M, Moore T, Ferraguti F, eds. eLife 11:e78815.

Tetzlaff T, Helias M, Einevoll GT, Diesmann M (2012) Decorrelation of Neural-Network Activity by Inhibitory Feedback. PLOS Computational Biology 8:e1002596.

Tolhurst DJ, Smyth D, Thompson ID (2009) The Sparseness of Neuronal Responses in Ferret Primary Visual Cortex. J Neurosci 29:2355–2370.

Theeuwes J (2013) Feature-based attention: it is all bottom-up priming. Philos Trans R Soc Lond B Biol Sci 368:20130055.

Tremblay R, Lee S, Rudy B (2016) GABAergic interneurons in the neocortex: From cellular properties to circuits. Neuron 91:260–292.

Treue S, Martínez-Trujillo JCM (1999) Feature-based attention influences motion processing gain in macaque visual cortex. Nature 399:575–579.

Treue S, Maunsell JHR (1996) Attentional modulation of visual motion processing in cortical areas MT and MST. Nature 382:539–541.

Treves A, Rolls ET (1991) What determines the capacity of autoassociative memories in the brain? Network: Computation in Neural Systems 2:371–397.

Tsodyks MV, Skaggs WE, Sejnowski TJ, McNaughton BL (1997) Paradoxical Effects of External Modulation of Inhibitory Interneurons. J Neurosci 17:4382–4388.

van Beest EH, Mukherjee S, Kirchberger L, Schnabel UH, van der Togt C, Teeuwen RRM, Barsegyan A, Meyer AF, Poort J, Roelfsema PR, Self MW (2021) Mouse visual cortex contains a region of enhanced spatial resolution. Nat Commun 12:4029.

van Versendaal D, Rajendran R, Saiepour MH, Klooster J, Smit-Rigter L, Sommeijer J-P, De Zeeuw CI, Hofer SB, Heimel JA, Levelt CN (2012) Elimination of Inhibitory Synapses Is a Major Component of Adult Ocular Dominance Plasticity. Neuron 74:374–383.

Veit J, Hakim R, Jadi MP, Sejnowski TJ, Adesnik H (2017) Cortical gamma band synchronization through somatostatin interneurons. Nat Neurosci 20:951–959.

Ventura-Antunes L, Mota B, Herculano-Houzel S (2013) Different scaling of white matter volume, cortical connectivity, and gyrification across rodent and primate brains. Frontiers in Neuroanatomy 7 Available at: https://www.frontiersin.org/articles/10.3389/fnana.2013.00003 [Accessed December 8, 2022].

Vinck M, Batista-Brito R, Knoblich U, Cardin JA (2015) Arousal and Locomotion Make Distinct Contributions to Cortical Activity Patterns and Visual Encoding. Neuron 86:740–754.

Vogels TP, Abbott LF (2009) Gating multiple signals through detailed balance of excitation and inhibition in spiking networks. Nat Neurosci 12:483–491.

Vogt BA, Miller MW (1983) Cortical connections between rat cingulate cortex and visual, motor, and postsubicular cortices. Journal of Comparative Neurology 216:192–210.

Voitov I, Mrsic-Flogel TD (2022) Cortical feedback loops bind distributed representations of working memory. Nature 608:381–389.

Vu ET, Krasne FB (1992) Evidence for a Computational Distinction Between Proximal and Distal Neuronal Inhibition. Science 255:1710–1712.

Vyas S, Golub MD, Sussillo D, Shenoy KV (2020) Computation Through Neural Population Dynamics. Annual Review of Neuroscience 43:249–275.

Wagor E, Mangini NJ, Pearlman AL (1980) Retinotopic organization of striate and extrastriate visual cortex in the mouse. J Comp Neurol 193:187–202.

Walker F, Möck M, Feyerabend M, Guy J, Wagener RJ, Schubert D, Staiger JF, Witte M (2016) Parvalbumin- and vasoactive intestinal polypeptide-expressing neocortical interneurons impose differential inhibition on Martinotti cells. Nat Commun 7:13664.

Wall NR, Parra MDL, Sorokin JM, Taniguchi H, Huang ZJ, Callaway EM (2016) Brain-Wide Maps of Synaptic Input to Cortical Interneurons. J Neurosci 36:4000–4009.

Wang L, Krauzlis RJ (2018) Visual Selective Attention in Mice. Current Biology 28:676-685.e4.

Wang L, Krauzlis RJ (2020) Involvement of Striatal Direct Pathway in Visual Spatial Attention in Mice. Current Biology 30:4739-4744.e5.

Wang L, Rangarajan KV, Gerfen CR, Krauzlis RJ (2018) Activation of Striatal Neurons Causes a Perceptual Decision Bias during Visual Change Detection in Mice. Neuron 97:1369-1381.e5.

Wang Q, Burkhalter A (2007) Area map of mouse visual cortex. Journal of Comparative Neurology 502:339–357.

Wang Q, Burkhalter A (2013) Stream-Related Preferences of Inputs to the Superior Colliculus from Areas of Dorsal and Ventral Streams of Mouse Visual Cortex. J Neurosci 33:1696–1705.

Wang Q, Gao E, Burkhalter A (2011) Gateways of Ventral and Dorsal Streams in Mouse Visual Cortex. J Neurosci 31:1905–1918.

Wang Q, Sporns O, Burkhalter A (2012) Network Analysis of Corticocortical Connections Reveals Ventral and Dorsal Processing Streams in Mouse Visual Cortex. J Neurosci 32:4386–4399.

Wang Y, Toledo-Rodriguez M, Gupta A, Wu C, Silberberg G, Luo J, Markram H (2004) Anatomical, physiological and molecular properties of Martinotti cells in the somatosensory cortex of the juvenile rat. The Journal of Physiology 561:65–90.

Warden MR, Selimbeyoglu A, Mirzabekov JJ, Lo M, Thompson KR, Kim SY, Adhikari A, Tye KM, Frank LM, Deisseroth K (2012) A prefrontal cortex-brainstem neuronal projection that

controls response to behavioural challenge. Nature 492:428–432.

Wehr M, Zador AM (2003) Balanced inhibition underlies tuning and sharpens spike timing in auditory cortex. Nature 426:442–446.

Wiederman SD, O'Carroll DC (2013) Selective Attention in an Insect Visual Neuron. Current Biology 23:156–161.

Wilent WB, Contreras D (2005) Dynamics of excitation and inhibition underlying stimulus selectivity in rat somatosensory cortex. Nat Neurosci 8:1364–1370.

Willmore B, Tolhurst DJ (2001) Characterizing the sparseness of neural codes. Network 12:255–270.

Williams LE, Holtmaat A (2019) Higher-Order Thalamocortical Inputs Gate Synaptic Long-Term Potentiation via Disinhibition. Neuron 101:91-102.e4.

Wilson NR, Runyan CA, Wang FL, Sur M (2012) Division and subtraction by distinct cortical inhibitory networks in vivo. Nature 488:343–348.

Wimmer RD, Schmitt LI, Davidson TJ, Nakajima M, Deisseroth K, Halassa MM (2015) Thalamic control of sensory selection in divided attention. Nature 526:705–709.

Wolff SB, Ölveczky BP (2018) The promise and perils of causal circuit manipulations. Current Opinion in Neurobiology 49:84–94.

Woods DL, Alho K, Algazi A (1992) Intermodal selective attention. I. Effects on event-related potentials to lateralized auditory and visual stimuli. Electroencephalogr Clin Neurophysiol 82:341–355.

Xiong Q, Znamenskiy P, Zador AM (2015) Selective corticostriatal plasticity during acquisition of an auditory discrimination task. Nature 521:348–351.

Xu X, Roby KD, Callaway EM (2010) Immunochemical characterization of inhibitory mouse cortical neurons: Three chemically distinct classes of inhibitory cells. Journal of Comparative Neurology 518:389–404.

Yang W, Carrasquillo Y, Hooks BM, Nerbonne JM, Burkhalter A (2013) Distinct Balance of Excitation and Inhibition in an Interareal Feedforward and Feedback Circuit of Mouse Visual Cortex. J Neurosci 33:17373–17384.

You W-K, Mysore SP (2020) Endogenous and exogenous control of visuospatial selective attention in freely behaving mice. Nat Commun 11:1986.

Yu J, Gutnisky DA, Hires SA, Svoboda K (2016) Layer 4 fast-spiking interneurons filter thalamocortical signals during active somatosensation. Nat Neurosci 19:1647–1657.

Zariwala HA, Kepecs A, Uchida N, Hirokawa J, Mainen ZF (2013) The limits of deliberation in

a perceptual decision task. Neuron 78:339–351.

Zénon A, Krauzlis RJ (2012) Attention deficits without cortical neuronal deficits. Nature 489:434–437.

Zhang S, Xu M, Chang W-C, Ma C, Hoang Do JP, Jeong D, Lei T, Fan JL, Dan Y (2016) Organization of long-range inputs and outputs of frontal cortex for top-down control. Nature Neuroscience 19:1733–1742.

Zhang S, Xu M, Kamigaki T, Do JPH, Chang W-C, Jenvay S, Miyamichi K, Luo L, Dan Y (2014) Long-range and local circuits for top-down modulation of visual cortex processing. Science 345:660–665.

Zhou H, Schafer RJ, Desimone R (2016) Pulvinar-Cortex Interactions in Vision and Attention. Neuron 89:209–220.

Zhou Y, Mesik L, Sun YJ, Liang F, Xiao Z, Tao HW, Zhang LI (2012) Generation of Spike Latency Tuning by Thalamocortical Circuits in Auditory Cortex. J Neurosci 32:9969–9980.

Zhuang J, Ng L, Williams D, Valley M, Li Y, Garrett M, Waters J (2017) An extended retinotopic map of mouse cortex. eLife 6.

Zilles K, Kálmán M, Hajós F, Schleicher A (1991) Developmental gradients of vasoactive intestinal polypeptide (VIP)-containing neurons in the rat visual cortex detected by image analysis. Developmental Brain Research 60:137–144.

Znamenskiy P, Zador AM (2013) Corticostriatal neurons in auditory cortex drive decisions during auditory discrimination. Nature 497:482–485.